Nancy-Université

UFR S.T.M.I.A.
École Doctorale IAEM
Université Henri Poincaré - Nancy I
D.F.D. Mathématiques

THÈSE présenté par

Nicolae Cîndea

en vue d'obtenir le titre de

DOCTEUR DE L'UNIVERSITÉ
Spécialité : Mathématiques.

Problèmes inverses et contrôlabilité avec applications en élasticité et IRM

soutenue le 29 Mars 2010

devant le jury composé de Messieurs les Professeurs :

Président du jury	Jean-Pierre PUEL	Université de Versaille St Quentin
Raporteurs	Philip BATCHELOR	King's College London
	Emmanuel TRELAT	Université d'Orléans
Examinateurs	Dominique CHAPELLE	INRIA-Rocquencourt
	Jacques FELBLINGER	Université Henri Poincaré Nancy 1
Directeurs de thèse	Marius TUCSNAK	Université Henri Poincaré Nancy 1
	Pierre-André VUISSOZ	Université Henri Poincaré Nancy 1

Institut Élie Cartan Nancy
Laboratoire Imagerie Adaptative Diagnostique et Interventionnelle (IADI)

Problèmes inverses et contrôlabilité avec applications en élasticité et IRM

Nicolae Cîndea

29 Mars 2010

Remerciements

Je tiens avant tout à remercier les deux personnes qui ont dirigé cette thèse : Marius Tucsnak et Pierre-André Vuissoz. Travailler avec eux fut un réel plaisir.

Je remercie Marius Tucsnak pour m'avoir guidé dans le monde de la contrôlabilité, pour sa disponibilité et sa bon humeur. Commençant avec le master, il m'a toujours encouragé. Ses hautes compétences pédagogiques et scientifiques ont été essentielles pour l'élaboration de cette thèse. Nos discussions, en langue roumaine, m'ont beaucoup aidé à supporter le mal du pays. Pour tout cela, je ne l'en remercierai jamais assez.

Je remercie également Pierre-André Vuissoz pour m'avoir introduit gentiment à l'imagerie par résonance magnétique. Il a fait preuve de beaucoup de patience et sens pédagogique durant toutes nos réunions des lundis après-midis. J'apprécie particulièrement sa grande culture en imagerie et sa capacité de trouver un langage commun entre mathématiciens et médecins.

Ma gratitude va à Philip Batchelor et à Emmanuel Trélat pour m'avoir fait l'honneur d'accepter de rapporter cette thèse. Leur remarques ont été précieuses.

Je remercie chaleureusement Dominique Chapelle, Jacques Felblinger et Jean-Pierre Puel pour leur participation à mon jury. Merci particulièrement à Jacques Felblinger pour avoir suivis de près mes travaux en IRM.

J'exprime ma reconnaissance à Sorin Micu et à Constantin Niculescu pour m'avoir guidé dans mes études et pour leur chaleureux accueils à l'Université de Craiova. Je remercie également à Ileana Costa pour m'avoir fait découvrir les mathématiques.

Je souhaite aussi remercier tous les membres de IECN et de IADI pour m'avoir accueilli comme collègue. Ces quatre derniers années ont été agréables.

Je remercie Christophe, mon collègue de bureau, pour son amitié. Merci également Julien, Aline, Arnaud, Aurélien, Fernando, Julie, Ghislain, Michael et Renaud pour nos pauses café de tous les jours. Un grand merci également aux collègues de l'équipe Corida : Bertrand, Pauline, Yuning, Erica, Takeo, Mario et Jérôme.

A mes amis extérieurs de l'université Adrian, Irina, Oana, Claudia et Tom qui m'ont aidé à faire d'autres choses que des mathématiques. A mes amis roumains Florea, Mircea, Emil, Cornel et Cristi pour tous les bons moments vécus ensembles.

Un merci tout particulier va à Cristina, pour m'avoir supporté ces dernières années.

En fin, je souhaite remercier ma famille : mes parents, ma soeur, mes grands-parents. Même loin, ils ont toujours été à mes cotés. Je les remercie de tout mon coeur.

Table des matières

Table des figures

Introduction

Dans cette thèse on s'intéresse à la contrôlabilité et l'observabilité exacte de quelques équations de plaques vibrantes ainsi q'aux problèmes inverses associés, appliquant les résultats obtenus pour la reconstruction des images par résonance magnétique d'organes en mouvement. L'exemple typique d'images par résonance magnétique qu'on veut reconstruire est donnée par l'imagerie cardiaque.

La relation entre l'observabilité d'un système et la reconstruction des images par résonance magnétique d'un objet en mouvement n'est pas évidente. Dans l'imagerie par résonance magnétique (IRM) on visualise la densité de protons pour chaque unité de volume de l'objet à imager. Supposons alors que la variation en temps de cette densité, notée par la suite $z(t)$, est donnée par une équation de la forme suivante :

$$\dot{z}(t) = Az(t), \qquad (t \geqslant 0) \tag{0.1}$$
$$z(0) = z_0. \tag{0.2}$$

On peut réduire le problème de la reconstruction de la densité $z(t)$ (qui nous donne les images), à partir d'une certaine mesure

$$y(t) = Cz(t), \qquad (t \geqslant 0) \tag{0.3}$$

à l'observabilité du système (0.1)-(0.3). Pour fixer les idées, notons $\dot{z}$ la dérivée de z par rapport au temps t, z_0 la donnée initiale appartenant à un espace de Hilbert X et $A : \mathcal{D}(A) \to X$ un opérateur non borné. L'opérateur d'observation C est un opérateur borné, appartenant à $\mathcal{L}(X, Y)$, où Y est un autre espace de Hilbert. L'observabilité du système (0.1)-(0.2) doit être comprise au sens de la définition suivante :

Définition 0.1. Le système (0.1)-(0.3) est dit exactement observable en temps $\tau > 0$ s'il existe une constante $k_\tau > 0$ telle que toute solution de (0.1)-(0.2) satisfait

$$\int_0^\tau \|Cz(t)\|^2 \, \mathrm{d}t \geqslant k_\tau^2 \|z_0\|_X^2, \qquad (z_0 \in \mathcal{D}(A)). \tag{0.4}$$

On dit que le système (0.1)-(0.2) est exactement observable, ou que le couple (A, C) est exactement observable, s'il est exactement observable en un temps $\tau > 0$.

Dans ce contexte, l'observabilité exacte du système (0.1)-(0.3) nous donne l'unicité et la stabilité (en un sens qui reste à préciser) de la reconstruction de la donnée initiale à partir de l'observation.

Pour l'IRM, l'observation $y(t)$ correspond à la restriction de la transformée de Fourier de $z(t)$ à un certain ensemble de l'espace de Fourier, qu'on va noter $\mathcal{O}$. Si l'observation est bien connue dans le cas de l'IRM, la question difficile est de trouver l'opérateur A qui, a priori, n'est pas connu. Dans Sermesant et al. [72], des images cardiaques obtenues par résonance magnétique sont utilisées pour calibrer les paramètres d'un modèle différentiel de la forme (0.1)-(0.2). Contrairement à cette démarche, nous supposons que le modèle du mouvement (l'opérateur A) est connu et nous voulons utiliser cette information pour améliorer la qualité des images reconstruites. Pour valider cette approche, on considère que le mouvement de l'objet qu'on veux imager (ou plutôt d'une section bidimensionnelle de l'objet) est gouverné par une équation des plaques vibrantes ou une équation des ondes, une grande partie de cette thèse étant dédiée à l'étude de l'observabilité ou de la contrôlabilité des différents modèles pour les plaques.

La notion duale de l'observabilité est celle de la contrôlabilité. On considère désormais le système suivant :

$$\begin{aligned} \dot{z}(t) &= Az(t) + Bu(t), \qquad (t \geqslant 0) && (0.5)\\ z(0) &= z_0, && (0.6) \end{aligned}$$

où $B \in \mathcal{L}(U, X)$ et U est un espace de Hilbert.

Définition 0.2. On dit que le système (0.5)-(0.6) est exactement contrôlable en temps $\tau > 0$ si pour toute donnée initiale $z_0 \in X$ et toute donnée finale $z_1 \in X$ il existe un contrôle $u \in L^2([0,\tau]; U)$ tel que toute solution de (0.5)-(0.6) satisfasse

$$z(\tau) = z_1.$$

On dit que le système (0.5)-(0.6), ou que le couple (A, B) est exactement contrôlable, si le système (0.5)-(0.6) est exactement contrôlable en un certain temps $\tau > 0$.

La dualité entre la contrôlabilité exacte et l'observabilité exacte est formalisée par la proposition suivante, voir Dolecki et Russell [23].

Proposition 0.3. *Avec les notations précédentes, le couple (A, B), est exactement contrôlable si et seulement si le couple (A^*, B^*) est exactement observable, c'est à dire, s'il existe un temps $\tau > 0$ et $k_\tau > 0$ tels que*

$$\int_0^\tau \|B^*\phi(t)\|_U^2 \; dt \geqslant k_\tau^2 \|\phi_0\|_X^2, \qquad (\phi \in \mathcal{D}(A^*),$$

où ϕ est la solution du système

$$\begin{cases} \dot{\phi}(t) = A^*\phi(t), \qquad (t \geqslant 0) \\ \phi(0) = \phi_0. \end{cases}$$

Les problèmes de la contrôlabilité et de l'observabilité des systèmes ont beaucoup plus d'applications que l'exemple de l'imagerie que nous avons étudié dans cette thèse.

Durant ces derniers décennies une riche littérature s'est développé sur ce sujet. Nous renvoyons le lecteur, par exemple aux livres de Lions [48], Tucsnak et Weiss [80], etc.

Cette thèse est structurée en deux parties. Dans la première partie on étudie l'observabilité exacte et la contrôlabilité exacte des deux modèles mathématiques des plaques vibrantes en donnant une méthode numérique pour la construction des contrôles pour une classe d'équations d'ordre deux en temps. La deuxième partie est centrée sur les problèmes inverses provenant de l'imagerie par résonance magnétique des organes en mouvement.

Dans le premier chapitre de cette thèse on recueille quelques résultats préliminaires sur la contrôlabilité et l'observabilité exacte des systèmes infinis dimensionnels. La plus-part des résultats sont donnés sans preuves en indiquant les références bibliographiques pour les démonstrations.

Le Chapitre 2 répond à la question de l'observabilité exacte d'une équation des plaques perturbée avec des termes linéaires d'ordre inférieur. Plus précisément, on prouve l'observabilité exacte de l'équation d'Euler-Bernoulli perturbée par un terme de la forme $(-a\Delta + b(x)\cdot\nabla + c(x))(\cdot)$.

Dans le Chapitre 3 on traite la contrôlabilité exacte interne d'une équation des plaques non linéaire attribuée à Berger :

$$\ddot{w}(x,t) + \Delta^2 w(x,t) - \left(a + b\int_\Omega |\nabla w|^2 \mathrm{d}x\right)\Delta w(x,t) = u(x,t)\chi_{\mathcal{O}}, \quad \Omega\times(0,\infty), \tag{0.7}$$

$$w(x,t) = \Delta w(x,t) = 0, \qquad (x,t)\in\partial\Omega\times(0,\infty), \tag{0.8}$$

$$w(x,0) = \dot{w}(x,0) = 0, \qquad x\in\Omega. \tag{0.9}$$

Dans ces équations $\Omega\subset\mathbb{R}^2$ est un ensemble ouvert et non vide de $\mathbb{R}^2$ et $\mathcal{O}$ est un sous-ensemble ouvert de Ω. On designe $\chi_{\mathcal{O}}$ la fonction caractéristique de l'ensemble $\mathcal{O}$. Plus précisément, nous avons prouvé la contrôlabilité exacte locale du système (0.7)-(0.9) en deux étapes :

- dans une première étape, on prouve la contrôlabilité exacte de la partie linéaire du système en utilisant le même genre d'arguments qu'au Chapitre 2 ;
- pour la partie non linéaire, on applique une méthode de point fixe, afin d'obtenir la contrôlabilité exacte locale de l'équation (0.7)-(0.9), en gardant le même temps de contrôlabilité que pour l'équation linéarisée.

Le Chapitre 4 est dédié à une nouvelle méthode d'approximation numérique des contrôles exactes pour les équations différentielles de la forme

$$\ddot{q}(t) + A_0 q(t) + B_0 u(t) = 0 \qquad (t\geqslant 0), \tag{0.10}$$

$$q(0) = q_0,\ \dot{q}(0) = q_1. \tag{0.11}$$

Avec de bonnes hypothèses sur les opérateurs A_0 et B_0, qu'on ne détaille pas pour le moment, et supposant que (0.10)-(0.11) est exactement observable, on prouve des estimations précise pour l'erreur commise en l'approximant le contrôle u avec des contrôles

finis dimensionnels. Dans ce cadre abstrait, on obtient des résultats pour l'approximation des contrôles pour l'équation des ondes et pour l'équation des plaques. Ces résultats sont ilustrés par des simulations numériques.

Le Chapitre 5 est une breve introduction à l'imagerie par résonance magnétique. Dans une première partie de ce chapitre, on décrit le principe physique de l'obtention des images par IRM. La deuxième partie du chapitre évoque la problématique de l'imagerie par résonance magnétique des objets en mouvement, en donnant l'exemple de l'imagerie cardiaque et de l'imagerie cardiaque en respiration libre.

Dans le Chapitre 6 on donne une méthode, assez différente du reste de la thèse, mais très efficace, pour la reconstruction d'images cardiaques à partir de données enregistrées en respiration libre. Cette méthode réduit la reconstruction des images pour toute phase cardiaque et respiratoire à la résolution d'un problème des moments dans un espace de Hilbert. Ce genre de problèmes des moments intervient aussi dans la théorie du contrôle des systèmes distribués (voir, par exemple, le livre de Avdonin et Ivanov [6]).

Notre méthode de reconstruction utilise les propriétés des espaces de Hilbert à noyau reproductif et a été validée par des tests effectués sur des données cliniques de cinq sujets sains et sur des données simulées.

Le dernier chapitre de cette thèse montre un exemple de reconstruction d'un terme source dans un système dynamique à partir d'une observation correspondante aux données enregistrées par un appareil IRM.

Plus précisément, on considère une équation des ondes en dimension deux et on prend comme sortie la restriction de la transformée de Fourier sur un ouvert de $\mathbb{R}^2$. Utilisant une variante de la méthode numérique présentée au Chapitre 4 pour la reconstruction des contrôles, on arrive reconstruire très précisément les termes source dans l'équation des ondes. On présente les résultats des simulations numériques associées, ainsi qu'un premier test d'une expérience sur la visualisation des ondes de surface dans un bac avec une faible épaisseur d'eau, par l'intermèdiaire de données enregistrées par un appareil IRM.

Dans la suite de cette introduction, nous présentons plus précisément le contenu de chaque chapitre.

Partie I : Contrôlabilité et observabilité de quelques équations des plaques

Dans cette partie de la thèse on étudie l'observabilité exacte et la contrôlabilité exacte des deux modèles mathématiques des plaques vibrantes en donnant une méthode numérique pour l'approximation des contrôles exacte pour une classe d'équations d'ordre deux en temps.

Chapitre 1 : Rappels sur la contrôlabilité et l'observabilité des systèmes de dimension infinie

Dans ce chapitre on rappelle quelques notions et résultats concernant la contrôlabilité exacte et l'observabilité exacte des systèmes inifini-dimensionnels. La majorité de ces résultats est donnée ici sans preuves et on renvoie le lecteur vers les références précises où les preuves se trouvent.

On suppose que le lecteur est familier avec la théorie des semi-groupes telle qu'elle est décrite dans le livre de Pazy [59]. On adopte les notations de la monographie "Observation and Control for Operator Semigroups" de Tucsnak et Weiss [80].

Tout au long de la première partie de la thèse X, Y et U sont des espaces de Hilbert identifiés avec leurs duals. Soit $A : \mathcal{D}(A) \to X$ un opérateur de domaine dense engendrant un semigroupe C_0 noté $(\mathbb{T}_t)_{t\geqslant 0}$. C'est facile à prouver que l'ensemble resolvente de l'opérateur A, noté dans la suite $\rho(A)$, est non-vide. Pour commencer nous allons rappeler un premier résultat d'analyse fonctionnelle (pour une preuve voir [80, Proposition 2.10.3]).

Proposition 0.4. *Soit $\beta \in \rho(A)$ et soit $X_1 = \mathcal{D}(A)$ avec la norme de graphe et soit X_{-1} l'espace X complété par rapport à la norme*

$$\|z\|_{-1} = \|(\beta I - A)^{-1} z\|_X, \qquad (z \in X).$$

Alors $A \in \mathcal{L}(X_1, X)$ et A a une unique extension à un opérateur de $\mathcal{L}(X, X_{-1})$, que l'on notera également par A. De plus,

$$(\beta I - A)^{-1} \in \mathcal{L}(X, X_1), \qquad (\beta I - A)^{-1} \in \mathcal{L}(X_{-1}, X)$$

et ces opérateurs sont unitaires.

Dans la suite on note par X_1 l'espace $\mathcal{D}(A)$ doté de la norme $\|\cdot\|_1$ avec un $\beta \in \rho(A)$ fixé, et par X_{-1} l'espace X complété par rapport à la norme $\|\cdot\|_{-1}$. La restriction de $\mathbb{T}_t$ à X_1 est l'image de $\mathbb{T}_t \in \mathcal{L}(X)$ par l'opérateur $(\beta I - A)^{-1} \in \mathcal{L}(X, X_1)$. Ainsi, ces opérateurs forment un semi-groupe fortement continu en X_1 engendré par la restriction de l'opérateur A à $\mathcal{D}(A^2)$. Les images de $\mathbb{T}_t \in \mathcal{L}(X)$ par l'opérateur $\beta I - A \in \mathcal{L}(X, X_{-1})$ forment un semi-groupe fortement continu engendré par l'extension de A à X_{-1}. La construction des espaces X_1 et X_{-1} peut être itérée, dans les deux directions, pour obtenir une suite infinie d'espaces

$$\cdots \subset X_2 \subset X_1 \subset X \subset X_{-1} \subset X_{-2} \subset \cdots$$

toutes les inclusions étant denses et continues.

Soit $B \in \mathcal{L}(U, X)$ un opérateur de contrôle. On considère l'équation suivante :

$$\dot{z}(t) = Az(t) + Bu(t), \qquad z(0) = z_0. \tag{0.12}$$

Il est bien connu que si $u \in L^2([0,\tau];U)$ et $z_0 \in X_1$ alors la solution z de (0.12) vérifie

$$z \in C^1([0,\tau];X) \cap C([0,\tau];X_1)$$

et $z(\tau)$ est donnée par

$$z(\tau) = \mathbb{T}_\tau z_0 + \Phi_\tau u,$$

où $\Phi_\tau \in \mathcal{L}(L^2([0,\tau];U),X)$,

$$\Phi_\tau u = \int_0^\tau \mathbb{T}_{\tau-t} B u(t)\ \mathrm{d}t.$$

La contrôlabilité exacte en temps τ de l'équation (0.12), introduite dans la Définition 0.2, revient à montrer que Im $\Phi_\tau = X$. Pour tout $\tau > 0$ on définit le Grammien de contrôlabilité $R_\tau \in \mathcal{L}(X)$ par

$$R_\tau = \Phi_\tau \Phi_\tau^*.$$

Alors, (A,B) est exactement contrôlable en temps τ si et seulement si R_τ est inversible. La proposition suivante donne une construction explicite du contrôle de norme minimale qui mène la solution de (0.12) de 0 à z_0 en temps τ.

Proposition 0.5. *On suppose que (A,B) est exactement contrôlable en temps τ. Alors il existe un opérateur $F_\tau \in \mathcal{L}(X, L^2([0,\tau];U))$ tel que :*

1. $\Phi_\tau F_\tau = \mathbb{I}_X$;
2. *Si u est un contrôle qui mène de 0 à z_0 la solution de (0.12) en temps τ, alors*

$$\|u\|_{L^2([0,\tau];U)} \geqslant \|F_\tau z_0\|_{L^2([0,\tau];U)}.$$

De plus, F_τ admet l'expression suivante :

$$F_\tau z_0 = \Phi_\tau^* R_\tau^{-1} z_0, \qquad (z_0 \in X).$$

Dans la partie qui reste du Chapitre 1 on donne deux résultats très utiles sur l'observabilité exacte et on rappelle quelques notions et résultats sur les séries de Fourier non-harmoniques.

Le résultat suivant est une conséquence d'un résultat de contrôlabilité simultanée (voir Tucsnak and Weiss [78] ou [80, Proposition 6.4.4]).

Proposition 0.6. *Soit $A : \mathcal{D}(A) \to X$ un opérateur tel qu'il existe une base orthonormale $(\phi_k)_{k\in\mathbb{N}}$ de X formée par les vecteurs propres de A, dont les valeurs propres associés λ_k satisfont $\lim_{k\to\infty} |\lambda_k| = \infty$ et soit $(\mathbb{T}_t)_{t\geqslant 0}$ le semi-groupe engendré par A. Soit $C \in \mathcal{L}(X,Y)$ un opérateur d'observation. Pour un ensemble $J \subset \mathbb{C}$ borné, on note*

$$V = span\{\phi_k \,|\, \lambda_k \in J\}^\perp$$

et soit A_V la restriction de A à $\mathcal{D}(A) \cap V$ considérée comme opérateur sur V. Soit C_V la restriction de C à $\mathcal{D}(A_V)$ et supposons que (A_V, C_V) est exactement observable en temps τ_0 et, de plus, que $C\Psi \neq 0$ pour tout vecteur propre Ψ de A. Alors (A,C) est exactement observable en tout temps $\tau > \tau_0$.

Une partie importante de cette thèse est dédiée à l'étude de l'observabilité interne et, par dualité, de la contrôlabilité interne exacte des systèmes vibrants. Dans ce but, on considère des systèmes de la forme :

$$\dot{z}(t) = Az(t), \qquad z(0) = z_0 \tag{0.13}$$
$$y(t) = Cz(t), \tag{0.14}$$

où $A : \mathcal{D}(A) \to X$ est un opérateur non-borné anti-adjoint dont les resolventes sont compactes et $C \in \mathcal{L}(X, Y)$. Le spectre de l'opérateur A est concentré sur l'axe imaginaire et est formé par ses valeurs propres $(i\mu_n)_{n\in\mathbb{Z}^*}$, avec $\mu_n \in \mathbb{R}$. Les vecteurs propres associés à ces valeurs propres $(\Phi_n)_{n\in\mathbb{Z}^*}$ forment une base orthonormale en X. On définit alors le *paquet d'ondes de centre μ et de rayon $\rho > 0$* par la relation

$$z = \sum_{l\in J_\rho(\mu)} c_l \Phi_l,$$

où

$$J_\rho(\mu) = \{l \in \mathbb{Z}^* \text{ tel que } |\mu_l - \mu| < \rho\}. \tag{0.15}$$

Le théorème suivant est une caractérisation spectrale de l'observabilité exacte du système (0.13)-(0.14). Une première caractérisation spectrale de l'observabilité exacte des systèmes de la forme (0.13)-(0.14) a été donnée par Ramdani, Takahashi, Tenenbaum et Tucsnak [64] et améliorée au niveau de l'estimation des constantes par Ervedoza [25]. Le Théorème 0.7 est un cas particulier du résultat obtenu en [25], en donnant ici des meilleures estimations des constantes pour le cas d'opérateurs de contrôle bornés.

Théorème 0.7. *Soit $A : \mathcal{D}(A) \to X$ un opérateur anti-adjoint en X ayant des résolventes compactes et $C \in \mathcal{L}(X, Y)$. Alors le système* (0.13)-(0.14) *est exactement observable si et seulement si il existe $\rho > 0$ et $d > 0$ tels que tout paquet d'ondes*

$$z = \sum_{l\in J_\rho(\mu)} c_l \Phi_l,$$

de centre μ et de rayon ρ, satisfasse

$$d^2 \|z\|_X^2 \leqslant \|Cz\|_Y^2,$$

où J_ρ est défini par (0.15)*. De plus, si l'inégalité précédente est satisfaite, alors le système* (0.13)-(0.14) *est exactement observable en tout temps $\tau > \tau^*$, pour*

$$\tau^* = \frac{2e}{\rho}\left(\frac{(1 + ln(L))\pi}{4}\right)^{1+\frac{1}{ln(L)}},$$

où

$$L = \frac{\pi \|C\|_{\mathcal{L}(X,Y)}^2}{3d^2}$$

et la constante k_τ dans l'inégalité d'observabilité est donnée par

$$k_\tau = \frac{\pi d^2}{\rho}\left(1 - \left(\frac{T^*}{T}\right)^{2n^*-1}\right), \text{ où } n^* = \left[\frac{1}{2}(\ln(L) + 1)\right]. \tag{0.16}$$

A la fin de ce chapitre, on rappelle quelques résultats d'analyse non-harmonique, issus d'un papier de Kahane [40].

Soit $n \in \mathbb{N}^*$ et $\mathcal{I} \subset \mathbb{Z}$ un ensemble d'indices On dit que $\Lambda = (\lambda_m)_{m\in\mathcal{I}}$ est une *suite régulière* s'il existe une constante $\gamma > 0$ telle que

$$\inf_{\substack{m,l\in\mathcal{I}\\ m\neq l}} |\lambda_m - \lambda_l| = \gamma. \tag{0.17}$$

La notion d'ensemble associé à une suite régulière sera utile pour exprimer quelques inégalités d'observabilité en termes de séries de Fourier.

Définition 0.8. On dit que l'ensemble $D \subset \mathbb{R}^n$ est un domaine associé à la suite régulière $\Lambda = (\lambda_m)_{m\in\mathcal{I}} \subset \mathbb{R}^n$ s'il existe deux constantes $\delta_1, \delta_2 > 0$ telles que, pour toute suite de nombres complexes $(a_m)_{m\in\mathcal{I}}$, ayant un nombre fini des termes non-nuls, on a

$$\delta_2(D) \sum_{m\in\mathcal{I}} |a_m|^2 \leqslant \int_D \left| \sum_{m\in\mathcal{I}} a_m e^{i\lambda_m\cdot x} \right|^2 \, \mathrm{d}x \leqslant \delta_1(D) \sum_{m\in\mathcal{I}} |a_m|^2.$$

La proposition suivante (voir [40, Proposition III.1.2]) est un équivalent $n-$dimensionnel du théorème d'Ingham [36].

Proposition 0.9. *Soit $\Lambda = (\lambda_m)_{m\in\mathcal{I}} \subset \mathbb{R}^n$ une suite régulière satisfaisant* (0.17)*. Alors il existe une constante positive α (α ne dépendant que de n) telle que toute boule de $\mathbb{R}^n$ de rayon $\frac{\alpha}{\gamma}$ est un domaine associé à Λ.*

Une notion utile dans le traitement des perturbations est celle de *suites asymptotiquement proches.*

Définition 0.10. Soit $\Lambda = (\lambda_m)_{m\in\mathcal{I}}$ et $\tilde{\Lambda} = (\tilde{\lambda}_m)_{m\in\mathcal{I}}$ deux suites régulières de $\mathbb{R}^n$. On dit que les suite Λ et $\tilde{\Lambda}$ sont asymptotiquement proches si pour tout $\alpha > 0$ il existe une boule ouverte $B \subset \mathbb{R}^n$ assez grande, telle que

$$|\lambda_m - \tilde{\lambda}_m| < \alpha \qquad (m \in \mathcal{I} \text{ tel que } \lambda_m, \tilde{\lambda}_m \in \mathbb{R}^n \setminus B).$$

Le théorème suivant dit que les suites qui sont asymptotiquement proches ont les mêmes domaines associés.

Théorème 0.11. *Soit $\Lambda = (\lambda_m)_{m\in\mathcal{I}}$ et $\tilde{\Lambda} = (\tilde{\lambda}_m)_{m\in\mathcal{I}}$ deux suites régulières asymptotiquement proches. Alors tout ensemble ouvert $D \subset \mathbb{R}^n$ est un domaine associé à Λ si et seulement si il est associé à $\tilde{\Lambda}$.*

Chapitre 2 : L'observabilité exacte interne d'une équation des plaques perturbée

Dans ce chapitre on étudie l'observabilité exacte interne d'une équation des plaques linéaire perturbée. Plus précisément, on prouve que l'observabilité exacte de l'équation

des plaques d'Euler-Bernoulli implique l'observabilité de l'équation d'Euler-Bernoulli perturbée avec des termes linéaires d'ordre inférieur.

Une grande partie de ce chapitre a été publiée dans Cîndea et Tucsnak [18].

Soit $\Omega \subset \mathbb{R}^n$ ($n \in \mathbb{N}^*$) un ensemble ouvert et non vide avec une frontière de classe C^2 ou un rectangle. On considère le système suivant :

$$\ddot{w}(x,t) + \Delta^2 w(x,t) - a\Delta w(x,t) + b(x)\cdot\nabla w(x,t) + c(x)w(x,t) = 0, \quad \Omega\times(0,\infty) \tag{0.18}$$

$$w(x,t) = \Delta w(x,t) = 0, \quad (x,t) \in \partial\Omega \times (0,\infty) \tag{0.19}$$

$$w(x,0) = w_0(x), \quad \dot{w}(x,0) = w_1(x), \quad x \in \Omega, \tag{0.20}$$

avec $a > 0$, $b \in (L^\infty(\Omega))^n$, $c \in L^\infty(\Omega)$, $w_0 \in H^2(\Omega)\cap H_0^1(\Omega)$ et $w_1 \in L^2(\Omega)$. On considère la sortie suivante

$$y(t) = \dot{w}(\cdot,t)|_{\mathcal{O}}, \tag{0.21}$$

où $\mathcal{O}$ est un ouvert non vide de Ω. Pour $n = 2$ le système (0.18)-(0.21) modélise les vibrations d'une plaque posée sur la frontière.

Le but de ce chapitre est d'étudier l'observabilité exacte du système (0.18)-(0.21) par rapport à l'observabilité exacte de l'équation d'Euler-Bernoulli non perturbée, c'est-à-dire le système (0.18)-(0.21) avec $a = 0$, $b = 0$ et $c = 0$. Plus précisément, le résultat principal de ce chapitre est le théorème suivant :

Théorème 0.12. *Soit $\mathcal{O}$ un sous-ensemble ouvert et non vide de Ω tel que* (0.18)-(0.21) *est exactement observable pour $a = 0$, $b = 0$ et $c = 0$. Alors* (0.18)-(0.21) *est exactement observable pour tout $a > 0$, $b \in (L^\infty(\Omega))$, $c \in L^\infty(\Omega)$.*

Une condition nécessaire et suffisante pour l'observabilité exacte de l'équation des ondes est que la région d'observation doit satisfaire la condition d'optique géométrique de Bardos, Lebeau and Rauch [9]. Pour l'équation des plaques d'Euler-Bernoulli, la condition d'optique géométrique est seulement une condition suffisante pour l'observabilité exacte (voir, par exemple, Lebeau [46]). Si Ω est un rectangle, l'équation des plaques d'Euler-Bernoulli est exactement observable dans un temps arbitrairement petit pour tout sous-ensemble ouvert $\mathcal{O}$ de Ω (voir, Jaffard [38] ou Komornik [42]). Ce résultat reste valable pour l'équation des plaques (0.18)-(0.21).

Théorème 0.13. *Supposons $n = 2$, Ω un rectangle et soit $\mathcal{O}$ un sous-ensemble ouvert et non vide de Ω. Alors* (0.18)-(0.21) *est exactement observable pour tout $a > 0$, $b \in (L^2(\Omega))^n$ et $c \in L^\infty(\Omega)$ en tout temps $\tau > 0$.*

Pour prouver ces deux théorèmes nous utilisons une formulation abstraite de notre problème d'observabilité. Soit H un espace de Hilbert muni de la norme $\|\cdot\|_H$ et $A_0 : \mathcal{D}(A_0) \to H$ un opérateur auto-adjoint, positif et inversible dont les résolventes sont compactes. Alors, l'opérateur A_0 est diagonalisable dans une base $(\varphi_k)_{k\geqslant 1}$ de vecteurs propres et les valeurs propres associées $(\lambda_k)_{k\geqslant 1}$ satisfont $\lim_{k\to\infty}\lambda_k = \infty$. De plus, on a

$$\mathcal{D}(A_0) = \left\{ z \in H \;\middle|\; \sum_{k\geqslant 1} \lambda_k^2 \left|\langle z, \varphi_k\rangle\right|^2 < \infty \right\},$$

et

$$A_0 z = \sum_{k \geqslant 1} \lambda_k \langle z, \varphi_k \rangle \varphi_k \qquad (z \in \mathcal{D}(A_0)).$$

Pour $\alpha \geqslant 0$, l'opérateur A_0^α est défini par

$$\mathcal{D}(A_0^\alpha) = \left\{ z \in H \;\middle|\; \sum_{k \geqslant 1} \lambda_k^{2\alpha} |\langle z, \varphi_k \rangle|^2 < \infty \right\},$$

et

$$A_0^\alpha z = \sum_{k \geqslant 1} \lambda_k^\alpha \langle z, \varphi_k \rangle \varphi_k \qquad (z \in \mathcal{D}(A_0^\alpha)).$$

Pour tout $\alpha \geqslant 0$, on note H_α l'espace $\mathcal{D}(A_0^\alpha)$ muni du produit scalaire

$$\langle \varphi, \psi \rangle_\alpha = \langle A_0^\alpha \varphi, A_0^\alpha \psi \rangle \qquad (\varphi,\ \psi \in H_\alpha)$$

et $H_{-\alpha}$ est l'espace dual de H_α par rapport à l'espace pivot H. La norme induite par ce produit scalaire est notée $\| \cdot \|_\alpha$. Alors, pour tout $\alpha \geqslant 0$, l'opérateur A_0 est unitaire de $H_{\alpha+1}$ dans H_α et A_0 est défini strictement positif dans H_α.

On considère le système suivant d'ordre deux :

$$\ddot{w}(t) + A_0^2 w(t) = 0, \tag{0.22}$$

$$w(0) = w_0, \qquad \dot{w}(0) = w_1 \tag{0.23}$$

et l'observation

$$y(t) = C_0 \dot{w}(t). \tag{0.24}$$

Dans une première étape, en utilisant la caractérisation spectrale donnée par le Théorème 0.7, on prouve que l'observabilité exacte de (0.22)-(0.24) implique l'observabilité du système suivant

$$\ddot{v}(t) + A_0^2 v(t) + a A_0 v(t) = 0 \tag{0.25}$$

$$v(0) = v_0, \qquad \dot{v}(0) = v_1 \tag{0.26}$$

par rapport à la même observation et pour tout $a > 0$.

Théorème 0.14. *Supposons que le système* (0.22)-(0.24) *est exactement observable, c'est-à-dire il existe $T > 0$ et $k_T > 0$ tels que*

$$\int_0^T \|C_0 \dot{w}(t)\|_Y^2 \, dt \geqslant k_T^2 \left(\|w_0\|_{H_1}^2 + \|w_1\|_H^2 \right), \qquad \left(\begin{bmatrix} w_0 \\ w_1 \end{bmatrix} \in H_2 \times H_1 \right). \tag{0.27}$$

Alors le système (0.25)-(0.26) *est exactement observable par rapport à l'observation* (0.24)*, c'est-à-dire il existe un temps $\tau > 0$ et une constante k_τ positive tel que toute solution de* (0.25)-(0.26) *satisfasse*

$$\int_0^\tau \|C_0 \dot{v}(t)\|_Y^2 \, dt \geqslant k_\tau^2 \left(\|v_0\|_{H_1}^2 + \|v_1\|_H^2 \right), \qquad \left(\begin{bmatrix} v_0 \\ v_1 \end{bmatrix} \in H_2 \times H_1 \right). \tag{0.28}$$

Dans la deuxième étape on prouve l'observabilité exacte du système

$$\ddot{v}(t) + \widetilde{A}_a^2 v(t) + P_0 v(t) = 0 \tag{0.29}$$
$$v(0) = v_0, \qquad \dot{v}(0) = v_1, \tag{0.30}$$

où $P_0 \in \mathcal{L}(H_{1-\varepsilon}, H)$, $\widetilde{A}_a^2 = A_0^2 + aA_0$ et $0 < \varepsilon < \frac{1}{2}$. Plus précisément, en utilisant une variante de la méthode compacité-unicité introduite par Bardos, Lebeau et Rauch [9], on prouve le théorème suivant :

Théorème 0.15. *Soit H un espace de Hilbert muni de la norme $\|\cdot\|_H$, soit $A_0 : \mathcal{D}(A_0) \to H$ un opérateur autoadjoint, positif et inversible dont les résolventes sont compactes et $P_0 \in \mathcal{L}(H_{1-\varepsilon}, H)$ avec $0 < \varepsilon < \frac{1}{2}$. Si*

(i) (0.22)-(0.24) *est exactement observable, c'est-à-dire q'il existe $\tau > 0$ et $k_\tau > 0$ tels que*

$$\int_0^\tau \|C_0 \dot{w}(t)\|_Y^2 \, dt \geqslant k_\tau^2 \left(\|w_0\|_{H_1}^2 + \|w_1\|_H^2 \right), \qquad \left(\begin{bmatrix} w_0 \\ w_1 \end{bmatrix} \in H_2 \times H_1 \right);$$

(ii) $C_0 \phi \neq 0$ *pour tout vecteur propre ϕ de $\widetilde{A}_a^2 + P_0$,*

alors (0.29)-(0.30) *est exactement observable en tout temps $T > \tau$, c'est à dire q'il existe $k_T > 0$ telle que toute solution v de* (0.29)-(0.30) *vérifie*

$$\int_0^T \|C_0 \dot{v}(t)\|_Y^2 \, dt \geqslant k_T^2 \left(\|v_0\|_{H_1}^2 + \|v_1\|_H^2 \right), \qquad \left(\begin{bmatrix} v_0 \\ v_1 \end{bmatrix} \in H_2 \times H_1 \right).$$

Une fois prouvés ces deux théorèmes abstraits, pour démontrer l'observabilité de l'équation des plaques perturbée on prend $H = L^2(\Omega)$, $Y = L^2(\mathcal{O})$ et $A_0 : H_1 \to H$, $C_0 \in \mathcal{L}(H, Y)$

$$H_1 = H^2(\Omega) \cap H_0^1(\Omega), \qquad A_0 \varphi = -\Delta \varphi, \qquad (\varphi \in H_1),$$

$$C_0 \varphi = \varphi|_{\mathcal{O}}, \qquad (\varphi \in H).$$

Nous définissons aussi les opérateurs $\widetilde{A}_a : H_1 \to H$

$$\widetilde{A}_a \varphi = (\Delta^2 - a\Delta)^{\frac{1}{2}} \varphi, \qquad (\varphi \in H_1)$$

et $P_0 \in \mathcal{L}(H_{1-\varepsilon}, H)$

$$P_0 \varphi = b \cdot \nabla \varphi + c\varphi, \qquad (\varphi \in H_{1-\varepsilon}).$$

Le Théorème 0.14 nous dit que si (A_0^2, C_0) est exactement observable (autrement dit (0.22)-(0.24) est exactement observable) en temps T alors $(\widetilde{A}_a^2, C_0)$ est exactement observable (autrement dit (0.25)-(0.26) est exactement observable) en temps $T > \tau$. Dans les applications pour vérifier la consdition *(ii)* de Théorème 0.15 nous utilisons l'estimation de Carleman suivante :

Théorème 0.16. *Avec les notations précédentes, soit $\psi \in \mathcal{C}^2(\Omega)$ une fonction telle que*

$$\begin{aligned} \psi &= 0, \qquad \text{sur } \partial\Omega \\ \psi(x) &> 0, \qquad \forall\, x \in \Omega \\ |\nabla\psi(x)| &> 0, \quad \forall\, x \in \overline{\Omega \setminus \mathcal{O}} \end{aligned}$$

et soit $\varphi(x) = e^{\lambda\psi(x)}$ pour tout $x \in \Omega$ et $\lambda \geqslant 1$. Soit u la solution du problème suivant :

$$\begin{aligned} \Delta^2 u - a\Delta u + b\cdot\nabla u + cu &= \mu^2 u \quad \text{dans } \Omega \\ u = \Delta u &= 0 \quad \text{sur } \partial\Omega. \end{aligned}$$

Alors il existe $\hat{s} > 1$, $\hat{\lambda} > 1$ et une constante $C > 0$ indépendante de $s \geqslant \hat{s}$ et $\lambda > \hat{\lambda}$, tel que

$$\begin{aligned} s\lambda^2 \int_\Omega \left(|\nabla(\Delta u)|^2 + s^3\lambda^4|\nabla u|^2 + s^5\lambda^6|u|^2\varphi^2\right) e^{2s\varphi}\mathrm{d}x \leqslant C \Bigg(\int_\Omega \frac{|g|^2}{\varphi} e^{2s\varphi}\mathrm{d}x \\ + s\lambda^2 \int_{\mathcal{O}} (|\nabla(\Delta u)|^2 + s^2\lambda^2\varphi^2|\Delta u|^2 + s^3\lambda^4|\nabla u|^2 + s^5\lambda^6\varphi^2|u|^2) e^{2s\varphi}\mathrm{d}x \Bigg). \end{aligned}$$

Ce théorème nous donne le résultat d'unicité du prolongement nécessaire pour l'application du Théorème 0.15. On obtient l'observabilité de $(A_a^2 + P_0, C_0)$, ce qui permet d'achever la preuve du Théorème 0.12. Pour prouver le Théorème 0.13, il suffit d'utiliser une méthode spectrale pour obtenir un temps arbitrairement petit pour l'observabilité exacte de (0.25)-(0.26).

Chapitre 3 : La contrôlabilité exacte locale de l'équation de Berger

Dans ce chapitre on étudie le problème de la contrôlabilité exacte interne d'un système des plaques non linéaire. Le résultat principal de ce chapitre est que si l'équation des plaques d'Euler-Bernoulli est exactement contrôlable alors ce système est aussi exactement contrôlable.

Ce chapitre fait l'objet d'un article publié en collaboration avec Marius Tucsnak [19].

Ces derniers décennies, une littérature riche a été consacrée à la contrôlabilité exacte des différentes équations linéaires qui modélisent les vibrations de plaques élastiques (voir, par exemple, Zuazua [87], Lasiecka and Triggiani [45], Jaffard [38]). Un des modèles le plus étudié est le modèle d'Euler-Bernoulli avec contrôle distribué, c'est-à-dire le système suivant :

$$\ddot{w}(x,t) + \Delta^2 w(x,t) = u(x,t)\chi_{\mathcal{O}} \qquad (x,t) \in \Omega \times (0,\infty), \tag{0.31}$$

$$w(x,t) = \Delta w(x,t) = 0 \qquad (x,t) \in \partial\Omega \times (0,\infty), \tag{0.32}$$

$$w(x,0) = \dot{w}(x,0) = 0 \qquad x \in \Omega. \tag{0.33}$$

Dans ces équations, $\Omega \subset \mathbb{R}^2$ est un ensemble ouvert et non vide et $\mathcal{O}$ est un sous-ensemble ouvert et non vide de Ω. Le contrôle, noté $u \in L^2([0,\infty); U)$ est prolongé par zéro à l'extérieur de $\mathcal{O}$, et $\chi_{\mathcal{O}}$ est la fonction caractéristique de $\mathcal{O}$.

Une condition suffisante pour la contrôlabilité exacte de (0.31)-(0.33) est que Ω et $\mathcal{O}$ doivent satisfaire la condition d'optique géométrique de Bardos, Lebeau et Rauch [9]. Ce résultat a été initialement prouvé par Lebeau [46] utilisant l'analyse microlocale. La preuve a été successivement simplifiée par Miller [52] et par Tucsnak et Weiss [80, Exemple 11.2.4]. La condition d'optique géométrique n'est pas une condition nécessaire pour la contrôlabilité de (0.31)-(0.33). Dans [38] Jaffard prouve que si Ω est un rectangle (0.31)-(0.33) est exactement contrôlable pour tout ouvert non vide $\mathcal{O} \subset \Omega$. Des situations plus compliquées pour lesquelles la condition d'optique géométrique n'est pas satisfaite bien que (0.31)-(0.33) soit exactement contrôlable ont été étudiés dans Burq et Zworski [14].

Le but de ce chapitre est d'étudier la contrôlabilité exacte locale d'un système modélisant les vibrations non linéaires de plaques élastiques. Le modèle, proposé par Berger [10] est équivalent dans un espace unidimensionnel avec les équations de Von Karman (voir Perla Menzala et Zuazua [51]). Dans le cas bidimensionnel le système peut être considéré comme la limite asymptotique du modèle de Von Karman (voir Perla Menzala, Pazoto et Zuazua [60], Nayfeh et Mook [54]).

Le modèle de Berger pour une plaque élastique remplissant le domaine Ω est formalisé par le système suivant

$$\ddot{w}(x,t) + \Delta^2 w(x,t) - \left(a + b\int_\Omega |\nabla w|^2 \, \mathrm{d}x\right)\Delta w(x,t) = u(x,t)\chi_{\mathcal{O}}, \quad \Omega \times (0,\infty), \tag{0.34}$$

$$w(x,t) = \Delta w(x,t) = 0, \qquad (x,t) \in \partial\Omega \times (0,\infty), \tag{0.35}$$

$$w(x,0) = \dot{w}(x,0) = 0, \qquad x \in \Omega. \tag{0.36}$$

La constante a est plus grande que $-\lambda_1$, avec λ_1 la première valeur propre du Laplacien Dirichlet en Ω, et correspond à une compression ($a > 0$) ou à une dilatation ($a < 0$) plane de la plaque élastique. La constante b est supposée positive.

Le résultat principal de ce chapitre est le théorème suivant :

Théorème 0.17. *Soit $\Omega \subset \mathbb{R}^2$ un ensemble ouvert et borné ayant une frontière de classe C^2 et soit $\mathcal{O} \subset \Omega$ un sous-ensemble ouvert et non vide de Ω tel que* (0.31)-(0.33) *est exactement contrôlable (en un certain temps $\tau_0 > 0$). Alors le système* (0.35)-(0.36) *est localement exactement contrôlable, c'est-à-dire, qu'il existe un temps $\tau > 0$ et $M > 0$ tels que pour tout $\left[\begin{smallmatrix} w_0 \\ w_1 \end{smallmatrix}\right] \in (H^2(\Omega) \cap H_0^1(\Omega)) \times L^2(\Omega)$ satisfaisant*

$$\|w_0\|^2_{H^2(\Omega)} + \|w_1\|^2_{L^2(\Omega)} \leqslant M^2,$$

il existe $u \in L^2([0,\tau]; L^2(\mathcal{O}))$ tel que la solution de (0.35)-(0.36) *vérifie*

$$w(\cdot,\tau) = w_0, \qquad \dot{w}(\cdot,\tau) = w_1.$$

La partie la plus intéressante du Théorème 0.17 est que, étant un résultat de perturbation, il repose seulement sur la contrôlabilité de l'équation des plaques d'Euler-Bernoulli (0.31)-(0.33) qui a beaucoup été étudiée. Observons que (0.31)-(0.33) n'est

pas la linéarisation de (0.35)-(0.36) autour de zéro. Notre argument de perturbation est divisé en deux étapes : premièrement on traite le cas $b = 0$ en utilisant des techniques spectrales, puis on passe à l'équation non linéaire par un argument de point fixe. Le seul problème est qu'on n'obtient pas un temps de contrôlabilité arbitrairement petit. Le deuxième résultat de ce chapitre va donner un temps arbitrairement petit pour la contrôlabilité locale exacte de l'équation de Berger (0.35)-(0.36) si Ω est un rectangle.

Théorème 0.18. *Soit $\Omega \subset \mathbb{R}^2$ et soit $\mathcal{O}$ un sous-ensemble ouvert et non vide de Ω. Alors* (0.35)-(0.36) *est localement exactement contrôlable en tout temps $\tau > 0$. Autrement dit, pour tout $\tau > 0$ il existe une constante $M > 0$ telle que pour tout $\left[\begin{smallmatrix} w_0 \\ w_1 \end{smallmatrix}\right] \in (H^2(\Omega) \cap H_0^1(\Omega)) \times L^2(\Omega)$, satisfaisant*

$$\|w_0\|^2_{H^2(\Omega)} + \|w_1\|^2_{L^2(\Omega)} \leqslant M^2,$$

il existe $u \in L^2([0,\tau]; L^2(\mathcal{O}))$ tel que la solution de (0.35)-(0.36) *vérifie*

$$w(\cdot,\tau) = w_0, \qquad \dot{w}(\cdot,\tau) = w_1.$$

Chapitre 4 : Une méthode d'approximation pour les contrôles exacts des systèmes vibrants

On propose une nouvelle méthode pour l'approximation des contrôles exacts des systèmes infinis dimensionnels d'ordre deux avec des opérateurs de contrôle bornés. L'algorithme combine le principe de Russell "stabilité implique contrôlabilité" et la méthode de Galerkin. La principale nouveauté de cette approche est l'obtention d'estimations d'erreur assez précises. Pour illustrer l'efficacité de cette méthode, on considère deux exemples, concernant l'équation des ondes et l'équation des poutres, et on décrit les simulations numériques associées.

Ce chapitre est un travail en collaboration avec Sorin Micu et Marius Tucsnak et fait l'objet d'un article soumis [16].

L'étude numérique des contrôles exacts pour les systèmes infini-dimensionnels a commencé dans les années '90 par une série d'articles de Glowinski et Lions (voir [31, 32]) où ils donnent des algorithmes pour déterminer les contrôles exactes de norme L^2 minimale (les contrôles HUM). Plusieurs anormalités apparues dans ces travaux sont à l'origine d'un grand nombre de papiers, dans lequel sont présentés et analysés des nombreuses méthodes numériques pour l'approximation des contrôles (voir, par exemple, [88], [27] ainse que leur références). A notre connaissance, avec l'exception du travail [26] où des approximations des contrôles HUM pour l'équations des ondes unidimensionnelle sont données, il n'existe pas de résultats sur la vitesse de convergence des contrôles approximatifs.

Le but de ce chapitre est de donner une méthode numérique efficace pour le calcul des contrôles exacts pour une classe de systèmes infinis-dimensionnels modélisant les vibrations élastiques. Notre résultat principal donne la vitesse de convergence de

nos approximations vers un contrôle exact. Pour illustrer l'efficacité de cette approche, nous l'avons appliquée à quelques systèmes gouvernés par des EDP et nous avons décrit les simulations numériques associées. Notre méthodologie combine le principe de Russell "stabilité implique contrôlabilité" avec les estimations d'erreur pour les approximations obtenues par la méthode des éléments finis pour les systèmes infinis-dimensionnels considérés. On se concentre sur les opérateurs de contrôle bornés, mais notre méthode peut être partiellement étendue aus cas d'opérateurs de contrôle non bornés.

Pour donner une formulation précise de nos résultats, nous avons besoin d'introduire au préalable quelques notations. Soit H un espace de Hilbert et soit $A_0 : \mathcal{D}(A_0) \to H$ un opérateur auto-adjoint, strictement positif défini dont les résolventes sont compactes. Dans la suite, on utilise la famille des espaces H_α est les puissances de l'opérateur A_0 introduites dans le Chapitre 2.

Soit U un autre espace de Hilbert et soit $B_0 \in \mathcal{L}(U, H)$ un opérateur de contrôle. On considère le système :

$$\ddot{q}(t) + A_0 q(t) + B_0 u(t) = 0 \qquad (t \geqslant 0), \tag{0.37}$$

$$q(0) = q_0,\ \dot{q}(0) = q_1. \tag{0.38}$$

Le système (0.37)-(0.38) est dit *exactement contrôlable en temps* $\tau > 0$ si pour tout $q_0 \in H_{\frac{1}{2}}$ et $q_1 \in H$ il existe un contrôle $u \in L^2([0,\tau]; U)$ tel que $q(\tau) = \dot{q}(\tau) = 0$. Pour donner une méthode d'approximation d'un tel contrôle u, nous avons besoin d'autres hypothèses et notations.

Supposons qu'il existe une famille $(V_h)_{h>0}$ de sous-espaces fini-dimensionnels de $H_{\frac{1}{2}}$ et qu'il existe $\theta > 0$, $h^* > 0$, $C_0 > 0$ tels que, pour tout $h \in (0, h^*)$

$$\|\pi_h \varphi - \varphi\|_{\frac{1}{2}} \leqslant C_0\, h^\theta \|\varphi\|_1 \qquad (\varphi \in H_1), \tag{0.39}$$

$$\|\pi_h \varphi - \varphi\| \leqslant C_0\, h^\theta \|\varphi\|_{\frac{1}{2}} \qquad (\varphi \in H_{\frac{1}{2}}), \tag{0.40}$$

où π_h est le projecteur orthogonal de $H_{\frac{1}{2}}$ sur V_h. Les relations (0.39)-(0.40) sont vérifiés quand la méthode des éléments finis est utilisée pour l'approximation des espaces de Sobolev. Le produit scalaire sur V_h est la restriction du produit scalaire sur H et est encore noté $\langle \cdot, \cdot \rangle$. On définit l'opérateur A_{0h} par :

$$\langle A_{0h}\varphi_h, \psi_h \rangle = \langle A_0^{\frac{1}{2}} \varphi_h, A_0^{\frac{1}{2}} \psi_h \rangle \qquad (\varphi_h,\ \psi_h \in V_h). \tag{0.41}$$

L'opérateur A_{0h} est clairement symétrique et défini strictement positif.

On note $U_h = B_0^* V_h \subset U$ et on définit les opérateurs $B_{0h} \in \mathcal{L}(U, H)$ par

$$B_{0h} u = \widetilde{\pi}_h B_0 u \qquad (u \in U), \tag{0.42}$$

où $\widetilde{\pi}_h$ est la projection orthonormale de H sur V_h. Remarquons que Im $B_{0h} \subset V_h$. Comme $\widetilde{\pi}_h$ est un projecteur, on obtient que $\widetilde{\pi}_h \in \mathcal{L}(H)$ est auto-adjoint. De plus, à partir de (0.40), on obtient

$$\|\varphi - \widetilde{\pi}_h \varphi\| \leqslant \|\varphi - \pi_h \varphi\| \leqslant C_0\, h^\theta \|\varphi\|_{\frac{1}{2}} \qquad (\varphi \in H_{\frac{1}{2}}).$$

L'opérateur adjoint de B_{0h} est $B_{0h}^* \in \mathcal{L}(H, U)$:

$$B_{0h}^*\varphi = B_0^*\widetilde{\pi}_h\varphi \qquad (\varphi \in H).$$

Puisque $U_h = B_0^*V_h$ on obtient que Ran $B_{0h}^* = U_h$ et donc

$$\langle B_{0h}^*\varphi_h, B_{0h}^*\psi_h\rangle_U = \langle B_0^*\varphi_h, B_0^*\psi_h\rangle_U \qquad (\varphi_h,\ \psi_h \in V_h). \tag{0.43}$$

Sous les hypothèses précédentes, on a que pour tout $h^* > 0$ la famille $(\|B_{0h}\|_{\mathcal{L}(U,H)})_{h\in(0,h^*)}$ est bornée.

Dans la suite, on donne notre algorithme pour le calcul d'une approximation $u_h \in C([0,\tau];U_h)$ pour un contrôle exact $u \in C([0,\tau];U)$ qui conduit la solution de (0.37)-(0.38) de $\left[\begin{smallmatrix} q_0 \\ q_1 \end{smallmatrix}\right] \in H_1 \times H_{\frac{1}{2}}$ à 0 en temps τ. Pour tout $h > 0$ et $N(h) \in \mathbb{N}$ on considère le système d'équations différentielles ordinaires suivant :

$$\ddot{w}_h^n(t) + A_{0h}w_h^n(t) + B_{0h}B_{0h}^*\dot{w}_h^n(t) = 0 \qquad (t \geqslant 0) \tag{0.44}$$

$$w_h^n(0) = \begin{cases} \pi_h q_0, & \text{si } n = 1 \\ w_{b,h}^{n-1}(0), & \text{si } n > 1 \end{cases} \qquad \dot{w}_h^n(0) = \begin{cases} \pi_h q_1, & \text{si } n = 1 \\ \dot{w}_{b,h}^{n-1}(0), & \text{si } n > 1, \end{cases} \tag{0.45}$$

et

$$\ddot{w}_{b,h}^n(t) + A_{0h}w_{b,h}^n(t) - B_{0h}B_{0h}^*\dot{w}_{b,h}^n(t) = 0 \qquad (t \leqslant \tau) \tag{0.46}$$

$$w_{b,h}^n(\tau) = w_h^n(\tau), \qquad \dot{w}_{b,h}^n(\tau) = \dot{w}_h^n(\tau). \tag{0.47}$$

Pour tout $h > 0$ on choisit $N(h)$ et on pose

$$\begin{bmatrix} w_{0h} \\ w_{1h} \end{bmatrix} = \begin{bmatrix} \pi_h q_0 \\ \pi_h q_1 \end{bmatrix} + \sum_{n=1}^{N(h)} \begin{bmatrix} w_{b,h}^n(0) \\ \dot{w}_{b,h}^n(0) \end{bmatrix} \tag{0.48}$$

Avec ces notations, u_h est défini par

$$u_h = B_{0h}^*\dot{w}_h + B_{0h}^*\dot{w}_{b,h}, \tag{0.49}$$

où w_h et $w_{b,h}$ sont les solutions de

$$\ddot{w}_h(t) + A_{0h}w_h(t) + B_{0h}B_{0h}^*\dot{w}_h(t) = 0 \qquad (t \geqslant 0) \tag{0.50}$$

$$w_h(0) = w_{0h}, \quad \dot{w}_h(0) = w_{1h}, \tag{0.51}$$

$$\ddot{w}_{b,h}(t) + A_{0h}w_{b,h}(t) - B_{0h}B_{0h}^*\dot{w}_{b,h}(t) = 0 \qquad (t \leqslant \tau) \tag{0.52}$$

$$w_{b,h}(\tau) = w_h(\tau), \qquad \dot{w}_{b,h}(\tau) = \dot{w}_h(\tau). \tag{0.53}$$

Nous pouvons maintenant formuler le résultat principal de ce chapitre.

Théorème 0.19. *En plus des notations et hypothèses précédentes, on suppose que* (0.37)-(0.38) *est exactement observable et que* $B_0 B_0^* \in \mathcal{L}(H_1, H_{\frac{1}{2}})$. *Alors il existe une constante* m_τ *telle que pour tout* $Q_0 = \left[\begin{smallmatrix} q_0 \\ q_1 \end{smallmatrix}\right] \in H_{\frac{3}{2}} \times H_1$ *la suite* $(u_h)_{h\geqslant 0} \subset C([0,\tau]; U_h)$ *définie par* (0.49) *avec* $N(h) = [\theta m_\tau \ln(h^{-1})]$ *converges quand* $h \to 0$ *vers un contrôle exact de* (0.37)-(0.38)*, noté par* u. *De plus, il existe des constantes* $h^* > 0$ *et* $C := C_\tau > 0$ *telles que*

$$\|u - u_h\|_{C([0,\tau];U)} \leqslant C h^\theta \ln^2(h^{-1}) \|Q_0\|_{H_{\frac{3}{2}} \times H_1} \qquad (0 < h < h^*).$$

Pour illustrer l'efficacité de cette méthode nous l'avons appliquée afin de calculer des approximations des contrôles exacts pour l'équation des ondes et pour l'équation des poutres élastiques.

Partie II : Problèmes inverses en IRM

Cette deuxième partie est centrée sur les problèmes inverses provenant de l'imagerie par résonance magnétique des objets en mouvement.

Chapitre 5 : Introduction à l'imagerie par résonance magnétique

Dans ce chapitre on présente quelques notions d'imagerie par résonance magnétique (IRM) nécessaires à la compréhension de cette partie de la thèse.

Dans la première section du chapitre nous expliquons les bases physiques de l'IRM, en passant rapidement de la résonance des spins à l'équation du signal IRM et à la formation des images. Dans la deuxième section, on discute la problématique du mouvement pendant l'acquisition du signal IRM, en s'intéressant principalement à l'imagerie cardiaque.

Les bases physiques de l'imagerie par résonance magnétique

Cette section est une breve introduction à la physique de l'imagerie par résonance magnétique. Le lecteur intéressé pourra se référer à la monographie Haacke et al [33].

La résonance magnétique est basée sur les propriétés magnétiques des noyaux atomiques, ou plus précisément, sur les propriétés des nucléons (les protons et les neutrons). Une notion qui décrit ces propriétés est la notion de spin, découverte par Pauli en 1924.

Le spin nucléaire $\overrightarrow{S}$ est une mesure du moment angulaire intrinsèque de la particule. Dans cette thèse nous allons considérer les spins $\frac{1}{2}$, pour lesquels on a besoin de deux nombres $a_{\pm\frac{1}{2}}$ qui donnent les amplitudes des projections des moments angulaires, égales à $\frac{\hbar}{2}$ et $-\frac{\hbar}{2}$. Les noyaux importants pour l'IRM (l'hydrogène ^1H par exemple) ont des spins $\frac{1}{2}$). Alors, dans ce cas, le noyau a deux états de spins possibles : $m = \frac{1}{2}$ ou $m = -\frac{1}{2}$. Ces états ont la même énergie, le nombre d'atomes dans ces deux états étant similaire.

La relation entre le moment angulaire $\overrightarrow{\mu}$ et le spin $\overrightarrow{S}$ est la suivante :

$$\overrightarrow{\mu}(p) = \gamma \overrightarrow{S}(p),$$

où γ est une constante caractéristique du noyau étudié et p est une certaine particule (proton).

S'il n'existe pas de champ magnétique externe, les spins sont orientés aléatoirement. Si un champ magnétique statique $\overrightarrow{B}_0$ est appliqué, tous les moments magnétiques s'orientent dans la direction de $\overrightarrow{B}_0$. L'évolution en temps du moment magnétique $\overrightarrow{\mu}(p)$ est donnée par l'équation suivante (l'équation de Bloch simplifiée) :

$$\frac{\mathrm{d}\overrightarrow{\mu}(p,t)}{dt} = \gamma \overrightarrow{\mu}(p,t) \times \overrightarrow{B}_0. \tag{0.54}$$

Le phénomène de résonance magnétique est obtenu par l'application d'un autre champ magnétique $\overrightarrow{B}_1$ orienté dans un plan perpendiculaire à $\overrightarrow{B}_0$ et avec une vitesse angulaire ω. Pour modéliser l'application d'un champ magnétique à un volume V, on note $\overrightarrow{M}$ la somme des tous les protons dans V :

$$\overrightarrow{M}(t) = \int_V \overrightarrow{\mu}(p,t)\ \mathrm{d}p.$$

Cette quantité $\overrightarrow{M}(t)$ est gouvernée par une équation de Bloch de la forme suivante :

$$\frac{d\overrightarrow{M}}{dt}(t) = \gamma \overrightarrow{M}(t) \times (\overrightarrow{B}_0 + \overrightarrow{B}_1(t)) + \frac{1}{T_1}(M_0 - M_Z)\overrightarrow{z} - \frac{1}{T_2}\overrightarrow{M}_\perp. \tag{0.55}$$

La variation en temps de $\overrightarrow{M}(t)$ provoque une variation du flux dans les antennes et donc un signal mesurable. Pour obtenir une image, il faut localiser dans l'espace le signal enregistré par les antennes. Cela est possible du fait que la fréquence de résonance dépend linéairement du champ magnétique appliqué. Alors, en faisant varier le champ magnétique $\overrightarrow{B}$ dans l'espace, les spins de différentes positions vont osciller avec des fréquences différentes.

Supposons que nous voulions obtenir une image bidimensionnelle dans un plan perpendiculaire à la direction $\overrightarrow{\alpha}$ donnée. On considère alors un champ magnétique $\overrightarrow{B}$ qui dépend linéairement de $\overrightarrow{\alpha}$

$$\overrightarrow{B}(\alpha) = \overrightarrow{B}_0 + G_\alpha \overrightarrow{\alpha}.$$

La fonction G_α est nommée gradient du champ magnétique $\overrightarrow{B}$ de direction $\overrightarrow{\alpha}$. Pour une impulsion magnétique $\overrightarrow{B}_1$ seuls les spins de la section perpendiculaire à $\overrightarrow{\alpha}$ sélectionnée sont excités.

Pour localiser le signal qui provient d'une position donnée (x, y) dans ce plan, on va utiliser un encodage en fréquence et en phase. Plus précisément, en appliquant un

gradient linéaire dans la direction y pendant un court temps τ, les spins de ce plan vont osciller avec des fréquences différentes en fonction de leur position par rapport à la direction y. Après l'arrêt de l'impulsion du gradient G_y, la phase de magnétisation va dépendre linéairement de y.

Pour discriminer dans la direction x, on va appliquer un impulsion magnétique avec un gradient G_x linéaire en x. Pendant l'application de cette impulsion les spins vont osciller avec des fréquences différentes en fonction de x, ce qui nous permettra de savoir d'où provient le signal, puis de l'enregistrer.

Soit $g(\overrightarrow{k}, t)$ le signal IRM enregistré pour la position $\overrightarrow{k} = (k_x, k_y)$ et le temps t. La densité des protons dans le plan sélectionné est notée par $f(x, y)$ avec $(x, y) \subset \Omega$, où Ω est le domaine où f est non nulle (FOV). La relation entre le signal et la densité des protons est donnée par

$$g(G_x, G_y, t) = \iint_\Omega f(x, y) e^{-2\pi i(k_x x + k_y y)} \, \mathrm{d}x \, \mathrm{d}y, \tag{0.56}$$

où k_x et k_y sont définis par

$$\begin{cases} k_x = \dfrac{\gamma}{2\pi} G_x \int_0^t G_x(s) \, \mathrm{d}s = \dfrac{\gamma}{2\pi} G_x t \\ k_y = \dfrac{\gamma}{2\pi} G_y \int_0^\tau G_y(s) \, \mathrm{d}s = \dfrac{\gamma}{2\pi} G_y \tau. \end{cases} \tag{0.57}$$

Autrement dit, (0.56) est équivalente à

$$g(\vec{k}(t), t) = \int_\Omega f(\vec{r}, t) e^{-2\pi i \vec{k} \cdot \vec{r}} \, \mathrm{d}\vec{r}.$$

Pour reconstruire l'image f à partir du signal g donné par (0.56), il faut faire varier les gradients G_y et G_x de sorte que (k_x, k_y) couvrent l'espace de Fourier (k-space) avec une "bonne" densité. L'image f est alors obtenue par une transformée de Fourier inverse.

La problématique du mouvement et l'IRM cardiaque

Dans la première section de ce chapitre nous avons supposé que la densité des protons $f(x, y)$ était constante au cours du temps. Ce n'est pas le cas pour une expérience IRM, car des mouvements involontaires du patient (notamment le mouvement du cœur dans l'IRM cardiaque) peuvent apparaître pendant l'acquisition. Néanmoins, on suppose que la durée des impulsions magnétiques utilisées pour l'acquisition du signal $g(k_x, k_y)$ est assez courte de sorte que la densité des protons n'ait pas le temps de changer.

L'effet des mouvements pendant l'acquisition correspond à l'apparition d'artéfacts. Il existe une littérature riche sur ce sujet. Un des premiers articles qui mentionnent ces effets est du à Schultz et al. [70].

Un des défis majeurs de l'IRM est d'imager les objets en mouvement. Dans cette thèse on va considérer que la densité des protons f dépend du temps. Ainsi la relation (0.56) devient

$$s(k_x, k_y, t) = \iint_\Omega f(x, y, t) e^{-i(k_x(t)x + k_y(t)y)} \, \mathrm{d}x \, \mathrm{d}y. \tag{0.58}$$

L'exemple typique d'organe en mouvement et donné par le cœur. Notamment, dans l'IRM cardiaque, le temps d'acquisition des données est de même ordre de grandeur que la contraction cardiaque.

L'approche standard pour l'IRM cardiaque est de supposer que le mouvement du cœur est périodique au cours du temps. Les protocoles standards d'IRM utilisent les données acquises en continu pendant plusieurs cycles cardiaque et une seule apnée pour reconstruire des images cardiaques pour différentes phases cardiaques. Ces protocoles sont groupés sous le nom de "retrospective gating". Nous généralisons cette approche pour la reconstruction d'images cardiaques à partir de données enregistrées en respiration libre dans le Chapitre 6.

Chapitre 6 : Un problème des moments en IRM cardiaque en respiration libre

Ce chapitre décrit rigoureusement une méthodologie pour la reconstruction d'images par résonance magnétique du cœur à partir des données enregistrées continument le long de plusieurs cycles cardiaques et respiratoires. Cette méthode généralise les techniques existantes et est basée sur les propriétés des espaces de Hilbert à noyau reproductif. Le problème de la reconstruction est formulé comme un problème des moments dans un espace de Hilbert à noyau reproductif. Les images obtenues en utilisant plusieurs espaces de Hilbert à noyau reproductif (qui correspondent aux espaces utilisés dans les techniques usuelles d'interpolation), sont comparées.

Ce chapitre est un travail en collaboration avec Freddy Odille, Gilles Bosser, Jacques Felblinger et Pierre-André Vuissoz. Une partie importante de ce chapitre a été publiée dans Cîndea et al [20].

L'IRM cardiaque est devenue un outil clinique standard pour l'évaluation des différents paramètres de la fonction cardiaque dans de nombreux centres médicaux. Un des inconvénients de l'IRM est le fait que l'acquisition des données est relativement lente, notamment du même ordre de grandeur que les mouvements physiologiques tels que la contraction cardiaque ou la respiration. Ainsi, des artéfacts de mouvement peuvent apparaître dans les images reconstruites à partir des données acquises pendant le mouvement [70, 85].

Plusieurs strategies ont été proposées pour supprimer ces artéfacts. Les protocoles standards utilisent les données acquises en continu pendant plusieurs cycles cardiaques et une ou plusieurs apnées. Le mouvement cardiaque peut être estimé alors à partir de l'électrocardiogramme (ECG). Par cette approche, les données sont triées et interpolées pour reconstruire plusieurs phases cardiaques. Ces images présentent un lissage temporel qui est provoquée par l'algorithme de reconstruction. De plus, la qualité de ces images dépend de la qualité de l'apnée. Dans certaines situations, l'apnée n'est pas possible et cette méthode n'est donc pas appliquable. Au vue ces difficultés, on comprend bien les motivations cliniques pour le développement des méthodes de reconstruction qui prendent en compte les mouvements physiologiques a beaucoup des motivation cliniques.

Une alternative à ces approches est l'IRM cardiaque en respiration libre, qui utilise pour la reconstruction les données acquises en respiration libre. Les techniques pour l'IRM cardiaque en respiration libre peuvent être séparées en deux catégories : les méthodes de correction et les méthodes d'interpolation. Les méthodes de correction ont pour but de combiner les données acquises pendant plusieurs cycles respiratoires et de reconstruire une image de référence. Des études récentes ont prouvé qu'il est possible d'estimer et d'utiliser le champ de déformation non-rigide provoqué par la respitation à partir d'un nombre réduit de capteurs [41, 47, 39, 58]. En collaboration avec Freddy Odille, Damien Mandry, Cédric Pasquier, Pierre-André Vuissoz et Jacques Felblinger, nous avons développé une autre méthode de reconstruction pour l'IRM cardiaque en respiration libre supposant que toutes les mouvements qui apparaissent sont déterminables, à partir d'un nombres des capteurs, comme des mouvements élastiques. De point de vue mathématique, cette méthode revient à résoudre une équation intégrale de Fredholm de premier type et pour garder la cohérence, on ne va pas détailler cette méthode dans la thèse. Pour détails, on renvoie le lecteur à Odille et al. [56]. L'idée des méthodes d'interpolation est de traiter le mouvement respiratoire de la même façon que le mouvement cardiaque, c'est-à-dire en interpolant les données acquises pour différents temps aux phases respiratoires à reconstruire [29, 77, 73]. Comme pour le mouvement cardiaque, cette approche suppose que le mouvement respiratoire est formé de copies (après un changement d'échelle) d'un cycle respiratoire idéal.

Ce chapitre présente une méthode d'interpolation pour l'IRM cardiaque en respiration libre. Une approche rigoureuse a été proposée, en généralisant les méthodes existantes. Nous utilisons les propriétés des espaces de Hilbert à noyau reproductif pour formuler le problème de la reconstruction des images cardiaques à partir des données acquises en respiration libre comme un problème des moments dans un espace de Hilbert à noyau reproductif. Plus précisément, on veut reconstruire une série d'images cardiaques pour différentes phases cardiaques et respiratoires, ce qui revient à trouver la solution $f \in L^2(D, H)$ du problème des moments suivant

$$\langle f,\, \varphi_{k,i} e^{\mathrm{i}k\cdot x} \rangle_{L^2(D,H)} = g_{k,i}, \qquad (k \in \mathbb{K}, i \in \mathbb{Z}),$$

où $(\varphi_{k,i})_{k,i} \subset H$ est une famille des fonction en H, avec H un espace de Hilbert à noyau reproductif. On note $g_{k,i}$ la valeur du signal IRM enregistré pour la position k dans l'espace de Fourier, i nous donnant le temps (notée T_i) de l'enregistrement du signal.

Cette approche nous a menés à tester plusieurs espaces de Hilbert à noyau reproductif qui correspondent aux techniques standards d'interpolation (l'espaces des splines cubiques et l'espace de Paley-Wiener) et des espaces moins utilisés en interpolation comme les espaces de Sobolev. Nous avons validé cette méthode en recontruisant des images à partir de données acquises en respiration libre provenant de cinq volontaires sains et de données simulées.

Chapitre 7 : Propagation d'une onde vue par IRM

Dans ce chapitre, on considère le problème de la reconstruction d'un terme source dans l'équation des ondes à partir de la restriction de la transformée de Fourier de la solution de l'équation des ondes à un ensemble ouvert et non-vide. On prouve la propriété d'identifiabilité de la source et on donne quelques exemples numériques.

Soit $\Omega = (0,1)^2$ le carré unité de $\mathbb{R}^2$. On considère l'équation des ondes suivante :

$$\ddot{w}(\boldsymbol{x},t) - \Delta w(\boldsymbol{x},t) = \lambda(t) f(\boldsymbol{x}), \qquad \boldsymbol{x} \in \Omega,\ t > 0 \tag{0.59}$$

$$w(\boldsymbol{x},t) = 0, \qquad \boldsymbol{x} \in \partial\Omega,\ t > 0 \tag{0.60}$$

$$w(\boldsymbol{x},0) = \dot{w}(\boldsymbol{x},0) = 0, \qquad \boldsymbol{x} \in \Omega, \tag{0.61}$$

avec f un terme source qu'on suppose inconnu. Dans ce chapitre on étudie le problème inverse de la reconstruction de la source f à partir de l'observation

$$y(t) = \widehat{w}(\cdot,t)|_{\mathcal{O}}, \tag{0.62}$$

où nous avons noté $\widehat{w}$ la transformée de Fourier de w et $\mathcal{O}$ un ensemble ouvert et non-vide de $\mathbb{R}^2$. Ce problème correspond à l'identification du terme source dans une équation des ondes à partir d'un signal enregistré par un appareil IRM (voir Chapitre 5).

Pour résoudre ce problème inverse, une question importante est *l'identifiabilité* de f

l'application qui associe à f l'observation y est injective ?

On donne une réponse positive à cette question en combinant quelques résultats classiques d'analyse de Fourier avec une version adaptée de la méthode de résolution des problèmes inverse pour la reconstruction des terme source décrite dans Alves, Silvestre, Takahashi et Tucsnak [2].

Le résultat principal de ce chapitre est le théorème suivant :

Théorème 0.20. *Soit $\tau > 0$ et soit $\lambda \in H^1(0,\tau)$ une fonction satisfaisant $\lambda(0) \neq 0$. L'application*

$$\mathbb{E}_\tau : L^2(\Omega) \to L^2(0,\tau; L^2(\mathcal{O}))$$

qui associe à la source f l'observation y, définie par (0.62), est injective.

Ce théorème nous donne l'identifiabilité du terme source f à partir de l'obervation y, et donc l'unicité de la solution de notre problème inverse.

Nous avons réalisé des simulations numériques pour reconstruire la source inconnue (mais sachant que f a un nombre fini de modes propres) dans (0.59)-(0.62). Nous avons utilisé la méthode d'observateurs itératifs qui est la méthode duale de la méthode décrite dans le Chapitre 4 pour l'approximation des contrôles exacts.

Finalement, nous avons essayé de réaliser un système expérimental gouverné par l'équation des ondes et de reconstruire un terme source à partir de vraies données IRM. Ce travail est en cours.

Dans ce chapitre introductif nous avons essayé de donner une vision d'ensemble de cette thèse. Les chapitres suivants sont en anglais, et la majorité correspondent à des articles publiés ou soumis.

Part I

Controlability and observability of some plate equations

1. Background of controllability and observability of infinite dimensional systems

In this chapter we recall some basic concepts and results concerning the exact controllability and exact observability of infinite dimensional systems. The majority of these results are stated here without proofs and we give precise references to the papers where the proofs can be found.

We suppose that the reader is familiar with the theory of semigroups, such is described, for instance, in Pazy [59]. Our notations follow closely the notation from the textbook Tucsnak and Weiss [80].

1.1 Notions of exact controllability and exact observability

In the remaining part of this chapter X, Y and U are complex Hilbert spaces which are identified with their duals. Let $A : \mathcal{D}(A) \to X$ be a densely defined operator with the resolvent $\rho(A) \neq \emptyset$ and let $(\mathbb{T}_t)_{t\geqslant 0}$ be the strongly continuos semigroup on X generated by A. We introduce the scale of Hilbert spaces $(X_\alpha)_{\alpha\in\mathbb{R}}$. For that, we need the following known result (see, for instance, Tucsnak and Weiss [80, Proposition 2.10.3]).

Proposition 1.1. *Let X be a Hilbert space, let $A : \mathcal{D}(A) \to X$ be a densely defined operator with the resolvent set $\rho(A) \neq \emptyset$, let $\beta \in \rho(A)$, let X_1 be $\mathcal{D}(A)$ with the graph norm and let X_{-1} be the completion of X with respect to the norm*

$$\|z\|_{-1} = \|(\beta I - A)^{-1} z\|_X, \qquad (z \in X).$$

Then $A \in \mathcal{L}(X_1, X)$ and A has a unique extension to an operator in $\mathcal{L}(X, X_{-1})$, also denoted by A. Moreover,

$$(\beta I - A)^{-1} \in \mathcal{L}(X, X_1), \quad (\beta I - A)^{-1} \in \mathcal{L}(X_{-1}, X)$$

and these two operators are unitary.

We denote by X_1 the space $\mathcal{D}(A)$ with the norm $\|z\|_1 = \|(\beta I - A)z\|_X$, where $\beta \in \rho(A)$ is fixed, and by X_{-1} the completion of X with respect to the norm $\|z\|_{-1} = \|(\beta I - A)^{-1}z\|_X$. The restriction of $\mathbb{T}_t$ to X_1 is the image of $\mathbb{T}_t \in \mathcal{L}(X)$ through the unitary operator $(\beta I - A)^{-1} \in \mathcal{L}(X, X_1)$. Therefore, these operators forms a strongly continuous semigroup on X_1, whose generator is the restriction of A to $\mathcal{D}(A^2)$. The images of $\mathbb{T}_t \in \mathcal{L}(X)$ through the operator $(\beta I - A) \in \mathcal{L}(X, X_{-1})$ form a strongly continuous semigroup, whose generator is the extension of A to X_{-1}. The construction of X_1 and X_{-1} can be iterated, in both directions, to obtain the infinite sequence of spaces

$$\cdots X_2 \subset X_1 \subset X \subset X_{-1} \subset X_{-2} \cdots$$

each inclusion being dense and with continuous embedding. This scale of Hilbert spaces can be extended, using the fractionar power of the operator $\beta I - A$ defined in Arendt, Batty, Hieber and Neubrander[3, Section 3.8], to a scale $(X_\alpha)_{\alpha\in\mathbb{R}}$ by setting $X_\alpha = (\beta I - A)^{-\alpha}(X)$ and $X_{-\alpha}$ is the dual space of X_α with respect to the pivot space X, for every $\alpha \geqslant 0$.

We consider the following infinite dimensional system :

$$\dot{z}(t) = Az(t) + Bu(t), \qquad z(0) = z_0, \tag{1.1}$$

where $B \in \mathcal{L}(U, X)$ is a bounded control operator and $z_0 \in X_1$. Here and henceforth, a dot denotes differentiation with respect to the time t. It is known (see, for instance [80, Section 4.2]) that, if $\tau > 0$ and $u \in L^2([0, \tau]; U)$, then the solution of (1.1) is $z \in C^1([0, \tau]; X) \cap C([0, \tau]; X_1)$ and z at the time τ is given by

$$z(\tau) = \mathbb{T}_\tau z_0 + \Phi_\tau u, \tag{1.2}$$

where $\Phi_\tau \in \mathcal{L}(L^2([0, \tau]; U), X)$ is defined by

$$\Phi_\tau u = \int_0^\tau \mathbb{T}_{\tau-t} Bu(t)\ \mathrm{d}t. \tag{1.3}$$

We can now give the definition of the exact controllability.

Definition 1.2. The pair (A, B) is exactly controllable in time $\tau > 0$ if $\mathrm{Ran}\Phi_\tau = X$. The pair (A, B) is exactly controllable if it is exactly controllable in some time $\tau > 0$.

The dual concept of exact controllability is the exact observability. For introducing this concept we consider the following system :

$$\dot{z}(t) = Az(t), \qquad z(0) = z_0 \tag{1.4}$$

$$y(t) = Cz(t), \tag{1.5}$$

where $C \in \mathcal{L}(\mathcal{D}(A), Y)$. We assume that the operator C is admissible in the sense of the following definition :

Definition 1.3. The operator $C \in \mathcal{L}(\mathcal{D}(A), Y)$ is an admissible observation operator for (1.4)-(1.5) if, for every $\tau > 0$, there exists a constant $K_\tau > 0$ such that any solution of (1.4) satisfies

$$\int_0^\tau \|Cz(t)\|_Y^2 \, \mathrm{d}t \leqslant K_\tau^2 \|z_0\|_X^2, \qquad (z_0 \in \mathcal{D}(A)). \tag{1.6}$$

Note that every bounded operator $C \in \mathcal{L}(X, Y)$ is admissible. In the remaining part of this thesis we are interested by bounded observation operators, but most of the results are true for unbounded admissible observation operators.

Definition 1.4. We say that the pair (A, C) is exactly observable in time $\tau > 0$, or that the system (1.4)-(1.5) is exactly observable in time $\tau > 0$, if there exists a constant $k_\tau > 0$ such that any solution z of (1.4) satisfies

$$k_\tau^2 \|z_0\|_X^2 \leqslant \int_0^\tau \|Cz(t)\|_Y^2 \, \mathrm{d}t, \qquad (z_0 \in \mathcal{D}(A)). \tag{1.7}$$

The pair (A, C) is exactly observable if it is exactly observable in some time $\tau > 0$.

The duality between exact controllability and exact observability is formalized by the result bellow, see Dolecki and Russell [23].

Proposition 1.5. *With the above assumptions on A and B, the pair (A, B) is exactly controllable if and only if the pair (A^*, B^*) is exactly observable, i.e., if there exist $\tau > 0$ and $k_\tau > 0$ such that*

$$k_\tau^2 \|\phi\|_X^2 \leqslant \int_0^\tau \|B^* \mathbb{T}_t^* \phi\|_U^2 \, dt, \qquad (\phi \in \mathcal{D}(A^*)).$$

1.1.1 Gramians and controllability

In this subsection we introduce controllability Gramians, which are useful in the explicit construction of minimal norm control driving the solution of (1.1) from an initial state z_0 to a final state $z_1 \in X$. As at the beginning of this section, we denote by $\Phi_\tau \in \mathcal{L}(L^2([0, \tau]; U), X)$ the operator defined by (1.3). For each $\tau > 0$, we define the controllability Gramian $R_\tau \in \mathcal{L}(X)$ by

$$R_\tau = \Phi_\tau \Phi_\tau^*. \tag{1.8}$$

Moreover, it is clear that (A, B) is exactly controllable in time τ if and only if R_τ is invertible. Using the definition (1.8) of the controllability Gramian and (1.3), we can write

$$R_\tau x = \int_0^\tau \mathbb{T}_t B B^* \mathbb{T}_t^* x \, \mathrm{d}t.$$

The following proposition give an explicit construction of the minimal norm control which drives the solution z of (1.1) from 0 to z_0 in time τ.

Proposition 1.6. *Suppose that (A, B) is exactly controllable in time $\tau > 0$. Then there exists an operator $F_\tau \in \mathcal{L}(X, L^2([0,\tau];U))$ such that :*

1. $\Phi_\tau F_\tau = \mathbb{I}_X$;
2. *If u is a control driving the solution of (1.1) from 0 to z_0 in time τ, then we have*

$$\|u\|_{L^2([0,\tau];U)} \geqslant \|F_\tau z_0\|_{L^2([0,\tau];U)}. \tag{1.9}$$

Proof. 1) Let $x \in X$. From the exact controllability of the pair (A, C) the operator Φ_τ is onto, so, there exists $u \in L^2([0,\tau];U)$ such that $\Phi_\tau u = x$. We define $F_\tau x = u$. It remains to prove that the operator F_τ, defined in this way, is bounded. We show that the graph of F_τ is closed. Let (x_n, u_n) be a sequence in the graph of the operator F_τ such that $(x_n, u_n) \to (x, u)$ in $X \times L^2([0,\tau];U)$. Then $x_n \to x$, $u_n \to u$ and $\Phi_\tau u_n \to \Phi_\tau u$. Thus, $x = \Phi_\tau u$ and, since $(\text{Ker } \Phi_\tau)^\perp$ is closed, $u \in (\text{Ker } \Phi_\tau)^\perp$, so that $F_\tau x = u$.

2) Is easy to verify that F_τ has the following expression:

$$F_\tau z_0 = \Phi_\tau^* R_\tau^{-1} z_0, \qquad (z_0 \in X).$$

Let $u \in L^2([0,\tau];U)$ be a control such that $\Phi_\tau u = z_0$. Then u can be written in the form $u = \Phi_\tau^* R_\tau^{-1} z_0 + v$, where $v \in \text{Ker } \Phi_\tau = (\text{Ran } \Phi_\tau^*)^\perp$. Since $\Phi_\tau^* R_\tau^{-1} z_0$ are orthogonal one to each other, $\|u\|^2 = \|\Phi_\tau^* R_\tau^{-1} z_0\|^2 + \|v\|^2$. Then, the minimum of $\|u\|$ is achieved only for $v = 0$, i.e. for $u = F_\tau z_0$. □

A simple consequence of Proposition 1.6 shows that we can steer the solution of

$$\dot{z}(t) = Az(t) + Bu(t) + F(t), \qquad z(0) = 0, \tag{1.10}$$

to an arbitrarily state in X by the mean of a control $U \in L^2([0,\tau];U)$, where $F \in L^2([0,\tau];X)$. More precisely we have the following corollary :

Corollary 1.7. *Let $\tau > 0$ and assume that the pair (A, B) is exactly controllable in time τ. Let $z_0 \in X$ and*

$$u = F_\tau z_0 - F_\tau \int_0^\tau \mathbb{T}_{\tau-s} F(s)\, ds, \tag{1.11}$$

where F_τ is the operator from Proposition 1.6. Then the solution z of (1.10) satisfies $z(\tau) = z_0$.

1.1.2 A simultaneous controllability result

Definition 1.8. Let $V \subset X$ be a closed invariant subspace for $\mathbb{T}_t$. The part of A in V, denoted by A_V, is the restriction of A to $\mathcal{D}(A_V) = \mathcal{D}(A) \cap V$, regarded as an (possibly unbounded) operator on V.

Clearly, A_V is the generator of the restriction of $\mathbb{T}_t$ to V. The following proposition follows directly from Proposition 6.4.4 form [80] and Proposition 1.5 above (see also Tucsnak and Weiss [78]).

Proposition 1.9. *Assume that there exists an orthonormal basis $(\Phi_n)_{n\in\mathbb{N}}$ formed by eigenvectors of A and the corresponding eigenvalues λ_n satisfy $\lim_{n\to\infty}|\lambda_n| = \infty$. For some bounded set $J \subset \mathbb{C}$ denote*

$$V = span\ \{\Phi_n \mid \lambda_n \in J\}^{\perp},$$

let A_V^* be the part of A^* in V and let B_V^* be the restriction of B^* to $\mathcal{D}(A_V^*)$. Assume that (A_V^*, B_V^*) is exactly controllable in time $\tau_0 > 0$ and that $B^*\Psi \neq 0$ for every eigenvector Ψ of A. Then (A, B) is exactly controllable in any time $\tau > \tau_0$.

As a corollary of this proposition we have the following dual result :

Proposition 1.10. *Let $A : \mathcal{D}(A) \to X$ be the generator of a strongly continuos semigroup $(\mathbb{T}_t)_{t\geqslant 0}$ on X. Assume that there exists an orthonormal basis $(\phi_k)_{k\in\mathbb{N}}$ of X, formed by eigenvectors of A and the corresponding eigenvalues λ_k satisfy $\lim_{k\to\infty}|\lambda_k| = \infty$. Let $C \in \mathcal{L}(X, Y)$ be a bounded observation operator. For some bounded set $J \subset \mathbb{C}$ denote*

$$V = span\ \{\phi_k \mid \lambda_k \in J\}^{\perp}$$

and let A_V be the part of A in V. Let C_V be the restriction of C to $\mathcal{D}(A_V)$. Assume that (A_V, C_V) is exactly observable in time $\tau_0 > 0$ and that $C\Psi \neq 0$ for every eigenvector Ψ of A. Then (A, C) is exactly observable in any time $\tau > \tau_0$.

1.2 A spectral criterium for the exact observability

An important part of this thesis is dedicated to the study of exact internal observability and, by duality, of exact internal controllability, of vibrating elastic systems. For this reason, we consider systems of the form :

$$\dot{z}(t) = Az(t), \qquad z(0) = z_0 \tag{1.12}$$

$$y(t) = Cz(t), \tag{1.13}$$

where $A : \mathcal{D}(A) \to X$ is an unbounded skew-adjoint operator with compact resolvents and $C \in \mathcal{L}(X, Y)$. The spectrum of the operator A is concentrated on the imaginary axis and is formed by the eigenvalues $(i\mu_n)_{n\in\mathbb{Z}^*}$, where $\mu_n \in \mathbb{R}$. The corresponding eigenvectors $(\mathbf{\Phi}_n)_{n\in\mathbb{Z}^*}$ form an orthonormal basis of X. Then a *wave packet of center μ and radius ρ* is defined by

$$z = \sum_{l\in J_\rho(\mu)} c_l \mathbf{\Phi}_l,$$

where

$$J_\rho(\mu) = \{l \in \mathbb{Z}^* \text{ such that } |\mu_l - \mu| < \rho\}. \tag{1.14}$$

This section focuses on a spectral characterization of the exact observability of the system (1.12)-(1.13) for this kind of operators, based on the results obtained by Ervedoza [25] and Ramdani, Takahashi, Tenenbaum and Tucsnak [64]. The following theorem is the main result of this section.

Theorem 1.11. *Let $A : \mathcal{D}(A) \to X$ be a skew-adjoint operator on X with compact resolvent and $C \in \mathcal{L}(X, Y)$. Then the system* (1.12)-(1.13) *is exactly observable if and only if there exists $\rho > 0$ and $d > 0$ such that for every wave packet*

$$z = \sum_{l \in J_\rho(\mu)} c_l \mathbf{\Phi}_l$$

of center $\mu \in \mathbb{R}$ and radius ρ we have

$$d^2 \|z\|_X^2 \leqslant \|Cz\|_Y^2, \tag{1.15}$$

where $J_\rho(\mu)$ is as in (1.14)*.*

Moreover, if (1.15) *holds, then system* (1.12)-(1.13) *is exactly observable in any time $\tau > \tau^*$, for*

$$\tau^* = \frac{2e}{\rho} \left(\frac{(1 + ln(L))\pi}{4} \right)^{1 + \frac{1}{ln(L)}}, \tag{1.16}$$

where

$$L = \frac{\pi \|C\|_{\mathcal{L}(X,Y)}^2}{3d^2} \tag{1.17}$$

and the constant k_τ in the observability inequality can be chosen as

$$k_\tau = \frac{\pi d^2}{\rho} \left(1 - \left(\frac{T^*}{T} \right)^{2n^* - 1} \right), \text{ where } n^* = \left[\frac{1}{2} (\ln(L) + 1) \right]. \tag{1.18}$$

Proof. For the proof of the first part of the theorem we send the interested reader to [64]. For the second part of the theorem we follow closely the proof of Theorem 2.5 from [25], only few calculus being different because of the choice of a bounded observation operator C. We give the details of the proof bellow.

Let z be the solution of (1.12) and $g(t) = \chi(t)z(t)$, where $\chi : \mathbb{R} \to \mathbb{R}$ is a function whose Fourier transform is smooth and with compact support, satisfying

$$\text{supp } \hat{\chi} \subset (-\rho, \rho). \tag{1.19}$$

Then χ is in the Schwartz class $\mathcal{S}(\mathbb{R})$ and therefore $g, \hat{g} \in L^2(\mathbb{R}; X)$. Writing z_0 and z in the basis formed by $(\mathbf{\Phi}_j)_j$ we obtain

$$z_0 = \sum_{j \in \mathbb{Z}^*} a_j \mathbf{\Phi}_j, \qquad z(t) = \sum_{j \in \mathbb{Z}^*} a_j e^{i\mu_j t} \mathbf{\Phi}_j.$$

Therefore,

$$\begin{aligned}\hat{g}(\omega) &= \frac{1}{\sqrt{2\pi}}\int_{\mathbb{R}} g(t)e^{-i\omega t}\,\mathrm{d}t = \frac{1}{\sqrt{2\pi}}\int_{\mathbb{R}} \chi(t)z(t)e^{-i\omega t}\,\mathrm{d}t \\ &= \frac{1}{\sqrt{2\pi}}\sum_{j\in\mathbb{Z}^*} a_j\mathbf{\Phi}_j\int_{\mathbb{R}}\chi(t)e^{-i(\omega-\mu_j)t}\,\mathrm{d}t \\ &= \sum_{j\in\mathbb{Z}^*} a_j\hat{\chi}(\omega-\mu_j)\mathbf{\Phi}_j.\end{aligned}$$

In particular, because the support of $\hat{\chi}$ is included in $(-\rho,\rho)$, $\hat{g}(\omega)$ is a wave packet and applying (1.15) we obtain

$$d^2\|\hat{g}(\omega)\|_X^2 \leqslant \|C\hat{g}(\omega)\|_Y^2. \tag{1.20}$$

Integrating with respect to ω, replacing $\hat{g}(\omega)$ with his expansion in the basis $(\mathbf{\Phi}_j)$, and using Parseval's identity, (1.20) becomes

$$d^2\left(\int_{\mathbb{R}}|\hat{\chi}(\omega)|^2\,\mathrm{d}\omega\right)\|z_0\|_X^2 \leqslant \int_{\mathbb{R}}|\chi(t)|^2\|Cz(t)\|_Y^2\,\mathrm{d}t. \tag{1.21}$$

From the inverse Fourier transform, and integrating by parts we can write

$$\chi(t) = \frac{1}{\sqrt{2\pi}}\int_{\mathbb{R}}\hat{\chi}(\omega)e^{i\omega t}\,\mathrm{d}\omega = \frac{1}{\sqrt{2\pi}(it)^n}\int_{\mathbb{R}}\hat{\chi}^{(n)}(\omega)e^{i\omega t}\,\mathrm{d}\omega.$$

Then

$$|\chi(t)| = \frac{1}{\sqrt{2\pi}|t|^n}\left(\int_{\mathbb{R}}\left|\hat{\chi}^{(n)}(\omega)\right|^2\,\mathrm{d}\omega\right)^{\frac{1}{2}}\left(\int_{-\rho}^{\rho}|e^{i\omega t}|^2\,\mathrm{d}\omega\right)^{\frac{1}{2}},$$

so, therefore

$$|\chi(t)|^2 \leqslant \frac{\rho}{\pi}\left(\frac{1}{|t|}\right)^{2n}\int_{\mathbb{R}}\left|\hat{\chi}^{(n)}(\omega)\right|^2\,\mathrm{d}\omega. \tag{1.22}$$

Evaluating the right hand side of (1.21) and using (1.22), we obtain

$$\begin{aligned}\int_{\mathbb{R}}|\chi(t)|^2\|Cz(t)\|_Y^2\,\mathrm{d}t &= \int_{-T}^{T}|\chi(t)|^2\|Cz(t)\|_Y^2\,\mathrm{d}t + 2\int_T^{\infty}|\chi(t)|^2\|Cz(t)\|_Y^2\,\mathrm{d}t \\ &\leqslant \int_{-T}^{T}|\chi(t)|^2\|Cz(t)\|_Y^2\,\mathrm{d}t + \frac{2\rho}{\pi}\int_{\mathbb{R}}\left|\hat{\chi}^{(n)}(\omega)\right|^2\,\mathrm{d}\omega\int_T^{\infty}\frac{1}{t^{2n}}\|Cz(t)\|_Y^2\,\mathrm{d}t \\ \leqslant \int_{-T}^{T}|\chi(t)|^2\|Cz(t)\|_Y^2\,\mathrm{d}t + \frac{2\rho}{\pi}\int_{\mathbb{R}}\left|\hat{\chi}^{(n)}(\omega)\right|^2\,\mathrm{d}\omega\sum_{k=1}^{\infty}\frac{1}{(kT)^{2n}}\int_{kT}^{(k+1)T}&\|Cz(t)\|_Y^2\,\mathrm{d}t\end{aligned}$$

We recall that C is a bounded operator in $\mathcal{L}(X,Y)$ and that the semigroup generated by A is in fact a unitary group. Therefore, we can rewrite the above inequality as

$$\int_{\mathbb{R}}|\chi(t)|^2\|Cz(t)\|_Y^2\,\mathrm{d}t \leqslant \int_{-T}^{T}|\chi(t)|^2\|Cz(t)\|_Y^2\,\mathrm{d}t + \frac{\rho\pi\|C\|_{\mathcal{L}(X,Y)}^2}{3T^{2n-1}}\int_{\mathbb{R}}\left|\hat{\chi}^{(n)}(\omega)\right|^2\,\mathrm{d}\omega\|z_0\|_X^2. \tag{1.23}$$

From (1.21) and (1.23) we obtain

$$\left[d^2\int_{\mathbb{R}}|\hat{\chi}(\omega)|^2\ \mathrm{d}\omega-\frac{\rho\pi\|C\|^2_{\mathcal{L}(X,Y)}}{3T^{2n-1}}\int_{\mathbb{R}}\left|\hat{\chi}^{(n)}(\omega)\right|^2\ \mathrm{d}\omega\right]\|z_0\|^2_X\leqslant\int_{-T}^{T}|\chi(t)|^2\|Cz(t)\|^2_Y\ \mathrm{d}t. \tag{1.24}$$

We can estimate $|\chi(t)|$ in the right hand member in the following way :

$$|\chi(t)|^2=\frac{1}{2\pi}\left|\int_{\mathbb{R}}\hat{\chi}(\omega)e^{i\omega t}\ \mathrm{d}\omega\right|^2\leqslant\frac{\rho}{\pi}\int_{\mathbb{R}}|\hat{\chi}(\omega)|^2\ \mathrm{d}\omega$$

and then (1.24) becomes

$$\left[d^2-\frac{\rho\pi\|C\|^2_{\mathcal{L}(X,Y)}}{3T^{2n-1}}\frac{\int_{\mathbb{R}}\left|\hat{\chi}^{(n)}(\omega)\right|^2\ \mathrm{d}\omega}{\int_{\mathbb{R}}|\hat{\chi}(\omega)|^2\ \mathrm{d}\omega}\right]\|z_0\|^2_X\leqslant\frac{\rho}{\pi}\int_{-T}^{T}\|Cz(t)\|^2_Y\ \mathrm{d}t. \tag{1.25}$$

We impose that the left part of (1.25) is positive. This is equivalent to

$$T>\inf_{n\in\mathbb{N}^*}\left\{\left(\frac{\rho\pi\|C\|^2_{\mathcal{L}(X,Y)}}{3d^2}\right)^{\frac{1}{2n-1}}\gamma_n^{\frac{2n}{2n-1}}\right\}, \tag{1.26}$$

where

$$\gamma_n=\left(\inf_{\phi\in\mathcal{D}(-\rho,\rho)}\frac{\|\phi^{(n)}\|^2_{L^2}}{\|\phi\|^2_{L^2}}\right)^{\frac{1}{2n}}.$$

By a slightly modification of Lemma 2.7 from [25] we obtain the following majoration for γ_n :

$$\gamma_n\leqslant\frac{n\pi}{2\rho},\qquad(n\in\mathbb{N}^*). \tag{1.27}$$

From (1.26) and (1.27) we can write

$$T\rho>\inf_{n\in\mathbb{N}^*}\left[\left(\frac{\pi\|C\|^2_{\mathcal{L}(X,Y)}}{3d^2}\right)^{\frac{1}{2n-1}}\left(\frac{n\pi}{2}\right)^{\frac{2n}{2n-1}}\right]. \tag{1.28}$$

We denote $f(n)=L^{\frac{1}{2n-1}}\left(\frac{n\pi}{2}\right)^{\frac{2n}{2n-1}}$ and

$$g(n)=\frac{1}{2n-1}\ln(L)+\frac{2n}{2n-1}\ln(\frac{n\pi}{2}),$$

where L is given by (1.17). Is easy to see that

$$g'(n)=\frac{2}{(2n-1)^2}\left[2n-1-\ln(L)-\ln(\frac{n\pi}{2})\right]$$

and, so, the minumum in $\mathbb{R}$ of g is atteined in $\tilde{n}$ given by

$$2\tilde{n}-1=\ln(L)+\ln(\frac{\tilde{n}\pi}{2}).$$

For L large, we approximate the minimum $g(n^*)$ of g by putting $2n-1=\ln(L)$. We have

$$g(n^*) \leqslant 1+(1+\ln(L))\ln\left(\frac{(1+\ln(L))\pi}{4}\right)$$

or, equivalently,

$$f(n^*) \leqslant e\left(\frac{(1+\ln(L))\pi}{4}\right)^{1+\frac{1}{\ln(L)}} = \frac{T^*\rho}{2}. \tag{1.29}$$

Combining (1.25), (1.27) and (1.29), we can write

$$\begin{aligned}\int_{-T}^{T} \|Cz(t)\|_Y^2 \,\mathrm{d}t &\geqslant \frac{\pi d^2}{\rho}\left[1-\frac{L}{T^{2n^*-1}}\left(\frac{n^*\pi}{2\rho}\right)^{2n^*}\right]\|z_0\|_X^2\\ &\geqslant \frac{\pi d^2}{\rho}\left[1-\frac{\left(\frac{T^*\rho}{2}\right)^{2n^*-1}}{(\rho T)^{2n^*-1}}\right]\|z_0\|_X^2\\ &= \frac{\pi d^2}{\rho}\left[1-\left(\frac{T^*}{2T}\right)^{2n^*-1}\right]\|z_0\|_X^2.\end{aligned}$$

Since the semigroup $(\mathbb{T}_t)$ generated by A is unitary, for any $z_0 \in \mathcal{D}(A)$ we can rewrite the above inequality as

$$\int_0^{2T} \|Cz(t)\|_Y^2 \,\mathrm{d}t \geqslant \frac{\pi d^2}{\rho}\left[1-\left(\frac{T^*}{2T}\right)^{2n^*-1}\right]\|z_0\|_X^2$$

and the proof of the theorem is complete. □

1.3 Non-harmonic Fourier series and observability

In this section we recall some non-harmonic Fourier analysis results and notions, borrowed from a paper of Kahane [40].

Let $n \in \mathbb{N}^*$ be a natural number and $\mathcal{I} \subset \mathbb{Z}$ a set of indices. We say that $\Lambda = (\lambda_m)_{m\in\mathcal{I}} \subset \mathbb{R}^n$ is a *regular sequence* if there exists a constant $\gamma > 0$ such that

$$\inf_{\substack{m,l\in\mathcal{I}\\ m\neq l}} |\lambda_m - \lambda_l| = \gamma. \tag{1.30}$$

We introduce the notion of domain associated to a regular sequence, which allows to express some observability inequalities in terms of Fourier series.

Definition 1.12. We say that the open subset $D \subset \mathbb{R}^n$ is a domain associated to the regular sequence $\Lambda = (\lambda_m)_{m\in\mathcal{I}} \subset \mathbb{R}^n$ if there exist constants $\delta_1(D), \delta_2(D) > 0$ such that,

for every sequence of complex numbers $(a_m)_{m\in\mathcal{I}}$ with a finite number of non-vanishing terms, we have

$$\delta_2(D)\sum_{m\in\mathcal{I}}|a_m|^2 \leqslant \int_D \left|\sum_{m\in\mathcal{I}} a_m e^{i\lambda_m\cdot x}\right|^2 \mathrm{d}x \leqslant \delta_1(D)\sum_{m\in\mathcal{I}}|a_m|^2. \tag{1.31}$$

The following proposition (see Proposition III.1.2 from [40]) is a n-dimensional equivalent of the classical Ingham inequality (Ingham [36]).

Proposition 1.13. *Let $\Lambda = (\lambda_m)_{m\in\mathcal{I}} \subset \mathbb{R}^n$ be a regular sequence satisfying* (1.30)*. Then there exists a positive constant α (depending only on the space dimension n) such that every ball in $\mathbb{R}^n$ of radius $\frac{\alpha}{\gamma}$ is a domain associated to Λ.*

Note that in the one dimensional case, the constant α, provided by the theorem of Ingham, is explicit and is equal to 2π. A consequence of this proposition is that we can prove easily the exact observability for systems with skew-adjoint generator and scalar output. More precisely, Tucsnak and Weiss proved the following result [80, Proposition 8.1.3].

Proposition 1.14. *Let $A : \mathcal{D}(A) \to X$ be a skew-adjoint operator generating the unitary group $\mathbb{T}$. Assume that A is diagonalisable with an orthonormal basis $(\phi_m)_{m\in\mathcal{I}}$ in X formed by its eigenvectors and denote by $(i\lambda_m)_m \subset i\mathbb{R}$ the eigenvalues corresponding to (ϕ_m). Assume that the eigenvalues of A are simple and there exists a bounded set $J \subset i\mathbb{R}$ such that*

$$\inf_{\substack{\lambda,\mu\in\sigma(A)\setminus J\\ \lambda\neq\mu}} |\lambda-\mu| = \gamma > 0.$$

Moreover, let $C \in \mathcal{L}(X_1, \mathbb{C})$ be an observation operator for the semigroup $\mathbb{T}$ generated by A such that

$$\inf_{m\in\mathcal{I}} |C\phi_m| > 0 \text{ and } \sup_{m\in\mathcal{I}} |C\phi_m| < \infty.$$

Then C is an admissible observation operator for $\mathbb{T}$ and the pair (A, C) is exactly observable in any time $\tau > \frac{2\pi}{\gamma}$.

Idea of the proof of Proposition 1.14. Using the facts that A is diagonalisable, that the eigenvalues of A are simple and that $\sup|C\phi_m| < \infty$ we can easily obtain, applying Ingham inequality, the admissibility of C. For the observability of the pair (A, C), we firstly denote

$$V = \text{span}\,\{\phi_k \,|\, \lambda_k \in J\}^\perp.$$

Applying Proposition 1.13 we have that (A_V, C_V) is exactly observable in any time $\tau > \frac{\alpha}{\gamma}$. Then, from Proposition 1.9 and using that $C\Phi_m \neq 0$, we obtain that (A, C) is exactly observable in any time $\tau > \frac{2\pi}{\gamma}$. □

The following results will be necessary for the proof of some exact observability and controllability results in Chapters 2 and 3.

Theorem 1.15 (Theorem III.3.1, Kahane [40]). *Let Λ_1, Λ_2 be two regular sequences in $\mathbb{R}^n$, and D_1, $D_2 \subset \mathbb{R}^n$ two domains associated to Λ_1, respectively Λ_2. If $\Lambda = \Lambda_1 \cup \Lambda_2$ is a regular sequence, then every set which contains the closure of $D_1 + D_2$ is a domain associated to Λ.*

The following theorem, proven in the same paper of Kahane [40], gives a condition on the density of a regular sequence such that any ball in $\mathbb{R}^n$ is a domain associated to this sequence.

Theorem 1.16. *Let Λ be a regular sequence in $\mathbb{R}^n$. For $d > 0$ denote by $\omega(d)$ the upper limit when $|b| \to \infty$ of the number of terms of Λ contained in the ball of center b and radius d. If $\omega(d) = o(d)$ when $d \to \infty$ then every ball in $\mathbb{R}^n$ of strictly positive radius is a domain associated to Λ.*

In Chapter 3 we consider the linearized Berger equation (3.4)-(3.6) as a pertubation of the Euler-Bernoulli plates equation (3.1)-(3.3), and the eigenvalues of the perturbed operator have a "similar" asymptotic behavior as the eigenvalues of the unperturbed operator. For quantify this "similarity" we introduce the definition of asymptotically close sequences.

Definition 1.17. Let $\Lambda = (\lambda_m)_{m\in\mathcal{I}}$ and $\tilde{\Lambda} = (\tilde{\lambda}_m)_{m\in\mathcal{I}}$ be two regular sequences in $\mathbb{R}^n$. We say that the sequences Λ and $\tilde{\Lambda}$ are asymptotically close if for every $\alpha > 0$ there exists an open ball $B \subset \mathbb{R}^n$ large enough such that

$$|\lambda_m - \tilde{\lambda}_m| < \alpha \qquad (m \in \mathcal{I} \text{ such that } \lambda_m, \tilde{\lambda}_m \in \mathbb{R}^n \setminus B).$$

The following theorem says that sequence wich are asymptotically close have the same associated domains.

Theorem 1.18 (Theorem III.2.2, Kahane [40]). *Let Λ and $\tilde{\Lambda}$ be two regular sequences asymptotically close. Then an open set $D \subset \mathbb{R}^n$ is an associated domain to Λ if and only if is an associated domain to $\tilde{\Lambda}$.*

2. Internal exact observability of a perturbed plate equation

In this chapter we study the exact internal observability of a linear perturbed plate equation. More precisely, we prove that the exact observability of the unperturbed Euler-Bernoulli plate equation implies the exact observability of the perturbed equation. If the plate is rectangular, the results from the unperturbed case are conserved, in particular, we have the exact observability in an arbitrarily small time.

Parts of this chapter were published in Cîndea and Tucsnak [18].

2.1 Introduction and main results

Let $\Omega \subset \mathbb{R}^n$ ($n \in \mathbb{N}^*$) be an open and nonempty set with a C^2 boundary or a rectangle. We consider the following initial and boundary value problem :

$$\ddot{w}(x,t)+\Delta^2 w(x,t)-a\Delta w(x,t)+b(x)\cdot\nabla w(x,t)+c(x)w(x,t)=0, (x,t)\in\Omega\times(0,\infty) \quad (2.1)$$

$$w(x,t)=\Delta w(x,t)=0, \quad (x,t)\in\partial\Omega\times(0,\infty) \quad (2.2)$$

$$w(x,0)=w_0(x), \quad \dot{w}(x,0)=w_1(x), \quad x\in\Omega, \quad (2.3)$$

where $a>0$, $b\in(L^\infty(\Omega))^n$, $c\in L^\infty(\Omega)$, $w_0\in H^2(\Omega)\cap H_0^1(\Omega)$ and $w_1\in L^2(\Omega)$. We consider the following output

$$y(t)=\dot{w}(\cdot,t)|_{\mathcal{O}}, \quad (2.4)$$

where $\mathcal{O}$ is an open and nonempty subset of Ω and a dot denotes differentiation with respect to the time t:

$$\dot{w}=\frac{\partial w}{\partial t}, \quad \ddot{w}=\frac{\partial^2 w}{\partial t^2}.$$

For $n=2$ the equations (2.1)-(2.3) model the vibration of a perturbed Euler-Bernoulli plate with a hinged boundary.

The aim of this chapter is to study the exact observability of the system (2.1)-(2.4) in rapport with the exact observability of the unperturbed Euler-Bernoulli plate equation, i.e. (2.1)-(2.4) with $a=0$, $b=0$ and $c=0$. More precisely, the main result of this chapter is the following theorem :

Theorem 2.1. *Let $\mathcal{O} \in \Omega$ be an open and nonempty subset of Ω such that* (2.1)-(2.4) *is exactly observable for $a = 0$, $b = 0$, $c = 0$. Then* (2.1)-(2.4) *is exactly observable for every $a > 0$, $b \in (L^\infty(\Omega))^n$, $c \in L^\infty(\Omega)$.*

A necessary and sufficient condition for the exact observability of the wave equation is that the observation region $\mathcal{O}$ satisfies the geometric optic condition of Bardos, Lebeau and Rauch [9]. For the Euler-Bernoulli plate equation, it is known that the geometric optic condition is only a sufficient condition for the exact observability (see, for instance, Lebeau [46]). For example, if Ω is a rectangle, the Euler-Bernoulli plate equation is exactly observable in an arbitrarily small time for any open and nonempty observation region $\mathcal{O}$ (see, for instance, Jaffard [38] or Komornik [42]). This result is preserved for the perturbed plate equation (2.1)-(2.4), as it is formalized in the following theorem:

Theorem 2.2. *Assume that $n = 2$, Ω is a rectangle and let $\mathcal{O}$ be an open and nonempty subset of Ω. Then* $(2.1) - (2.4)$ *is exactly observable for every $a > 0$, $b \in (L^\infty(\Omega))^n$, $c \in L^\infty(\Omega)$ in any time $\tau > 0$.*

For proving the above two theorems, we consider an abstract formulation of our exact observability problem. More precisely, in Section 2.2 we prove two observability results for two linear abstract perturbed systems.

In the third section of this chapter, we prove the theorems 2.1 and 2.2, applying the abstract results from Section 2.2. A unique continuation result for the bi-Laplacian is proved in Section 2.3.1. For the proof of Theorem 2.2 we use some results of non-harmonic Fourier analysis introduced in Section 1.3.

2.2 Two exact observability results for second-order perturbed systems

Let H be a Hilbert space equipped with the norm $\|\cdot\|_H$ and let $A_0 : \mathcal{D}(A_0) \to H$ be a self-adjoint, positive and boundedly invertible operator, with compact resolvents. For such an operator A_0 we denote H_α the Hilbert space defined by $H_\alpha = (\beta I - A_0)^{-\alpha}(H)$ for any $\alpha \geqslant 0$ ($\beta \in \rho(A_0)$ is fixed) and $H_{-\alpha}$ is the dual space of H_α with respect to the pivot space H. In this section we prove the exact observability of two second-order abstract systems treated as linear perturbations of the following system :

$$\ddot{w}(t) + A_0^2 w(t) = 0, \tag{2.5}$$

$$w(0) = w_0, \quad \dot{w}(0) = w_1. \tag{2.6}$$

The system (2.5)-(2.6) can be described by a first order system. Indeed, if we denotes $X = H_1 \times H$, $\mathcal{D}(A) = H_2 \times H_1$ and

$$A : \mathcal{D}(A) \to X, \quad A \begin{bmatrix} f \\ g \end{bmatrix} = \begin{bmatrix} g \\ -A_0^2 f \end{bmatrix} \tag{2.7}$$

we can write (2.5)-(2.6) as

$$\dot{z}(t) = Az(t), \qquad z(0) = z_0,$$

where $z(t) = \begin{bmatrix} w(t) \\ \dot{w}(t) \end{bmatrix}$, $z_0 = \begin{bmatrix} w_0 \\ w_1 \end{bmatrix}$. The operator A defined above is a skew-adjoint operator and, therefore, generates a strongly continuous semigroup $(\mathbb{T}_t)_t$ on X.

Let $C_0 \in \mathcal{L}(H, Y)$ be an observation operator and let $C \in \mathcal{L}(X, Y)$ be its associated operator defined by $C = [0\, C_0]$, where Y is a Hilbert space equipped with the norm $\|\cdot\|_Y$. We say that (2.5)-(2.6) is exactly observable in rapport with the output $y(t) = C_0\dot{w}(t)$ if the pair (A, C) is exactly observable in the sense of Definition 1.4.

This section has two subsections. In subsection 2.2.1 we study the exact observability of equation (2.5)-(2.6) perturbed with the term aA_0w and in subsection 2.2.2 we study the exact observability of the same equation perturbed with a linear first-order term denoted P_0w.

2.2.1 From $\ddot{w} + A_0^2 w = 0$ to $\ddot{w} + A_0^2 w + aA_0 w = 0$

In this subsection we prove that the exact observability of the system (2.5)-(2.6), in rapport with the output $y(t) = C_0\dot{w}(t)$, implies the exact observability of the following initial value problem:

$$\ddot{v}(t) + A_0^2 v(t) + aA_0 v(t) = 0 \tag{2.8}$$

$$v(0) = v_0, \quad \dot{v}(0) = v_1, \tag{2.9}$$

in rapport with the same output, where $a > 0$.

We can state here the main result of this subsection.

Theorem 2.3. *Assume that the system* (2.5)-(2.6) *is exactly observable, i.e., there exist* $T > 0$ *and a constant* $k_T > 0$ *such that*

$$\int_0^T \|C_0\dot{w}(t)\|_Y^2 \, dt \geqslant k_T^2 \left(\|w_0\|_{H_1}^2 + \|w_1\|_H^2\right), \qquad \left(\begin{bmatrix} w_0 \\ w_1 \end{bmatrix} \in H_2 \times H_1\right). \tag{2.10}$$

Then the system (2.8)-(2.9) *is exactly observable in rapport with the observation* $y(t) = C_0\dot{v}(t)$, *i.e., there exist a time* $\tau > 0$ *and a constant* $k_\tau > 0$ *such that every solution of* (2.8)-(2.9) *satisfies*

$$\int_0^\tau \|C_0\dot{v}(t)\|_Y^2 \, dt \geqslant k_\tau^2 \left(\|v_0\|_{H_1}^2 + \|v_1\|_H^2\right), \qquad \left(\begin{bmatrix} v_0 \\ v_1 \end{bmatrix} \in H_2 \times H_1\right). \tag{2.11}$$

In order to write (2.8)-(2.9) as a first order system, we introduce the family of operators $(\widetilde{A_a})_{a>0}$, $\widetilde{A_a} : \mathcal{D}(\widetilde{A_a}) \to X$ defined by

$$\mathcal{D}(\widetilde{A_a}) = H_2 \times H_1, \qquad \widetilde{A_a} = \begin{bmatrix} 0 & I \\ -A_0^2 - aA_0 & 0 \end{bmatrix}. \tag{2.12}$$

Denoting $z(t) = \begin{bmatrix} v(t) \\ \dot{v}(t) \end{bmatrix}$ and $z_0 = \begin{bmatrix} v_0 \\ v_1 \end{bmatrix}$, (2.8)-(2.9) can be written as

$$\dot{z}(t) = \widetilde{A_a} z(t), \qquad z(0) = z_0.$$

The principal tool of the proof of the above theorem is Theorem 1.11. Applying the Hautus like spectral criterium, given by Theorem 1.11, is not enough for proving Theorem 2.3. We will need to separate the spectrum in two parts: a higher frequency part, which is observable with the spectral criterium, and a lower frequency part, wich is exactly observable from the exact observability of the unperturbed system. These ideas are formalized by Proposition 1.10.

We firstly prove the following lemma which give some information about the operator $\widetilde{A_a}$.

Lemma 2.4. *The operator $\widetilde{A_a} : \mathcal{D}(\widetilde{A_a}) \to X$ defined by (2.12) generates a strongly continuous group $(\mathbb{T}_t^a)_t$ on X. Every eigenvector of $\widetilde{A_a}$ is of the form*

$$\mathbf{\Phi}(a) = \frac{1}{\sqrt{2}} \begin{bmatrix} \frac{1}{i\mu(a)}\phi \\ \phi \end{bmatrix}, \tag{2.13}$$

the correspondig eigenvalue being $i\mu(a)$, where $\mu(a) = \pm\lambda(a)$ and ϕ, respectively $\lambda(a)$, are the eigenvectors, respectively the eigenvalues, of the operator $(A_0^2 + aA_0)^{\frac{1}{2}}$. Moreover, there exists an ortohormal basis of X formed by the eigenvectors $(\Phi_n(a))_{n\in\mathbb{Z}^*}$ of $\widetilde{A_a}$, and the corresponding family of eigenvalues $(i\mu_n(a))_{n\in\mathbb{Z}^*}$ satisfies $\lim_{n\to\infty} |\mu_n(a)| = +\infty$.

Proof. It is easy to prove that $(A_0^2 + aA_0)^{\frac{1}{2}}$ is a self-adjoint operator with compact resolvents. Then $\widetilde{A_a}$ is a skew-adjoint operator and, applying the classical Stone's theorem, $\widetilde{A_a}$ generates a strongly continuous group in X which we denote $(\mathbb{T}_t^a)_t$. The part of the lemma concerning the form of eigenvectors and eigenvalues of $\widetilde{A_a}$ is a direct consequence of Proposition 3.7.7 in [80]. □

Proof of Theorem 2.3. If we reformulate the systems (2.5)-(2.6) and (2.8)-(2.9) as first order systems, then the theorem can be enounced as : if the pair $(\widetilde{A_0}, C)$ is exactly observable then the pair $(\widetilde{A_a}, C)$ is exactly observable for any $a > 0$.

The proof is based on the spectral criterium for exact observability given by Theorem 1.11. In this purpose, for each $\omega \in \mathbb{R}$ and $\varepsilon > 0$ we denote

$$J_\varepsilon(\omega, a) = \{m \in \mathbb{Z}^* \text{ such that } |\mu_m(a) - \omega| < \varepsilon\}. \tag{2.14}$$

We say that φ_a, given by

$$\varphi_a = \sum_{m\in J_\varepsilon(\omega,a)} c_m \mathbf{\Phi}_m(a), \tag{2.15}$$

is a *wave package of center ω and radius ε* associated with the operator $\widetilde{A_a}$.

We assume that $(\widetilde{A_0}, C)$ is exactly observable. Then, from Theorem 1.11, there exist $\varepsilon > 0$ and $\delta > 0$ such that for any $\omega \in \mathbb{R}$ and $\varphi_0 = \sum_{m \in J_\varepsilon(\omega,0)} c_m \mathbf{\Phi}_m(0)$ we have

$$\|C\varphi_0\|_Y \geqslant \delta \|\varphi_0\|.$$

It is easy to see that

$$\lambda_m(a) = \lambda_m(0)\sqrt{1 + \frac{a}{\lambda_m(0)}} = \lambda_m(0) + \frac{a}{2} + \frac{a}{8} o(\lambda_m(0)^{-1}). \tag{2.16}$$

Nevertheless, $(\lambda_m(0))_m$ are the eigenvalues of A_0 and from the hypotheses that we supposed on A_0, we have that $|\lambda_m(0)| \to \infty$ when $m \to \infty$. Therefore, using the values of $\mu_m(a)$ from Lemma 2.4 and (2.16) we obtain that there exists $\omega(a) > 0$ such that for every $\omega \geqslant \omega(a)$ and $m \in J_\varepsilon(\omega, a)$ we have $|\mu_m(a)|^{-1} \leqslant 4$. Then, if $\omega \geqslant \omega(a)$, $m \in J_\varepsilon(\omega, a)$ is equivalent to

$$\left|\mu_m(0) - \frac{a}{2} - \frac{a}{8} o(\lambda_m(0)^{-1}) - \omega\right| < \varepsilon,$$

which is equivalent to

$$|\mu_m(0) - a - \omega| < \varepsilon$$

and, therefore, $m \in J_\varepsilon(\omega + a, 0)$. Also, we proved that $J_\varepsilon(\omega, a) = J_\varepsilon(\omega + a, 0)$ for every $\omega \geqslant \omega(a)$. For $a > 0$ fixed, we denote $J = \{\omega \in \mathbb{R} \text{ with } |\omega| < \omega(a)\}$ and

$$V = \text{span } \{\mathbf{\Phi}_m(a) \text{ such that } \mu_m(a) \in J\}.$$

Then we have the same wave packages for $\widetilde{A_{0V}}$ and $\widetilde{A_{aV}}$. Using the spectral criterium and the fact that $C\mathbf{\Psi}_m(a) = C\mathbf{\Phi}_m(0)$ for every $m \in \mathbb{Z}^*$, we have that the exact observability of $(\widetilde{A_{0V}}, C|_V)$ implies the exact observability of $(\widetilde{A_{aV}}, C|_V)$.

Since for every eigenvector $\mathbf{\Psi}(a)$ of $\widetilde{A_a}$ there exists an eigenvector $\mathbf{\Psi}(0)$ of $\widetilde{A_0}$ such that

$$C\mathbf{\Psi}(a) = C\mathbf{\Psi}(0),$$

using Proposition 1.10, we obtain the conclusion of the theorem. □

2.2.2 From $\ddot{w} + A_0^2 w = 0$ to $\ddot{w} + A_0^2 w + P_0 w = 0$

Let $0 < \varepsilon < \frac{1}{2}$ be a fixed constant and let $P_0 \in \mathcal{L}(H_{1-\varepsilon}, H)$ be a linear operator. We consider the following second-order system:

$$\ddot{v}(t) + A_0^2 v(t) + P_0 v(t) = 0, \qquad t > 0 \tag{2.17}$$

$$v(0) = v_0, \qquad \dot{v}(0) = v_1, \tag{2.18}$$

seen as a pertubation of (2.5)-(2.6). The aim of this subsection is to prove that the exact observability of (2.5)-(2.6) in rapport with the output $y(t) = C_0 \dot{w}(t)$, where $C_0 \in L(H, Y)$, implies the exact observability of (2.17)-(2.18) in rapport with the same output. The main result of this subsection is the following theorem.

Theorem 2.5. *Let H be a Hilbert space with the norm $\|\cdot\|_H$, let $A_0 : H_1 \to H$ be a self-adjoint, positive, boundedly invertible operator, with compact resolvents and let $P_0 \in \mathcal{L}(H_{1-\varepsilon}, H)$, with $0 < \varepsilon < 1$. Assume that (2.5)-(2.6) is exactly observable in time $\tau > 0$ with respect to the observation $y(t) = C_0\dot{w}(t)$, i.e., there exists a constant $k_\tau > 0$ such that any solution w of (2.5)-(2.6) satisfies*

$$\int_0^\tau \|C_0\dot{w}(t)\|_Y^2 \, dt \geqslant k_\tau^2 \left(\|w_0\|_{H_1}^2 + \|w_1\|_H^2\right), \qquad \left(\begin{bmatrix} w_0 \\ w_1 \end{bmatrix} \in H_2 \times H_1\right).$$

If $C_0\phi \neq 0$ for every eigenvector ϕ of $A_0^2 + P_0$ then (2.17)-(2.18) is exactly observable in any time $T \geqslant \tau$, i.e., there exists a constant $k_T > 0$ such that any solution v of (2.17)-(2.18) satisfies

$$\int_0^T \|C_0\dot{v}(t)\|_Y^2 \, dt \geqslant k_T^2 \left(\|v_0\|_{H_1}^2 + \|v_1\|_H^2\right), \qquad \left(\begin{bmatrix} v_0 \\ v_1 \end{bmatrix} \in H_2 \times H_1\right).$$

If $A : H_2 \times H_1 \to H_1 \times H$ is the operator defined by (2.7), we denote $P = \left[\begin{smallmatrix} 0 & 0 \\ -P_0 & 0 \end{smallmatrix}\right]$ and $C = [0 \; C_0] \in \mathcal{L}(H_1 \times H, Y)$. We can consider $P \in \mathcal{L}(H_{1-\varepsilon} \times H_{-\varepsilon}, H_1 \times H)$. Then $A_P : H_2 \times H_1 \to H_1 \times H$, with $A_P = A + P$, is well defined. Since P can be seen as an operator in $\mathcal{L}(H_1 \times H)$, according to Theorem 1.1 from Pazy [59, p.76], A_P is the generator of a strongly continuous semigroup in $H_1 \times H$, denoted $\left(\mathbb{T}_t^P\right)_{t\geqslant 0}$.

The following lemmas are usefull for the proof of Theorem 2.5.

Lemma 2.6. *Let $\beta \in \rho(A) \cap \rho(A_P)$, $0 < \varepsilon < \frac{1}{2}$ and let $G \in \mathcal{L}(H_{1-\varepsilon} \times H_{-\varepsilon}, H_1 \times H)$ be the compact operator defined by*

$$G = (\beta I - A_P)^{-\varepsilon}. \tag{2.19}$$

In the hypotheses of Theorem 2.5, there exists a positive constant C_T such that

$$\int_0^T \|C_0\dot{\psi}(t)\|_Y^2 \, dt \leqslant C_T \left\| G \begin{bmatrix} w_0 \\ w_1 \end{bmatrix} \right\|_{H_1 \times H}^2, \qquad \left(\begin{bmatrix} w_0 \\ w_1 \end{bmatrix} \in H_1 \times H\right), \tag{2.20}$$

where ψ is the solution of

$$\ddot{\psi}(t) + A_0^2\psi(t) + P_0\psi(t) = -P_0 w(t), \qquad t \in (0, \infty) \tag{2.21}$$

$$\psi(0) = \dot{\psi}(0) = 0 \tag{2.22}$$

and w is the solution of (2.5)-(2.6).

Proof. Since $C_0 \in \mathcal{L}(H, Y)$ we have the following estimate:

$$\|C_0\dot{\psi}\|_{C([0,T];Y)} \leqslant \|C_0\|_{\mathcal{L}(H,Y)} \|\dot{\psi}\|_{C([0,T];H)} \leqslant \|C_0\|_{\mathcal{L}(H,Y)} \|\Psi\|_{C([0,T];H_1\times H)},$$

where $\Psi(t) = \begin{bmatrix} \psi(t) \\ \dot{\psi}(t) \end{bmatrix}$ is the solution of the following initial value problem

$$\dot{\Psi}(t) = A_P\Psi(t) + P \begin{bmatrix} w(t) \\ \dot{w}(t) \end{bmatrix}, \qquad \Psi(0) = 0. \tag{2.23}$$

Then, there exists a constant $\tilde{C}_T > 0$ such that

$$\|\Psi\|_{C([0,T];H_1\times H)} \leqslant \tilde{C}_T \left\| P \begin{bmatrix} w \\ \dot{w} \end{bmatrix} \right\|_{L^1([0,T];H_1\times H)} = \tilde{C}_T \|P_0 w\|_{L^1([0,T];H)}.$$

Since $P_0 \in \mathcal{L}(H_{1-\varepsilon}, H)$, combining the above inequalities, we obtain

$$\|C_0\dot{\psi}\|_{C([0,T];Y)} \leqslant \tilde{C}_T \|C_0\|_{\mathcal{L}(H,Y)} \|P_0\|_{\mathcal{L}(H_{1-\varepsilon},H)} \|w\|_{L^1([0,T];H_{1-\varepsilon})}. \tag{2.24}$$

We recall that w is the solution of (2.5)-(2.6) and, therefore, we can bound its L^1 norm by the norm of the initial data. We have that

$$\|w\|_{L^1([0,T];H_{1-\varepsilon})} \leqslant C_T \left\| \begin{bmatrix} w_0 \\ w_1 \end{bmatrix} \right\|_{H_{1-\varepsilon}\times H_{-\varepsilon}}. \tag{2.25}$$

Using the fact that $(\beta I - A)^{-\varepsilon}$ is a unitary operator from $H_{1-\varepsilon} \times H_{-\varepsilon}$ onto $H_1 \times H$, we obtain

$$\left\| \begin{bmatrix} w_0 \\ w_1 \end{bmatrix} \right\|_{H_{1-\varepsilon}\times H_{-\varepsilon}} = \left\| (\beta I - A)^{-\varepsilon} \begin{bmatrix} w_0 \\ w_1 \end{bmatrix} \right\|_{H_1\times H}. \tag{2.26}$$

Since P can be seen as a bounded operator in $\mathcal{L}(H_1 \times H)$, the norm $\|(\beta I - A_P)^{-1} z\|$ is an equivalent norm to $\|(\beta I - A)^{-1} z\|$ in $H_1 \times H$ (see for a proof, for instance [80, Section 2.10]). Using an interpolation argument and the estimates (2.24)-(2.26), we can conclude that there exists a constant $C_T > 0$ such that

$$\|C_0\dot{\psi}\|_{C([0,T];Y)} \leqslant C_T \left\| G \begin{bmatrix} w_0 \\ w_1 \end{bmatrix} \right\|_{H_1\times H}$$

and the proof of the lemma is complete. □

Lemma 2.7. *Denote*

$$\mathcal{N}(T) = \left\{ W_0 = \begin{bmatrix} w_0 \\ w_1 \end{bmatrix} \in H_1 \times H \mid C\mathbb{T}_t^P W_0 = 0, \quad \textit{for any } t \in [0,T] \right\}. \tag{2.27}$$

In the hypotheses of Theorem 2.5, the set $\mathcal{N}(T)$ contains only the zero element.

Proof. The solution v of (2.17)-(2.18) can be written as $v = w + \psi$, where w is the solution of the unperturbed system (2.5)-(2.6) and ψ is the solution of (2.21)-(2.22). Then we have

$$\int_0^T \|C_0\dot{v}(t)\|_Y^2 \, \mathrm{d}t + \int_0^T \|C_0\dot{\psi}(t)\|_Y^2 \, \mathrm{d}t \geqslant \frac{1}{2} \int_0^T \|C_0\dot{w}(t)\|_Y^2 \, \mathrm{d}t. \tag{2.28}$$

Using the observability of the unperturbed equation (2.5)-(2.6), we obtain from (2.28) that exists a constant $k_T > 0$ such that

$$\int_0^T \|C_0\dot{v}(t)\|_Y^2 \, \mathrm{d}t + \int_0^T \|C_0\dot{\psi}(t)\|_Y^2 \, \mathrm{d}t \geqslant \frac{k_T^2}{2} (\|w_0\|_{H_1}^2 + \|w_1\|_H^2). \tag{2.29}$$

From (2.29) and Lemma 2.6 we obtain

$$\int_0^T \|C_0\dot{v}(t)\|_Y^2 \, \mathrm{d}t + C_T \left\| G \begin{bmatrix} w_0 \\ w_1 \end{bmatrix} \right\|_{H_1\times H}^2 \geqslant \frac{1}{2} k_T^2 (\|w_0\|_{H_{\frac{1}{2}}}^2 + \|w_1\|^2), \qquad \left(\begin{bmatrix} w_0 \\ w_1 \end{bmatrix} \in H_1 \times H \right), \tag{2.30}$$

where G is the operator defined by (2.19).

Let $W_0 = [\begin{smallmatrix} w_0 \\ w_1 \end{smallmatrix}]$ be an element of $\mathcal{N}(T)$. Then from (2.30) we have

$$C_T \|GW_0\|_{H_1\times H}^2 \geqslant \frac{1}{2} k_T^2 \|W_0\|_{H_1\times H}^2. \tag{2.31}$$

Using a classical compacity and unicity argument, it follows that $\mathcal{N}(T)$ is a finite dimensional space. It is clear that for $\delta \in (0,T)$, if $W_0 \in \mathcal{N}(T)$ then $\mathbb{T}_t^P W_0 \in \mathcal{N}(T-\delta)$ for each $0 < t < \delta$. Since A_P commutes with $(\beta I - A_P)^{-1}$, we can write

$$G^{\frac{1}{\varepsilon}} \frac{\mathbb{T}_t^P - I}{t} W_0 = \frac{\mathbb{T}_t^P - I}{t} G^{\frac{1}{\varepsilon}} W_0 \to A_P G^{\frac{1}{\varepsilon}} W_0 = G^{\frac{1}{\varepsilon}} A_P W_0, \text{ when } t \to 0.$$

So, $\left(\frac{\mathbb{T}_t^P - I}{t} W_0 \right)_t$ is a Cauchy family for the norm $W \mapsto \|(\beta I - A_P)^{-1} W\|$ in $\mathcal{N}(T-\delta)$ and, also, for the norm $W \mapsto \|W\|$. Then $\mathcal{N}(T) \subset \mathcal{D}(A_P)$. Moreover, we will show that $\mathcal{N}(T)$ is stable in rapport with A_P. Let $W_0 = \begin{bmatrix} w_0 \\ w_1 \end{bmatrix} \in \mathcal{N}(T)$. From (2.27) we have

$$C\mathbb{T}_t^P W_0 = 0, \qquad (t \in [0,T]).$$

After differentiation in rapport with t, the relation above becomes

$$C\mathbb{T}_t^P A_P W_0 = 0, \qquad (t \in [0,T]),$$

and, therefore, $\mathcal{N}(T)$ is A_P-stable.

Assume that $\mathcal{N}(t) \neq \{0\}$. Since $\mathcal{N}(T)$ is finite dimensional and A_P-stable, then it contains an eigenvector of A_P. Let $W_0 = \begin{bmatrix} w_0 \\ w_1 \end{bmatrix} \in \mathcal{N}(T)$ be a eigenvector of A_P. Then exists $\lambda \neq 0$ such that

$$A_P W_0 = \lambda W_0,$$

and, so, w_1 is an eigenvector of $A_0^2 + P_0$. From the definition of $\mathcal{N}(T)$ we obtain that $C_0 w_1 = 0$ which contradicts the assumtion of Theorem 2.5 that $C_0\phi \neq 0$ for every eigenvector ϕ of $A_0^2 + P_0$. □

Proof of Theorem 2.5 . The idea of the proof is to show that in (2.30), from Lemma 2.6, we can remove the term $C_T\|GW_0\|_{H_1\times H}^2$ and thus we obtain the requested observability inequality

$$\int_0^T \|C\mathbb{T}_t^P W_0\|_Y^2 \, \mathrm{d}t \geqslant \frac{1}{2} k_T^2 \|W_0\|_{H_1\times H}^2, \qquad (W_0 \in H_2 \times H_1). \tag{2.32}$$

Assume that there exists a sequence $(W_0^n)_n \in H_1 \times H$ such that $\|W_0^n\|_{H_1\times H} = 1$ and

$$\int_0^T \|C\mathbb{T}_t^P W_0^n\|_Y^2 \, \mathrm{d}t \to 0, \quad \text{when } n \to \infty,$$

which contradicts (2.32). Since the operator $G = (\beta I - A_P)^{-\varepsilon}$, given by Lemma 2.6, is compact, we can extract a subsequence of $(W_0^n)_n$, denoted with the same notation, such that

$$GW_0^n \to GW_0 \in H_1 \times H, \text{ when } n \to \infty,$$

where $W_0 \in H_1 \times H$. Passing to the limit in (2.30), we obtain

$$C_T \|GW_0\|_{H_1\times H}^2 \geqslant \frac{1}{2} k_T^2$$

that is

$$\|GW_0\|_{H_1\times H}^2 \geqslant \frac{k_T^2}{2C_T} > 0,$$

and so, $W_0 \neq 0$. Recall that

$$\int_0^T \|C\mathbb{T}_t^P W_0\|_Y^2 \, \mathrm{d}t = 0,$$

which implies

$$C\mathbb{T}_t^P W_0 = 0, \qquad (t \in (0,T)).$$

Also, we proved that $W_0 \in \mathcal{N}(T)$ and $W_0 \neq 0$. This is in contradiction with the result of Lemma 2.7, and so the observability inequality (2.32) is true. □

2.3 Proof of main results

In this section, before proving the main results announced in Section 2.1, we prove two exact observability results for a simpler problem. More precisely, consider the following initial and boundary value problem :

$$\ddot{w}(x,t) + \Delta^2 w(x,t) - a\Delta w(x,t) = 0, \qquad (x,t) \in \Omega \times (0,\infty) \tag{2.33}$$

$$w(x,t) = \Delta w(x,t) = 0, \qquad (x,t) \in \partial\Omega \times (0,\infty), \tag{2.34}$$

$$w(x,0) = w_0(x), \qquad \dot{w}(0) = w_1(x), \qquad x \in \Omega, \tag{2.35}$$

where $a \geqslant 0$, $w_0 \in H^2(\Omega) \cap H_0^1(\Omega)$, $w_1 \in L^2(\Omega)$ and Ω is an open and nonempty set in $\mathbb{R}^n$ for a certain $n \in \mathbb{N}^*$. Consider the observation output given by:

$$y(t) = \dot{w}(\cdot,t)|_{\mathcal{O}}, \tag{2.36}$$

where $\mathcal{O}$ is an open subset of Ω.

Proposition 2.8. *Let $\mathcal{O}$ be an open and nonempty subset of Ω such that* (2.33)-(2.35) *is exactly observable in rapport with the observation* (2.36) *for $a = 0$. Then the system* (2.33)-(2.36) *is exactly observable for every $a > 0$.*

Proof. Denote, for the remaining part of this section, $H = L^2(\Omega)$ and $A_0 : H_1 \to H$

$$H_1 = H^2(\Omega) \cap H_0^1(\Omega), \qquad A_0\varphi = -\Delta\varphi, \qquad (\varphi \in H_1).$$

Using these notation, (2.33)-(2.35) can be written as

$$\ddot{w}(t) + A_0^2 w(t) + aA_0 w(t) = 0, \qquad t > 0$$

$$w(0) = w_0, \qquad \dot{w}(0) = w_1.$$

It is well known that the operator A_0 defined above is a self-adjoint, positive and boundedly invertible operator, with compact resolvents and we assumed that the corresponding unperturbed equation is exactly observable. Then, applying Theorem 2.3, we obtain the exact observability of (2.33)-(2.36). □

Proposition 2.9. *Let $\Omega = (0, l_1) \times (0, l_2)$ be a rectangle in $\mathbb{R}^2$ and $\mathcal{O}$ an open and nonempty subset of Ω. Then* (2.33)-(2.36) *is exactly observable in any time $\tau > 0$.*

Our approach for proving Proposition 2.9 follows closely the ideas from Tucsnak and Weiss [80, Section 8.5] and Jaffard [38]. Here we use the results on the pseudo-periodic functions, borrowed from Kahane [40], and recalled in Section 1.3. Before proving Proposition 2.9, we prove the following proposition:

Proposition 2.10. *Let $r, s, a > 0$ and let $\Lambda \in l^2(\mathbb{Z}^2, \mathbb{R}^3)$ be defined by*

$$\lambda_{mn} = \begin{bmatrix} m\sqrt{r} \\ n\sqrt{s} \\ rm^2 + sn^2 + \frac{a}{2} + \varepsilon_{mn} \end{bmatrix}, \tag{2.37}$$

where $(\varepsilon_{mn})_{m,n} \in l^2(\mathbb{Z}^2, \mathbb{R})$ is a sequence such that $\varepsilon_{mn} \to 0$ when $m^2 + n^2 \to \infty$. Then any ball of strictly positive radius in $\mathbb{R}^3$ is a domain associated to Λ.

In order to prove Proposition 2.10, we need some notation and a lemma. For the remaining part of this section, we denote $(\varepsilon_{mn})_{m,n} \in l^2(\mathbb{Z}^2, \mathbb{R})$ a sequence such that $\varepsilon_{mn} \to 0$ when $m^2 + n^2 \to \infty$. For any $R > 0$ and $\left[\begin{smallmatrix} k \\ l \end{smallmatrix}\right] \in \mathbb{Z}^2 \setminus \left[\begin{smallmatrix} 0 \\ 0 \end{smallmatrix}\right]$ with $|k| < R$ and $|l| < R$ we define

$$S_{R,k,l} = \left\{ \begin{bmatrix} m \\ n \end{bmatrix} \in \mathbb{Z}^2 \text{ such that } |2rkm + 2sln + \varepsilon_{m+k,n+l} - \varepsilon_{mn}| < 3R^2 \right\}, \tag{2.38}$$

and we introduce the subsequence $\Lambda_{R,k,l} = (\lambda_{mn})_{\left[\begin{smallmatrix} m \\ n \end{smallmatrix}\right] \in S_{R,k,l}}$ of Λ.

Lemma 2.11. *With the above notation, any ball in $\mathbb{R}^3$ of strictly positive radius is a domain associated to $\Lambda_{R,k,l}$.*

Proof. Without loss of generality we can assume that $k \neq 0$. Then the condition $\left[\begin{smallmatrix} m \\ n \end{smallmatrix}\right] \in S_{R,k,l}$ implies that exists a constant $c > 0$ such that

$$rm^2 + sn^2 + \frac{a}{2} + \varepsilon_{mn} = cn^2 + O(n). \tag{2.39}$$

Indeed, from (2.38), denoting $\delta_{mn} = \varepsilon_{m+k,n+l} - \varepsilon_{mn}$, we have

$$-3R^2 < 2rkm + 2sln + \delta_{mn} < 3R^2$$

and, so,

$$4r^2k^2m^2 < 9R^4 - 6\delta_{mn}R^2 + \delta_{mn}^2 + 4sln(\delta_{mn} - 3R^2) + 4s^2l^2n^2.$$

Dividing with $4rk^2$ we can write the relation bellow as

$$rm^2 + sn^2 = \left(\frac{s^2l^2}{rk^2} + s\right)n^2 + \frac{9R^4 - 6\delta_{mn}R^2 + \delta_{mn}^2 + 4sln(\delta_{mn} - 3R^2)}{4rk^2}$$

But, $\delta_{mn} \to 0$ when $m^2 + n^2 \to \infty$ so the estimation (2.39) is proved. Then the number of terms of $\Lambda_{R,k,l}$ contained in a ball of center $b = \left[\begin{smallmatrix} b_1 \\ b_2 \\ b_3 \end{smallmatrix}\right]$ and of radius $d > 0$ is bounded by the number of terms of the sequence $(rm^2 + sn^2 + \frac{a}{2} + \varepsilon_{mn})_{\left[\begin{smallmatrix} m \\ n \end{smallmatrix}\right] \in S_{R,k,l}}$ in $(b_3 - d, b_3 + d)$. Relation (2.39) implies that, after possibly eliminating a finite number of terms, the sequence $\Lambda_{R,k,l}$ can be rewritten as a sequence $\left[\begin{smallmatrix} \alpha_n \\ \beta_n \\ \gamma_n \end{smallmatrix}\right]$ with γ_n strictly increasing and

$$\gamma_{n+p} - \gamma_n \geqslant c(2np + p^2) + O(n).$$

By choosing p large enough it follows

$$\gamma_{n+p} - \gamma_n \geqslant np.$$

Consequently, the number of terms of $\Lambda_{R,k,l}$, contained in a ball of center b and of radius d is smaller then $c(\sqrt{|b_3| + d} - \sqrt{|b_3| - d} + 1)$, which tends to 1 when $b_3 \to \infty$. The conclusion follows now by applying Theorem 1.16. □

Proof of Proposition 2.10. We can assume without loss of generality that $r, s \in (0, 1]$. Let $\varepsilon > 0, R > max(1, 2\alpha/\varepsilon)$, where α is the constant given by Proposition 1.13, and let $\mathcal{I}_R$ be the union of all strips $s_{R,k,l}$ with $k^2 + l^2 \neq 0$, $|k| \leqslant R$ and $|l| \leqslant R$. Denote $\Lambda_1 = (\lambda_{mn})_{\left[\begin{smallmatrix} m \\ n \end{smallmatrix}\right] \in \mathcal{I}_R}$. Then

$$\Lambda_1 = \bigcup_{\substack{k,l \in [-R,R] \\ k^2 + l^2 \neq 0}} \Lambda_{R,k,l}.$$

Applying Theorem 1.15 and Lemma 2.11, any ball in $\mathbb{R}^3$ of strictly positive radius is a domain associated to Λ_1.

Let $\mathcal{J}_R = \mathbb{Z}^2 \setminus \mathcal{I}_R$ and let $\Lambda_2 = (\lambda_{mn})_{\left[\begin{smallmatrix} m \\ n \end{smallmatrix}\right] \in \mathcal{J}(R)}$, so that $\Lambda = \Lambda_1 \cup \Lambda_2$. Let $\left[\begin{smallmatrix} m \\ n \end{smallmatrix}\right], \left[\begin{smallmatrix} m' \\ n' \end{smallmatrix}\right] \in \mathcal{J}_R$ with $\left[\begin{smallmatrix} m \\ n \end{smallmatrix}\right] \neq \left[\begin{smallmatrix} m' \\ n' \end{smallmatrix}\right]$. If $|m - m'| \geqslant R$ or $|n - n'| \geqslant R$ then $|\lambda_{mn} - \lambda_{m'n'}| \geqslant R$. If

$|m-m'|<R$ and $|n-n'|<R$ then there exist $k,l\in[-R,R]\cap\mathbb{Z}$ with $k^2+l^2\neq 0$ such that

$$m'=m+k,\quad n'=n+l.$$

Then, by using the facts that $\left[\begin{smallmatrix}m\\n\end{smallmatrix}\right]\notin\mathcal{I}_R$, $r,s\in(0,1]$ and $R>1$, it follows that

$$\begin{aligned}\left|rm^2+sn^2+\varepsilon_{mn}-rm'^2-sn'^2-\varepsilon_{m'n'}\right|&=|\varepsilon_{mn}-2rmk-2snl-rk^2-sl^2-\varepsilon_{m'n'}|\\&\geqslant|2rmk+2snl+\varepsilon_{m+k,n+l}-\varepsilon_{mn}|-|rk^2+sl^2|>3R^2-rR^2-sR^2\geqslant R^2\geqslant R.\end{aligned}$$

Therefore we proved that

$$\inf_{\substack{\lambda,\mu\in\Lambda_2\\ \lambda\neq\mu}}|\lambda-\mu|\geqslant R,$$

then, by Proposition 1.13, we have that any ball of radius $\varepsilon/2$ is a domain associated to Λ_2 so that, by applying Theorem 1.15, we obtain that any ball of radius ε is a domain associated to Λ. □

Proof of Proposition 2.9. We use the same notation as in the proof of Proposition 2.8, and we denote $A_1:H_1\to H$

$$A_1=\left(A_0^2+aA_0\right)^{\frac{1}{2}}.$$

Denote $(\mu_{mn})_{m,n\in\mathbb{Z}^*}$ the eigenvalues and $(\phi_{mn})_{m,n\in\mathbb{N}^*}$ the eigenvectors of $A_0=-\Delta$:

$$\mu_{mn}=rm^2+sn^2,\qquad(m,n\in\mathbb{N}^*),$$

where $r=\left(\frac{\pi}{l_1}\right)^2$ and $s=\left(\frac{\pi}{l_2}\right)^2$ and the corresponding orthonormal basis of eigenvectors of A_0 is given by

$$\phi_{mn}(x,y)=\frac{2}{\sqrt{l_1l_2}}\sin(\sqrt{r}mx)\sin(\sqrt{s}ny),\qquad(m,n\in\mathbb{N}^*).$$

It is easy to see that the operator A_1 has the same eigenvectors (ϕ_{mn}) and the eigenvalues $\tilde{\lambda}_{mn}$ given by

$$\tilde{\mu}_{mn}=rm^2+sn^2+\frac{a}{2}+\varepsilon_{mn},$$

where $\varepsilon_{mn}\to 0$ when $m^2+n^2\to\infty$.

The above facts imply that the semigroup $\mathbb{S}$ generated by iA_1 satisfies

$$\mathbb{S}_tz=\sum_{m,n}z_{mn}e^{i(rm^2+sn^2+\frac{a}{2}+\varepsilon_{mn})t}\phi_{mn},\quad\forall z\in\mathcal{D}(A_0^{\frac{1}{2}}),$$

where we denoted

$$z_{mn}=\langle z,\phi_{mn}\rangle,\quad\forall m,n\in\mathbb{N}.$$

Let $\tau > 0$ and let $C_0 z = z\,|_{\mathcal{O}}$. Then

$$\int_0^\tau \|C_0 \mathbb{S}_t z\|^2 \,\mathrm{d}t = \int_0^\tau \int_{\mathcal{O}} \left| \sum_{m,n\in\mathbb{N}} z_{mn} e^{i(rm^2+sn^2+\frac{a}{2}+\varepsilon_{mn})t} \phi_{mn}(x,y) \right|^2 \mathrm{d}x\mathrm{d}y\mathrm{d}t$$

$$= \frac{4}{l_1 l_2} \int_0^\tau \int_{\mathcal{O}} \left| \sum_{m,n\in\mathbb{N}} z_{mn} e^{i(rm^2+sn^2+\frac{a}{2}+\varepsilon_{mn})t} \sin(\sqrt{r}mx)\sin(\sqrt{s}ny) \right|^2 \mathrm{d}x\mathrm{d}y\mathrm{d}t \quad (2.40)$$

Let us extend the sequence (z_{mn}) by setting

$$z_{-m,n} = -z_{mn},\ z_{m,-n} = -z_{mn},\ z_{-m,-n} = z_{mn}, \quad \forall m,n \in \mathbb{N}.$$

Then (2.40) can be written as

$$\int_0^\tau \|C_0 \mathbb{S}_t z\|^2 \,\mathrm{d}t = \frac{1}{iab} \int_0^\tau \int_{\mathcal{O}} \left| \sum_{m,n\in\mathbb{Z}^*} z_{mn} e^{i\lambda_{mn}\cdot \begin{bmatrix} x \\ y \\ t \end{bmatrix}} \right|^2 \mathrm{d}x\mathrm{d}y\mathrm{d}t,$$

where (λ_{mn}) is defined by (2.37). By Proposition 2.10 $(\lambda_{mn})_{mn}$ is a sequence associated to the domain $\mathcal{O}\times(0,\tau)$ for any $\tau > 0$ and any open and nonempty $\mathcal{O} \in \Omega$. Using now the definition of associated sequence to a domain there exists a constant $c > 0$ such that

$$\int_0^\tau \|C_0 \mathbb{S}_t z\|^2 \,\mathrm{d}t \geqslant c^2 \sum_{m,n\in\mathbb{Z}^*} |z_{mn}|^2,$$

so that the pair (iA_1, C_0) is exactly observable in any time $\tau > 0$. Using Proposition 6.8.2 from [80] we have the exact observability of (2.33)-(2.36) in the rectangle $(0,l_1)\times(0,l_2)$ in any time $\tau > 0$. □

The idea of the proof of Theorem 2.2 and Theorem 2.1 is to apply Theorem 2.5, considering a linear perturbation of equation (2.33). In order to apply Theorem 2.5, we need a unique continuation result for bi-Laplacian which we be proved using a global Carleman estimate.

2.3.1 A unique continuation result for bi-Laplacian

The aim of this section is to prove the following proposition :

Proposition 2.12. *Let $a \in (0,\infty)$, $b \in (L^\infty(\Omega))^n$, $c \in L^\infty(\Omega)$, $\mu \in \mathbb{R}$ and let $u \in H^4(\Omega)$ be a function such that*

$$\Delta^2 u - a\Delta u + b\cdot\nabla u + cu = \mu^2 u \qquad \text{in } \Omega \quad (2.41)$$

$$u = \Delta u = 0 \qquad \text{on } \partial\Omega \quad (2.42)$$

and

$$u = 0 \quad \text{in } \mathcal{O}. \quad (2.43)$$

Then $u = 0$ in Ω.

The key of the proof of Proposition 2.12 is a global Carleman estimate for bi-Laplacian (Theorem 2.15), which we obtained applying two times a particular case of the global Carleman estimate proved by Imanuvilov and Puel in [35].

Let Ω be an nonempty open set of class C^2. Let $y \in H^2(\Omega) \cap H_0^1(\Omega)$ be the solution of the problem

$$\Delta y = f, \quad \text{in } \Omega \tag{2.44}$$
$$y = 0, \quad \text{on } \partial\Omega, \tag{2.45}$$

where $f \in L^2(\Omega)$. We use the following classic lemma stated in [35], and proved in Fursikov-Imanuvilov [30].

Lemma 2.13. *Let $\mathcal{O}$ be an open and nonempty subset of Ω. Then there exists a function $\psi \in C^2(\overline{\Omega})$ such that*

$$\psi = 0, \qquad \text{on } \partial\Omega \tag{2.46}$$
$$\psi(x) > 0, \qquad \forall\, x \in \Omega \tag{2.47}$$
$$|\nabla\psi(x)| > 0, \quad \forall\, x \in \overline{\Omega \setminus \mathcal{O}}. \tag{2.48}$$

We consider a weight function

$$\varphi(x) = e^{\lambda\psi(x)}, \tag{2.49}$$

where $\lambda \geqslant 1$ will be chosen later.

Using the definition of the function φ, and the properties of function ψ given by Lemma 2.13, we have

$$\frac{1}{\varphi(x)} = \frac{1}{e^{\lambda\psi(x)}} = e^{-\lambda\psi(x)} \leqslant 1 \leqslant e^{2\lambda\psi(x)} = \varphi^2(x), \tag{2.50}$$

for all $\lambda \geqslant 1$.

The following theorem is a particular case of the Carleman estimate proved by Imanuvilov Puel [35] for general elliptic operators.

Theorem 2.14. *Assume that hypotheses* (2.46)-(2.49) *are verified and let $y \in H^2(\Omega) \cap H_0^1(\Omega)$ be the solution of* (2.44)-(2.45)*. Then there exists a constant $C > 0$ independent of s and λ, and parameters $\widehat{\lambda} > 1$ and $\widehat{s} > 1$ such that for all $\lambda \geqslant \widehat{\lambda}$ and for all $s > \widehat{s}$ such that*

$$\int_\Omega |\nabla y|^2 e^{2s\varphi}\mathrm{d}x + s^2\lambda^2 \int_\Omega |y|^2\varphi^2 e^{2s\varphi}\mathrm{d}x \leqslant C\left(\frac{1}{s\lambda^2}\int_\Omega \frac{|f|^2}{\varphi}e^{2s\varphi}\mathrm{d}x + \int_{\mathcal{O}} \left(|\nabla y|^2 + s^2\lambda^2\varphi^2|y|^2\right) e^{2s\varphi}\mathrm{d}x\right). \tag{2.51}$$

Let $u \in H^4(\Omega)$ be the solution of the problem

$$\Delta^2 u - a\Delta u = g, \quad \text{in } \Omega \tag{2.52}$$
$$u = \Delta u = 0, \quad \text{on } \partial\Omega, \tag{2.53}$$

where $g \in L^2(\Omega)$.

Theorem 2.15. *Let $\psi \in C^2(\overline{\Omega})$ be a function such that (2.46)-(2.48) are verified and let φ given by (2.49). Let $u \in H^4(\Omega)$ be a solution of (2.52)-(2.53). Then there exist $\widehat{s} > 1$, $\widehat{\lambda} > 1$ and a constant $C > 0$ independent of $s \geqslant \widehat{s}$ and $\lambda \geqslant \widehat{\lambda}$, such that*

$$s\lambda^2 \int_\Omega \left(|\nabla(\Delta u)|^2 + s^3\lambda^4|\nabla u|^2 + s^5\lambda^6|u|^2\varphi^2\right) e^{2s\varphi}\mathrm{d}x \leqslant C\left(\int_\Omega \frac{|g|^2}{\varphi} e^{2s\varphi}\mathrm{d}x \right.$$
$$\left. + s\lambda^2 \int_{\mathcal{O}} (|\nabla(\Delta u)|^2 + s^2\lambda^2\varphi^2|\Delta u|^2 + s^3\lambda^4|\nabla u|^2 + s^5\lambda^6\varphi^2|u|^2) e^{2s\varphi}\mathrm{d}x\right). \tag{2.54}$$

Proof. We denote $y = \Delta u$ and $g_1 = g + a\Delta u$. Then (2.52) and the last part of (2.53) can be written as

$$\Delta y = g_1, \quad \text{in } \Omega \tag{2.55}$$
$$y = 0, \quad \text{on } \partial\Omega \tag{2.56}$$

Then we can apply Theorem 2.14, so there exists $s_1 > 1$, $\lambda_1 > 1$ and $C_1 > 0$ independent of s and λ such that for all $s \geqslant s_1$, $\lambda \geqslant \lambda_1$ the following estimate is satisfied

$$s\lambda^2 \int_\Omega |\nabla y|^2 e^{2s\varphi}\mathrm{d}x + s^3\lambda^4 \int_\Omega |y|^2\varphi^2 e^{2s\varphi}\mathrm{d}x \leqslant$$
$$C_1\left(\int_\Omega |g_1|^2\varphi^{-1}e^{2s\varphi}\mathrm{d}x + \int_{\mathcal{O}} \left(s\lambda^2|\nabla y|^2 + s^3\lambda^4\varphi^2|y|^2\right) e^{2s\varphi}\mathrm{d}x\right) \leqslant$$
$$C_1\left(2\int_\Omega (|g|^2\varphi^{-1} + a^2|\Delta u|^2\varphi^2) e^{2s\varphi}\mathrm{d}x + \int_{\mathcal{O}} \left(s\lambda^2|\nabla y|^2 + s^3\lambda^4\varphi^2|y|^2\right) e^{2s\varphi}\mathrm{d}x\right),$$

where bellow we used (2.50). Replacing y with Δu in the previous estimate, we obtain

$$s\lambda^2 \int_\Omega |\nabla(\Delta u)|^2 e^{2s\varphi}\mathrm{d}x + (s^3\lambda^4 - 2a^2C_1) \int_\Omega |\Delta u|^2\varphi^2 e^{2s\varphi}\mathrm{d}x \leqslant$$
$$C_1\left(2\int_\Omega |g|^2\varphi^{-1}e^{2s\varphi}\mathrm{d}x + \int_{\mathcal{O}} \left(s\lambda^2|\nabla(\Delta u)|^2 + s^3\lambda^4\varphi^2|\Delta u|^2\right) e^{2s\varphi}\mathrm{d}x\right). \tag{2.57}$$

Now consider the problem

$$\Delta u = y, \quad \text{in } \Omega \tag{2.58}$$
$$u = 0, \quad \text{on } \partial\Omega, \tag{2.59}$$

and apply Theorem 2.14. Then there exists a constant $C_2 > 0$, $s_2 > 1$, $\lambda_2 > 1$ such that for $s \geqslant s_2$ and $\lambda \geqslant \lambda_2$ we have

$$\begin{aligned} s\lambda^2 \int_\Omega |\nabla u|^2 e^{2s\varphi} \mathrm{d}x + s^3\lambda^4 \int_\Omega |u|^2 \varphi^2 e^{2s\varphi} \mathrm{d}x \leqslant \\ C_2 \left(\int_\Omega |\Delta u|^2 \varphi^{-1} e^{2s\varphi} \mathrm{d}x + \int_{\mathcal{O}} \left(s\lambda^2 |\nabla u|^2 + s^3\lambda^4 \varphi^2 |u|^2 \right) e^{2s\varphi} \mathrm{d}x \right) \leqslant \\ C_2 \left(\int_\Omega |\Delta u|^2 \varphi^2 e^{2s\varphi} \mathrm{d}x + \int_{\mathcal{O}} \left(s\lambda^2 |\nabla u|^2 + s^3\lambda^4 \varphi^2 |u|^2 \right) e^{2s\varphi} \mathrm{d}x \right), \end{aligned} \tag{2.60}$$

where for the last part of the inequality bellow we used estimation (2.50).

We denote $\widehat{\lambda} = \max\{\lambda_1, \lambda_2\}$ and $\widehat{s} = \max\{s_1, s_2\}$. For $s \geqslant \widehat{s}$ and $\lambda \geqslant \widehat{\lambda}$, combining (2.57) and (2.60) we have

$$\begin{aligned} s\lambda^2 \int_\Omega |\nabla(\Delta u)|^2 e^{2s\varphi} \mathrm{d}x + \frac{s^3\lambda^4 - 2a^2 C_1}{C_2} s\lambda^2 \int_\Omega (|\nabla u|^2 + s^2\lambda^2 |u|^2 \varphi^2) e^{2s\varphi} \mathrm{d}x \\ - (s^3\lambda^4 - a^2 C_1) \left(\int_{\mathcal{O}} \left(s\lambda^2 |\nabla u|^2 + s^3\lambda^4 \varphi^2 |u|^2 \right) e^{2s\varphi} \mathrm{d}x \right) \leqslant \\ C_1 \left(2 \int_\Omega |g|^2 \varphi^{-1} e^{2s\varphi} \mathrm{d}x + \int_{\mathcal{O}} \left(s\lambda^2 |\nabla(\Delta u)|^2 + s^3\lambda^4 \varphi^2 |\Delta u|^2 \right) e^{2s\varphi} \mathrm{d}x \right). \end{aligned} \tag{2.61}$$

Fixing λ in (2.61), there exists a constant $C > 0$ such that (2.54) is verified. Therefore, the proof of the theorem is complete. □

Proof of Proposition 2.12. The proof is a direct consequence of Theorem 2.15. Let us denote $g = (\mu^2 - a)u - b \cdot \nabla u \in L^2(\Omega)$. Applying Theorem 2.15 to (2.41)-(2.42) and using (2.43), we obtain

$$s\lambda^2 \int_\Omega (|\nabla(\Delta u)|^2 + s^3\lambda^4 |\nabla u|^2 + s^5\lambda^6 |u|^2 \varphi^2) e^{2s\varphi} \mathrm{d}x \leqslant C \int_\Omega \frac{|g|^2}{\varphi} e^{2s\varphi} \mathrm{d}x.$$

We can easily verify that

$$|g(x)|^2 \leqslant 2 \left(\mu^4 + \|a\|^2_{L^\infty(\Omega)} \right) |u(x)|^2 + 2\|b\|^2_{(L^\infty(\Omega))^n} |\nabla u(x)|^2, \qquad (x \in \Omega).$$

Combining the above inequality with (2.50), we obtain

$$\begin{aligned} s\lambda^2 \int_\Omega |\nabla(\Delta u)|^2 e^{2s\varphi} \mathrm{d}x + s^4\lambda^6 \int_\Omega |\nabla u|^2 e^{2s\varphi} \mathrm{d}x + s^6\lambda^8 \int_\Omega |u|^2 \varphi^2 e^{2s\varphi} \mathrm{d}x \leqslant \\ 2C \left(\left(\mu^4 + \|a\|^2_{L^\infty(\Omega)} \right) \int_\Omega |u|^2 \varphi^2 e^{2s\varphi} \mathrm{d}x + \|b\|^2_{(L^\infty(\Omega))^n} \int_\Omega |\nabla u|^2 e^{2s\varphi} \mathrm{d}x. \right) \end{aligned} \tag{2.62}$$

Taking $s \to \infty$ in (2.62), we easily obtain that $u = 0$ in Ω. □

2.3.2 Proof of Theorems 2.1 and 2.2

For the remaining part of this section, let $A_0 : H_1 \to H$ be the following operator

$$H_1 = H^2(\Omega) \cap H_0^1(\Omega)$$

$$A_0\varphi = (\Delta^2 - a\Delta)^{\frac{1}{2}}\varphi, \qquad (\varphi \in H_1)$$

and $P_0 \in \mathcal{L}(H_{1-\varepsilon}, H)$

$$P_0\varphi = b \cdot \nabla\varphi + c\varphi, \qquad (\varphi \in H_{1-\varepsilon}),$$

where a, b, c are like in the beginning of this section. Therefore (2.1)-(2.3) can be written as

$$\ddot{w}(t) + A_0^2 w(t) + P_0 w(t) = 0, \qquad t > 0 \tag{2.63}$$

$$w(0) = w_0, \qquad \dot{w}(0) = w_1 \tag{2.64}$$

and let $Y = L^2(\mathcal{O})$ and $C_0 \in \mathcal{L}(H, Y)$

$$C_0 w(t) = \dot{w}(\cdot, t)|_{\mathcal{O}}. \tag{2.65}$$

Proving Theorem 2.1 or Theorem 2.2 is equivalent now to prove the exact observability of (2.63)-(2.65), the only difference between the two theorems being the observation time.

Proof of Theorem 2.1. From Proposition 2.8 we have that the pair (A_0, C_0) is exactly observable, i.e., there exists a time $\tau_0 > 0$ such that (A_0, C_0) is exactly observable in time τ_0.

If we transcript the result of Proposition 2.12 in the language of A_0, P_0, C_0 we obtain that

$$A_0^2 u + P_0 u = \mu^2 u,$$

$$C_0 u = 0$$

implies $u = 0$. Then from Theorem 2.5 we obtain that (2.63)-(2.65) is exactly observable in any time $\tau \geqslant \tau_0$. □

Proof of Theorem 2.2. The only difference between this proof and the previous one is that we apply here Proposition 2.9 which give us the observability of (A_0, C_0) in any time $\tau > 0$ and similarly we have that (2.63)-(2.65) is exactly observable in any time $\tau > 0$. □

3. Local exact controllability for Berger plate equation

This chaper is a joint work with Marius Tucsnak. Important parts of this chapter were published in Cîndea and Tucsnak [19].

In this chapter we study the exact controllability of a nonlinear plate equation by the means of a control which acts on an internal region of the plate. The main result asserts that this system is locally exactly controllable if the associated linear Euler-Bernoulli system is exactly controllable. In particular, for rectangular domains we obtain that the Berger system is locally exactly controllable in arbitrarily small time and for every open and nonempty control region.

3.1 Introduction

During the last decades an important literature has been devoted to the exact controllability of various linear equations modeling the vibrations of elastic plates (see, for instance, Zuazua [87], Lasiecka and Triggiani [45], Jaffard [38]). A case of particular interest is the Euler-Bernoulli model with distributed control, i.e., the initial and boundary value problem

$$\ddot{w}(x,t) + \Delta^2 w(x,t) = u(x,t)\chi_{\mathcal{O}} \quad \text{for } (x,t) \in \Omega \times (0,\infty), \tag{3.1}$$

$$w(x,t) = \Delta w(x,t) = 0 \qquad \text{for} \quad (x,t) \in \partial\Omega \times (0,\infty), \tag{3.2}$$

$$w(x,0) = \dot{w}(x,0) = 0 \quad \text{for } x \in \Omega. \tag{3.3}$$

In the above equations, $\Omega \subset \mathbb{R}^2$ is an open nonempty set, $\mathcal{O}$ is an open subset of Ω and a dot denotes differentiation with respect to the time t, so that

$$\dot{w} = \frac{\partial w}{\partial t}, \quad \ddot{w} = \frac{\partial^2 w}{\partial t^2}.$$

The state trajectory of the above system is the function $t \mapsto \begin{bmatrix} w \\ \dot{w} \end{bmatrix}$, where w and $\dot{w}$ stand for the transverse displacement and the transverse velocity of the plate, respec-

tively. The input function is $u \in L^2([0,\infty); L^2(\mathcal{O}))$, extended by zero outside $\mathcal{O}$, and $\chi_{\mathcal{O}}$ is the characteristic function of $\mathcal{O}$.

A general sufficient condition for the exact controllability of (3.1)-(3.3) is that Ω and $\mathcal{O}$ satisfy the geometric optics condition of Bardos, Lebeau and Rauch [9]. This has been originally shown in Lebeau [46], using microlocal analysis. The proof has been successively simplified in Miller [52] and Tucsnak and Weiss [80, Example 11.2.4]. The geometric optics condition is not necessary for the exact controllability of (3.1)-(3.3). Indeed, as has been shown in Jaffard [38], if Ω is a rectangle then (3.1)-(3.3) is exactly controllable for every nonempty control region $\mathcal{O}$. More complicated situations in which the geometric optics condition fails but the exact controllability property holds have been recently investigated in Burq and Zworski [14] (see also Tenenbaum and Tucsnak [76] for boundary controllability). Note that the proofs of the exact controllability results in [14] and [38] are based on technics which are quite different of those used for the case in which the geometric optics condition holds.

The aim of this chapter is to study the local exact controllability of a system modeling the nonlinear vibrations of an elastic plate. This model, which has been proposed by Berger (see Berger [10]), is equivalent in one space dimension to the wider known Von Karman equations (see Perla Menzala and Zuazua [51]). In the two-dimensional case the system we consider can be seen as an asymptotic limit of the Von Karman equations (see Perla Menzala, Pazoto and Zuazua [60], Nayfeh and Mook [54]).

Berger's model for an elastic plate filling the domain Ω and hinged on the boundary $\partial\Omega$ consists in the following initial and boundary value problem:

$$\ddot{w}(x,t) + \Delta^2 w(x,t) - \left(a + b\int_\Omega |\nabla w|^2 \, \mathrm{d}x\right)\Delta w(x,t) = u\chi_{\mathcal{O}} \quad \text{for } (x,t) \in \Omega \times (0,\infty), \tag{3.4}$$

$$w(x,t) = \Delta w(x,t) = 0 \quad \text{for } (x,t) \in \partial\Omega \times (0,\infty), \tag{3.5}$$

$$w(x,0) = 0, \quad \dot{w}(x,0) = 0 \quad \text{for } x \in \Omega. \tag{3.6}$$

In the above system we continue to use the notation described after (3.1)-(3.3). Moreover, the constant a is supposed to be larger then $-\lambda_1$, where $\lambda_1 > 0$ denotes the first eigenvalue of the Dirichlet Laplacian in Ω and it corresponds to the in-plane stretching ($a < 0$) or compression ($a > 0$) of the plate. The constant b is supposed to be positive.

The first main result of this chapter is:

Theorem 3.1. *Let $\Omega \subset \mathbb{R}^2$ be an open bounded set with C^2 boundary and let $\mathcal{O} \subset \Omega$ be an open and nonempty subset of Ω such that* (3.1)-(3.3) *is exactly controllable (in some time $\tau_0 > 0$). Then the nonlinear system* (3.4)-(3.6) *is locally exactly controllable (in some time $\tau > 0$), i.e., there exist $\tau > 0$, $M > 0$ such that for every $\left[\begin{smallmatrix} w_0 \\ w_1 \end{smallmatrix}\right] \in (H^2(\Omega) \cap H_0^1(\Omega)) \times L^2(\Omega)$, with $\|w_0\|^2_{H^2(\Omega)} + \|w_1\|^2_{L^2(\Omega)} \leqslant M^2$, there exists $u \in L^2([0,\tau]; L^2(\mathcal{O}))$ such that the solution w of* (3.4)-(3.6) *satisfies*

$$w(\cdot,\tau) = w_0, \quad \dot{w}(\cdot,\tau) = w_1.$$

The main interest of Theorem 3.1 is that, being a perturbation result, it relies only on the exact controllability of (3.1)-(3.3), which is a well studied problem. Note that (3.1)-(3.3) is not the linearization around 0 of (3.4)-(3.6). Therefore our perturbation argument is divided in two steps: we first tackle the case $b = 0$, by using frequency domain techniques and then we go back to the original nonlinear problem by a fixed point argument. The main shortcoming of Theorem 3.1 is that it does not provide, as expected, the local exact controllability in arbitrarily small time. Our second main result is Theorem 3.2 below, which feels this gap, at least in the case of rectangular domains.

Theorem 3.2. *Let $\Omega \subset \mathbb{R}^2$ be a rectangle and let $\mathcal{O}$ be an open and nonempty subset of Ω. Then* (3.4)-(3.6) *is locally exactly controllable in any time $\tau > 0$. In other words, for every $\tau > 0$ there exists a constant $M > 0$ such that for every $\left[\begin{smallmatrix} w_0 \\ w_1 \end{smallmatrix}\right] \in (H^2(\Omega) \cap H_0^1(\Omega)) \times L^2(\Omega)$, with*

$$\|w_0\|^2_{H^2(\Omega)} + \|w_1\|^2_{L^2(\Omega)} \leqslant M^2,$$

there exists $u \in L^2([0,\tau]; L^2(\mathcal{O}))$ such that the solution w of (3.4)-(3.6) *satisfies*

$$w(\cdot,\tau) = w_0, \quad \dot{w}(\cdot,\tau) = w_1.$$

The remaining part of this chapter is organized as follows. In Section 3.2 we show that if an abstract plate equation is exactly controllable then the same result holds if we perturb the equation by a particular lower order linear term. Section 3.3 is devoted to the fixed point argument and to one example in one space dimension. Finally, the main results are proved in Section 3.4.

3.2 Exact controllability of an abstract second order system perturbed by a lower order term

In this section we introduce some notation and we give an exact controllability result for a second order system perturbed by a lower order term. This exact controllability result is the equivalent of the exact observability result for the perturbed second order system described in Section 2.2.1.

Let H be a Hilbert space which will be identified with its dual and let $A_0 : \mathcal{D}(A_0) \to H$ be a strictly positive operator. Whenever no confusion is possible, the inner product and the induced norm in H will be simply denoted $\langle \cdot, \cdot \rangle$ and $\| \cdot \|$ respectively. When saying that A_0 is *strictly positive* we mean that A_0 is self-adjoint and that there exists a constant $\gamma > 0$ such that

$$\langle A_0\varphi, \varphi \rangle \geqslant \gamma \|\varphi\|^2 \qquad (\varphi \in \mathcal{D}(A_0)).$$

Recall that such an operator A_0 has an orthonormal basis of eigenvectors $(\varphi_n)_{n\in\mathbb{N}^*}$ corresponding to the positive eigenvalues $(\lambda_n)_{n\in\mathbb{N}^*}$. We denote H_1 the Hilbert space

$\mathcal{D}(A_0)$ with the inner product $\langle \varphi, \psi \rangle_1 = \langle A_0\varphi, A_0\psi \rangle$ and the induced norm

$$\|\varphi\|_1 = \|A_0\varphi\| \qquad (\varphi \in H_1).$$

The Hilbert space H_2 is $\mathcal{D}(A_0^2)$ with the inner product $\langle \varphi, \psi \rangle = \langle A_0^2\varphi, A_0^2\psi \rangle$ and the induced norm

$$\|\varphi\|_2 = \|A_0^2\varphi\| \qquad (\varphi \in H_2).$$

Consider the second order evolution equation

$$\ddot{w}(t) + A_0^2 w(t) = B_0 u(t), \quad w(0) = 0, \quad \dot{w}(0) = 0, \tag{3.7}$$

where $B_0 \in \mathcal{L}(U, H)$. In order to write this equation as a first order system we introduce the Hilbert space $X = H_1 \times H$ and the family of operators $(\widetilde{A_a})_{a>-\lambda_1}$, $\widetilde{A_a} : \mathcal{D}(\widetilde{A_a}) \to X$ defined by

$$\mathcal{D}(\widetilde{A_a}) = H_2 \times H_1, \qquad \widetilde{A_a} = \begin{bmatrix} 0 & I \\ -A_0^2 - aA_0 & 0 \end{bmatrix}, \tag{3.8}$$

where λ_1 is the first eigenvalue of the operator A_0. Since A_0 is strictly positive, is easy to prove that $(A_0^2 + aA_0)$ is a strictly positive operator with compact resolvents and so, $\widetilde{A_a}$, defined by (3.8), is a skew-adjoint operator. Applying Stone's theorem, we have that $\widetilde{A_a}$ generates an unitary group $\mathbb{T}$ on $X = H_1 \times H$. Finally, we introduce the control operator $B \in \mathcal{L}(U, X)$ defined by

$$B\mathrm{v} = \begin{bmatrix} 0 \\ B_0\mathrm{v} \end{bmatrix} \qquad (\mathrm{v} \in U). \tag{3.9}$$

Then (3.7) can be written as

$$\dot{z}(t) = \widetilde{A_0} z(t) + Bu(t), \quad z(0) = 0,$$

where we have denoted $z(t) = \left[\begin{smallmatrix} w(t) \\ \dot{w}(t) \end{smallmatrix}\right]$.

In the remaining part of this sectionn we focus on the following initial data problem, consisting in a pertubation of (3.7) by the term $aA_0w(t)$:

$$\ddot{w}(t) + A_0^2 w(t) + aA_0 w(t) = B_0 u(t) \tag{3.10}$$

$$w(0) = 0, \quad \dot{w}(0) = 0, \tag{3.11}$$

with $a > -\lambda_1$. With notation from the beginning of the section, the system (3.10)-(3.11) can be written in the form

$$\dot{z}(t) = \widetilde{A_a} z(t) + Bu(t), \quad z(0) = 0, \tag{3.12}$$

where $z(t) = \begin{bmatrix} w(t) \\ \dot{w}(t) \end{bmatrix}$.

Our aim is to show that if (3.12) is exactly controllable for $a = 0$ then it is exactly controllable for every $a > -\lambda_1$, where λ_1 is the first eigenvalue of A_0. The main result of

this section is the following proposition, which gives no information on the controllability time. Note that $\left[\begin{smallmatrix} 0 \\ -aA_0 \end{smallmatrix}\right]$ is not a compact operator in the state space $X = H_1 \times H$, so that the compactness-uniqueness method introduced in [9] (see also [14]) cannot be applied. Our method is based on a spectral test of Hautus type introduced in [64].

Proposition 3.3. *Assume that the pair $(\widetilde{A_0}, B)$ is exactly controllable. Then for every $a > -\lambda_1$ the pair $(\widetilde{A_a}, B)$ is exactly controllable.*

Proof. This proof is similar to the proof of Theorem 2.3. For the completeness of the chapter we give however here the proof of this proposition. Recall from Section 2.2 that $\widetilde{A_a}$ is skew-adjoint operator with compact resolvents for every $a > -\lambda_1$. The conclusion of the proposition is obtained bellow by first showing that in "high frequency" a wave packet (as defined in Section 1.2) is exactly observable.

Denote $\varphi_{-n} = \varphi_n$ for all $n \in \mathbb{N}^*$. For every $a > -\lambda_1$ we denote by $(\lambda_n(a))_{n\in\mathbb{N}^*}$ the eigenvalues of the operator $(A_0^2 + aA_0)^{\frac{1}{2}}$ associated to the eigenvectors $(\varphi_n)_{n\in\mathbb{N}^*}$. It is easy to verify that

$$\lambda_n(a) = \lambda_n\sqrt{1 + a\lambda_n^{-1}} = \lambda_n + \frac{a}{2} + \frac{a}{8}o(\lambda_n^{-1}), \tag{3.13}$$

where $\lambda_n = \lambda_n(0)$ are the eigenvalues of the operator A_0. Then the family $(\Phi_n(a))_{n\in\mathbb{Z}^*}$ given by

$$\Phi_n(a) = \frac{1}{\sqrt{2}}\begin{bmatrix} \frac{1}{i\mu_n(a)}\varphi_n \\ \varphi_n \end{bmatrix} \qquad (n \in \mathbb{Z}^*) \tag{3.14}$$

is an orthonormal basis of eigenvectors of the operator $\widetilde{A_a}$ associated to the eigenvalues $(i\mu_n(a))_{n\in\mathbb{Z}^*}$, where

$$\mu_n(a) = \begin{cases} -\lambda_n(a), & \text{if } n \in \mathbb{N}^* \\ \lambda_n(a), & \text{if } -n \in \mathbb{N}^*, \end{cases} \tag{3.15}$$

for every $a > -\lambda_1$.

For $\varepsilon > 0$, $\omega \in \mathbb{R}$ and $a > -\lambda_1$ we define

$$J_\varepsilon(\omega, a) = \{m \in \mathbb{Z}^* \text{ such that } |\mu_m(a) - \omega| < \varepsilon\}. \tag{3.16}$$

Since the pair $(\widetilde{A_0}, B)$ is exactly controllable we know from Theorem 1.11 that there exist $\varepsilon, \delta > 0$ such that for all $\omega \in \mathbb{R}$ we have

$$\|B^*\varphi\|_U \geqslant \delta\|\varphi\|_X, \tag{3.17}$$

for every wave packet $\varphi = \sum\limits_{m\in J_\varepsilon(\omega,0)} c_m\Phi_m(0)$.

The idea is to prove that the inequality (3.17) implies a similar inequality for every wave package $\psi = \sum_{m\in J_\varepsilon(\omega,a)} c_m\Phi_m(a)$. For the remaining part of this proof we consider $a > -\lambda_1$ fixed. Since $|\mu_k(a)| \to \infty$ when $k \to \infty$, there exists an $\omega_a > 0$

such that for every $|\omega| \geqslant \omega_a$ if $m \in J_\varepsilon(\omega, a)$ then $\frac{1}{8}|\mu_m(a)^{-1}| \leqslant \frac{1}{2}$. Let ω be such that $|\omega| \geqslant \omega_a$. Then $m \in I_\varepsilon(\omega, 0)$ is equivalent to

$$|\lambda_m(a) - \frac{a}{2} - \frac{a}{8}o(\lambda_m^{-1}) - \omega| < \varepsilon \Leftrightarrow m \in J_\varepsilon(\omega + a, a),$$

so $J_\varepsilon(\omega, 0) = J_\varepsilon(\omega + a, a)$. Since

$$B^*\psi = \sum_{m \in J_\varepsilon(\omega,a)} c_m B^* \Phi_m(a) = \sum_{m \in J_\varepsilon(\omega-a,0)} c_m B^* \Phi_m(0),$$

from (3.17) we have for every ω with $|\omega| \geqslant \omega_a$ that

$$\|B^*\psi\|_U \geqslant \delta \|\psi\|_X.$$

Denote $V = \operatorname{span}\{\Phi_m(a) \mid |\tilde{\mu}_m(a)| < \omega_a\}^\perp$. From the above inequality and Theorem 1.11 we obtain that $(\widetilde{A_a}|_V, B_V)$, with $\widetilde{A_a}|_V$ as in Definition 1.8, is exactly controllable.

From the exact controllability of the pair $(\widetilde{A_0}, B)$ it is clear that for every eigenvector $\Psi(a)$ of $\widetilde{A_a}$ there exists an eigenvector $\Psi(a)$ of $\widetilde{A_0}$ such that

$$B^*\Psi(a) = B^*\Psi(0) \neq 0$$

and, using Proposition 1.9, the pair $(\widetilde{A_a}, B)$ is exactly controllable. □

The particular case where A_0 is the Dirichlet Laplacian is discussed in the following example.

Example 3.4. We consider the problem of exact controllability of the following linear plate equation

$$\ddot{w}(x,t) + \Delta^2 w(x,t) - a\Delta w(x,t) = u(x,t)\chi_{\mathcal{O}}, \quad \text{for } (x,t) \in \Omega \times (0,\infty) \tag{3.18}$$

$$w(x,t) = \Delta w(x,t) = 0, \quad \text{for } (x,t) \in \partial\Omega \times (0,\infty) \tag{3.19}$$

$$w(x,0) = 0, \quad \dot{w}(x,0) = 0, \quad \text{for } x \in \Omega. \tag{3.20}$$

Let $\Omega \subset \mathbb{R}^2$ be an open bounded set with its boundary $\partial\Omega$ of class C^2. Assume that Ω and its open subset $\mathcal{O}$ are such that the Bardos, Lebeau and Rauch geometric control condition is verified, i.e. that there exists $\tau > 0$ such that any light ray traveling in Ω at unit speed and reflected according to geometric optics laws when it hits $\partial\Omega$, will intersect $\mathcal{O}$ in a time smaller than τ (see [9]). Then the problem (3.18)-(3.20) is exactly controllable, i.e., there exists a time $\tau > 0$, such that for every $\left[\begin{smallmatrix} w_0 \\ w_1 \end{smallmatrix}\right] \in (H^2(\Omega) \cap H_0^1(\Omega)) \times L^2(\Omega)$ exists a control $u \in L^2([0,\tau]; L^2(\mathcal{O}))$ such that the solution w of (3.18)-(3.20) satisfies

$$w(x,\tau) = w_0(x), \quad \dot{w}(x,\tau) = w_1(x) \qquad (x \in \Omega).$$

Indeed, denote $H = L^2(\Omega)$, $H_1 = H^2(\Omega) \cap H_0^1(\Omega)$,

$$H_2 = \{\varphi \in H^4(\Omega) \mid \varphi = \Delta\varphi = 0 \text{ on } \partial\Omega\}$$

and $U = L^2(\mathcal{O})$. Let $A_0 : H_1 \to H$ be defined by

$$A_0\varphi = -\Delta\varphi \qquad (\varphi \in H_1)$$

and $B_0 u = u\chi_{\mathcal{O}}$. Introducing the operators $\widetilde{A_a}$ and B, given by (3.8) and (3.9), the system (3.18)-(3.20) can be written as

$$\dot{z}(t) = \widetilde{A}_a z(t) + Bu(t), \quad z(0) = 0,$$

where $z = \left[\begin{smallmatrix} w \\ \dot{w} \end{smallmatrix}\right]$. Since we supposed that Ω and $\mathcal{O}$ satisfy the geometric condition of Bardos, Lebeau and Rauch, $(\widetilde{A_0}, B)$ is exactly controllable in arbitrarily small time (see [46]). Then, from Proposition 3.3, we conclude that $(\widetilde{A_a}, B)$ is exactly controllable for every $a > -\lambda_1$, where λ_1 is the first eigenvalue of the Dirichlet Laplacian in Ω.

3.3 From $\ddot{w} + A_0^2 w + aA_0 w = B_0 u$ to $\ddot{w} + A_0^2 w + (a + b\|A_0^{\frac{1}{2}} w\|^2)A_0 w = B_0 u$

In this section we consider the following perturbation of the linear differential equation studied in Section 3.2:

$$\ddot{w}(t) + A_0^2 w(t) + (a + b\|A_0^{\frac{1}{2}} w(t)\|^2)A_0 w(t) = B_0 u(t) \tag{3.21}$$

$$w(0) = \dot{w}(0) = 0, \tag{3.22}$$

where $a > -\lambda_1$, $b > 0$ and $B_0 \in \mathcal{L}(U, H)$.

The principal result of this subsection is the following.

Theorem 3.5. *Assume that* (3.10)-(3.11) *is exactly controllable in time $\tau > 0$. Then* (3.21)-(3.22) *is locally exactly controllable in time τ, i.e., there exists a constant $M > 0$ such that for every $\left[\begin{smallmatrix} w_0 \\ w_1 \end{smallmatrix}\right] \in H_1 \times H$, with $\|w_0\|_{H_1}^2 + \|w_1\|_H^2 \leqslant M^2$ exists a control $u \in L^2([0,\tau]; U)$, such that the solution w of* (3.21)-(3.22) *satisfies*

$$w(\tau) = w_0, \quad \dot{w}(\tau) = w_1.$$

Proof. Recall that since $(A_0^2 + aA_0)$ is a strictly positive operator with compact resolvents, the operator $\widetilde{A_a}$ is skew-adjoint and, applying theorem of Stone, generates a unitary group $\mathbb{T}$ in $X = H_1 \times H$. We denote $G : H_1 \times H \to H_1 \times H$

$$G\begin{bmatrix} w_1 \\ w_2 \end{bmatrix} = \begin{bmatrix} 0 \\ b\|A_0^{\frac{1}{2}} w_1\|^2 A_0 w_1 \end{bmatrix}.$$

Then (3.21)-(3.22) can be written as

$$\dot{z}(t) = \widetilde{A_a} z(t) + Gz(t) + Bu(t), \quad z(0) = 0, \tag{3.23}$$

where $z = \left[\begin{smallmatrix} w \\ \dot{w} \end{smallmatrix}\right]$ and $Bu(t) = \left[\begin{smallmatrix} 0 \\ B_0 u(t) \end{smallmatrix}\right]$. Let us consider the following linear equation

$$\dot{z}(t) = \widetilde{A_a} z(t) + F(t) + Bu(t), \quad z(0) = 0, \tag{3.24}$$

where $F = \left[\begin{smallmatrix} 0 \\ f(t) \end{smallmatrix}\right]$ and $f \in L^2([0,T];H)$. Let $z_0 \in X$. Since the pair $(\widetilde{A_a}, B)$ is exactly controllable in time τ we can consider a control operator $F_\tau \in \mathcal{L}(X, L^2([0,\tau];U))$ as in Proposition 1.6. Using Corollary 1.7 we see that the input function u given by

$$u = F_\tau z_0 - F_\tau \int_0^\tau \mathbb{T}_{\tau - s} F(s)\, \mathrm{d}s. \tag{3.25}$$

is such that $z(\tau) = z_0$.

Consider the mapping $\mathcal{F} : L^2([0,\tau];H) \to L^2([0,\tau];H)$ defined by

$$\mathcal{F}(f) = b\|A_0^{\frac{1}{2}} w\|_{L^2(0,\tau;H)} A_0 w,$$

where $\left[\begin{smallmatrix} w \\ \dot{w} \end{smallmatrix}\right]$ is the solution of (3.24) with u given by (3.25).

To obtain the conclusion of the theorem it suffices to show that $\mathcal{F}$ has a fixed point. Let $M > 0$ to be fixed later and $f \in L^2([0,\tau];H)$ with $\|f\|_{L^2([0,\tau];H)} \leqslant M$. We first show that if M is small enough the ball $B(0,M)$ of center 0 and radius M is invariant for $\mathcal{F}$ in $L^2([0,\tau];H)$. Since the operator F_τ given by Proposition 1.6 is bounded, from (3.25) we obtain easily that there exists a constant $C_\tau > 0$ such that

$$\|u\|_{L^2([0,\tau];U)} \leqslant C_\tau(\|z_0\|_X + \|f\|_{L^2([0,\tau];H)}). \tag{3.26}$$

Using the formula

$$z(\tau) = \int_0^\tau \mathbb{T}_{\tau - s} F(s)\, \mathrm{d}s + \Phi_\tau u$$

combined to the inequality (3.26) and renoting the constant, we obtain

$$\|z\|_{C([0,\tau];X)} = \|w\|_{C([0,\tau];H_1)} + \|\dot{w}\|_{C([0,\tau];H)} \leqslant C_\tau(\|z_0\|_X + \|f\|_{L^2([0,\tau];H)}).$$

From the last estimate we can conclude that

$$\begin{aligned} \|\mathcal{F}(f)\|_{L^2([0,\tau];H)} = b\|A_0^{\frac{1}{2}} w\|^2_{L^2([0,\tau];H)} \|A_0 w\|_{L^2([0,T];H)} &\leqslant bC_\tau \|z\|^3_{C([0,\tau];X)} \\ &\leqslant bC_\tau \left(\|z_0\|_X + \|f\|_{L^2([0,\tau];H)}\right)^3. \end{aligned}$$

Then, assuming that $0 < M < \frac{1}{2bC_\tau\sqrt{2}}$ and $\|z_0\|_X < M$, we obtain from the previous estimate that $\mathcal{F}(B(0,M)) \subset B(0,M)$.

We next show that $\mathcal{F}$ is a contraction of $B(0,M)$. Let $f_1, f_2 \in L^2([0,\tau];H)$ two functions such that $\|f_1\|, \|f_2\| \leqslant M$. Let $u_1, u_2 \in L^2([0,\tau];U)$ be the controls given by (3.25) for $f = f_1$, respectively $f = f_2$, and denote z_1 and z_2 the solutions of

$$\dot{z}_1(t) = \widetilde{A_a} z_1(t) + \begin{bmatrix} 0 \\ f_1(t) \end{bmatrix} + Bu_1(t), \quad z_1(0) = 0, \tag{3.27}$$

$$\dot{z}_2(t) = \widetilde{A_a} z_2(t) + \begin{bmatrix} 0 \\ f_2(t) \end{bmatrix} + Bu_2(t), \quad z_2(0) = 0. \tag{3.28}$$

Then we have

$$\begin{aligned}\|\mathcal{F}(f_1) - \mathcal{F}(f_2)\|_{L^2([0,\tau];H)} &= \left\| \|A_0^{\frac{1}{2}} w_1\|^2_{L^2([0,\tau];H)} A_0 w_1 - \|A_0^{\frac{1}{2}} w_2\|^2_{L^2([0,\tau];H)} A_0 w_2 \right\|_{L^2([0,\tau];H)} \\ &\leqslant \|A_0^{\frac{1}{2}} w_1\|^2_{L^2([0,\tau];H)} \|A_0(w_1 - w_2)\|_{L^2([0,\tau];H)} \\ &+ \left\| A_0^{\frac{1}{2}}(w_1 - w_2) \right\|_{L^2([0,\tau];H)} \left(\|A_0^{\frac{1}{2}} w_1\|_{L^2([0,\tau];H)} + \|A_0^{\frac{1}{2}} w_2\|_{L^2([0,\tau];H)} \right) \|A_0 w_2\|_{L^2([0,\tau];H)},\end{aligned}$$

where $z_1 = \left[\begin{smallmatrix} w_1 \\ \dot{w}_1 \end{smallmatrix}\right]$ and $z_2 = \left[\begin{smallmatrix} w_2 \\ \dot{w}_2 \end{smallmatrix}\right]$. If we denote $\tilde{z} = z_1 - z_2$ then we have

$$\dot{\tilde{z}}(t) = \widetilde{A_a}\tilde{z}(t) + \begin{bmatrix} 0 \\ (f_1 - f_2)(t) \end{bmatrix} + B(u_1(t) - u_2(t)), \quad \tilde{z}(0) = \tilde{z}(\tau) = 0.$$

It is easily to prove that there exists a constant $C > 0$ such that

$$\|w_1 - w_2\|_{C([0,\tau];H)} \leqslant C(\|f_1 - f_2\|_{L^2([0,\tau],H)} + \|u_1 - u_2\|_{L^2([0,\tau];U)}).$$

Moreover, using the form of u_1 and u_2, we have

$$u_1 - u_2 = F_\tau \int_0^\tau \mathbb{T}_{\tau - s} \left[\begin{smallmatrix} 0 \\ (f_1 - f_2)(t) \end{smallmatrix}\right] \, \mathrm{d}s.$$

Therefore, there exist two constants $C_1, C_2 > 0$ such that

$$\|A_0(w_1 - w_2)\|_{L^2(0,\tau;H)} \leqslant C_1 \|f_1 - f_2\|_{L^2(0,\tau;H)},$$

$$\|A_0^{\frac{1}{2}}(w_1 - w_2)\|_{L^2(0,\tau;H)} \leqslant C_2 \|f_1 - f_2\|_{L^2(0,\tau;H)}.$$

Using the above estimates there exists a constant $\alpha > 0$, depending on the time τ, such that

$$\begin{aligned}&\|\mathcal{F}(f_1) - \mathcal{F}(f_2)\|_{L^2([0,\tau];H)} \leqslant \alpha \left[(\|z_0\| + \|f_1\|_{L^2([0,\tau];H)})^2 \right. \\ &\left. + (\|z_0\| + \|f_1\|_{L^2([0,\tau];H)})(\|z_0\| + \|f_2\|_{L^2([0,\tau];H)}) + (\|z_0\| + \|f_2\|_{L^2([0,\tau];H)})^2 \right] \|f_1 - f_2\|_{L^2([0,\tau];H)},\end{aligned}$$

for all $f_1, f_2 \in L^2([0,\tau];H)$ with $\|f_1\|_{L^2([0,\tau];H)}, \|f_2\|_{L^2([0,\tau];H)} \leqslant M$.

Then, choosing M small enough, $\|z_0\|_X < M$ and denoting

$$C = \alpha(\|z_0\| + \|f_1\|)^2 + (\|z_0\| + \|f_1\|)(\|z_0\| + \|f_2\|) + (\|z_0\| + \|f_2\|)^2 \in (0,1),$$

we can write the previous estimate as

$$\|\mathcal{F}(f_1) - \mathcal{F}(f_2)\|_{L^2([0,\tau];H)} \leqslant C \|f_1 - f_2\|_{L^2([0,\tau];H)},$$

so $\mathcal{F}$ is a contraction in $B(0, M)$.

Using Banach fixed point theorem, we obtain that $\mathcal{F}$ has a fixed point, and the proof of the theorem is completed. □

Example 3.6. In one space dimension, i.e. $\Omega = (0, \pi)$, the initial system (3.4)-(3.6) become

$$\ddot{w}(x,t) + \frac{\partial^4 w}{\partial x^4}(x,t) - \left(a + b \int_0^\pi \left| \frac{\partial w}{\partial x}(x,t) \right|^2 \, \mathrm{d}x \right) \frac{\partial^2 w}{\partial x^2}(x,t) = u\chi_{\mathcal{O}}, \quad x \in (0,\pi), t > 0 \tag{3.29}$$

$$w(0,t) = w(\pi,t) = \frac{\partial^2 w}{\partial x^2}(0,t) = \frac{\partial^2 w}{\partial x^2}(\pi,t), \quad t \in (0,\infty) \tag{3.30}$$

$$w(x,0) = 0, \quad \dot{w}(x,0) = 0, \quad x \in (0,\pi), \tag{3.31}$$

where $a > -1$, $b > 0$ and $\mathcal{O} \in \Omega$ is an open interval. The above equations are a model for the free vibrations of a hinged extensible beam compressed (if $a > 0$) or stretched (if $a < 0$) by an axial force, which has been extensively studied in the literature (see Dickey [21], [22], Ball [8]).

We claim that this problem is locally exactly controllable in arbitrarily small time. Indeed, denote $H = L^2(0,\pi)$, $H_1 = H^2(0,\pi) \cap H_0^1(0,\pi)$ and

$$H_2 = \left\{ \varphi \in H^4(0,\pi) \cap H_0^1(0,\pi) \text{ such that } \frac{\mathrm{d}^2\varphi}{\mathrm{d}x^2}(0) = \frac{\mathrm{d}^2\varphi}{\mathrm{d}x^2}(\pi) = 0 \right\}.$$

Let $A_0 : H_1 \to H$ be the operator defined by $A_0\varphi = -\frac{\mathrm{d}^2\varphi}{\mathrm{d}x^2}$ for all $\varphi \in H_1$. Using the operator $\widetilde{A_a}$, defined by (3.8), we can write (3.29)-(3.31) on the form of system (3.21)-(3.22). Denote $\varphi_n(x) = \sqrt{\frac{2}{\pi}}\sin(nx)$ the eigenvectors of $(A_0^2 + aA_0)^{\frac{1}{2}}$ associated to the eigenvalues $\lambda_n(a) = \sqrt{n^4 + an^2}$ and $\varphi_{-n} = \varphi_n$ for all $n \in \mathbb{N}^*$. It follows that $(\Phi_n)_{n\in\mathbb{Z}^*}$ given by

$$\Phi_n(x) = \frac{1}{\sqrt{2}} \begin{bmatrix} \frac{1}{i\mu_n(a)}\sqrt{\frac{2}{\pi}}\sin(nx) \\ \sqrt{\frac{2}{\pi}}\sin(nx) \end{bmatrix}$$

is an orthonormal basis formed by the eigenvectors of $\widetilde{A_a}$ associated to the eigenvalues $(i\mu_n(a))_{n\in\mathbb{Z}^*}$, where

$$\mu_n(a) = \begin{cases} -\lambda_n(a), & \text{if } n \in \mathbb{N}^* \\ \lambda_n(a), & \text{if } -n \in \mathbb{N}^*, \end{cases}$$

Is easy to verify that for any $a > -1$ we have

$$\lim_{n\to\infty} |\mu_{n+1}(a) - \mu_n(a)| = \infty.$$

Using Proposition 8.1.3 from [80], we obtain that the linear part of the (3.29) is exactly controllable in a time arbitrarily small. So, applying Theorem 3.5 we obtain the local exact controllability of equation (3.29)-(3.31) in a time arbitrarily small.

3.4 Proof of main results

In this section $\Omega \subset \mathbb{R}^2$ is a bounded open set with C^2 boundary or Ω is a rectangle and the operator A_0 is as in Example 3.4, i.e., $A_0 \in \mathcal{L}(H_1, H)$, where

$$H_1 = H^2(\Omega) \cap H_0^1(\Omega), \quad A_0\varphi = -\Delta\varphi \qquad (\varphi \in H_1).$$

Then, $H_2 = \mathcal{D}(A_0^2) = \{\varphi \in H^4(\Omega) \mid \varphi = \Delta\varphi = 0 \text{ on } \partial\Omega\}$ and

$$A_0^2\varphi = \Delta^2\varphi \qquad (\varphi \in H_2).$$

If $\mathcal{O} \subset \Omega$ is an open and nonempty set we denote $U = L^2(\mathcal{O})$ and we consider $B_0 \in \mathcal{L}(U, H)$ defined by $B_0 u = u\chi_{\mathcal{O}}$.

Proof of Theorem 3.1. With the above notation, the problem (3.4)-(3.6) can be written as

$$\ddot{w}(t) + A_0^2 w(t) + (a + b\|A_0^{\frac{1}{2}} w(t)\|^2) A_0 w(t) = B_0 u(t) \tag{3.32}$$

$$w(0) = 0, \quad \dot{w}(0) = 0. \tag{3.33}$$

By the hypothesis, for $a = b = 0$, the system (3.32)-(3.33) is exactly controllable in some time $\tau_0 > 0$. Applying Proposition 3.3 we have that (3.32)-(3.33), with A_0 and B_0 chosen like above, is exactly controllable in a time $\tau > 0$ for every $a > -\lambda_1$ and $b = 0$, where λ_1 is the first eigenvalue of Dirichlet Laplacian in Ω. Then from Theorem 3.5 we obtain that (3.32)-(3.33) is locally exactly controllable in time τ, which means that (3.4)-(3.6) is locally exactly controllable. □

As already mentioned the above result gives no information on the controllability time of (3.4)-(3.6). This shortcoming can be remedied in the case of a rectangular domain Ω by using the explicit knowledge of the eigenvectors and of the eigenvalues of A_0. We prove first an exact observability result for plate equation in a rectangular domain. Consider the initial and boundary value problem:

$$\ddot{w}(x,t) + \Delta^2 w(x,t) - a\Delta w(x,t) = 0, \quad \text{for } (x,t) \in \Omega \times (0,\infty) \tag{3.34}$$

$$w(x,t) = \Delta w(x,t) = 0, \quad \text{for } (x,t) \in \partial\Omega \times (0,\infty), \tag{3.35}$$

$$w(x,0) = w_0, \quad \dot{w}(x,0) = w_1, \quad \text{for } x \in \Omega, \tag{3.36}$$

where $a > -\lambda_1$. We consider the following output:

$$y(t) = \dot{w}(\cdot,t)|_{\mathcal{O}}. \tag{3.37}$$

The following proposition is a little variation of Proposition 2.9 in the sense that now the parameter a don't need to be positive (we assume only $a > -\lambda_1$).

Proposition 3.7. *Let $\Omega = (0, l_1) \times (0, l_2)$ be a rectangle in $\mathbb{R}^2$ and $\mathcal{O}$ an open and nonempty subset of Ω. Then* (3.34)-(3.37) *is exactly observable in the state space $H_1 \times H$ in any time $\tau > 0$.*

We use notation and results on pseudo-periodic functions which have been recalled in Section 1.3. The following proposition plays a central role in the proof of Proposition 3.7.

Proposition 3.8. *Let $r, s > 0$, $a > -(r+s)$ and let $\Lambda = (\mu_{mn})_{m,n\in\mathbb{Z}^*}$ be a sequence defined by*

$$\mu_{mn} = \begin{bmatrix} m\sqrt{r} \\ n\sqrt{s} \\ \sqrt{(rm^2+sn^2)^2 + a(rm^2+sn^2)} \end{bmatrix}. \tag{3.38}$$

Then any open and nonempty set in $\mathbb{R}^3$ is a domain associated to Λ in the sense of Definition 1.12.

The above proposition is a tiny variation of Proposition 2.10. For the completeness of the presentation we give here a proof of Proposition 3.8 that follows the same ideas as the proof of Proposition 2.10. The difference is that now we use in a different way the non-harmonic analysis results from Section 1.3.

Proof. Consider the sequence $(\alpha_{mn})_{m,n\in\mathbb{Z}^*}$ in $\mathbb{R}^3$ defined by

$$\alpha_{mn} = \begin{bmatrix} m\sqrt{r} \\ n\sqrt{s} \\ rm^2+sn^2 \end{bmatrix} \qquad (m,n\in\mathbb{Z}^*). \tag{3.39}$$

According to Jaffard [38], every open and nonempty set $D \subset \mathbb{R}^3$ is an associated domain to (α_{mn}). This clearly implies that every open and nonempty set in $\mathbb{R}^3$ is an associated domain to the sequence $\tilde{\Lambda} = (\tilde{\mu}_{m,n})_{m,n\in\mathbb{Z}^*}$ defined by

$$\tilde{\mu}_{mn} = \begin{bmatrix} m\sqrt{r} \\ n\sqrt{s} \\ rm^2+sn^2+\frac{a}{2} \end{bmatrix}.$$

It is easy to check that

$$\sqrt{(rm^2+sn^2)^2 + a(rm^2+sn^2)} = rm^2+sn^2+\frac{a}{2}+\varepsilon_{mn},$$

with $\lim\limits_{m^2+n^2\to\infty} \varepsilon_{mn} = 0$. From that it follows that the sequences Λ and $\tilde{\Lambda}$ are asymptotically close in the sense of Definition 1.17. Therefore, applying Theorem 1.18, every open nonempty set in $\mathbb{R}^3$ is an associated domain to Λ. □

To prove Proposition 3.7 we also need the following lemma:

Lemma 3.9. *With notation from the beginning of this section, let $C_0 \in \mathcal{L}(H,U)$ be the operator defined by $C_0 w = w|_{\mathcal{O}}$. The pair $(i(A_0^2+aA_0)^{\frac{1}{2}}, C_0)$ is exactly observable in H in every time $\tau > 0$, i.e., there exists a constant $k_\tau > 0$ such that*

$$\int_0^\tau \|C_0\mathbb{S}_t w_0\|_U^2 \, dt \geqslant k_\tau^2 \|w_0\|^2 \qquad (w_0 \in H),$$

where $(\mathbb{S}_t)$ is the semigroup generated by $i(A_0^2+aA_0)^{\frac{1}{2}}$.

Proof. Denote $(\lambda_{mn})_{m,n\in\mathbb{N}^*}$ the eigenvalues of Dirichlet Laplacian in Ω, given by

$$\lambda_{mn} = rm^2 + sn^2 \qquad (m,n \in \mathbb{N}^*),$$

where $r = \left(\frac{\pi}{l_1}\right)^2$, $s = \left(\frac{\pi}{l_2}\right)^2$ and denote by (φ_{mn}) a corresponding orthonormal basis formed by eigenvectors of A_0

$$\varphi_{mn}(x,y) = \frac{2}{\sqrt{l_1 l_2}} \sin(\sqrt{r}mx)\sin(\sqrt{s}ny) \qquad (m,n \in \mathbb{N}^*,\ (x,y) \in \Omega).$$

It is easy to check that for every $m,n \in \mathbb{N}^*$ φ_{mn} is an eigenvector of $(A_0^2 + aA_0)^{\frac{1}{2}}$ with corresponding eigenvalue

$$\lambda_{mn}(a) = \sqrt{(rm^2+sn^2)^2 + a(rm^2+sn^2)}.$$

The above facts imply that for every $a > -\lambda_{11}(0)$ the semigroup $\mathbb{S}$ generated by $i(A_0^2 + aA_0)^{\frac{1}{2}}$ verifies

$$\mathbb{S}_t z = \sum_{m,n} z_{mn} e^{i\lambda_{mn}(a)t}\varphi_{mn} \qquad (z \in H_1),$$

where we have denoted

$$z_{mn} = \langle z, \varphi_{mn}\rangle \qquad (m,n \in \mathbb{N}^*).$$

Therefore, we have

$$\begin{aligned}\int_0^\tau \|C_0\mathbb{S}_t z\|^2 \,\mathrm{d}t &= \int_0^\tau \int_{\mathcal{O}} \left|\sum_{m,n\in\mathbb{N}^*} z_{mn} e^{i\lambda_{mn}(a)t}\varphi_{mn}(x,y)\right|^2 \mathrm{d}x\mathrm{d}y\mathrm{d}t \\ &= \frac{4}{l_1 l_2}\int_0^\tau \int_{\mathcal{O}} \left|\sum_{m,n\in\mathbb{N}^*} z_{mn} e^{i\lambda_{mn}(a)t}\sin(\sqrt{r}mx)\sin(\sqrt{s}ny)\right|^2 \mathrm{d}x\mathrm{d}y\mathrm{d}t \quad (3.40)\end{aligned}$$

Let us extend the sequence (z_{mn}) by setting

$$z_{-m,n} = -z_{mn},\ z_{m,-n} = -z_{mn},\ z_{-m,-n} = z_{mn}, \qquad (m,n \in \mathbb{N}^*).$$

Then (3.40) can be written as

$$\int_0^\tau \|C_0\mathbb{S}_t z\|^2 \,\mathrm{d}t = \frac{1}{l_1 l_2}\int_0^\tau \int_{\mathcal{O}} \left|\sum_{m,n\in\mathbb{Z}^*} z_{mn} e^{i\mu_{mn}\cdot\begin{bmatrix}x\\y\\t\end{bmatrix}}\right|^2 \mathrm{d}x\mathrm{d}y\mathrm{d}t,$$

where (μ_{mn}) is defined by (3.38). By Proposition 3.8, $(\mu_{mn})_{mn}$ is a sequence associated to the domain $\mathcal{O}\times(0,\tau)$ for any $\tau > 0$ and any open and nonempty $\mathcal{O} \in \Omega$. Using the definition of an associated sequence to a domain it follows that there exists a constant $c > 0$ such that

$$\int_0^\tau \|C_0\mathbb{S}_t z\|^2 \,\mathrm{d}t \geqslant c^2 \sum_{m,n\in\mathbb{Z}^*} |z_{mn}|^2.$$

We have thus swown that the pair $(i(A_0^2 + aA_0)^{\frac{1}{2}}, C_0)$ is exactly observable in any time $\tau > 0$. □

Proof of Proposition 3.7. Let $C_0 \in \mathcal{L}(U, H)$ be the operator introduced by Lemma 3.9. From this lemma we have that the pair $(i(A_0^2 + aA_0)^{\frac{1}{2}}, C_0)$ is exactly observable in any time $\tau > 0$. Applying Proposition 6.8.2 from [80] (with A_0 replaced by $(A_0^2 + aA_0)^{\frac{1}{2}}$), we obtain that the pair $(\widetilde{A_a}, C)$, with $C = \left[\begin{smallmatrix} 0 \\ C_0 \end{smallmatrix}\right]$, is exactly observable in any time $\tau > 0$. □

A direct consequence of Proposition 3.7 and Proposition 1.5 is the following corollary.

Corollary 3.10. *Let $\Omega = (0, l_1) \times (0, l_2)$ be a rectangle and $\mathcal{O}$ an open and nonempty subset of Ω. Then for every $a > -\lambda_1$ and $b = 0$ the system* (3.4)-(3.6) *is exactly controllable in any time $\tau > 0$.*

Proof of Theorem 3.2. With notation from the beginning of this section the system (3.4)-(3.6) can be written, like in the proof of Theorem 3.1, as an abstract system (3.32)-(3.33). From Corollary 3.10 we obtain that for $b = 0$ and for every $a > -\lambda_1$ the system (3.32)-(3.33) is exactly controllable in a time $\tau > 0$ arbitrarily small. Then, applying Theorem 3.5, we can conclude that (3.32)-(3.33) is locally exactly controllable in time $\tau > 0$, so we proved that, if Ω is a rectangle, Berger equation (3.4)-(3.6) is locally exactly controllable in a time arbitrarily small. □

4. An approximation method for exact controls of vibrating systems

This chaper is a joint work with Sorin Micu and Marius Tucsnak and makes the object of a submitted article [16].

We propose a new method for the approximation of exact controls of a second order infinite dimensional system with bounded input operator. The algorithm combines Russell's "stabilizability implies controllability" principle with the Galerkin's method. The main new feature brought in by this approach consists in giving precise error estimates. In order to test the efficiency of the method, we consider two illustrative examples (with the finite element approximations of the wave and the beam equations) and we describe the corresponding simulations.

4.1 Introduction

The numerical study of the exact controls of infinite dimensional systems started in the 90's with a series of papers of Glowinski and Lions (see [31, 32]) where algorithms to determine the minimal L^2-norm exact controls (sometimes called HUM controls) are provided. Several abnormalities presented in these works stand at the origin of a large number of articles in which a great variety of numerical methods are presented and analyzed (see, for instance, [88], [27] and the references therein). However, except the recent work [26], where the approximation of the HUM controls for the one dimensional wave equation is considered, to our knowledge, there are no results on the rate of convergence of the approximative controls.

The aim of this work is to provide an efficient numerical method for computing exact controls for a class of infinite dimensional systems modeling elastic vibrations. Our main theoretical result gives the rate of convergence of our approximations to an exact control. Moreover, to illustrate the efficiency of this approach, we apply it to several systems governed by PDE's and we describe the associated numerical simulations. Our methodology combines Russell's "stabilizability implies controllability" principle with error estimates for finite element type approximations of the considered infinite dimensional systems. We focus on the case of bounded input operators which excludes

boundary control for systems governed by partial differential equations. However, the method can be partially extended to the unbounded input operator case, see Remark 4.8 below.

In order to give the precise statement of our results we need some notation. Let H be a Hilbert space and assume that $A_0 : \mathcal{D}(A_0) \to H$ is a self-adjoint, strictly positive operator with compact resolvents. Then, according to classical results, the operator A_0 is diagonalizable with an orthonormal basis $(\varphi_k)_{k\geqslant 1}$ of eigenvectors and the corresponding family of positive eigenvalues $(\lambda_k)_{k\geqslant 1}$ satisfies $\lim_{k\to\infty} \lambda_k = \infty$. Moreover, we have

$$\mathcal{D}(A_0) = \left\{ z \in H \;\middle|\; \sum_{k\geqslant 1} \lambda_k^2 \left|\langle z, \varphi_k\rangle\right|^2 < \infty \right\},$$

and

$$A_0 z = \sum_{k\geqslant 1} \lambda_k \langle z, \varphi_k\rangle \varphi_k \qquad (z \in \mathcal{D}(A_0)).$$

For $\alpha \geqslant 0$ the operator A_0^α is defined by

$$\mathcal{D}(A_0^\alpha) = \left\{ z \in H \;\middle|\; \sum_{k\geqslant 1} \lambda_k^{2\alpha} \left|\langle z, \varphi_k\rangle\right|^2 < \infty \right\}, \tag{4.1}$$

and

$$A_0^\alpha z = \sum_{k\geqslant 1} \lambda_k^\alpha \langle z, \varphi_k\rangle \varphi_k \qquad (z \in \mathcal{D}(A_0^\alpha)).$$

For every $\alpha \geqslant 0$ we denote by H_α the space $\mathcal{D}(A_0^\alpha)$ endowed with the inner product

$$\langle \varphi, \psi\rangle_\alpha = \langle A_0^\alpha \varphi, A_0^\alpha \psi\rangle \qquad (\varphi,\ \psi \in H_\alpha).$$

The induced norm is denoted by $\|\cdot\|_\alpha$. From the above facts it follows that for every $\alpha \geqslant 0$ the operator A_0 is a unitary operator from $H_{\alpha+1}$ onto H_α and A_0 is strictly positive on H_α.

Let U be another Hilbert space and let $B_0 \in \mathcal{L}(U, H)$ be an input operator. Consider the system

$$\ddot{q}(t) + A_0 q(t) + B_0 u(t) = 0 \qquad (t \geqslant 0), \tag{4.2}$$

$$q(0) = q_0,\ \dot{q}(0) = q_1. \tag{4.3}$$

The above system is said *exactly controllable in time* $\tau > 0$ if for every $q_0 \in H_{\frac{1}{2}},\ q_1 \in H$ there exists a control $u \in L^2([0,\tau], U)$ such that $q(\tau) = \dot{q}(\tau) = 0$. In order to provide a numerical method to approximate such a control u, we need more assumptions and notation.

Assume that there exists family $(V_h)_{h>0}$ of finite dimensional subspaces of $H_{\frac{1}{2}}$ and that there exist $\theta > 0$, $h^* > 0$, $C_0 > 0$ such that, for every $h \in (0, h^*)$,

$$\|\pi_h \varphi - \varphi\|_{\frac{1}{2}} \leqslant C_0\, h^\theta \|\varphi\|_1 \qquad (\varphi \in H_1), \tag{4.4}$$

$$\|\pi_h\varphi - \varphi\| \leqslant C_0\, h^\theta \|\varphi\|_{\frac{1}{2}} \qquad (\varphi \in H_{\frac{1}{2}}), \tag{4.5}$$

where π_h is the orthogonal projector from $H_{\frac{1}{2}}$ onto V_h. Assumptions (4.4)-(4.5) are, in particular, satisfied when finite elements are used for the approximation of Sobolev spaces. The inner product in V_h is the restriction of the inner product on H and it is still denoted by $\langle\cdot,\cdot\rangle$. We define the linear operator $A_{0h} \in \mathcal{L}(V_h)$ by

$$\langle A_{0h}\varphi_h, \psi_h\rangle = \langle A_0^{\frac{1}{2}}\varphi_h, A_0^{\frac{1}{2}}\psi_h\rangle \qquad (\varphi_h,\ \psi_h \in V_h). \tag{4.6}$$

The operator A_{0h} is clearly symmetric and strictly positive.

Denote $U_h = B_0^* V_h \subset U$ and define the operators $B_{0h} \in \mathcal{L}(U,H)$ by

$$B_{0h}u = \widetilde{\pi}_h B_0 u \qquad (u \in U), \tag{4.7}$$

where $\widetilde{\pi}_h$ is the orthogonal projection of H onto V_h. Note that $\operatorname{Ran} B_{0h} \subset V_h$. As well-known, since it is a projector, the operator $\widetilde{\pi}_h \in \mathcal{L}(H)$ is self-adjoint. Moreover, from (4.5) we deduce that

$$\|\varphi - \widetilde{\pi}_h\varphi\| \leqslant \|\varphi - \pi_h\varphi\| \leqslant C_0\, h^\theta \|\varphi\|_{\frac{1}{2}} \qquad (\varphi \in H_{\frac{1}{2}}). \tag{4.8}$$

The adjoint $B_{0h}^* \in \mathcal{L}(H,U)$ of B_{0h} is

$$B_{0h}^*\varphi = B_0^*\widetilde{\pi}_h\varphi \qquad (\varphi \in H). \tag{4.9}$$

Since $U_h = B_0^* V_h$, from (4.9) it follows that $\operatorname{Ran} B_{0h}^* = U_h$ and that

$$\langle B_{0h}^*\varphi_h, B_{0h}^*\psi_h\rangle_U = \langle B_0^*\varphi_h, B_0^*\psi_h\rangle_U \qquad (\varphi_h,\ \psi_h \in V_h). \tag{4.10}$$

The above assumptions imply that, for every $h^* > 0$, the family $\Big(\|B_{0h}\|_{\mathcal{L}(U,H)}\Big)_{h\in(0,h^*)}$ is bounded.

In what follows, we give an algorithm to compute an approximation $u_h \in C([0,\tau];U_h)$ of an exact control $u \in C([0,\tau];U)$, which drives the solution of (4.2)-(4.3) from the initial state $\left[\begin{smallmatrix} q_0 \\ q_1 \end{smallmatrix}\right] \in H_1 \times H_{\frac{1}{2}}$ to rest in time τ. For every $h > 0$ and $n \geqslant 1$ we consider the following second order ODE's :

$$\ddot{w}_h^n(t) + A_{0h} w_h^n(t) + B_{0h}B_{0h}^*\dot{w}_h^n(t) = 0 \qquad (t \geqslant 0) \tag{4.11}$$

$$w_h^n(0) = \begin{cases} \pi_h q_0, & \text{if } n = 1 \\ w_{b,h}^{n-1}(0), & \text{if } n > 1 \end{cases} \qquad \dot{w}_h^n(0) = \begin{cases} \pi_h q_1, & \text{if } n = 1 \\ \dot{w}_{b,h}^{n-1}(0), & \text{if } n > 1, \end{cases} \tag{4.12}$$

and

$$\ddot{w}_{b,h}^n(t) + A_{0h} w_{b,h}^n(t) - B_{0h}B_{0h}^*\dot{w}_{b,h}^n(t) = 0 \qquad (t \leqslant \tau) \tag{4.13}$$

$$w_{b,h}^n(\tau) = w_h^n(\tau), \qquad \dot{w}_{b,h}^n(\tau) = \dot{w}_h^n(\tau). \tag{4.14}$$

For every $h > 0$ we appropriately choose $N(h) \in \mathbb{N}$ (see Theorem 4.1 below) and we define

$$\begin{bmatrix} w_{0h} \\ w_{1h} \end{bmatrix} = \begin{bmatrix} \pi_h q_0 \\ \pi_h q_1 \end{bmatrix} + \sum_{n=1}^{N(h)} \begin{bmatrix} w_{b,h}^n(0) \\ \dot{w}_{b,h}^n(0) \end{bmatrix} \tag{4.15}$$

With this notation, u_h is defined by

$$u_h = B_{0h}^* \dot{w}_h + B_{0h}^* \dot{w}_{b,h}, \tag{4.16}$$

where w_h and $w_{b,h}$ are the solution of

$$\ddot{w}_h(t) + A_{0h} w_h(t) + B_{0h} B_{0h}^* \dot{w}_h(t) = 0 \qquad (t \geqslant 0) \tag{4.17}$$

$$w_h(0) = w_{0h}, \quad \dot{w}_h(0) = w_{1h}, \tag{4.18}$$

$$\ddot{w}_{b,h}(t) + A_{0h} w_{b,h}(t) - B_{0h} B_{0h}^* \dot{w}_{b,h}(t) = 0 \qquad (t \leqslant \tau) \tag{4.19}$$

$$w_{b,h}(\tau) = w_h(\tau), \qquad \dot{w}_{b,h}(\tau) = \dot{w}_h(\tau). \tag{4.20}$$

We can now formulate the main result of this paper.

Theorem 4.1. *With the above notation and assumptions, assume furthermore that the system* (4.2), (4.3) *is exactly controllable in some time* $\tau > 0$ *and that* $B_0 B_0^* \in \mathcal{L}(H_1, H_{\frac{1}{2}})$. *Then there exists a constant* $m_\tau > 0$ *such that the sequence* $(u_h)_{h \geqslant 0}$ *of* $C([0,\tau]; U_h)$ *defined in* (4.16) *with* $N(h) = [\theta\, m_\tau \ln(h^{-1})]$, *converges when* $h \to 0$ *to an exact control in time* τ *of* (4.2), (4.3), *denoted by* u, *for every* $Q_0 = \left[\begin{smallmatrix} q_0 \\ q_1 \end{smallmatrix}\right] \in H_{\frac{3}{2}} \times H_1$. *Moreover, there exist constants* $h^* > 0$ *and* $C := C_\tau$ *such that we have*

$$\|u - u_h\|_{C([0,\tau];U)} \leqslant C h^\theta \ln^2(h^{-1}) \|Q_0\|_{H_{\frac{3}{2}} \times H_1} \qquad (0 < h < h^*). \tag{4.21}$$

We prove this theorem in Section 4.4. In the second section we recall some background on exact controllability and stabilizability. Section 4.3 provides some error estimates. In Section 5 we apply our results to the wave equation in two space dimensions and to the Euler-Bernoulli beam equation, providing numerical simulations.

4.2 Some background on exact controllability and uniform stabilization

In this section we recall, with no claim of originality, some background concerning the exact controllability and uniform stabilizability of the system (4.2), (4.3). We give, in particular, a short proof, adapted to our case, of Russell's "stabilizability implies controllability" principle. This principle has been originally stated in Russell [68, 69] (see also Chen [15]).

Consider the second order differential equation

$$\ddot{w}(t) + A_0 w(t) + B_0 B_0^* \dot{w}(t) = 0 \qquad (t \geqslant 0), \tag{4.1}$$

$$w(0) = w_0,\ \dot{w}(0) = w_1. \tag{4.2}$$

It is well known that the above equation defines a well posed dynamical system in the state space $X = H_{\frac{1}{2}} \times H$. More precisely, the solution $\left[\begin{smallmatrix} w \\ \dot{w} \end{smallmatrix}\right]$ of (4.1), (4.2) is given by

$$\begin{bmatrix} w(t) \\ \dot{w}(t) \end{bmatrix} = \mathbb{T}_t \begin{bmatrix} w_0 \\ w_1 \end{bmatrix} \qquad \left(\begin{bmatrix} w_0 \\ w_1 \end{bmatrix} \in X, \quad t \geqslant 0 \right), \tag{4.3}$$

where $\mathbb{T}$ is the contraction semigroup on X generated by $\mathcal{A} - \mathcal{B}\mathcal{B}^*$ and $\mathcal{A} : \mathcal{D}(\mathcal{A}) \to X$, $\mathcal{B} \in \mathcal{L}(U, X)$ are defined by

$$\mathcal{D}(\mathcal{A}) = H_1 \times H_{\frac{1}{2}}, \qquad \mathcal{A} = \begin{bmatrix} 0 & I \\ -A_0 & 0 \end{bmatrix}, \quad \mathcal{B} = \begin{bmatrix} 0 \\ B_0 \end{bmatrix}.$$

We also consider the backwards system

$$\ddot{w}_b(t) + A_0 w_b(t) - B_0 B_0^* \dot{w}_b(t) = 0 \qquad (t \leqslant \tau), \tag{4.4}$$

$$w_b(\tau) = w(\tau),\ \dot{w}_b(\tau) = \dot{w}(\tau). \tag{4.5}$$

It is not difficult to check that the solution $\left[\begin{smallmatrix} w_b \\ \dot{w}_b \end{smallmatrix}\right]$ of (4.4), (4.5) is given by

$$\begin{bmatrix} w_b(t) \\ \dot{w}_b(t) \end{bmatrix} = \mathbb{S}_{\tau - t} \begin{bmatrix} w(\tau) \\ \dot{w}(\tau) \end{bmatrix} \qquad (t \in [0, \tau]), \tag{4.6}$$

where $\mathbb{S}$ is the contraction semigroup in X generated by $-\mathcal{A} - \mathcal{B}\mathcal{B}^*$.

We define $L_\tau \in \mathcal{L}(X)$ by

$$L_\tau \begin{bmatrix} w_0 \\ w_1 \end{bmatrix} = \begin{bmatrix} w_b(0) \\ \dot{w}_b(0) \end{bmatrix} \qquad \left(\begin{bmatrix} w_0 \\ w_1 \end{bmatrix} \in X \right). \tag{4.7}$$

With the above notation, the operator L_τ clearly satisfies $L_\tau = \mathbb{S}_\tau \mathbb{T}_\tau$.

Proposition 4.2. *With the above notation, assume that the system* (4.2), (4.3) *is exactly controllable in some time $\tau > 0$. Then the semigroups $\mathbb{T}$ and $\mathbb{S}$ are exponentially stable and we have $\|\mathbb{T}_\tau\|_{\mathcal{L}(X)} < 1$ and $\|\mathbb{S}_\tau\|_{\mathcal{L}(X)} < 1$. Moreover, the operator $I - L_\tau$ is invertible and we have*

$$(I - L_\tau)^{-1} = \sum_{n \geqslant 0} L_\tau^n. \tag{4.8}$$

Proof. The fact that $\mathbb{T}$ and $\mathbb{S}$ are exponentially stable is well-known (see, for instance, Haraux [34] and Liu [49]). The more precise facts that $\|\mathbb{T}_\tau\|_{\mathcal{L}(X)} < 1$ and $\|\mathbb{S}_\tau\|_{\mathcal{L}(X)} < 1$ are easy to establish (see, for instance, Lemma 2.2 in Ito, Ramdani and Tucsnak [37]). Finally, (4.8) follows from $\|L_\tau\|_{\mathcal{L}(X)} < 1$. □

The particular case of Russell's principle [69], which we need in this work, is given by the following result:

Proposition 4.3. *Assume that* (4.2), (4.3) *is exactly controllable in time* $\tau > 0$. *Then a control* $u \in C([0,\tau];U)$ *for* (4.2), (4.3) *steering the initial state* $\left[\begin{smallmatrix} q_0 \\ q_1 \end{smallmatrix}\right] \in X$ *to rest in time* τ *is given by*

$$u = B_0^* \dot{w} + B_0^* \dot{w}_b, \tag{4.9}$$

where w *and* w_b *are the solutions of* (4.1)-(4.2) *and* (4.4)-(4.5) *respectively, with*

$$\begin{bmatrix} w_0 \\ w_1 \end{bmatrix} = (I - L_\tau)^{-1} \begin{bmatrix} q_0 \\ q_1 \end{bmatrix}. \tag{4.10}$$

Remark 4.4. The original assumption of Russell's principle was essentially the exponential stability of the semigroups $\mathbb{T}$ and $\mathbb{S}$, whence the name "stabilizability implies controllability". Since, according to Proposition 4.2, these stability properties are equivalent to the exact controllability of (4.2), (4.3), we made this assumption explicitly in Proposition 4.3. The essential thing retained from the original Russell's principle is the specific form (4.9) of u, obtained using the "closed loop semigroups" $\mathbb{T}$ and $\mathbb{S}$.

Proof of Proposition 4.3. Denote

$$q(t) = w(t) - w_b(t) \qquad (t \in [0,\tau]).$$

Then q clearly satisfies (4.2) with u given by (4.9). Moreover, from (4.10) it follows that q satisfies the initial conditions (4.3). Finally, from (4.5) it follows that

$$q(\tau) = \dot{q}(\tau) = 0.$$

□

Remark 4.5. Using the semigroup notation, an alternative way of writing (4.9) is

$$u(t) = \mathcal{B}^* \mathbb{T}_t \begin{bmatrix} w_0 \\ w_1 \end{bmatrix} + \mathcal{B}^* \mathbb{S}_{\tau - t} \mathbb{T}_\tau \begin{bmatrix} w_0 \\ w_1 \end{bmatrix} \qquad (t \in [0,\tau]), \tag{4.11}$$

where $w_0,\ w_1$ satisfy (4.10).

We need below the fact that the restrictions of $\mathbb{T}$ and $\mathbb{S}$ to $H_1 \times H_{\frac{1}{2}}$ and $H_{\frac{3}{2}} \times H_1$ are exponentially stable semigroups. Sufficient conditions for this are given in the result below.

Proposition 4.6. *Assume that* $B_0 B_0^* \in \mathcal{L}(H_1, H_{\frac{1}{2}})$. *Then the restrictions of* $\mathbb{T}$ *and* $\mathbb{S}$ *to* $H_1 \times H_{\frac{1}{2}}$ *and* $H_{\frac{3}{2}} \times H_1$ *are contraction semigroups on these spaces with generators the restrictions of* $\mathcal{A} - \mathcal{B}\mathcal{B}^*$ *and* $-\mathcal{A} - \mathcal{B}\mathcal{B}^*$ *to* $H_{\frac{3}{2}} \times H_1$ *and* $H_2 \times H_{\frac{3}{2}}$ *respectively. Moreover, if* (4.2), (4.3) *is exactly controllable in time* $\tau > 0$ *then*

$$\|\mathbb{T}_\tau\|_{\mathcal{L}(H_{\frac{3}{2}} \times H_1)} < 1, \qquad \|\mathbb{S}_\tau\|_{\mathcal{L}(H_{\frac{3}{2}} \times H_1)} < 1. \tag{4.12}$$

Proof. From a well-known result (see, for instance, [80, Proposition 2.10.4]) it follows that the restriction of $\mathbb{T}$ to $\mathcal{D}(\mathcal{A}-\mathcal{B}\mathcal{B}^*) = H_1 \times H_{\frac{1}{2}}$ is a contraction semigroup on $\mathcal{D}(\mathcal{A}-\mathcal{B}\mathcal{B}^*)$ (endowed with the graph norm) whose generator is the restriction of $\mathcal{A}-\mathcal{B}\mathcal{B}^*$ to $\mathcal{D}((\mathcal{A}-\mathcal{B}\mathcal{B}^*)^2)$. Since $B_0B_0^* \in \mathcal{L}(H_1, H_{\frac{1}{2}})$, it is easy to check that $\mathcal{D}((\mathcal{A}-\mathcal{B}\mathcal{B}^*)^2) = H_{\frac{3}{2}} \times H_1$. It follows that indeed the restriction of $\mathbb{T}$ to $H_1 \times H_{\frac{1}{2}}$ is a contraction semigroup on this space with generator the restriction of $\mathcal{A}-\mathcal{B}\mathcal{B}^*$ to $H_{\frac{3}{2}} \times H_1$. The second assertion on $\mathbb{T}$ can be easily obtained by iterating this argument. The corresponding assertions for $\mathbb{S}$ can be proved in a completely similar manner. Finally, the estimates (4.12) follow from the corresponding estimates for the norms in $\mathcal{L}(H_1 \times H_{\frac{1}{2}})$ (see Proposition 4.2) by applying again Proposition 2.10.4 in [80]. □

Remark 4.7. An important property of the control u constructed in (4.16) is that, under appropriate assumptions on B_0, its regularity increases when the initial data are more regular. For instance, if $B_0B_0^* \in \mathcal{L}(H_1, H_{\frac{1}{2}})$ and $\left[\begin{smallmatrix} q_0 \\ q_1 \end{smallmatrix}\right] \in H_{\frac{3}{2}} \times H_1$ then, by Proposition 4.6, $\left[\begin{smallmatrix} w_0 \\ w_1 \end{smallmatrix}\right] = (I - L_\tau)^{-1} \left[\begin{smallmatrix} q_0 \\ q_1 \end{smallmatrix}\right] \in H_{\frac{3}{2}} \times H_1$ so that $u \in C^1([0,\tau]; U)$ and $B_0u \in C([0,\tau]; H_{\frac{1}{2}})$.

Remark 4.8. Russell's principle can be extended to the the case of unbounded input operators $B_0 \in \mathcal{L}(U, H_{-\frac{1}{2}})$, where $H_{-\frac{1}{2}}$ is the dual of $H_{\frac{1}{2}}$ with respect to the pivot space H. In this case the system (4.1)-(4.2) is still well-posed and it keeps most of the properties holding for bounded B_0 (see, for instance, [82], [79] and references therein). For a quite general form of Russell's principle for unbounded input operators we refer to [66].

4.3 An approximation result

The aim of this section is to provide error estimates for the approximations of (4.1) by finite-dimensional systems. Using the notation in Section 1 for the families of spaces $(V_h)_{h>0}$, $(U_h)_{h>0}$ and the families of operators $(\pi_h)_{h>0}$, $(A_{0h})_{h>0}$, $(B_{0h})_{h>0}$, we consider the family of finite dimensional systems

$$\ddot{w}_h(t) + A_{0h}w_h(t) + B_{0h}B_{0h}^*\dot{w}_h(t) = 0\,, \tag{4.1}$$

$$w_h(0) = \pi_h w_0\,, \quad \dot{w}_h(0) = \pi_h w_1\,. \tag{4.2}$$

In the case in which $B_0 = 0$ and A_0 is the Dirichlet Laplacian, it has been shown in Baker [7] that, given $w_0 \in H_{\frac{3}{2}}$, $w_1 \in H_1$, the solutions of (4.1) converge when $h \to 0$ to the solution of (4.1). Moreover, [7] contains precise estimates of the convergence rate. The result below shows that the same error estimates hold when A_0 is an arbitrary positive operator and $B_0 \neq 0$. Throughout this section we assume that $B_0B_0^* \in \mathcal{L}(H_1, H_{\frac{1}{2}})$.

Proposition 4.9. *Let $w_0 \in H_{\frac{3}{2}}, w_1 \in H_1$ and let w, w_h be the corresponding solutions of* (4.1), (4.2) *and* (4.1), (4.2). *Moreover, assume that $B_0B_0^* \in \mathcal{L}(H_1, H_{\frac{1}{2}})$. Then there exist three constants K_0, K_1, $h^* > 0$ such that, for every $h \in (0, h^*)$, we have*

$$\|\dot{w}(t) - \dot{w}_h(t)\| + \|w(t) - w_h(t)\|_{\frac{1}{2}} \leqslant (K_0 + K_1\,t)h^\theta \left(\|w_0\|_{\frac{3}{2}} + \|w_1\|_1\right) \qquad (t \geqslant 0). \tag{4.3}$$

Proof. We first note that, according to Proposition 4.6, we have

$$w \in C([0,\infty);H_{\frac{3}{2}}) \cap C^1([0,\infty);H_1) \cap C^2([0,\infty);H_{\frac{1}{2}}),$$
$$\|\ddot{w}(t)\|_{\frac{1}{2}} + \|\dot{w}(t)\|_1 + \|w(t)\|_{\frac{3}{2}} \leqslant \|w_1\|_1 + \|w_0\|_{\frac{3}{2}} \qquad (t \geqslant 0). \tag{4.4}$$

Equation (4.1) can be written

$$\langle \ddot{w}, v\rangle + \langle A_0^{\frac{1}{2}} w, A_0^{\frac{1}{2}} v\rangle + \langle B_0^*\dot{w}, B_0^* v\rangle_U = 0 \qquad (v \in H_{\frac{1}{2}}),$$

whereas, using (4.6) and (4.10), we see that (4.1) is equivalent to

$$\langle \ddot{w}_h, v_h\rangle + \langle A_0^{\frac{1}{2}} w_h, A_0^{\frac{1}{2}} v_h\rangle + \langle B_0^*\dot{w}_h, B_0^* v_h\rangle_U = 0 \qquad (v_h \in V_h).$$

Taking $v = v_h$ in the first one of the above relations and subtracting side by side it follows that

$$\langle \ddot{w} - \ddot{w}_h, v_h\rangle + \langle A_0^{\frac{1}{2}}(w - w_h), A_0^{\frac{1}{2}} v_h\rangle + \langle B_0^*\dot{w} - B_0^*\dot{w}_h, B_0^* v_h\rangle_U = 0 \qquad (v_h \in V_h),$$

which yields (recall that π_h is the orthogonal projector from $H_{\frac{1}{2}}$ onto V_h) that

$$\begin{aligned}\langle \pi_h\ddot{w} - \ddot{w}_h, v_h\rangle + \langle A_0^{\frac{1}{2}}(\pi_h w - w_h), A_0^{\frac{1}{2}} v_h\rangle \\ = \langle \pi_h\ddot{w} - \ddot{w}, v_h\rangle - \langle B_0^*\dot{w} - B_0^*\dot{w}_h, B_0^* v_h\rangle_U \qquad (v_h \in V_h).\end{aligned} \tag{4.5}$$

We set

$$\mathcal{E}_h(t) = \frac{1}{2}\|\pi_h\dot{w} - \dot{w}_h\|^2 + \frac{1}{2}\|A_0^{\frac{1}{2}}(\pi_h w - w_h)\|^2.$$

Using (4.5) it follows that

$$\begin{aligned}\dot{\mathcal{E}}_h(t) &= \langle \pi_h\ddot{w} - \ddot{w}, \pi_h\dot{w} - \dot{w}_h\rangle - \langle B_0^*(\dot{w} - \dot{w}_h), B_0^*(\pi_h\dot{w} - \dot{w}_h)\rangle_U \\ &= \langle \pi_h\ddot{w} - \ddot{w}, \pi_h\dot{w} - \dot{w}_h\rangle - \|B_0^*(\pi_h\dot{w} - \dot{w}_h)\|_U^2 + \langle B_0 B_0^*(\pi_h\dot{w} - \dot{w}), (\pi_h\dot{w} - \dot{w}_h)\rangle.\end{aligned}$$

We have thus shown that

$$\dot{\mathcal{E}}_h(t) \leqslant M\left(\|\pi_h\ddot{w} - \ddot{w}\| + \|\pi_h\dot{w} - \dot{w}\|\right)\|\pi_h\dot{w} - \dot{w}_h\|,$$

where $M = 1 + \|B_0 B_0^*\|$. It follows that

$$2\,\mathcal{E}_h^{\frac{1}{2}}(t)\frac{\mathrm{d}}{\mathrm{d}t}\mathcal{E}_h^{\frac{1}{2}}(t) \leqslant M\sqrt{2}\,\left(\|\pi_h\ddot{w} - \ddot{w}\| + \|\pi_h\dot{w} - \dot{w}\|\right)\mathcal{E}_h^{\frac{1}{2}}(t),$$

which yields

$$\mathcal{E}_h^{\frac{1}{2}}(t) \leqslant \mathcal{E}_h^{\frac{1}{2}}(0) + M\sqrt{2}\int_0^t \left(\|\pi_h\ddot{w} - \ddot{w}\| + \|\pi_h\dot{w} - \dot{w}\|\right)\mathrm{d}t \qquad (t \geqslant 0).$$

The above estimate, combined with (4.4), to the fact that $\mathcal{E}_h(0) = 0$ and to (4.5), implies that there exist two constants $\widetilde{K},\ \widetilde{h}^* > 0$ such that, for every $h \in (0, \widetilde{h}^*)$, we have

$$\mathcal{E}_h^{\frac{1}{2}}(t) \leqslant t\,\widetilde{K}h^\theta\left(\|w_0\|_{\frac{3}{2}} + \|w_1\|_1\right) \qquad (t \geqslant 0). \tag{4.6}$$

On the other hand, using (4.4), combined with (4.4) and (4.5), we have that there exists a constant $\widehat{h}^* > 0$ such that, for every $h \in (0, \widehat{h}^*)$,

$$\begin{aligned}\|\dot{w}(t) - \dot{w}_h(t)\| &\leqslant \|\dot{w}(t) - \pi_h \dot{w}(t)\| + \|\pi_h \dot{w}(t) - \dot{w}_h(t)\| \\ &\leqslant K\left[h^\theta\left(\|w_0\|_{\frac{3}{2}} + \|w_1\|_1\right) + \mathcal{E}_h^{\frac{1}{2}}(t)\right],\end{aligned}$$

$$\begin{aligned}\|w(t) - w_h(t)\|_{\frac{1}{2}} &\leqslant \|w(t) - \pi_h w(t)\|_{\frac{1}{2}} + \|\pi_h w(t) - w_h(t)\|_{\frac{1}{2}} \\ &\leqslant K\left[h^\theta\left(\|w_0\|_{\frac{3}{2}} + \|w_1\|_1\right) + \mathcal{E}_h^{\frac{1}{2}}(t)\right],\end{aligned}$$

for some constant $K > 0$. The last two inequalities, combined to (4.6) yield the conclusion (4.3). □

For $h > 0$ we denote $X_h = V_h \times V_h$ and we consider the operators

$$\mathcal{A}_h = \begin{bmatrix} 0 & I \\ -A_{0h} & 0 \end{bmatrix}, \quad \mathcal{B}_h = \begin{bmatrix} 0 \\ B_{0h} \end{bmatrix}. \tag{4.7}$$

The discrete analogues of the semigroups $\mathbb{T}$, $\mathbb{S}$ and of the operator L_t, denoted by $\mathbb{T}_h$, $\mathbb{S}_h$ and $L_{h,t}$ respectively, are defined, for every $h > 0$, by

$$\mathbb{T}_{h,t} = \mathrm{e}^{t(\mathcal{A}_h - \mathcal{B}_h\mathcal{B}_h^*)}, \quad \mathbb{S}_{h,t} = \mathrm{e}^{t(-\mathcal{A}_h - \mathcal{B}_h\mathcal{B}_h^*)}, \quad L_{h,t} = \mathbb{S}_{h,t}\mathbb{T}_{h,t} \qquad (t \geqslant 0). \tag{4.8}$$

For every $h > 0$ we define $\Pi_h \in \mathcal{L}(H_{\frac{1}{2}} \times H_{\frac{1}{2}}, X_h)$ by

$$\Pi_h = \begin{bmatrix} \pi_h & 0 \\ 0 & \pi_h \end{bmatrix}. \tag{4.9}$$

The following two results are consequences of Proposition 4.9.

Corollary 4.10. *There exist two constants C_1, $h^* > 0$ such that, for every $h \in (0, h^*)$ and $t > 0$, we have (recall that $L_t = \mathbb{S}_t\mathbb{T}_t$ for every $t \geqslant 0$):*

$$\|\Pi_h\mathbb{T}_t Z_0 - \mathbb{T}_{h,t}\Pi_h Z_0\|_X \leqslant C_1 t h^\theta \|Z_0\|_{H_{\frac{3}{2}} \times H_1} \qquad (Z_0 \in H_{\frac{3}{2}} \times H_1), \tag{4.10}$$

$$\|\Pi_h\mathbb{S}_t Z_0 - \mathbb{S}_{h,t}\Pi_h Z_0\|_X \leqslant C_1 t h^\theta \|Z_0\|_{H_{\frac{3}{2}} \times H_1} \qquad (Z_0 \in H_{\frac{3}{2}} \times H_1), \tag{4.11}$$

$$\|\Pi_h L_t Z_0 - L_{h,t}\Pi_h Z_0\|_X \leqslant C_1 t h^\theta \|Z_0\|_{H_{\frac{3}{2}} \times H_1} \qquad (Z_0 \in H_{\frac{3}{2}} \times H_1). \tag{4.12}$$

Proof. The estimate (4.10) is nothing else but (4.6) rewritten in semigroup terms. To prove (4.11), it suffices to notice that $P\mathbb{S}_t = \mathbb{T}_t P$ where

$$P\begin{bmatrix} w_0 \\ w_1 \end{bmatrix} = \begin{bmatrix} w_0 \\ -w_1 \end{bmatrix} \qquad \left(\begin{bmatrix} w_0 \\ w_1 \end{bmatrix} \in X\right).$$

Finally, estimate (4.12) can be easily obtained from (4.10) and (4.11). □

Corollary 4.11. *There exist three constants $C_0,\ C_1,\ h^*>0$ such that, for every $t>0$, $h\in(0,h^*)$ and $k\in\mathbb{N}$ we have*

$$\|L_t^kZ_0-L_{h,t}^k\Pi_hZ_0\|_X\leqslant(C_0+kC_1t)h^\theta\|Z_0\|_{H_{\frac{3}{2}}\times H_1}\qquad(Z_0\in H_{\frac{3}{2}}\times H_1).$$

Proof. We have

$$\|L_t^kZ_0-L_{h,t}^k\Pi_hZ_0\|_X\leqslant\|L_t^kZ_0-\Pi_hL_t^kZ_0\|_X+\|\Pi_hL_t^kZ_0-L_{h,t}^k\Pi_hZ_0\|_X.\tag{4.13}$$

From Proposition 4.6 it follows that, for every $t\geqslant0$, $H_{\frac{3}{2}}\times H_1$ is an invariant space for L_t. Using this fact combined to (4.4) and (4.5) we obtain that there exists a constant $C_0>0$ such that the first term of the right-hand side of the above inequality satisfies

$$\|L_t^kZ_0-\Pi_hL_t^kZ_0\|_X\leqslant C_0h^\theta\|Z_0\|_{H_{\frac{3}{2}}\times H_1}.\tag{4.14}$$

For the second term of the right-hand side in (4.13) we have

$$\begin{aligned}\|\Pi_hL_t^kZ_0-L_{h,t}^k\Pi_hZ_0\|_X&\leqslant\|\Pi_hL_t^kZ_0-L_{h,t}\Pi_hL_t^{k-1}Z_0\|_X+\|L_{h,t}\Pi_hL_t^{k-1}Z_0-L_{h,t}^k\Pi_hZ_0\|_X\\&=\|\Pi_hL_t(L_t^{k-1}Z_0)-L_{h,t}\Pi_hL_t^{k-1}Z_0\|_X+\|L_{h,t}(\Pi_hL_t^{k-1}Z_0-L_{h,t}^{k-1}\Pi_hZ_0)\|_X.\end{aligned}$$

Applying (4.12), we obtain

$$\|\Pi_hL_t^kZ_0-L_{h,t}^k\Pi_hZ_0\|_X\leqslant C_1th^\theta\|Z_0\|_{H_{\frac{3}{2}}\times H_1}+\|\Pi_hL_t^{k-1}Z_0-L_{h,t}^{k-1}\Pi_hZ_0\|_X.$$

By an obvious induction argument it follows that

$$\|\Pi_hL_t^kZ_0-L_{h,t}^k\Pi_hZ_0\|_X\leqslant C_1tkh^\theta\|Z_0\|_{H_{\frac{3}{2}}\times H_1}\qquad(Z_0\in H_{\frac{3}{2}}\times H_1).\tag{4.15}$$

Finally, combining (4.13)-(4.15), we obtain the conclusion of the corollary. □

4.4 Proof of the main result

In this section we continue to use the notation from (4.7)-(4.9) for $\mathcal{A}_h$, $\mathcal{B}_h$, $\mathbb{T}_h$, $\mathbb{S}_h$, L_h and Π_h. We first give the following result:

Lemma 4.12. *Suppose that the system (4.2), (4.3) is exactly controllable in time $\tau>0$ and that $B_0B_0^*\in\mathcal{L}(H_1,H_{\frac{1}{2}})$. Let $Q_0=\left[\begin{smallmatrix}q_0\\q_1\end{smallmatrix}\right]\in H_{\frac{3}{2}}\times H_1$ and let u be the control given by (4.11), where $W_0=\left[\begin{smallmatrix}w_0\\w_1\end{smallmatrix}\right]$ is given by (4.10). Let $v_h:[0,\tau]\to U_h$ be defined by*

$$v_h(t)=\mathcal{B}_h^*\mathbb{T}_{h,t}\Pi_hW_0+\mathcal{B}_h^*\mathbb{S}_{h,\tau-t}\mathbb{T}_{h,\tau}\Pi_hW_0\qquad(t\in[0,\tau]).\tag{4.1}$$

Then there exist three constants $C_2,\ C_3,\ h^*>0$ such that, for every $h\in(0,h^*)$, we have

$$\|(u-v_h)(t)\|_U\leqslant\frac{C_2+tC_3}{1-\|L_\tau\|_{\mathcal{L}(H_{\frac{3}{2}}\times H_1)}}h^\theta\|Q_0\|_{H_{\frac{3}{2}}\times H_1}\qquad(t\in[0,\tau]).\tag{4.2}$$

Proof. We first note that from Proposition 4.6 and the fact that $Q_0 \in H_{\frac{3}{2}} \times H_1$ it follows that W_0 given by (4.10) still belongs to $H_{\frac{3}{2}} \times H_1$. Using (4.11), (4.1), (4.9) and (4.7) we see that for every $t \in [0, \tau]$ we have :

$$\begin{aligned}\|(u - v_h)(t)\|_U &= \|\mathcal{B}^*\mathbb{T}_t W_0 + \mathcal{B}^*\mathbb{S}_{\tau-t}\mathbb{T}_\tau W_0 - \mathcal{B}_h^*\mathbb{T}_{h,t}\Pi_h W_0 - \mathcal{B}_h^*\mathbb{S}_{h,\tau-t}\mathbb{T}_{h,\tau}\Pi_h W_0\|_U \\ &\leqslant \left\|\mathcal{B}^*\mathbb{T}_t W_0 - \begin{bmatrix}0 & B_{0h}^*\end{bmatrix}\mathbb{T}_t W_0\right\|_U + \left\|\begin{bmatrix}0 & B_{0h}^*\end{bmatrix}(\mathbb{T}_t W_0 - \mathbb{T}_{h,t}\Pi_h W_0)\right\|_U \\ &\quad + \left\|\mathcal{B}^*\mathbb{S}_{\tau-t}\mathbb{T}_\tau W_0 - \begin{bmatrix}0 & B_{0h}^*\end{bmatrix}\mathbb{S}_{\tau-t}\mathbb{T}_\tau W_0\right\|_U \\ &\quad + \left\|\begin{bmatrix}0 & B_{0h}^*\end{bmatrix}(\mathbb{S}_{\tau-t}\mathbb{T}_\tau W_0 - \mathbb{S}_{h,\tau-t}\mathbb{T}_{h,\tau}\Pi_h W_0)\right\|_U . \quad (4.3)\end{aligned}$$

Let $h^* > 0$ be chosen like in Proposition 4.9. To bound the first term in the right hand side of (4.3) we note that since $\mathcal{B}^* = \begin{bmatrix}0 & B_0^*\end{bmatrix}$ and $B_{0h}^* = B_0^*\widetilde{\pi}_h$ we have that

$$\left\|\mathcal{B}^*\mathbb{T}_t W_0 - \begin{bmatrix}0 & B_{0h}^*\end{bmatrix}\mathbb{T}_t W_0\right\|_U = \|B_0^*(\dot{w}(t) - \widetilde{\pi}_h\dot{w}(t))\|_U \leqslant \|B_0^*\|_{\mathcal{L}(H,U)}\|\dot{w}(t) - \widetilde{\pi}_h\dot{w}(t)\|,$$

where we have denoted $\mathbb{T}_t W_0 = \begin{bmatrix}w(t)\\ \dot{w}(t)\end{bmatrix}$. Using next (4.8) and Proposition 4.6 we obtain that there exists a constant $C_0 > 0$ such that

$$\left\|\mathcal{B}^*\mathbb{T}_t W_0 - \begin{bmatrix}0 & B_{0h}^*\end{bmatrix}\mathbb{T}_t W_0\right\|_U \leqslant C_0 h^\theta \|\dot{w}(t)\|_{\frac{1}{2}} \leqslant C_0 h^\theta \|W_0\|_{H_{\frac{3}{2}}\times H_1}. \quad (4.4)$$

Similarly we show that the third term in the right hand side of (4.3) satisfies

$$\left\|\mathcal{B}^*\mathbb{S}_{\tau-t}\mathbb{T}_\tau W_0 - \begin{bmatrix}0 & B_{0h}^*\end{bmatrix}\mathbb{S}_{\tau-t}\mathbb{T}_\tau W_0\right\|_U \leqslant C_0 h^\theta \|W_0\|_{H_{\frac{3}{2}}\times H_1}. \quad (4.5)$$

To bound the second term in the right hand side of (4.3) we use the uniform boundedness of the family of operators $(B_{0h}^*)_{h\in(0,h^*)}$ in $\mathcal{L}(H, U)$ and Proposition 4.9 to get

$$\left\|\begin{bmatrix}0 & B_{0h}^*\end{bmatrix}(\mathbb{T}_t W_0 - \mathbb{T}_{h,t}\Pi_h W_0)\right\|_U \leqslant (K_0 + K_1\, t)h^\theta \|W_0\|_{H_{\frac{3}{2}}\times H_1}. \quad (4.6)$$

The forth term in the right hand side of (4.3) can be estimated similarly to get

$$\left\|\begin{bmatrix}0 & B_{0h}^*\end{bmatrix}(\mathbb{S}_{\tau-t}\mathbb{T}_\tau W_0 - \mathbb{S}_{h,\tau-t}\mathbb{T}_{h,\tau}\Pi_h W_0)\right\|_U \leqslant (K_0 + K_1\, t)h^\theta \|W_0\|_{H_{\frac{3}{2}}\times H_1}. \quad (4.7)$$

Using (4.4)-(4.7), relation (4.3) yields

$$\|(u - v_h)(t)\|_U \leqslant (C_2 + tC_3)h^\theta \|W_0\|_{H_{\frac{3}{2}}\times H_1},$$

for some constants $C_2,\ C_3 > 0$ and $h \in (0, h^*)$. Using in the above estimate the fact, following from Proposition 4.6 and (4.10), that

$$\|W_0\|_{H_{\frac{3}{2}}\times H_1} \leqslant \frac{1}{1 - \|L_\tau\|_{\mathcal{L}(H_{\frac{3}{2}}\times H_1)}}\|Q_0\|_{H_{\frac{3}{2}}\times H_1},$$

we obtain the conclusion of this lemma. □

We are now in a position to prove the main result of this work.

Proof of Theorem 4.1. Using the semigroup notation introduced in Section 2 we can write u_h given by (4.16) as

$$u_h(t) = \mathcal{B}_h^* \mathbb{T}_{h,t} \begin{bmatrix} w_{0h} \\ w_{1h} \end{bmatrix} + \mathcal{B}_h^* \mathbb{S}_{h,\tau-t} \mathbb{T}_{h,\tau} \begin{bmatrix} w_{0h} \\ w_{1h} \end{bmatrix} \qquad (t \in [0,\tau]), \tag{4.8}$$

where

$$\begin{bmatrix} w_{0h} \\ w_{1h} \end{bmatrix} = \sum_{n=0}^{N(h)} L_{h,\tau}^n \Pi_h \begin{bmatrix} q_0 \\ q_1 \end{bmatrix}. \tag{4.9}$$

Since

$$\|u - u_h\|_{L^2([0,\tau],U)} \leqslant \|u - v_h\|_{L^2([0,\tau],U)} + \|v_h - u_h\|_{L^2([0,\tau],U)}, \tag{4.10}$$

it suffices to evaluate the two terms from the right, where v_h is given by (4.1).

To estimate the second term in the right-hand side of (4.10) we first note that

$$\begin{aligned}
&(v_h - u_h)(t) \\
&\quad = \mathcal{B}_h^* \mathbb{T}_{h,t} \Pi_h W_0 + \mathcal{B}_h^* \mathbb{S}_{h,\tau-t} \mathbb{T}_{h,\tau} \Pi_h W_0 - \mathcal{B}_h^* \mathbb{T}_{h,t} \Pi_h \begin{bmatrix} w_{0h} \\ w_{1h} \end{bmatrix} - \mathcal{B}_h^* \mathbb{S}_{h,\tau-t} \mathbb{T}_{h,\tau} \Pi_h \begin{bmatrix} w_{0h} \\ w_{1h} \end{bmatrix}.
\end{aligned}$$

It follows that there exists a positive constant C with

$$\begin{aligned}
\|(v_h - u_h)(t)\|_U &\leqslant \left\| \mathcal{B}_h^* \mathbb{T}_{h,t} \Pi_h W_0 - \mathcal{B}_h^* \mathbb{T}_{h,t} \Pi_h \begin{bmatrix} w_{0h} \\ w_{1h} \end{bmatrix} \right\|_U \\
&\quad + \left\| \mathcal{B}_h^* \mathbb{S}_{h,\tau-t} \mathbb{T}_{h,\tau} \Pi_h W_0 - \mathcal{B}_h^* \mathbb{S}_{h,\tau-t} \mathbb{T}_{h,\tau} \Pi_h \begin{bmatrix} w_{0h} \\ w_{1h} \end{bmatrix} \right\|_U \\
&\leqslant C \left\| W_0 - \begin{bmatrix} w_{0h} \\ w_{1h} \end{bmatrix} \right\|_X = C \left\| \sum_{n=0}^{\infty} L_\tau^n Q_0 - \sum_{n=0}^{N(h)} L_{h,\tau}^n \Pi_h Q_0 \right\|_X \\
&\leqslant C \sum_{n=N(h)+1}^{\infty} \|L_\tau\|_{\mathcal{L}(X)}^n \|Q_0\|_X + C \sum_{n=0}^{N(h)} \|(L_\tau^n - L_{h,\tau}^n \Pi_h) Q_0\|_X.
\end{aligned}$$

The above estimate and Corollary 4.11 imply that there exists $\widetilde{C} > 0$ such that

$$\begin{aligned}
\|(v_h - u_h)(t)\|_U &\leqslant C \frac{\|L_\tau\|_{\mathcal{L}(X)}^{N(h)+1}}{1 - \|L_\tau\|_{\mathcal{L}(X)}} \|Q_0\|_X + C h^\theta \sum_{n=0}^{N} (C_0 + n C_1 \tau) \|Q_0\|_{H_{\frac{3}{2}} \times H_1} \\
&= C \frac{\|L_\tau\|_{\mathcal{L}(X)}^{N(h)+1}}{1 - \|L_\tau\|_{\mathcal{L}(X)}} \|Q_0\|_X + \widetilde{C} N^2(h) (1+\tau) h^\theta \|Q_0\|_{H_{\frac{3}{2}} \times H_1} \\
&\leqslant \frac{\widetilde{C}(1+\tau)}{1 - \|L_\tau\|_{\mathcal{L}(X)}} \left(\|L_\tau\|_{\mathcal{L}(X)}^{N(h)} + N^2(h) h^\theta \right) \|Q_0\|_{H_{\frac{3}{2}} \times H_1},
\end{aligned}$$

By choosing $N(h) = \left[\frac{\theta}{\ln(\|L_\tau\|_{\mathcal{L}(X)})}\ln(h)\right]$ we deduce that

$$\|(v_h - u_h)(t)\|_U \leqslant \frac{\widetilde{C}(1+\tau)}{(1-\|L_\tau\|_{\mathcal{L}(X)})\ln^2(\|L_\tau\|^{-1}_{\mathcal{L}(X)})}\ln^2(h^{-1})\, h^\theta \|Q_0\|_{H_{\frac{3}{2}}\times H_1}.$$

Combining this last estimate with (4.2) and taking $m_\tau = \frac{1}{\ln(\|L_\tau\|^{-1}_{\mathcal{L}(X)})}$ we obtain the conclusion (4.21). □

Remark 4.13. The functions u_h given by (4.16) or v_h from (4.1) should not be confused with the exact control ζ_h, obtained by applying Russell's principle to the finite-dimensional system

$$\ddot{q}_h(t) + A_{0h}q_h(t) + B_{0h}u = 0, \tag{4.11}$$

$$q_h(0) = \pi_h q_0, \quad \dot{q}_h(0) = \pi_h q_1. \tag{4.12}$$

Indeed, this control ζ_h is given by the formula

$$\zeta_h(t) = \mathcal{B}_h^*\mathbb{T}_{h,t}Z_{h0} + \mathcal{B}_h^*\mathbb{S}_{h,\tau-t}\mathbb{T}_{h,\tau}Z_{h0}, \qquad Z_{h0} = (I - L_{h,\tau})^{-1}\Pi_h\left[\begin{smallmatrix} q_0 \\ q_1 \end{smallmatrix}\right], \tag{4.13}$$

so that u_h is obtained by "filtering" (in an appropriate sense) ζ_h. Note that, since $\mathbb{T}_h$ and $\mathbb{S}_h$ are not, in general, uniformly exponentially stable (with respect to h), the control ζ_h does not, in general, converge to u (see, for instance, [88]).

4.5 Examples and numerical results

In this section we apply our numerical method to approximate exact controls for the two dimensional wave equation and for the Euler-Bernoulli beam equation. For both examples we consider distributed controls.

4.5.1 The wave equation

In this subsection we consider the approximation of an internal distributed exact control for the wave equation with homogeneous Dirichlet boundary condition.

Let $\Omega \subset \mathbb{R}^2$ be an open connected set with boundary of class C^2 or let Ω be a rectangular domain. Let $\mathcal{O} \subset \Omega$, $\mathcal{O} \neq \Omega$ be an open set. We consider the control problem

$$\ddot{q}(x,t) - \Delta q(x,t) + \chi_{\mathcal{O}}(x)u(x,t) = 0, \quad (x,t) \in \Omega \times [0,\tau] \tag{4.1}$$

$$q(x,t) = 0, \quad (x,t) \in \partial\Omega \times [0,\tau] \tag{4.2}$$

$$q(x,0) = q_0(x), \quad \dot{q}(x,0) = q_1(x), \quad x \in \Omega, \tag{4.3}$$

where $\chi_{\mathcal{O}} \in \mathcal{D}(\Omega)$ is such that $\chi_{\mathcal{O}}(x) = 1$ for $x \in \mathcal{O}$ and $\chi_{\mathcal{O}}(x) \geqslant 0$ for $x \in \Omega$.

In order to apply the method described in (4.11)-(4.20) to this case we need appropriate choices of spaces and operators. We take $H = L^2(\Omega)$, $U = H$ and $A_0 : \mathcal{D}(A_0) \to H$ with

$$\mathcal{D}(A_0) = \mathcal{H}^2(\Omega) \cap \mathcal{H}_0^1(\Omega), \quad A_0\varphi = -\Delta\varphi \qquad (\varphi \in \mathcal{D}(A_0)),$$

where we use the notation $\mathcal{H}^m(\Omega)$, with $m \in \mathbb{N}$, for the standard Sobolev spaces. It is well known that A_0 is a self-adjoint, strictly positive operator with compact resolvents. The corresponding spaces $H_{\frac{3}{2}}$, H_1 and $H_{\frac{1}{2}}$ introduced in Section 1 are in this case given by

$$H_{\frac{3}{2}} = \left\{\varphi \in \mathcal{H}^3(\Omega) \cap \mathcal{H}_0^1(\Omega) \;\mid\; \Delta\varphi = 0 \;\text{ on }\; \partial\Omega\right\},$$
$$H_1 = \mathcal{H}^2(\Omega) \cap \mathcal{H}_0^1(\Omega), \qquad H_{\frac{1}{2}} = \mathcal{H}_0^1(\Omega).$$

The control operator $B_0 \in \mathcal{L}(H)$ is defined by

$$B_0 u = \chi_{\mathcal{O}} u \qquad (u \in H).$$

The operator B_0 is clearly self-adjoint and $B_0 B_0^* \in \mathcal{L}(H_1, H_{\frac{1}{2}})$. Moreover, we assume that τ and $\mathcal{O}$ are such that the system (4.1)-(4.3) is exactly controllable in time τ, i.e., that for every $\left[\begin{smallmatrix} q_0 \\ q_1 \end{smallmatrix}\right] \in H_0^1(\Omega) \times L^2(\Omega)$ there exists a control $u \in L^2([0,\tau], U)$ such that $q(\tau) = \dot{q}(\tau) = 0$. Sufficient conditions in which this assumption holds are give in various works, see Lions [48], Bardos, Lebeau and Rauch [9], Liu [49].

To construct an approximating family of spaces $(V_h)_{h>0}$ we consider a quasi-uniform triangulation $\mathcal{T}_h$ of Ω of diameter h, as defined, for instance, in [13, p.106]. For each $h > 0$ we define V_h by

$$V_h = \left\{\varphi \in C(\overline{\Omega}) \;\middle|\; \varphi_{|T} \in P_1(T) \;\text{ for every }\; T \in \mathcal{T}_h,\; \varphi_{|\partial\Omega} = 0\right\},$$

where $P_1(T)$ is the set of affine functions on T. It is well-known (see, for instance, [63, p.96-97]) that the orthogonal projector π_h from $H_{\frac{1}{2}} = \mathcal{H}_0^1(\Omega)$ onto V_h satisfies (4.4) and (4.5) for $\theta = 1$.

We define $U_h = \{\chi_{\mathcal{O}} v_h \;|v_h \in V_h\} \subset U$ and let $B_{0h} \in \mathcal{L}(H)$ be given by $B_{0h}\varphi = \widetilde{\pi}_h(\chi_{\mathcal{O}}\varphi)$ for every $\varphi \in H$. Note that $B_{0h}^*\varphi_h = \chi_{\mathcal{O}}\varphi_h$ and $\langle B_{0h}B_{0h}^*\varphi_h, \psi_h\rangle = \langle \chi_{\mathcal{O}}^2\varphi_h, \psi_h\rangle$ for every $\varphi_h, \psi_h \in V_h$, where $\langle\cdot,\cdot\rangle$ denotes the inner product in $L^2(\Omega)$.

With the above choice of spaces and operators, denoting by $N(h) = \left[\frac{\theta}{\ln\|L_\tau\|}\ln h\right]$, the first part of the general method described in (4.11)-(4.20) reduces to the computation of the families of functions $(w_h^n)_{1\leqslant n\leqslant N(h)}$, $(w_{b,h}^n)_{1\leqslant n\leqslant N(h)}$ satisfying, for every $v_h \in V_h$,

$$\langle \ddot{w}_h^n(t), v_h\rangle + \langle \nabla w_h^n(t), \nabla v_h\rangle + \langle \chi_{\mathcal{O}}^2 \dot{w}_h^n(t), v_h\rangle = 0 \qquad (t \in [0,\tau]) \tag{4.4}$$

$$w_h^n(0) = \begin{cases} \pi_h q_0, & \text{if } n = 1 \\ w_{b,h}^{n-1}(0), & \text{if } n > 1 \end{cases} \qquad \dot{w}_h^n(0) = \begin{cases} \pi_h q_1, & \text{if } n = 1 \\ \dot{w}_{b,h}^{n-1}(0), & \text{if } n > 1, \end{cases} \tag{4.5}$$

and

$$\langle \ddot{w}_{b,h}^n(t), v_h\rangle + \langle \nabla w_{b,h}^n(t), \nabla v_h\rangle - \langle \chi_{\mathcal{O}}^2 \dot{w}_{b,h}^n(t), v_h\rangle = 0 \qquad (t \in [0,\tau]) \tag{4.6}$$

$$w_{b,h}^n(\tau) = w_h^n(\tau), \qquad \dot{w}_{b,h}^n(\tau) = \dot{w}_h^n(\tau). \tag{4.7}$$

The second part of the method described in (4.11)-(4.20) reduces to the computation of w_{0h} and w_{1h} defined by

$$\begin{bmatrix} w_{0h} \\ w_{1h} \end{bmatrix} = \begin{bmatrix} \pi_h q_0 \\ \pi_h q_1 \end{bmatrix} + \sum_{n=1}^{N(h)} \begin{bmatrix} w_{b,h}^n(0) \\ \dot{w}_{b,h}^n(0) \end{bmatrix}. \tag{4.8}$$

Finally, the approximation u_h of the exact control u is given by

$$u_h = \chi_{\mathcal{O}} \dot{w}_h + \chi_{\mathcal{O}} \dot{w}_{b,h}, \tag{4.9}$$

where w_h and $w_{b,h}$ are the solution of

$$\langle \ddot{w}_h(t), v_h \rangle + \langle \nabla w_h(t), \nabla v_h \rangle + \langle \chi_{\mathcal{O}}^2 \dot{w}_h(t), v_h \rangle = 0 \qquad (v_h \in V_h,\ t \in [0,\tau]) \tag{4.10}$$

$$w_h(0) = w_{0h}, \quad \dot{w}_h(0) = w_{1h} \tag{4.11}$$

$$\langle \ddot{w}_{b,h}(t), v_h \rangle + \langle \nabla w_{b,h}(t), \nabla v_h \rangle - \langle \chi_{\mathcal{O}}^2 \dot{w}_{b,h}(t), v_h \rangle = 0 \qquad (v_h \in V_h,\ t \in [0,\tau]) \tag{4.12}$$

$$w_{b,h}(\tau) = w_h(\tau), \qquad \dot{w}_{b,h}(\tau) = \dot{w}_h(\tau). \tag{4.13}$$

Since we checked above all the necessary assumptions, we can apply Theorem 4.1 to obtain that (u_h) converges in $C([0,\tau]; L^2(\Omega))$ to an exact control u such that

$$\|u - u_h\|_{C([0,\tau];L^2(\Omega))} \leqslant Ch \ln^2(h^{-1})(\|q_0\|_{\mathcal{H}^3(\Omega)} + \|q_1\|_{\mathcal{H}^2(\Omega)}) \qquad (0 < h < h^*). \tag{4.14}$$

for some constants $h^*,\ C > 0$.

The efficiency of the algorithm has been tested in the case $\Omega = [0,1]^2$ and $\mathcal{O} = [(x_1, x_2) \times (0,1)] \cup [(0,1) \times (y_1, y_2)]$, where $x_1, x_2, y_1, y_2 \in (0,1)$ are such that $x_1 < x_2$ and $y_1 < y_2$. The initial data that we want to steer to zero are the "bubble" functions $q_0(x,y) = q_1(x,y) = x^3y^3(1-x)^3(1-y)^3$ and the control time is $\tau = 2\sqrt{2}$. Note that $\left[\begin{smallmatrix} q_0 \\ q_1 \end{smallmatrix}\right] \in H_{\frac{3}{2}} \times H_{\frac{1}{2}}$. We use 60 points of discretization in each space direction. For the time discretization we used a classical centered-difference implicit scheme and the CFL number is $\alpha = 1/20$.

Figure 4.1 shows the norm decay of the solution of the discretized wave equation coresponding to (4.1)-(4.3), with a control u_h given by (4.16).

Figure 4.2 displays the norm of the solution of the controlled discretized wave equation, corresponding to (4.1)-(4.3), at the time τ for different values of N used in calculus of $\left[\begin{smallmatrix} w_{0h} \\ w_{1h} \end{smallmatrix}\right]$.

4.5.2 The Euler-Bernoulli beam equation

This subsection is dedicated to the problem of the approximation of an internal distributed exact control for the Euler-Bernoulli beam equation.

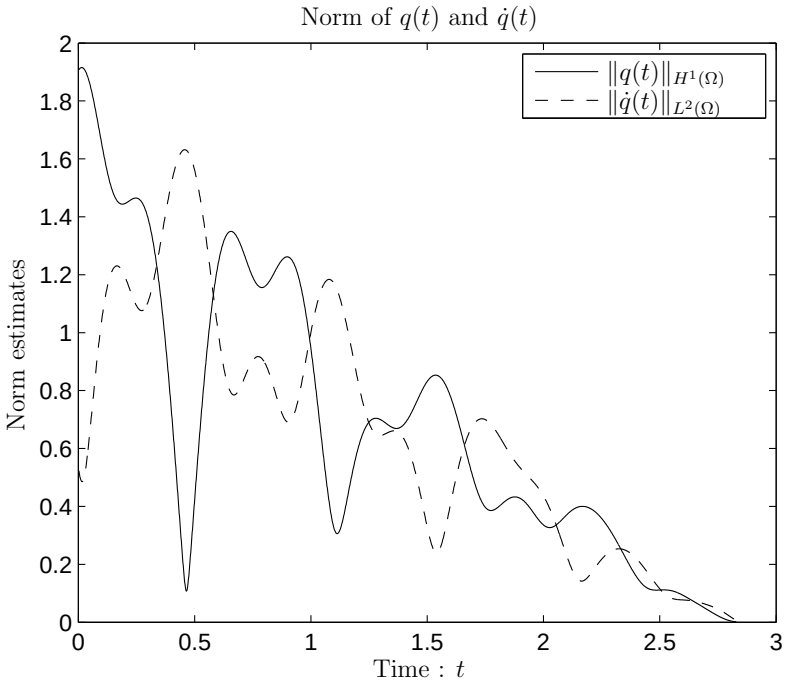

Figure 4.1: The norms of the solution of the controlled wave equation with the control u_h given by (4.16). In continuous line is the norm H_0^1 of $q(t)$ and in dashed line the norm L^2 of $\dot{q}(t)$.

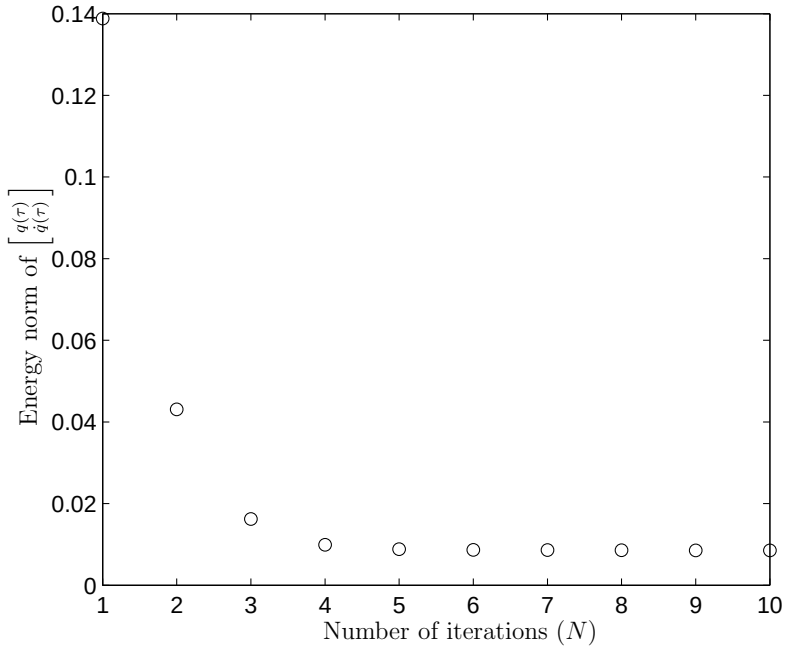

Figure 4.2: The energy of the controlled wave equation solution at the time τ versus the number of terms N in the approximation of the control u_h.

Let $\Omega = (0, 1)$ and let $\mathcal{O} \subset \Omega$ be an open and nonempty interval included in Ω. We

consider the following problem

$$\ddot{q}(x,t) + \frac{\partial^4 q}{\partial x^4}(x,t) + \chi_{\mathcal{O}}(x)u(x,t) = 0, \quad (x,t) \in \Omega \times [0,\tau] \tag{4.15}$$

$$q(0,t) = \frac{\partial^2 q}{\partial x^2}(0,t) = q(1,t) = \frac{\partial^2 q}{\partial x^2}(1,t) = 0, \quad t \in [0,\tau] \tag{4.16}$$

$$q(x,0) = q_0(x), \quad \dot{q}(x,0) = q_1(x), \quad x \in \Omega, \tag{4.17}$$

modeling a beam hinged at the both ends with a control u applied in an internal region. We denote by $\chi_{\mathcal{O}} \in \mathcal{D}(\Omega)$ a positive function which satisfies $\chi_{\mathcal{O}}(x) = 1$ for every $x \in \mathcal{O}$. It is well known (see, for instance, [80, Example 6.8.3]) that the system (4.15)-(4.17) is exactly controllable in any time $\tau > 0$.

In order to apply the method described in this paper we need to choose appropriate spaces and operators. Let $H = L^2(\Omega)$, $U = H$ and consider the operator $A_0 : \mathcal{D}(A_0) \to H$, defined by

$$\mathcal{D}(A_0) = \left\{ \varphi \in \mathcal{H}^4(\Omega) \;\mid\; \varphi(0) = \frac{d^2\varphi}{dx^2}(0) = \varphi(1) = \frac{d^2\varphi}{dx^2}(1) = 0 \right\},$$

$$A_0\varphi = \frac{d^4\varphi}{dx^4} \qquad (\varphi \in \mathcal{D}(A_0)).$$

It is well known that A_0 is a self-adjoint, strictly positive operator with compact resolvents. The corresponding spaces $H_{\frac{3}{2}}$, H_1 and $H_{\frac{1}{2}}$ introduced in Section 4.1 are now given by

$$H_{\frac{3}{2}} = \left\{ \varphi \in \mathcal{H}^6(\Omega) \;\mid\; \varphi(0) = \varphi(1) = \frac{d^2\varphi}{dx^2}(0) = \frac{d^2\varphi}{dx^2}(1) = \frac{d^4\varphi}{dx^4}(0) = \frac{d^4\varphi}{dx^4}(1) = 0 \right\},$$

$$H_1 = \left\{ \varphi \in \mathcal{H}^4(\Omega) \;\mid\; \varphi(0) = \frac{d^2\varphi}{dx^2}(0) = \varphi(1) = \frac{d^2\varphi}{dx^2}(1) = 0 \right\}, \quad H_{\frac{1}{2}} = \mathcal{H}^2(\Omega) \cap \mathcal{H}_0^1(\Omega).$$

As in the case of the wave equation the control operator $B_0 \in \mathcal{L}(H)$ is defined by $B_0 u = \chi_{\mathcal{O}} u$ for every $u \in H$. Clearly B_0 is self-adjoint and $B_0 \in \mathcal{L}(H_1, H_{\frac{1}{2}})$.

To construct an approximating family of spaces $(V_h)_{h>0}$ we consider an uniform discretization $\mathcal{I}_h$ of the interval $(0,1)$ formed by $\mathcal{N}$ points and $h = 1/(\mathcal{N}-1)$. For each $h > 0$ we define V_h by

$$V_h = \{\varphi \in C^1([0,1]) \mid \varphi_{|I} \in P_3(T) \text{ for every } I \in \mathcal{I}_h, \;\; \varphi(0) = \varphi(1) = 0\},$$

where $P_3(I)$ is the set of polynomial functions of degree 3 on I. Note that V_h is the cubic Hermite finite element space. Denoting by π_h the orthogonal projector from $H_{\frac{1}{2}}$ to V_h and applying the Theorem 3.3 from Strang and Fix [75, p. 144] we obtain estimates (4.4) and (4.5) with $\theta = 2$.

Indeed, Theorem 3.3 from [75, p. 144] has the following statement:

Theorem 4.14. *Suppose that V_h is of degree $k-1$ and its basis is uniform to order q. Suppose also that the derivatives D_j associated with the nodal parameters are all of order $|D_j| < k - \frac{n}{2}$. Then for any function $u \in \mathcal{H}^k(\Omega)$ and for every $s \leqslant q$ there exists a positive constant C_s such that the following estimate is verified*

$$\|\pi_h u - u\|_{\mathcal{H}^s(\Omega)} \leqslant C_s h^{k-s} \|u\|_{\mathcal{H}^k(\Omega)}. \tag{4.18}$$

Remark 4.15. For Hermite cubic interpolation we have $k = 4$ and $q = 2$. Moreover, the orthogonal projector π_h from H_1 to V_h is the restriction of the orthogonal projector from $H_{\frac{1}{2}}$ to V_h. This can be easily verified using the definition of this projector :

$$\pi_h f = \sum_{i=1}^{\mathcal{N}} f((i-1)h)\varphi_i \qquad (f \in H_{\frac{1}{2}}),$$

where φ_i is the basis of V_h.

Remark 4.16. Estimate (4.18) gives directly only (4.4) for our spaces. To prove (4.5) we use the same ideas as in the proof of Theorem (4.14) in [75, p. 144]. Under the same hypotheses we prove in general case that for every $u \in \mathcal{H}^{k-2}(\Omega)$ and for every $s \leqslant q-2$ there exists $C_s > 0$ such that

$$\|\pi_h u - u\|_{\mathcal{H}^s(\Omega)} \leqslant C_s h^{k-2-s} \|u\|_{k-2},$$

this givin precisely (4.5) with $\theta = 2$.

The method described by (4.11)-(4.20) reduces to the computation of the families of functions $(w_h^n)_{1\leqslant n\leqslant N(h)}$, $(w_{b,h}^n)_{1\leqslant n\leqslant N(h)}$ satisfying, for every $v_h \in V_h$,

$$\langle \ddot{w}_h^n(t), v_h\rangle + \left\langle \frac{\partial^2 w_h^n}{\partial x^2}(t), \frac{\mathrm{d}^2 v_h}{\mathrm{d}x^2}\right\rangle + \langle \chi_{\mathcal{O}}^2 \dot{w}_h^n(t), v_h\rangle = 0 \qquad (t \in [0,\tau]) \tag{4.19}$$

$$w_h^n(0) = \begin{cases} \pi_h q_0, & \text{if } n = 1 \\ w_{b,h}^{n-1}(0), & \text{if } n > 1 \end{cases} \qquad \dot{w}_h^n(0) = \begin{cases} \pi_h q_1, & \text{if } n = 1 \\ \dot{w}_{b,h}^{n-1}(0), & \text{if } n > 1, \end{cases} \tag{4.20}$$

and

$$\langle \ddot{w}_{b,h}^n(t), v_h\rangle + \left\langle \frac{\partial^2 w_{b,h}^n}{\partial x^2}(t), \frac{\mathrm{d}^2 v_h}{\mathrm{d}x^2}\right\rangle - \langle \chi_{\mathcal{O}}^2 \dot{w}_{b,h}^n(t), v_h\rangle = 0 \qquad (t \in [0,\tau]) \tag{4.21}$$

$$w_{b,h}^n(\tau) = w_h^n(\tau), \qquad \dot{w}_{b,h}^n(\tau) = \dot{w}_h^n(\tau). \tag{4.22}$$

The second part of the method described in (4.11)-(4.20) reduces to the computation of w_{0h} and w_{1h} defined by

$$\begin{bmatrix} w_{0h} \\ w_{1h} \end{bmatrix} = \begin{bmatrix} \pi_h q_0 \\ \pi_h q_1 \end{bmatrix} + \sum_{n=1}^{N(h)} \begin{bmatrix} w_{b,h}^n(0) \\ \dot{w}_{b,h}^n(0) \end{bmatrix}. \tag{4.23}$$

Finally, the approximation u_h of the exact control u is given by

$$u_h = \chi_{\mathcal{O}} \dot{w}_h + \chi_{\mathcal{O}} \dot{w}_{b,h}, \tag{4.24}$$

where w_h and $w_{b,h}$ are the solution of

$$\langle \ddot{w}_h(t), v_h \rangle + \left\langle \frac{\partial^2 w_h}{\partial x^2}(t), \frac{\mathrm{d}^2 v_h}{\mathrm{d}x^2} \right\rangle + \langle \chi^2_{\mathcal{O}} \dot{w}_h(t), v_h \rangle = 0 \qquad (t \in [0, \tau]) \tag{4.25}$$

$$w_h(0) = w_{0h}, \quad \dot{w}_h(0) = w_{1h} \tag{4.26}$$

$$\langle \ddot{w}_{b,h}(t), v_h \rangle + \left\langle \frac{\partial^2 w_{b,h}}{\partial x^2}(t), \frac{\mathrm{d}^2 v_h}{\mathrm{d}x^2} \right\rangle - \langle \chi^2_{\mathcal{O}} \dot{w}_{b,h}(t), v_h \rangle = 0 \qquad (t \in [0, \tau]) \tag{4.27}$$

$$w_{b,h}(\tau) = w_h(\tau), \qquad \dot{w}_{b,h}(\tau) = \dot{w}_h(\tau). \tag{4.28}$$

From Theorem 4.1 we obtain that (u_h) converges in $C([0,\tau]; L^2(\Omega))$ to an exact control u such that

$$\|u - u_h\|_{C([0,\tau];L^2(\Omega))} \leqslant C h^2 \ln^2(h^{-1})(\|q_0\|_{\mathcal{H}^6(\Omega)} + \|q_1\|_{\mathcal{H}^4(\Omega)}) \qquad (0 < h < h^*). \tag{4.29}$$

for some constants $h^*,\ C > 0$.

We tested the algorithm in the case $\mathcal{O} = (\frac{1}{3}, \frac{2}{3})$ and the initial data that we want to steer to zero are $q_0(x) = x^5(1-x)^5$, $q_1(x) = -q_0(x)$ and the control time is $\tau = 1$. Note that $\left[\begin{smallmatrix} q_0 \\ q_1 \end{smallmatrix}\right] \in H_{\frac{3}{2}} \times H_1$. We used $\mathcal{N} = 100$ discretization points in space and in time an implicit centered-difference scheme with the CFL number equal to 0.1.

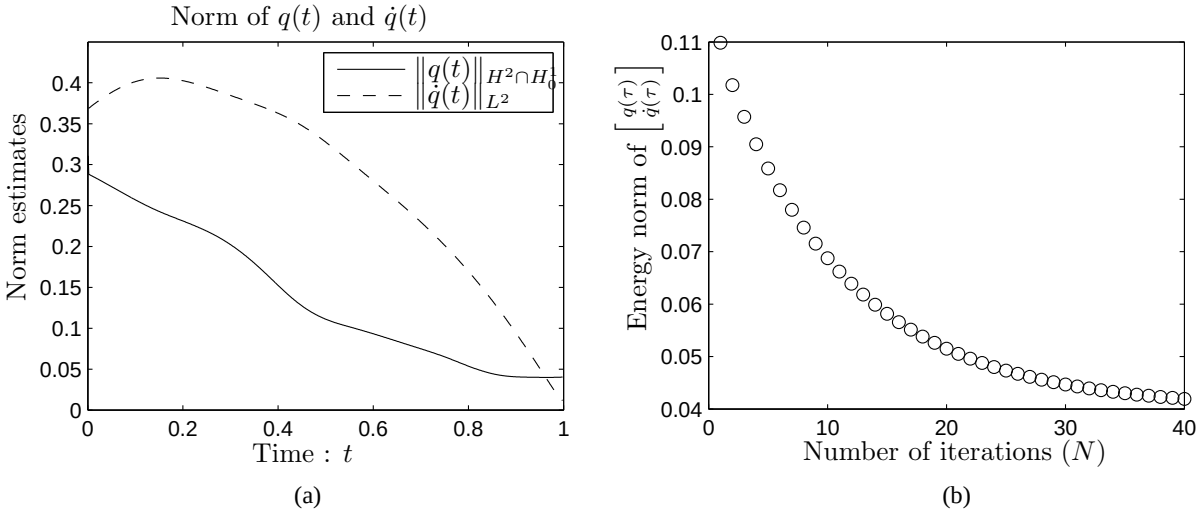

Figure 4.3: (a) The norm of the solution of the controlled beam equation, with $u = u_h$ and the initial state $q_0(x) = x^5(1-x)^5$, $q_1(x) = -q_0(x)$. (b) The energy of the solution of the controlled beam at time τ versus the number of terms N in the approximation of u_h.

Figure 4.3(a) shows the norm decay of the solution of the discretized beam equation coresponding to (4.15)-(4.17), with a control u_h given by (4.16). Figure 4.3(b) displays

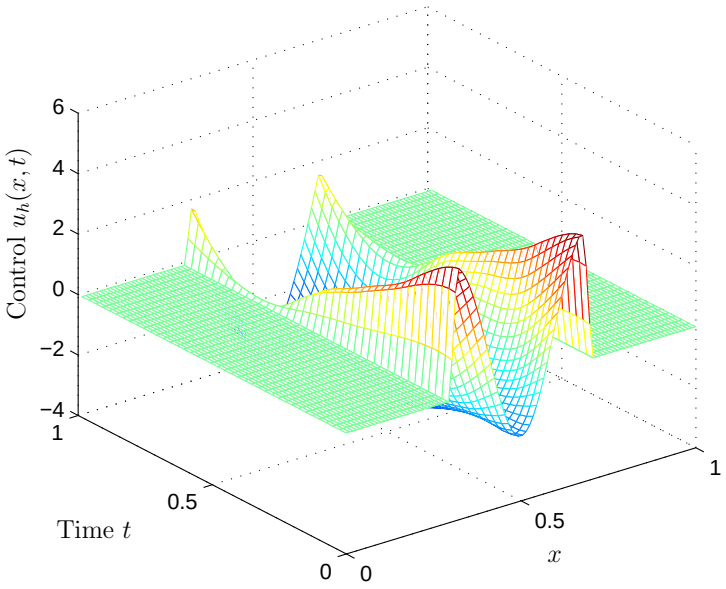

Figure 4.4: The approximation u_h with the initial state $q_0(x) = x^5(1-x)^5$, $q_1(x) = -q_0(x)$ and the control time $\tau = 1$.

the dependence of the norm of the solution of (4.15)-(4.17), at the time τ, to the number N of terms used in the calculus of $\left[\begin{smallmatrix} w_{0h} \\ w_{1h} \end{smallmatrix}\right]$.

In Figure 4.4 is given the form of the approximate control u_h corresponding to the initial data $\left[\begin{smallmatrix} q_0 \\ q_1 \end{smallmatrix}\right]$ considered in the example below.

Conclusion and perspectives

In this part of the thesis, we proved some exact observability and controllability results for two types of perturbed plate equations and we studied a numerical method for the approximation of the exact controls of vibrating systems.

In Chapter 1 we gathered some basic results on exact controllability and observability of infinite dimensional systems wich were necessary to give a unitary structure of this part.

In Chapter 2 we proved the exact observability of an Euler-Bernoulli plate equation perturbed by a linear lower order term of a general form. We used a spectral criterium for the exact observability combined with a simultaneous observability result to manage the pertubation.

In Chapter 3 we proved the local exact observability of a nonlinear plate equation, due to Berger, by means of a control acting in an internal region of the plate. We tackle this equation as a pertubation of Euler-Bernoulli plate equation. The pertubing term has a linear part, wich can be tackled by the same spectral criterium used in Chapter 2, and a nonlinear part wich we tackled by a fixed point argument. This fixed point argument gives us the local character of the controllability result obtained for the Berger equation.

For both plate equations studied in Chapters 2 and 3 we obtained the exact obsevability and, respectively, the exact controllability, in an arbitrarily small time if the plate is rectangular. One intersting perspective is to study the influence of the shape of the domain on the controllability or observability time : in particular can we obtain an arbitrarily small controllability time for other domains than rectangular ones?

In Chapter 4 we described a method to approximate the exact controls of vibrating systèmes modeled by equations of second order in time and with bounded control operators. We proved the error estimates for this approximations of the exact controls and we illustrated this method by numerical simulations for wave and plate equations.

One interesting future development of this numerical method is to study the error estimates in the approximation of the controls in the case of unbounded control operators. In this way we can approximate the boundary controls for PDEs. Another intersting development is to combine a full space-time discretization with this method.

Another research perspective is to develop numerical methods to approximate the exact controls for pertubed second order systems and for first order systems such that we can tackle the pertubed, eventualy nonlinear, systems studied in Chapters 2 and 3.

Part II

Inverse problems in MRI

5. Introduction to cardiac MRI

In this chapter we give some notions of MRI, which are necessary for the comprehension of this part of the thesis.

In the first section we explain the basic physics of magnetic resonance imaging (MRI) passing rapidely from magnetic spin resonance to the equation of the MRI signal and image formation. The second section focuses to the problematic of motion during MRI acquisition, particularly being interested to cardiac MRI.

5.1 Basic physics of magnetic resonance

This section is a short introduction to the basic MRI physics. For details, a good textbook is Haacke et al [33].

5.1.1 Nuclear spin resonance and Bloch equation

Nuclear magnetic resonance is based on the magnetic properties of the atom's nuclei, or more precisely, on the properties of nucleons (neutrons and protons). A notion wich describes these properties is the nuclear spin, discovered by Pauli in 1924.

The nuclear spin $\overrightarrow{S}$ is a measure of the particle's intrinsic angular momentum. More precisely, a quantum mechanical description of particle's spin consists in a set of complex numbers corresponding to projection of the angular momentum of the particle on a given axis. In the remaining part of this chapter we consider spin $\frac{1}{2}$ particle, for which we need two numbers $a_{\pm\frac{1}{2}}$, giving amplitudes of finding it with projection of angular momentum equal to $\frac{\hbar}{2}$ and $-\frac{\hbar}{2}$. Particularly, in MRI are important nuclei wich have a spin of one-half, like ${}^1H$. Therefore, the nucleus has two possible spin states: $m = 1/2$ or $m = -1/2$. These states have the same energy, the number of atoms in these two states being approximatively equal. The relation between a spin and its magnetic moment $\overrightarrow{\mu}$ is the following.

$$\overrightarrow{\mu}(p) = \gamma \overrightarrow{S}(p), \tag{5.1}$$

where γ is a constant characteristic of the studied nucleum and by p we denote a given particule (proton).

If there is no external magnetic field the spins are randomly oriented. If a static magnetic field $\overrightarrow{B}_0$ is applied all magnetic momentum $\overrightarrow{\mu}(p)$ are oriented in the direction of the field $\overrightarrow{B}_0$. The evolution in time of the magnetic moment $\overrightarrow{\mu}(p)$ is governed by the following equation (simplified Bloch equation) :

$$\frac{d\overrightarrow{\mu}(p,t)}{dt} = \gamma\,\overrightarrow{\mu}(p,t) \times \overrightarrow{B}_0, \tag{5.2}$$

for every isolated proton p placed in the constant magnetic field $\overrightarrow{B}_0$.

The solution of this equation is a precession motion of the vector $\overrightarrow{\mu}$ around the direction of $\overrightarrow{B}_0$ (Figure 5.1). The angle of precession θ is given by the initial condition on $\overrightarrow{\mu}$ and the angular frequency ω (or Larmor frequency) is given by :

$$\omega = \gamma|\overrightarrow{B}_0|. \tag{5.3}$$

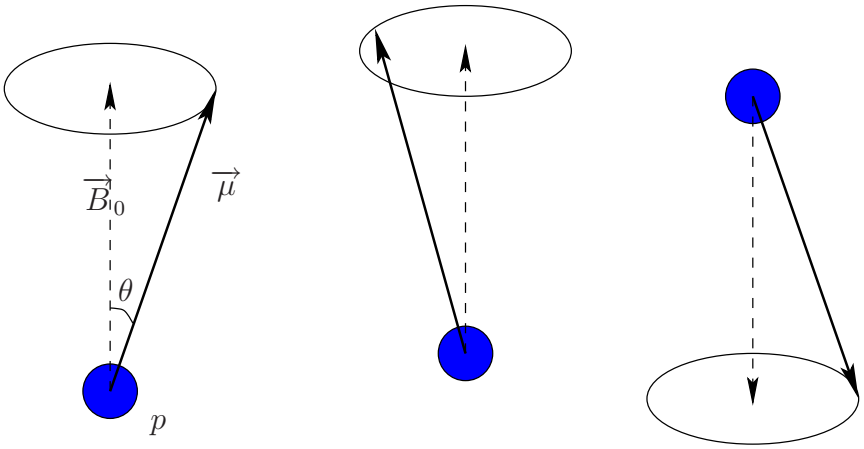

Figure 5.1: Motion of the nuclear spins placed in a external magnetic field B_0. The directions of the vector μ can be parallel or anti-parallel with the direction of B_0.

Magnetic resonance phenomenon

Magnetic resonance phenomenon is obtained by the application of an additional magnetic field $\overrightarrow{B}_1$ (a RF pulse) oriented in a perpendicular plane to the direction of $\overrightarrow{B}_0$ and with the angular speed ω. This field will basculate the spin $\overrightarrow{\mu}$ with an angle θ_0 such that the spin arrive usually in the transverse plane. The explanation of the necessity to use this kind of pulse $\overrightarrow{B}_1$ is that in MRI we need to consider all the nuclear spins from a volume and not an isolated spin. Supposing that the spins are placed under a constant magnetic field $\overrightarrow{B}_0$, the sum of all magnetic momentum $\overrightarrow{\mu}$ from a volume will be parallel with $\overrightarrow{B}_0$ (because all the spins precess around $\overrightarrow{B}_0$ with aleatory phases).

For modeling the result of the apllication of a magnetic field to a volume V we denote by $\overrightarrow{M}$ the summation of all the spin's magnetic momentum for all the protons in V, i.e.

$$\overrightarrow{M}(t) = \int_V \overrightarrow{\mu}(p,t)\ \mathrm{d}p. \tag{5.4}$$

Then $\overrightarrow{M}(t)$ will be governed by an equation similar to the Bloch equation for a single spin (5.2), with some suplementary terms given by the interactions between protons in V. There are two kind of interactions :

- After the stop of the RF pulse $\overrightarrow{B}_1$ the nuclear spins interact only with $\overrightarrow{B}_0$ and they tends to orient in the direction of $\overrightarrow{B}_0$. This is modeled by a longitudinal magnetization term M_Z wich increases exponentialy (with a rate T_1).
- The spin-spin interactions force the spins to go out from the resonance phase to an incoherent phase. These interactions are modeled by transversal magnetization term $M_\perp$ which decreases exponentialy (with the rate T_2).

Now, $\overrightarrow{M}(t)$ will verify the following Bloch equation :

$$\frac{d\overrightarrow{M}}{dt}(t) = \gamma\overrightarrow{M}(t) \times (\overrightarrow{B}_0 + \overrightarrow{B}_1(t)) + \frac{1}{T_1}(M_0 - M_Z)\overrightarrow{z} - \frac{1}{T_2}\overrightarrow{M}_\perp. \tag{5.5}$$

The importance of equation (5.5) is that in this way we know the resulting magnetization $\overrightarrow{M}$ for the protons in a volume V, corresponding to the known magnetic fields $\overrightarrow{B}_0$ and $\overrightarrow{B}_1$. The variation in time of $\overrightarrow{M}(t)$ induce a variation of flux in the coils and therefore we have a measurable signal (Figure 5.2).

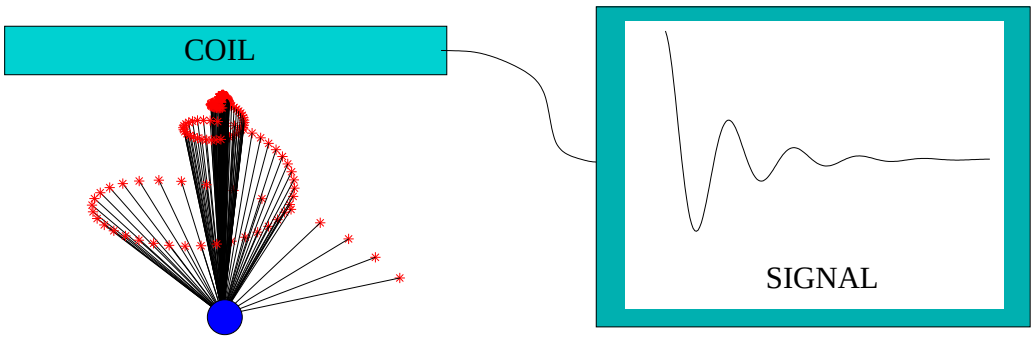

Figure 5.2: MR signal detection

5.1.2 Image formation

For obaining an image we need to localize in space the signal recorded as in previous section. This is possible because the resonance frequency depends linearly to the applied magnetic field $\overrightarrow{B}$ as in (5.3) and, therefore, varying $\overrightarrow{B}$ in space, the spins from different positions will oscilate with different frequencies.

Gradients and spatial encoding

Let suppose that we want to obtain a 2d image in a plane perpendicular to direction $\overrightarrow{\alpha}$. We consider then a magnetic field $\overrightarrow{B}$ depending linearly to the position in direction $\overrightarrow{\alpha}$

$$\overrightarrow{B}(\alpha) = \overrightarrow{B}_0 + G_\alpha \overrightarrow{\alpha}.$$

The function G_α is called gradient of the magnetic field $\overrightarrow{B}$ in direction $\overrightarrow{\alpha}$. Therefore, for a certain frequency of the RF pulse $\overrightarrow{B}_1$ only the spins from a slice in direction $\overrightarrow{\alpha}$ are excited.

Now it remains to localize the signal from a given position (x, y) in this selected plane. For this we use the frequency and phase encoding, respectively. More precisely, applying a linear gradient G_y in the direction y for a short time τ, the spins from this plane precess with different frequency depending on the position in the direction y. In this thesis we assume that this time τ is shorter than the time T_2 ($\tau \ll T_2 < T_1$). After this magnetic pulse of gradient G_y stops, the phase of the magnetization will depends linearly to y. This part of the process is called phase encoding.

For discriminate in x direction we will apply a magnetic pulse with a gradient G_x linearly dependent to x. During the apllication of this pulse the spins in direction x will precess with different frequency and is now that acquisition of signal take place (see Figure 5.3). This part is called frequency encoding.

Signal equation

We introduce some notation. Let $g(\overrightarrow{k}, t)$ the MR signal for the position $\overrightarrow{k} = (k_x, k_y)$ and the time t. The density of protons in the selected slice (the image) is denoted by $f(x, y)$, with $(x, y) \in \Omega$, where Ω is the spatial domain where the proton density is non zero. The relation between signal and proton density is given by the following equation:

$$g(G_x, G_y, t) = \iint_\Omega f(x, y) e^{-2\pi i(k_x x + k_y y)} \, \mathrm{d}x \, \mathrm{d}y, \tag{5.6}$$

where k_x and k_y are notations for

$$\begin{cases} k_x = \dfrac{\gamma}{2\pi} G_x \int_0^t G_x(s) \, \mathrm{d}s = \dfrac{\gamma}{2\pi} G_x t \\ k_y = \dfrac{\gamma}{2\pi} G_y \int_0^\tau G_y(s) \, \mathrm{d}s = \dfrac{\gamma}{2\pi} G_y \tau. \end{cases} \tag{5.7}$$

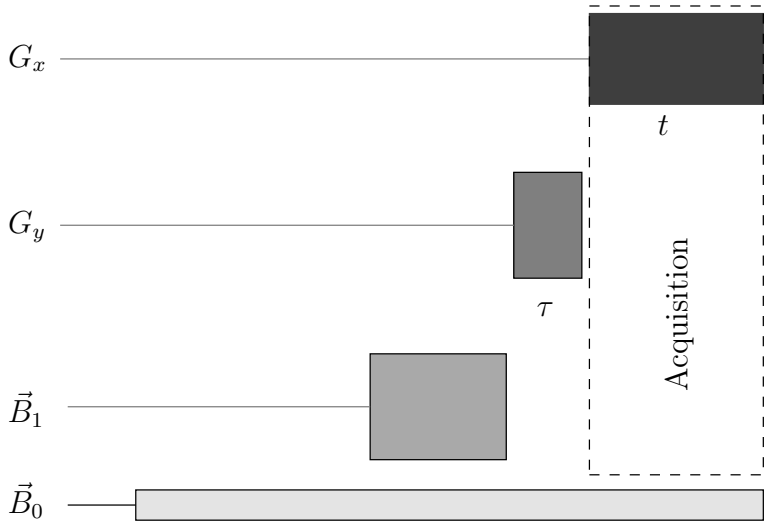

Figure 5.3: Magnetic gradients

Equivalently, relation (5.6) can be written as

$$g(\vec{k}(t), t) = \int_{\Omega} f(\vec{r}, t) e^{-2\pi i \vec{k} \cdot \vec{r}} \, \mathrm{d}\vec{r}.$$

To recover the image f from the signal g given by (5.6) we need to variate the gradients G_y and G_z such that (k_x, k_y) will cover the k-space with a "good" density. Then f is obtained as an inverse Fourier transform of g. There, "good" means that the sample's density (k_x, k_y) is in a direct relation with the field of view (FOV) of the reconstructed image and the support of the set formed by all acquired $g(k_x, k_y)$ with the resolution of the image.

5.2 Motion problematic and cardiac MRI

In Section 5.1 we assumed that the density of spins $f(x, y)$ is constant in time. This is not the case in a MRI experiment because of involuntary or physiological motions of patient. However, we assume that the duration of RF pulse used for acquisition is small enough such that there is no motion during the acquisition of the signal for a single position (k_x, k_y). Moreover, in this thesis we don't discuss the situation of motions that can appear in a time shorter than T_2.

The effect of motion consists in apparition of artifacts and there exists an important literature on this subject. Some of the first papers about motion artifacts in MRI are the following Schultz et al. [70], Wood and Henkelman [85].

We can see one example of motion artifacts on a simulated phantom (Figure 5.4) and an example of artifacts on a cardiac MRI acquired in free-breathing (Figure 5.5).

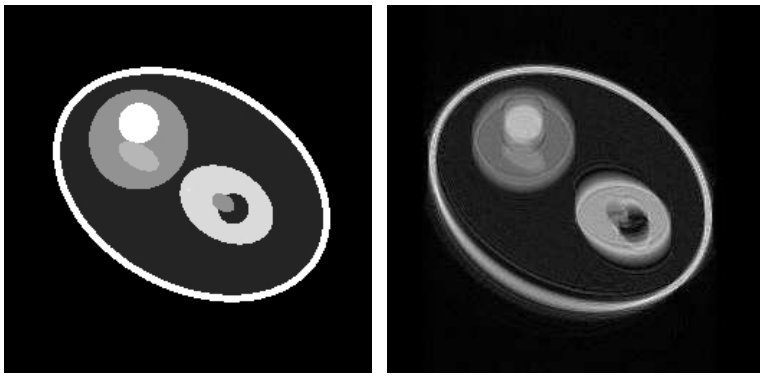

(a) (b)

Figure 5.4: Numerical simulated phantom with a periodic motion. (a) Exact static image. (b) Image with motion artifacts

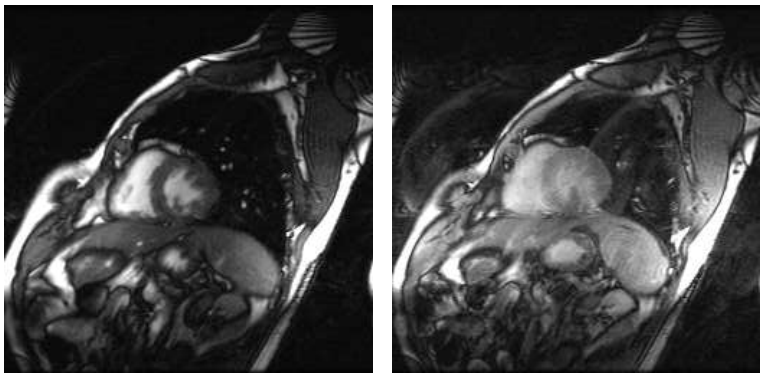

(a) (b)

Figure 5.5: Two images cardiac from a healthy volunteer acquired in free-breathing. (a) Image reconstructed using the method presented in Chapter 6. (b) Image reconstructed by an inverse Fourier transform.

One of the major chalenges in MRI is to image objects in motion as is the case for cardiac MRI.

In the remaining part of this thesis we assume that the density of protons in the imaged domain Ω is time dependent. Then the relation between the signal and image (5.6) can be written in the following form (after a change of variable) :

$$s(k_x, k_y, t) = \iint_{\Omega} f(x, y, t) e^{-i(k_x(t)x + k_y(t)y)} \, \mathrm{d}x \, \mathrm{d}y. \tag{5.8}$$

A first approach for recovering the image $f(x, y, t)$, assuming that the motion of the imaged subjet is known, is to make a change of variable to a fixed initial domain as in Odille et al. [56, 58] to compensate the respiratory and cardiac motions for a cardiac MRI acquisition in free-breathing. More precisely, in collaboration with Freddy Odille, Damien Mandry, Cédric Pasquier, Pierre-André Vuissoz and Jacques Felblinger, we developed a method for cardiac MRI in free-breathing, assuming that cardiac and

respiratory motions can be deduced from a small number of sensors as elastic motions. From a mathematical point of view, this method is equivalent to solving an integral Fredholm equation of first kind and, for simplicity and coherence reasons, we don't detail this method in this thesis. For details, we send the reader to Odille et al. [56].

A second approach, much more usual in cardiac MRI, is to assume only that the density of protons f is periodic in time, or, more generaly, that f is formed by rescaled copies of a standard motion. Standard cardiac MRI protocols usually involve continuous acquisition of data over multiple cycles during one breath-hold. Cardiac motion can then be resolved using electrocardiogram (ECG) information. By this approach, called retrospective gating, the raw data is sorted and ordered in a fixed number of cardiac phases (Figure 5.6). All cata acquired in a precise cardiac phase (for example in phase 3), marked in Figure 5.6 by a rectangle are used for the reconstruction of one image.

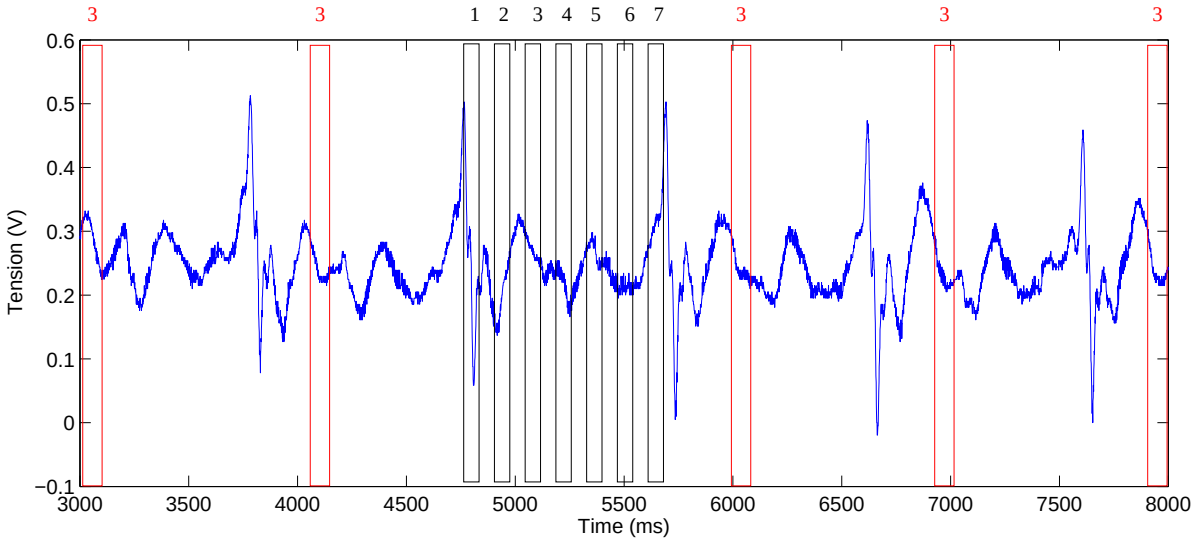

Figure 5.6: Cardiac retrospective gating using ECG.

The same approach can be used to reconstruct cardiac images acquired in free-breathing using in this case the ECG for resolving the cardiac motion and a thoracic belt for the respiratory motion (Figure 5.7) Fredrickson et al. [29]. All data included in a rectangle are used for the reconstruction of one image for the coresponding cardiores-piratory phase.

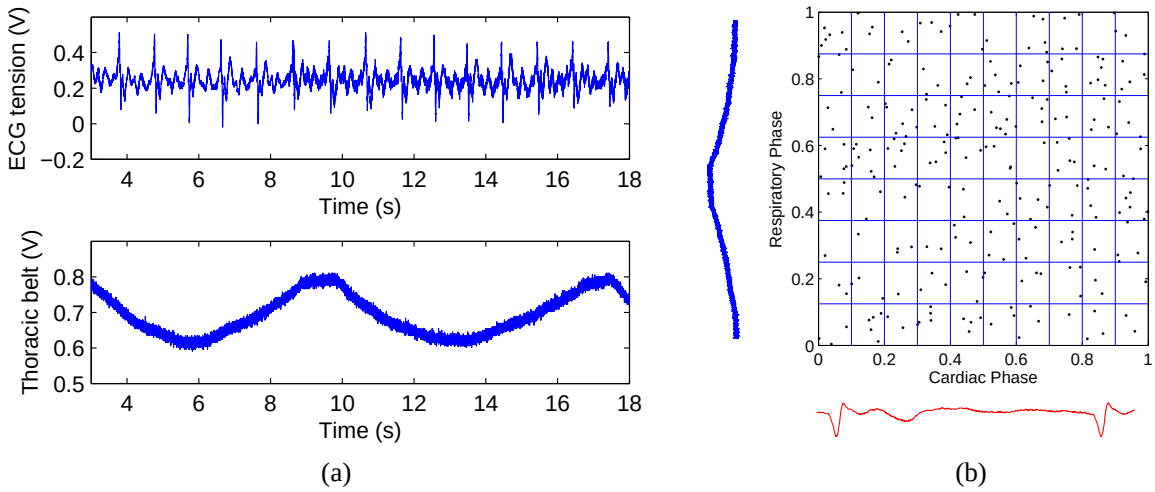

Figure 5.7: Cardiac retrospective gating in free-breathing using ECG and respiratory belt. (a) ECG and thoracic belt. (b) Normalized cardiac and respiratory times for the line $k_y = 64$ of the k-space. All data included in a rectangle are used for the reconstruction of one image for the coresponding cardiorespiratory phase.

6. A moments problem in cardiac-respiratory MRI in free-breathing

This chaper is a joint work with Freddy Odille, Gilles Bosser, Jacques Felblinger and Pierre-André Vuissoz. Important parts of this chapter were published in Cîndea et al. [20].

This chaper describes a rigorous framework for reconstructing MR images of the heart acquired continuously over the cardiac and respiratory cycle. The framework generalizes existing techniques, commonly referred to as retrospective gating, and is based on the properties of reproducing kernel Hilbert spaces (RKHS). The reconstruction problem is formulated as a moment problem in a multidimensional RKHS (a two-dimensional space for cardiac and respiratory resolved imaging). Several RKHS were tested and compared, including those corresponding to commonly used interpolation techniques (sinc-based and splines kernels), and a more specific kernel allowed by the framework (based on a first order Sobolev RKHS). The Sobolev RKHS was shown to allow improved reconstructions in both simulated and real data from healthy volunteers, acquired in free-breathing.

6.1 Introduction to the cardiorespiratory MRI reconstruction problem

Cardiac MRI is now becoming a standard clinical tool for the evaluation of many different cardiac function parameters in an increasing number of medical centers. It is problematic that MRI involves a relatively slow acquisition or sampling period, that is of the same order of magnitude as physiological motion, such as cardiac contraction and breathing. Therefore, flow or motion artifacts are likely to appear in the resulting MR images from FOV anatomy affected by involuntary physiological motions [70, 85].

Several imaging strategies have been proposed in order to counter these effects [71]. Standard protocols usually involve continuous acquisition of data over multiple cardiac

cycles during one or more patient breath-holds. Cardiac motion can then be resolved using ECG information. By this approach, the raw data is sorted and interpolated, effectively reordered from the arbitrarily acquired time samples to an ordering into the cardiac phases to be separately reconstructed. In breath-hold acquisition, the upper bound of the temporal interpolation is usually ensured by the prospective segmented acquisition [11]. Either in prospective segmented acquisition or in true retrospective gating, the reconstruction assumes that each heart beat is a rescaled copy of a standard heart beat. The resulting reconstructed images from retrospective gating therefore reveal spatial and temporal averaging, direct effects of the computational algorithm. Moreover, the method relies on efficient breath-holding, not always possible due to the patient compliance or unconscious state. Breath-holds themselves may also be affected by drift [61]. In some clinical situations (eg when imaging infants, patients with respiratory disease or those unable to maintain a stable breath-hold) free-breathing MRI data acquisition is the only possibility, but usually results in lower quality images related to motion artifacts due to inconsistent data and/or inadequate reconstruction process.

Given these difficulties, there is a clinical motivation to develop techniques to improve MR imaging quality in the presence of physiological motion, i.e. during free-breathing. Functional cardiac studies would also benefit from free-breathing MRI, eliminating undesirable effects of breath-holding which can modify intra-thoracic pressures and therefore ventricular filling, as with the Vasalva maneuver [84]. Free-breathing cardiac MRI would also benefit correspondence of MRI results to nuclear imaging or electrocardiography, both performed during free-breathing. A free-breathing cardiac MRI method that would eliminate respiration-induced motion artifacts as well as allow images to be reconstructed corresponding to the different phases of cardiac (systole / diastole) and respiratory (inspiration / expiration) cycles would be particularly valuable clinically. Respiration constantly modulates intra-thoracic pressures which, via complex cardiac-respiratory interactions, also modulates ventricular filling and stroke volume [55, 81].

As an alternative to breath-holding approaches, free-breathing cardiac MRI approaches have been proposed in order to reconstruct cardiac images from continuously acquired data, in free breathing, and thus overcome the limitations mentioned above. These techniques can be categorized as either correction methods [47, 39, 56, 58] or interpolation methods [29, 77, 73]. Correction methods aim at combining data acquired in different respiratory motion states. Recent studies [41, 47, 39, 56, 58] have shown that it is possible to estimate and take account of nonrigid deformation fields induced by respiration. These deformation fields can be computed either from a fast real-time imaging [41] or from a motion model driven by a reduced number of motion sensors [47, 39, 56, 58]. Interpolation methods aim at resolving respiratory motion in the same manner as cardiac motion, i.e. by interpolating the raw data from the acquisition time samples to the respiratory phases to be reconstructed [29, 77, 73]. As for interpolated cardiac motion, this approach assumes that each respiratory cycle occurring during image acquisition is a rescaled copy of a standard, idealized respiratory cycle. Although the latter technique requires a high level of motion reproducibility, it has the advantage over correction methods of not requiring an estimation of actual motion field, a difficult

problem, hence potentially a source of error.

This chaper focuses on development of interpolation methods for free-breathing cardiac MRI. A rigorous framework is proposed, generalizing existing methods, using the properties of reproducing kernel Hilbert spaces (RKHS) [86, pages 16-18]. Based on the work in [67], we formulate MRI reconstruction from free-breathing, continuously acquired data, as a moment problem in a multidimensional RKHS - a tensorial product of two RKHS for resolving both cardiac and respiratory motion. The framework suggests testing various RKHS, including those associated with standard interpolation techniques (sinc-based or splines kernels), and alternative ones, such as a first order Sobolev RKHS. The Sobolev RKHS involves searching for solutions in a class of functions that have weaker regularity properties. This is particularly relevant here, as the cardiac MRI computational problem represents scattered data interpolation in the cardiac-respiratory space. Our method has been validated using simulated data samples and cardiac scans from free-breathing healthy volunteers, with comparison of the different RKHS.

This chaper extends the use of reproducing kernel Hilbert spaces, from cardiac MR imaging during breath-holds [67] to cardiac MR imaging in free-breathing. In this context, we discuss the problem of nonuniform two-dimensional sampling density and the dependence of the quality of the reconstructed images to the sampling density, for each proposed interpolation technique.

6.2 Theory of RKHS reconstruction

6.2.1 Formulation of the cardiorespiratory-resolved imaging problem

In this section, we consider free-breathing, continuous acquisition of MR data. The k-space is assumed to be acquired in a Cartesian, sequential manner several times, independently of the heart and breathing patterns (non-Cartesian sampling would be treated similarly).

We denote $g(k,T) = \widehat{F}(k,T)$ the MR signal acquired at a certain position $k = (k_x, k_y)$ in k-space, and time $T \in [0, \infty)$, with $\hat{F}$ representing the Fourier transform of F.

It is assumed that the beginning of each cardiac and respiratory cycle is known, and is denoted by $(c_i)_i$ and $(r_i)_i$ respectively. For each time T there exist two positive integers i and j such that $T \in [c_i, c_{i+1})$ and $T \in [r_j, r_{j+1})$. Assuming that cardiac and respiratory cycles are periodic (up to a rescaling accounting for variations in cycle lengths), each time T can be associated with a pair $(s,\, t) \in [0,\, 1)^2$, representing the normalized cardiac and respiratory phases (i.e. time intervals during the normalized cardiac and respiratory cycles, as in (6.8)), respectively. The MR signal, expressed as a function of the normalized cardiac-respiratory phases, is denoted by $\hat{f}(k,s,t) =$

$\hat{F}(k,T)$. Restated, all MR samples can be mapped to some timepoint on both the time-scaled (ideal) cardiac and respiratory cycles. We assume that for each k-space point the associated time samples are different. If this is not the case we will repeat the acquisition of the same k-space point after a random small time. Reconstruction aims at finding a function $f(x,s,t)$, where

$$f : D \times [0,\,1)^2 \to \mathbb{C} \tag{6.1}$$

is the cardiac-respiratory resolved image (with D being the span of the field of view). The value $f(x,s,t)$ represents the intensity of a pixel x from the image at the given cardiac-respiratory phase (s,t).

Let $g_{k,i}$ be the actual measurements collected by the scanner, at position k in the k-space, and normalized time $(s_{k,i},\, t_{k,i})_i$. This measurements $g_{k,i}$ give the following constraint on the Fourier transform $\widehat{f}$ of f:

$$\hat{f}(k,\, s_{k,i},\, t_{k,i}) = g_{k,i}, \qquad (k \in \mathbb{K}, \quad i \in \mathbb{I}), \tag{6.2}$$

where $\mathbb{K} = \{1,\, \dots\, N_y\} \times \{1,\, \dots, N_x\}$ and $N_y \times N_x$ is the reconstructed image size in the spatial dimensions. Let $\mathbb{I}$ be, for the moment, the set of integer numbers. The case where $\mathbb{I}$ is a finite set of indices will be considered later. The reconstruction problem aims to find a function f such that it Fourier transform $\widehat{f}$ satisfy (6.2) for all the sparse data $g_{k,i}$.

6.2.2 Reconstruction as a moment problem in reproducing kernel Hilbert spaces

Based on the work of Roerdink and Zwaan [67], a solution f is sought in $L^2(D,H)$, where $D = [-\pi,\pi]^2$ is isomorphic to the FOV and H is a *reproducing kernel Hilbert space (RKHS)* [4].

Definition 6.1. We call a reproducing kernel Hilbert space a Hilbert space of functions

$$H = \{h : X \to \mathbb{C} \mid \exists K : X \times X \to \mathbb{C}\}$$

such that

(i) $K(\cdot,\, \boldsymbol{x}) \in H$, for every $\boldsymbol{x} \in X$

(ii) $\langle h(\cdot),\, K(\cdot,\, \boldsymbol{x})\rangle_H = h(\boldsymbol{x})$, for every $\boldsymbol{x} \in X$ and every function $h \in H$.

The function K is called the reproducing kernel of H.

Proposition 6.2. *If $(H_1, \langle\cdot,\cdot\rangle_1)$, $(H_2, \langle\cdot,\cdot\rangle_2)$ are two reproducing kernel Hilbert spaces with kernels K_1 and K_2 respectively then $H = H_1 \otimes H_2$ is a reproducing kernel Hilbert space with the kernel*

$$K(\boldsymbol{x},\boldsymbol{y}) = K_1(s_1,s_2)K_2(t_1,t_2),$$

where $\boldsymbol{x} = (s_1,t_1)$ and $\boldsymbol{y} = (s_2,t_2)$.

Proof. Recall that we define $H = H_1 \otimes H_2$ as

$$H = \{h : X \times X \to \mathbb{C} \,|\, h(s,t) = h_1(s)h_2(t) \text{ with } h_1 \in H_1 \text{ and } h_2 \in H_2\}.$$

It is easy to see that H is a Hilbert space with the scalar product

$$\langle h, g\rangle = \langle h_1, g_1\rangle_1 \langle h_2, g_2\rangle_2,$$

where $h = (h_1, h_2)$ and $g = (g_1, g_2)$.

From the definition of K and from the property (i) of the definition of the RKHS is obvious that $K((\cdot,\cdot),(s,t)) \in H$. Moreover

$$\langle h(\cdot,\cdot), K((\cdot,\cdot),(s,t))\rangle = \langle h_1(\cdot)h_2(\cdot), K_1(\cdot,s)K_2(\cdot,t))\rangle = \\ \langle h_1(\cdot), K_1(\cdot,s)\rangle_1 \langle h_2(\cdot), K_2(\cdot,t)\rangle_2 = h_1(s)h_2(t) = h(s,t)$$

and the proof of the proposition is complete. □

A well known example of reproducing kernel Hilbert space is the Paley-Wiener space $\mathbb{P}$ denotes the space of band-limited functions [86, pages 105-109]. In the remaining part of this chapter we are interested in the reproducing kernel Hilbert spaces of functins with two arguments, therefore we consider the space $H = \mathbb{P} \otimes \mathbb{P}$ which we call, in what follows, Paley-Wiener space (or sinc space). The kernel of this space is

$$K(s,t,u,v) = \text{sinc } (s-u)\text{sinc } (t-v),$$

where

$$\text{sinc } (t) = \begin{cases} \frac{\sin \pi t}{\pi t}, & t \neq 0 \\ 1, & t = 0. \end{cases}$$

We denote $\varphi_{k,i}(s,t) = K(s,t,s_{k,i},t_{k,i})$ the interpolation functions in the cardiac-respiratory cycle-space, spanning (s,t), that equals acquired MRI data $g_{k,i}$ at the known timepoints in the cardiac and respiratory phases in $(s_{k,i}, t_{k,i})$, and provides some estimate at all other timepoints in (s,t). (6.2) can be rewritten in the form

$$\langle f,\, \varphi_{k,i} e_k\rangle_{L^2(D,H)} = g_{k,i}, \qquad (k \in \mathbb{K}, i \in \mathbb{Z}), \tag{6.3}$$

where $e_k(x) = \exp(\mathrm{i}\, k \cdot x)$. Indeed, we have

$$\begin{aligned} \langle f, \varphi_{k,ie_k}\rangle_{L^2(D,H)} &= \int_D \langle f(x,\cdot,\cdot), \varphi_{k,i}(\cdot,\cdot)e_{k,i}(x)\rangle_H \, \mathrm{d}x \\ &= \left\langle \int_D f(x,\cdot,\cdot)e^{-ik\cdot x} \, \mathrm{d}x, K(\cdot,\cdot,s_{k,i},t_{k,i}) \right\rangle_H \\ &= \langle \hat{f}(k,\cdot,\cdot), K(\cdot,\cdot,s_{k,i},t_{k,i})\rangle = \hat{f}(k,s_{k,i},t_{k,i}). \end{aligned}$$

Remark that the left hand side of (6.3) can be rewritten as: $\langle f,\, e_k\varphi_{k,i}\rangle_{L^2(D,H)} = \left\langle \hat{f}(k),\, \varphi_{k,i} \right\rangle_H$ for all k. The reconstruction problem (6.3) can therefore be reformulated as a moment problem in the reproducing kernel space H:

$$\langle \hat{f}(k),\, \varphi_{k,i}\rangle_H = g_{k,i}, \qquad (i \in \mathbb{I}), \tag{6.4}$$

for each $k \in \mathbb{K}$ or, indeed, finding $\hat{f}$ such that its moments respective to all $\varphi_{k,i}$ are the respective collected data $g_{k,i}$. Solving the latter problem amounts to finding $\hat{f}$. Once $\hat{f}$ has been determined, f is given by the inverse Fourier transform of $\hat{f}$.

The RKHS theory provides theorems for the solution of moment problems such as the one in (6.4). In particular, if $(s_{k,i}, t_{k,i})$ are such that $(\varphi_{k,i})_i$ form a Riesz basis [86, pages 145-160], then (6.4) has the solution given by the formula

$$\hat{f}(k,s,t) = \sum_i g_{k,i} \sum_j \overline{G}^{-1}_{k,ij} \varphi_{k,j}(s,t) \quad \text{for all } (s,t), \tag{6.5}$$

where we introduced the Gramian matrix $G_{k,ij} = \langle \varphi_{k,i},\, \varphi_{k,j} \rangle_H$. Note that if $(\varphi_{k,i})_i$ is an orthogonal system the matrix $(G_{k,ij})_{ij}$ is the identity matrix. Having $\hat{f}$ from (6.5), f will be obtained by a Fourier inverse transform like in (6.6):

$$f(x,s,t) = \sum_{k \in \mathbb{K}} \sum_{i,j \in \mathbb{I}} g_{k,i} \overline{G}^{-1}_{k,ij} \varphi_{k,j}(s,t) e_k(x). \tag{6.6}$$

Let us remark that the reconstruction formula given by (6.6) is valid for any RKHS, all the above computation, independent of the space used.

Thus, in RKHS, the solution to the retrospectively gated reconstruction can be calculated by the simple formula (6.6), based on the k-space measurements and the chosen basis. If $\mathbb{I}$ is a finite set of samples $\{1,\, 2,\, \ldots, I\}$, as it is in practice, (6.2) does not have a unique solution. Nevertheless, the function f given by (6.6) is then the minimal norm solution, in the Hilbert space H, of the reconstruction problem (6.2) [86, Example 1, page 147].

In the present application, sampling in the temporal dimensions is nonuniform as it depends on patient physiology. It is possible to adapt the kernel to the sampling density by modifying the rate of decay (i.e. the envelope) of the kernel function away from the sampled timepoints

$$K_p(s,t,u,v) = K(p \cdot s, p \cdot t, p \cdot u, p \cdot v),$$

with $p > 0$. The parameter p is called the "kernel opening parameter" of K_p. In order to fulfill the requirements of a Nyquist like sampling density criterion [44, 1], p will be increased as the density of samples $(s_{k,i},\, t_{k,i})_i$ increases:

$$p = \frac{1}{d_{max}}, \tag{6.7}$$

where d_{max} is the diameter of the biggest disc that can be included in the square $(0,1) \times (0,1)$ that does not contain any pair $(s_{k,i},\, t_{k,i})$.

Remark 6.3. It is possible to adapt the kernel to sampling density modifying the decay rate of the kernel diferently for the cardiac and respitatory parameters, i.e., we can consider

$$K_{p,q}(s,t,u,v) = K(p \cdot s, q \cdot t, p \cdot u, q \cdot v).$$

6.2.3 Specific RKHS for cardiac MRI application

In addition to the Paley-Wiener space RKHS example (referred hereafter as the "sinc RKHS"), other RKHS were tested, including the bicubic spline function space $\mathcal{K}^3 \otimes \mathcal{K}^3$ and a first order Sobolev space $W^{1,2} \otimes W^{1,2}$.

The kernel of the bicubic spline functions space is given by

$$K(s,t,u,v) = \beta^3(s-u) \cdot \beta^3(t-v),$$

where $\beta^3(t) = \beta^3_+(t+2)$ and $\beta^3_+ = \beta^0_+ * \beta^0_+ * \beta^0_+ * \beta^0_+$. Here we noted $*$ as the convolution operator and β^0_+ is the characteristic function of the $[0,1)$ interval

$$\beta^0_+(t) = \begin{cases} 1, & \text{if } t \in [0,\,1) \\ 0, & \text{otherwise.} \end{cases}$$

The Sobolev space $W^{1,2}$ is defined by

$$W^{1,2}([0,1]) = \left\{ \begin{array}{l} w \mid w \text{ is an absolutely continuous function,} \\ w' \in L^2[0,1] \end{array} \right\}.$$

Therefore, the space $W^{1,2} \otimes W^{1,2}$ is a reproducing kernel space [24] with the kernel

$$\begin{aligned} K(s,t,u,v) &= 1/4\sinh^2(1)[\cosh(s+u-1) + \cosh(|s-u|-1)] \\ &\quad \times[\cosh(t+v-1) + \cosh(|t-v|-1)], \end{aligned}$$

where sinh and cosh are the hyperbolic sinus and cosinus, respectively.

6.3 Materials and methods

6.3.1 Computer simulation

All simulations and reconstructions were performed on a notebook PC (Hewlett-Packard, Houston, TX, 1,7Ghz processor, 1GB RAM), using code written in Matlab (MathWorks, Natick, MA).

First a thorax phantom was generated (256×256 matrix), formed by eight ellipses filled with different gray tones, and having two periodic oscillatory motions (Fig. 6.1).

Simulated respiratory and ECG waveforms were generated in order to drive deformation of the ellipses (Fig. 6.2) which form our cardiac-respiratory phantom. The MR acquisition process was simulated by applying the 2D Fast Fourier Transform (FFT) to each simulated image (without any noise addition) and selecting the k-space data in a Cartesian sequential fashion.

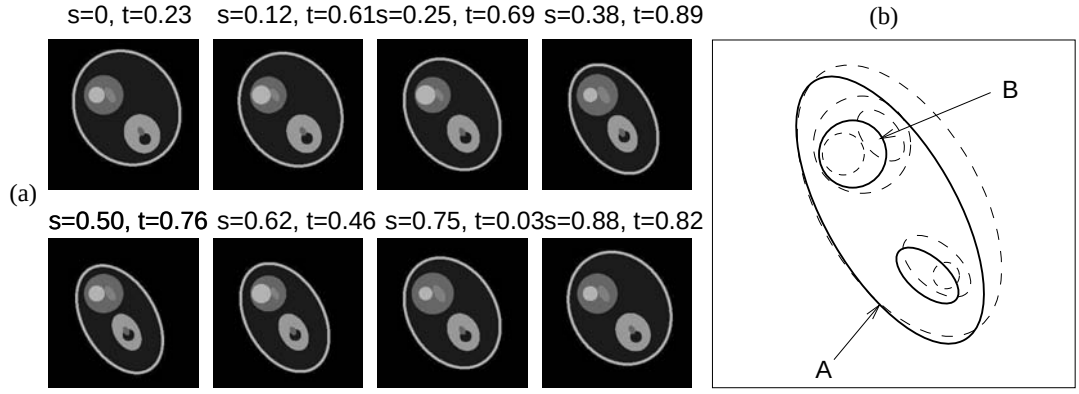

Figure 6.1: Cardiac-respiratory phantom. (a) Images of the numerical phantom simulating cardiac and respiratory motions at eight phases of motion. The respiratory phase is denoted by s and the cardiac phase by t. (b) A schematic description of the motion: the bold lines show the minimal surface of the phantom and the dashed lines, its maximal surface. We denote by A the biggest ellipse and by B the smaller ellipse corresponding to the heart.

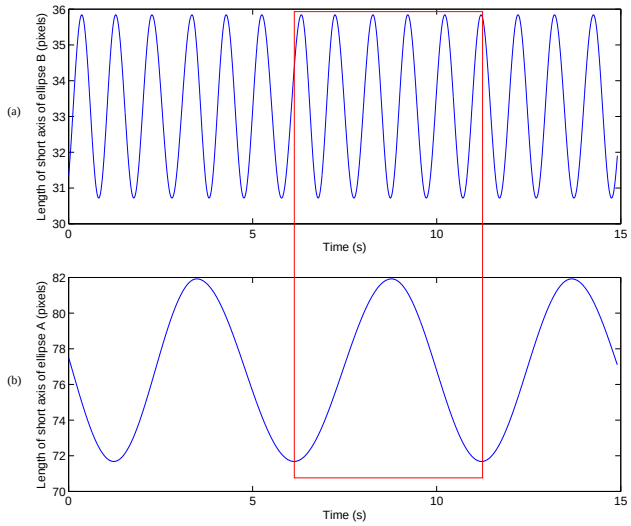

Figure 6.2: Simulated motion of the phantom. (a) Short axis of ellipse A. (b) Short axis of ellipse B.

To each time $T_{k,i}$ we associate the normalized acquisition times $(s_{k,i})$ and $(t_{k,i})$ for $i \in \{1, 2, \cdots, 300\}$, according to

$$s_{k,i} = \frac{T_{k,i} - r_j}{r_{j+1} - r_j} \text{ and } t_{k,i} = \frac{T_{k,i} - c_l}{c_{l+1} - c_l}, \tag{6.8}$$

where $T_{k,i} \in [r_j, r_{j+1}) \cap [c_l, c_{l+1})$ is the i-th acquisition time corresponding to the k-space sample k and r_j (respectively c_l) is the beginning time of the j-th respiratory cycle (respectively l-th cardiac cycle).

Three different RKHS were tested and compared: i) the space of band-limited sinc functions, $H = \mathbb{P} \otimes \mathbb{P}$, described in the previous section; ii) the space of 2D bicubic spline functions, $\mathcal{K}^3 \otimes \mathcal{K}^3$; iii) the 2D Sobolev space, $W^{1,2} \otimes W^{1,2}$. The reconstructions produced are compared with the method presented by Thompson and McVeigh in [77] (called "sinc-exp" interpolation in the remainder of this chapter).

The simulation was validated by comparing each reconstructed image with the exactly corresponding source image. To do this, two similarity criteria commonly used in image analysis were used : the correlation coefficient and the normalized mutual information [62]. We recall here that the correlation coefficient of two images F and G is defined by

$$c(F,G) = 1 - \frac{\sum_{i,j}(F(x_i,y_i) - \overline{F})(G(x_i^*,y_i^*) - \overline{G})}{\sqrt{\sum_{i,j}(F(x_i,y_i) - \overline{F})^2 (G(x_i^*,y_i^*) - \overline{G})^2}}$$

where $\overline{F}$ is the mean of F and

$$\begin{bmatrix} x_i^* \\ y_i^* \end{bmatrix} = T \begin{bmatrix} x_i \\ y_i \end{bmatrix}, \text{ with } T \text{ an affine tranformation.}$$

The normalized mutual information of two images F and G is defined by

$$\mathrm{NMI}(F,G) = \frac{\mathrm{I}(F,G)}{\mathrm{I}(F,F) + \mathrm{I}(G,G)},$$

where $\mathrm{I}(F,G)$ is the mutual information of F and G, i.e.,

$$\mathrm{I}(F,G) = \sum\sum p(F_{ij},G_{ij}) \log\left(\frac{p(F_{ij},G_{ij})}{p_1(F_{ij})p_2(G_{ij})}\right),$$

where $p(x,y)$ is the joint probability distribution function of F and G, and $p_1(x)$ and $p_2(y)$ are the marginal probability distribution functions of F and G respectively.

Description of cardiorespiratory phantom

In this paragraph we give a short and exact description of the cardiorespiratory phantom used in this section. For a given cardiac-respiratory phase $(s,t) \in [0,1]^2$ the thorax phantom is generated as in Algorithm 6.3.1. The notation $E(y,x,a,b,\alpha,c)$ describes an ellipse with the center (y,x), long axis a, short axis b and with angle α between the first axis and the horizontal axis. The parmeter $c \in [0,1]$ designes the gray level of the ellipse, and all the ellipses are fullfilled and are drawn in the order specified in the algorithm.

6.3.2 MR experiments

MR scans were performed using a 1.5 T GE SIGNA Excite HD MR system (General Electric, Milwaukee, WI). Physiological signals, collected using a modified version of the

Algorithm 6.3.1 Cardiorespiratory phantom

Require: $(s,t) \in [0,1]^2$

$x_m = 128,\ y_m = 128,\ \alpha = \frac{\pi}{2},\ a_0 = 100,\ b_0 = 80,\ r = 6,\ c = 3,\ r_h = 30$

$\delta_x = \cos(\alpha\left(\frac{1}{8}\cos(2\pi s) + \frac{3}{8}\right),\ \delta_y = \sin(\alpha\left(\frac{1}{8}\cos(2\pi s) + \frac{3}{8}\right)$

$x = x_m + r\cos(2\pi s)\cos(\alpha),\ y = y_m - r\cos(2\pi s)\sin(\alpha)$

$x_1 = x + a_0\delta_x,\ y_1 = y + a_0\delta_y$

$x_{1c} = x + (a_0 - 10)\delta_x,\ y_{1c} = y + (a_0 - 10)\delta_y$

$x_{2c} = x + (a_0 + 10)\delta_x,\ y_{2c} = y + (a_0 - 10)\delta_y$

$x_h = x - r_h$

$y_h = y - r_h$

$r = r_h + c\cos(2\pi t)$

$r_a = r_h/2 + c\cos((2t+1)\pi)$

$r_v = r_h/2 + c\cos(2\pi t)$

draw the ellipses

$E_1(y, x, a_0, b_0 + r\cos(2\pi s), \alpha, 0.7)$

$E_2(y, x, a_0 - 5, b_0 + r\cos(2\pi s) - 5, \alpha, 0.1)$

$E_3(y_1, x_1, a_0/3, (b_0 + r\cos(2\pi s))/3, \alpha, 0.6)$

$E_4(y_{1c}, x_{1c}, 10, 10, \alpha, 0.1)$

$E_5(y_{2c}, x_{2c}, 8, 5, \alpha, 0.4)$

$E_6(y_c, x_c, r_h, r_h, \alpha, 0.4)$

$E_7(y_c, x_c - 11, r_a, r_a, \alpha, 0.7)$

$E_8(y_c, x_c + 11, r_v, r_v, \alpha, 0.5)$

end draw

Maglife patient monitoring system (Schiller Medical, Wissembourg, France), were converted into optical signals, transmitted outside the MR bore through optical fibers, and then recorded on the signal analyzer and event controller (SAEC) computer described in [57]. A pneumatic belt was used to monitor respiration, and ECG sensors provided information about the cardiac phase. The SAEC system allows synchronous acquisition and recording of physiological signals (respiration and ECG) and MR signals (image acquisition windows and MR gradients), real-time correction of MR gradient switching interference on ECG waveforms, and R-wave detection [57],[28].

Five healthy volunteers underwent several fast MR imaging sequences available on clinical scanners (2D SSFP Gradient Echo, TE=1.7 ms, TR=3.5 ms, 256×128 raw data matrix, 2.8 mm square pixels, 8 mm slice thickness, no parallel imaging acceleration factor, FOV 360 mm, flip angle 45°, 256 images in the acquisition and an 8 element cardiac coil), resulting in a temporal resolution of 2.37 frames per second. Prospective segmented acquisition was not used for simplicity of the implementation, since in free breathing it does not insure a upper bound for the coverage of the cardio-respiratory phase space as in breath hold acquisition. For each volunteer we applied this sequence with three different imaging planes: cardiac transmitral short axis, horizontal axis and vertical long axis. Data were acquired with feedback in free-breathing and the subjects were instructed to maintain the respiratory curve between two predetermined limits.

We normalized the acquisition times to obtain a cardiac phase in the interval $[0, 1]$ (Fig. 6.3(a)) using the method presented by Bohning et al. [12]. This method is based on the linear dependence between systole length and RR duration, first observed by Weissler et al. [83]. For the respiratory phase, simple linear rescaling was used (Fig. 6.3(b)), with end inspiration corresponding to 0. As stated by (6.6), all the sampled data of the MRI acquisition are used as $g_{k,i}$ in the reconstruction of the image at a given cardiac-respiratory phase $f(x, s, t)$. For sake of clarity only the sampling of $(g_{1,i})_i$ was displayed in Fig. 6.3(c).

The images obtained in free breathing using the sinc, spline, and Sobolev RKHS reconstructions, as well as sinc-exp interpolation, were compared with standard clinical images reconstructed from the data acquired during a breath-hold.

To evaluate the clinical utility of the method, cine sequences in the short axis view at two different respiratory phases (respiratory phase 0.2 inspiration and respiratory phase 0.85 expiration) were produced for three subjects with the four different methods. The images were evaluated and compared by two experienced (regular practice of cardiac MRI) observers that were blinded to the methods used. The two cardiologists were instructed to evaluate the overall quality, artifacts and the diagnostic value of the cine sequences.

For each dataset, the kernel opening parameter chosen depended linearly on sampling density. The same value was used for the kernel opening parameter (p) for each kernel. When the value of p is not explicitly specified, it was set by the formula (6.7). In [77] is proposed to use the interpolation kernel $f_{kernel}(D_i) = \mathrm{sinc}(20D_i)\exp(-(20D_i)^2)$ where D_i is the distance from the timepoint (s_i, t_i) to the current point (s, t). An equivalent

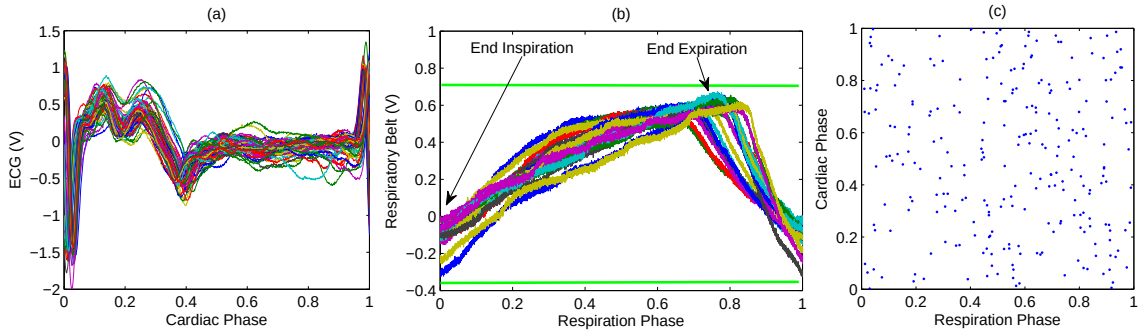

Figure 6.3: Physiological signals from one of the five volunteers. (a) ECG signal recorded during acquisition, with each R-R interval rescaled to the unit interval. (b) The respiratory signal recorded by a belt during acquisition, rescaled to [0, 1]. (c) The normalized acquisition times for one line of the k-space showing the irregular sampling of the cardiac-respiratory phase space. The respiratory phase is marked horizontally, and the cardiac phase vertically.

writing of this kernel in terms of our kernel opening parameter p given by (6.7) is

$$f_{kernel}(D_i) = \text{sinc}(2pD_i)\exp(-(2pD_i)^2) \tag{6.9}$$

6.4 Comparison of images obtained using different RKHS

6.4.1 Computer simulation

Reconstructions from the cardiac-respiratory phantom described in the previous section were performed for a fixed value of the normalized respiration time s ($s = 0.2$) and for 30 values of the normalized cardiac time t, uniformly distributed between 0 and 1. Reconstructed images resulting from use of a particular RKHS, i.e. sinc, splines, Sobolev RKHS, and the sinc-exp interpolation method [77] are shown in Fig. 6.4.

Image quality was assessed by computing the correlation coefficient and the normalized mutual information, with respect to the exact images, for all values of s and t mentioned above. The mean and standard deviation of these scores are summarized in Table 6.1. The best scores were obtained using the Sobolev RKHS. This concurs with visual inspection of the reconstructed images in Fig. 6.4, which shows a reduction in residual aliasing artifacts, due to the oscillatory motion of the phantom, in the Sobolev reconstruction compared with all other methods.

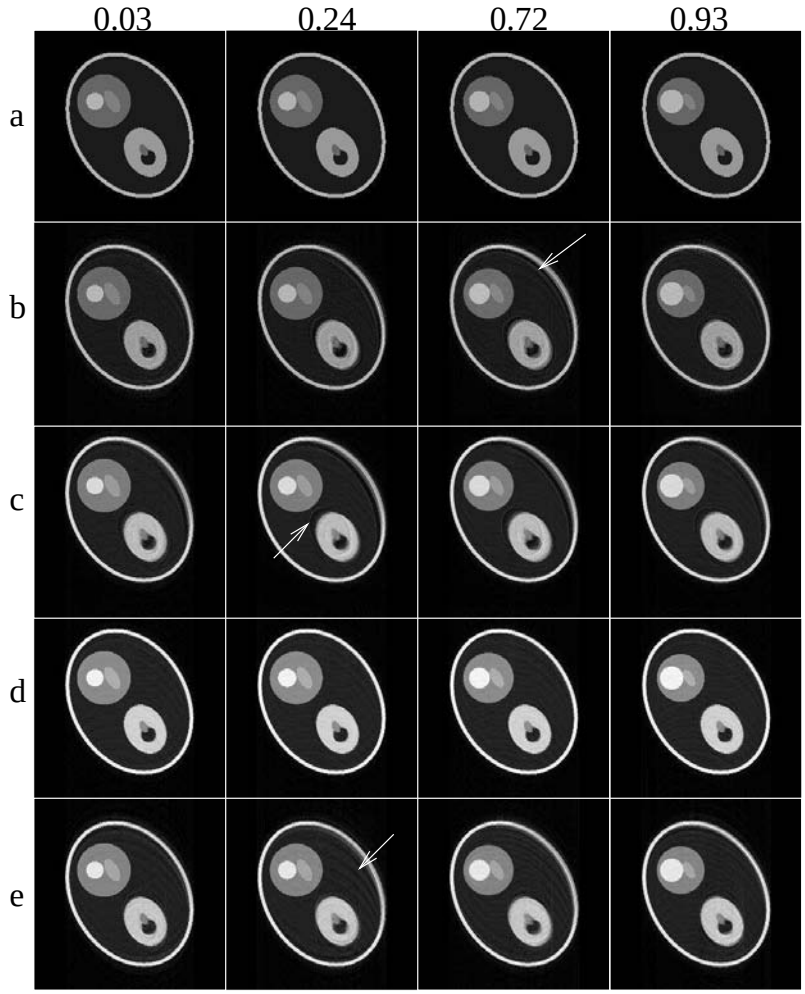

Figure 6.4: Exact and reconstructed images of the cardiac-respiratory phantom. Four cardiac phases are presented horizontally, for different reconstruction methods (marked vertically), and for a fixed respiratory phase. The arrows point to some visible artifacts. (a) The exact source image. (b) Reconstruction using the sinc RKHS method in the Paley-Wiener space.(c) Reconstruction in the bicubic spline functions RKHS. (d) Reconstruction in the first order Sobolev space. (e) Reconstruction using sinc-exp interpolation.

6.4.2 MR Results

Cardiac images were reconstructed from the volunteer data acquired during free-breathing. Images are able to be reconstructed in any cardiac and respiratory phase. One also has the ability to select a specific cardiac phase (such as end-diastole) and reconstruct cardiac images at different respiratory phases. This capability is highly useful for studying the influence of respiration on left ventricular filling for example.

Table 6.1: Comparison of exact source images and reconstructed images using the sinc RKHS method, the splines RKHS method, the Sobolev RKHS method, and sin-exp interpolation in computer simulated data.

Reconstruction method	Correlation coefficient		Normalized mutual information	
	Mean	Standard deviation	Mean	Standard deviation
Sinc RKHS	0.94	0.043	0.20	0.041
Splines RKHS	0.96	0.020	0.23	0.063
Sobolev RKHS	0.97	0.008	0.33	0.060
Sinc-exp	0.96	0.019	0.29	0.096

Breath-hold vs reconstruction from free-breathing data

Of all the possible motion states existing in the range of s and t, two in particular have been selected for comparison with standard clinical images acquired in breath-hold. Two cardiac timepoints corresponding to diastole and systole were first selected manually (the same as for the free-breathing and breath-hold reconstructions). The respiratory phase used for comparison was the closest to the breath-hold reference, as defined by the correlation coefficient, of the 30 respiratory phases reconstructed at uniformly distributed values of s between 0 and 1. For the two cardiac timepoints, images are shown in Fig. 6.5. The correlation coefficient was then computed between the reference images (breath-hold) and the reconstructions from free-breathing data (see Table 6.2) for all the 30 cardiac phases. As in the phantom experiment, imaging results obtained using the Sobolev RKHS exhibited a statistical advantage over the other RKHS methods and sinc-exp interpolation.

Table 6.2: The mean of correlation coefficient between images (the respiratory phase is s=0.55 fixed, and 30 different cardiac phases) reconstructed from free-breathing using sinc RKHS, splines RKHS, Sobolev RKHS, sinc-exp interpolation and standard clinical images obtained in breath-hold for a healthy volunteer.

Reconstruction Method	Correlation coefficient	Standard deviation
Sinc RKHS	0.433	0.035
Splines RKHS	0.433	0.030
Sobolev RKHS	0.448	0.028
Sinc-exp interpolation	0.447	0.029

Comparison of the different RKHS

Data from each of the five healthy volunteers were used to reconstruct 30 cardiac phases (at a fixed respiratory phase), as is usually done in standard protocols. Fig. 6.6 shows examples of such reconstructions using the different methods to be tested. The figure

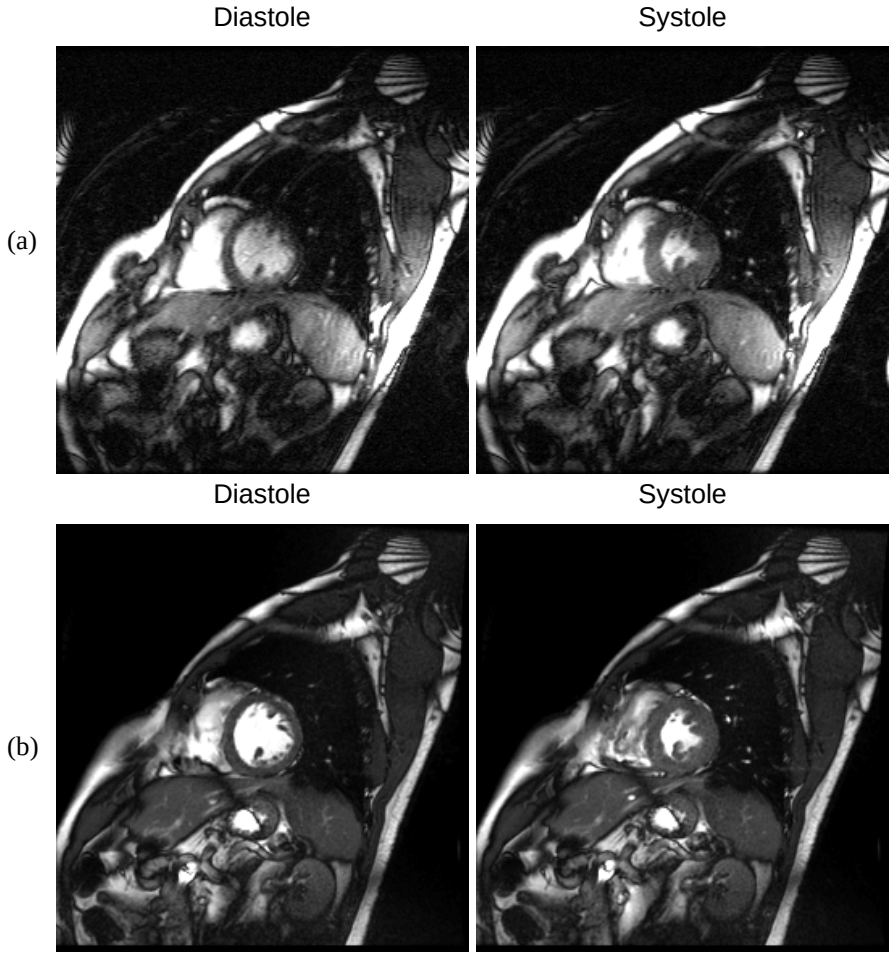

Figure 6.5: Cardiac images from a healthy volunteer, in two cardiac phases : diastole and systole respectively. (a) Images reconstructed using Sobolev RKHS from data acquired in free-breathing (for two cardiac phases and one respiratory phase corresponding to breath-hold: $s = 0.55$). (b) Standard clinical images obtained from data acquired during a breath-hold.

also shows a temporal profile accounting for cardiac motion along a line section drawn in the left ventricle. These profiles show less blurring using the Sobolev RKHS and sinc-exp interpolation compared with the sinc and splines RKHS. However a few residual aliasing artifacts can be seen.

This typical example illustrates the inherent compromise which has to be made between resolution (or equally, the amount of blurring) and aliasing artifacts, as the temporal sampling density is nonuniform. The results in Fig. 6.7 aim to give a better understanding of this compromise. Shannon entropy of images was used in order to assess the "effective" image resolution (in terms of the size of structures that can be detected). Entropy is a good choice for that as it has been used as an objective criterion

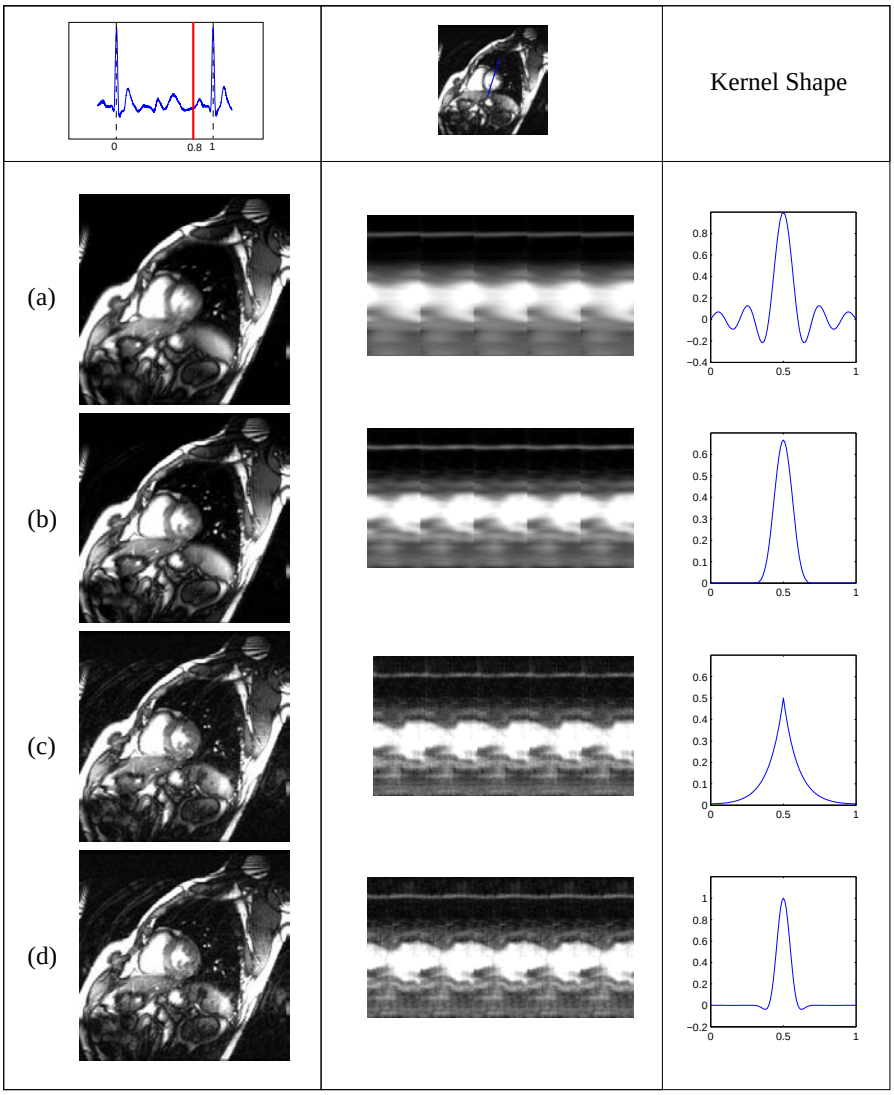

Figure 6.6: Images reconstructed for a fixed cardiac-respiratory phase from data acquired in free breathing (left column). The specific cardiac phase chosen for display is illustrated at the top of the left column with red line, and the respiratory phase is end-inspiration. Temporal profiles (midle column) correspond to the line marked in the image at the top of the middle column. The one dimensional profile of the interpolation kernel (right column) centered in 0.5 and for $p = 5$. (a) Sinc RKHS. (c) Splines RKHS. (c) Sobolev RKHS (d) Sinc-exp interpolation.

for such tasks as image restoration [53] or motion-compensated MRI reconstruction [5]. Generally speaking, entropy increases as the effective resolution is improved. This can be seen by varying the kernel opening parameter p (see Fig. 6.7). On the one hand, increasing p, results in narrower kernels. In the case of the sinc RKHS, increasing p, the interpolation kernel became very localized and we record a loss of signal that produce artifacts. On the other hand, significantly decreasing the magnitude of p will result in a loss of resolution (i.e. blurring). Results from Fig. 6.7 suggest that, compared to sinc

or splines RKHS, the Sobolev RKHS method is an efficient and robust choice, as its results exhibit a relatively weak dependence upon the opening parameter. The results obtained with Sobolev RKHS method are comparable with the results obtained with sinc-exp interpolation, even though for small values of p the entropy of images obtained with sinc-exp have lower entropy. These better results obtained using Sobolev RKHS or sinc-exp interpolation can be attributed to the exponential decay of both kernels. The exponential function represents a more rapid decay than any polynomial function, and has a more desirable effect than that obtained by varying p.

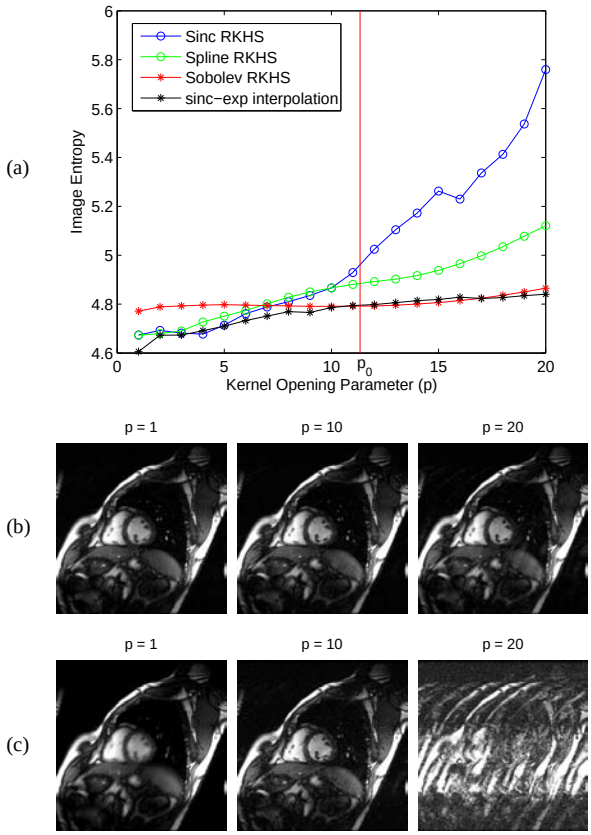

Figure 6.7: (a) The entropy of cardiac images from a healthy volunteer reconstructed with different kernel opening parameters. The parameter $p_0 = 11.34$ marked in the figure is the kernel opening parameter given by (6.7). (b) Cardiac images reconstructed using Sobolev RKHS, for different values of the kernel opening parameter p. (c) Cardiac images reconstructed using sinc RKHS, for different values of the kernel opening parameter p.

The analyses of the cine sequences produced for three subjects in inspiration and expiration by the two cardiologists blinded observers were consistent. Two of the methods, sinc RKHS and splines RKHS, produced images of very poor quality with many artifacts, and were of little diagnostic value. The two other methods, Sobolev RKHS and sinc-exp interpolation, were comparable with overall good image quality, much less artifacts and good diagnostic accuracy. Both observers agreed that the images pro-

duced with Sobolev RKHS contained slightly less artifacts than those using the sinc-exp interpolation.

The mean of the image entropy from further results is shown in Fig. 6.8 over the full range of cardiac phases from images from five healty volunteers. Here the kernel opening parameter was set as in (6.7). The graph shows again that the Sobolev RKHS and sinc-exp interpolation give more stable values compared with other kernels.

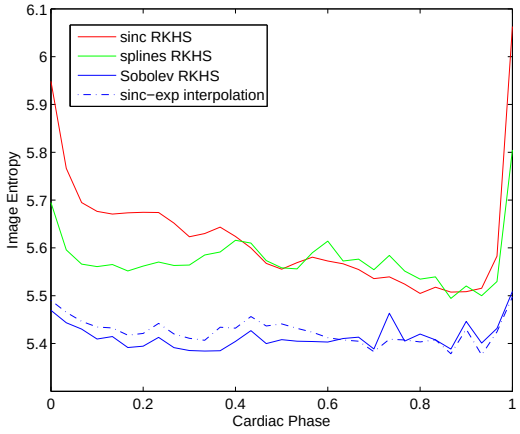

Figure 6.8: The mean of image entropy, over the images reconstructed for five healthy volunteers, for 30 cardiac phases uniformly distributed between 0 and 1.

6.5 Extension to three-dimensional RKHS

The framework presented in this chapter can be extended to three dimensional reproducing kernel Hilbert spaces as in Cîndea et al. [17]. The interest of such an extension is that we can study the variation of cardiac function during the respiration and for different lengths of the RR intervals.

The aim of this generalization is to provide a method for cardiac imaging reconstruction at each cardiac-respiratory phase and for every instantaneous heart rate.

6.5.1 Materials and methods

We used the same materials as in Section 6.3.2. We realize the usual normalizations for the cardiac and respiratory phases. For the heart rate we consider a linear normalization from the interval $[RR_{min}, RR_{max}]$ to $[0, 1]$, where RR_{min}, RR_{max} are the minimal, respectively the maximal, heart rate recorded for a given acquisition. Figure 6.9 displays 60 acquisitions of one line of the k-space represented in the volume of cardiac-respiratory phases and RR intervals.

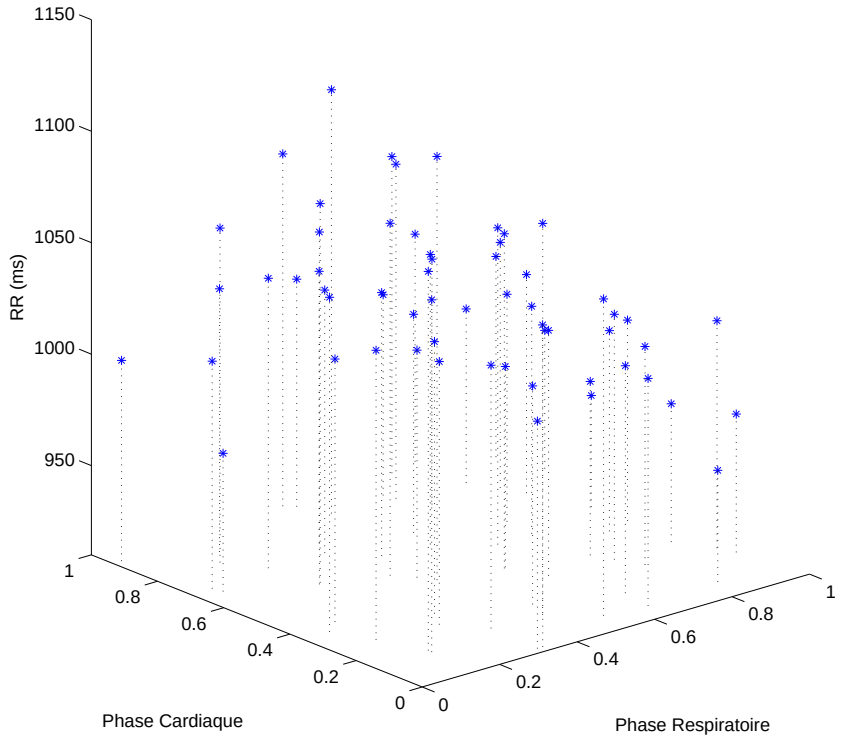

Figure 6.9: The normalized cardiac-respiratory phases and heart-rate for 60 acquisition of the line $k_y = 100$ of the k-space.

Figure 6.10 shows the dependency of the heart rate to the respiratory phase. Therefore, during the inspiration the cardiac rate is lower than the expiration, this fact being the principal motivation for this study.

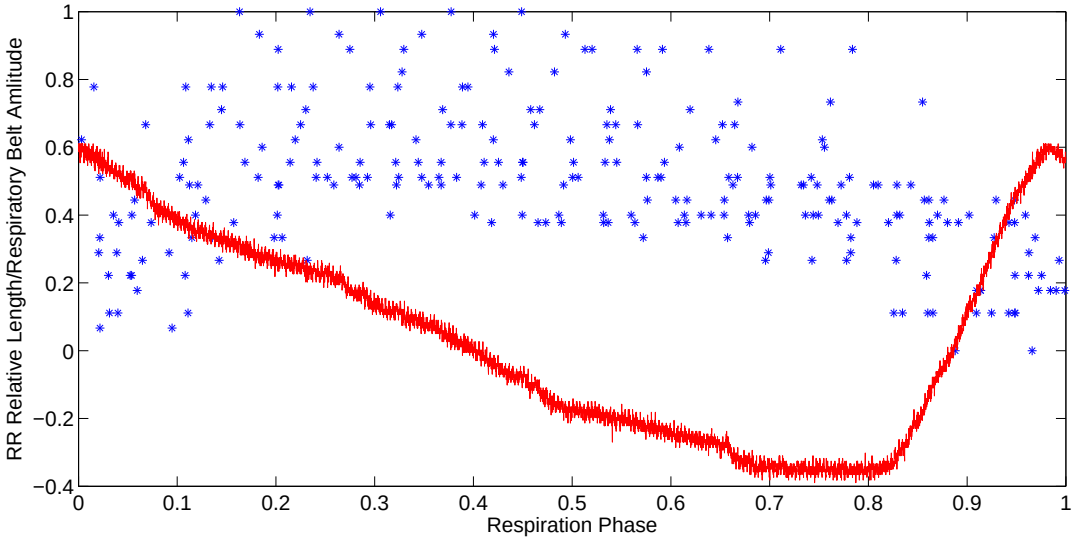

Figure 6.10: The heart rate function of the respiratory phase

From a strictly theoretical point of view the changes from two space dimensions to three dimensions are trivial. Reconstruction formula (6.6) becomes

$$f(x,s,t,r) = \sum_{k\in\mathbb{K}} \sum_{i,j\in\mathbb{I}} g_{k,i} \overline{G}^{-1}_{k,ij} \varphi_{k,j}(s,t,r) e_k(x),$$

where s is the cardiac phase, t the respiratory phase and r the normalized heart rate. Remark that $\varphi_{k,j}$ depends now on three parameters

$$\varphi_{k,j}(s,t,r) = K(s,t,r,s_{k,j},t_{k,j},r_{k,j})$$

and that K is the kernel of one of the following RKHS: $\mathbb{P}\otimes\mathbb{P}\otimes\mathbb{P}$, $\mathcal{K}^3\otimes\mathcal{K}^3\otimes\mathcal{K}^3$ or $W^{1,2}\otimes W^{1,2}\otimes W^{1,2}$. From a practical point of view we have longer aquisition time and more data to process, but the computation is still possible on a personal computer.

6.5.2 Results of three-dimensional RKHS recontruction

In this subsection we present some examples of images obtained using the three dimensional reconstruction framework.

Is possible to reconstruct images for different points of 3D cardiac-respiratory space. Images of short cardiac axis for a fixed respiratory phase were reconstructed from the data acquired in free-breathing (Figure 6.11). From the same data we can reconstruct images for a fixed cardiac phase and different RR intervals and respiratory phase (Figure 6.12).

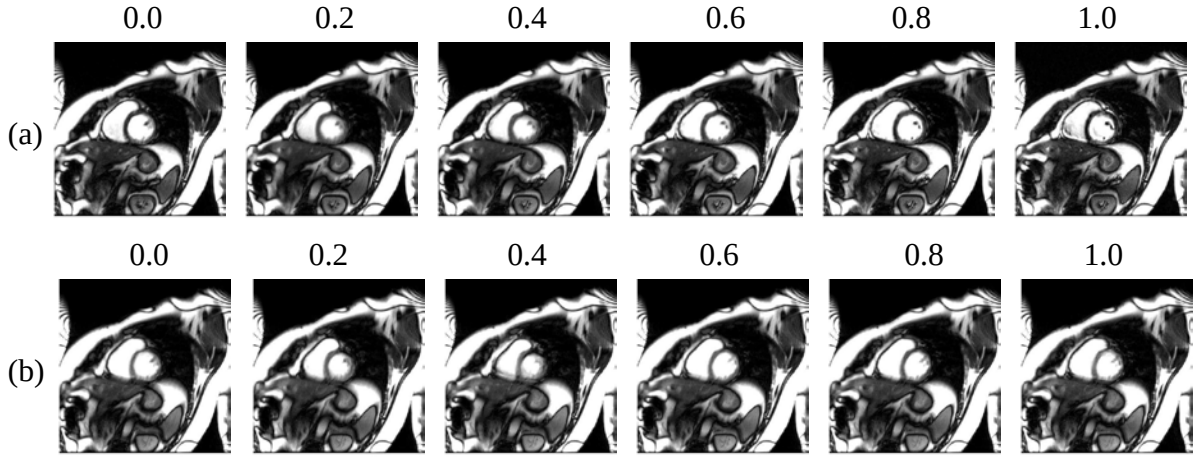

Figure 6.11: Two image series for fixed respiratory phase, for a medium RR interval (1030 ms) and for cardiac phases given in figure. (a) Respiratory phase corresponds to the end of expiration. (b) Respiratory phase coresponds to the end of inspiration.

In Figure 6.12 is visible a variation of the left ventricle "volume" (for the moment only two dimensional acquisition was performed). We claim that using this method we can visualize by MRI the variation of the left ventricle volume for different heart rates, but a more detailed set of subjects must be used (eventualy a clinical study) for validate our affirmation.

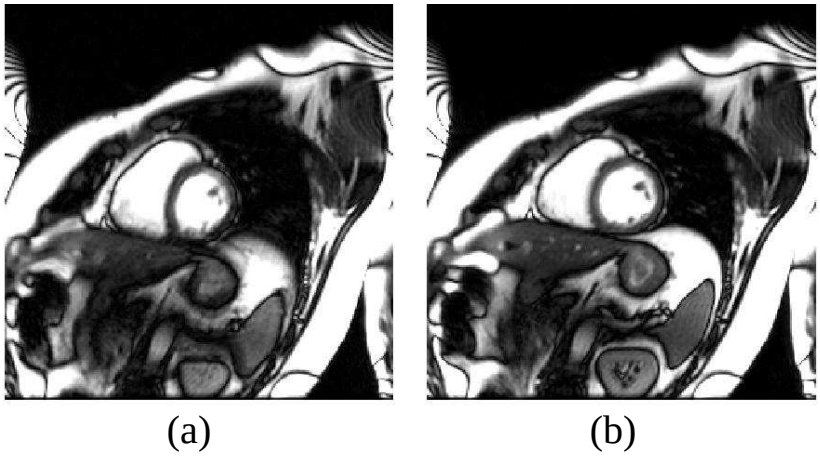

Figure 6.12: Images reconstructed for different RR values and different respiratory phases (the cardiac phase is 0.9). (a) The heart rate is 960 ms and the respiratory phase is 0.9. (b) The heart rate is 1100 ms and the respiratory phase is 0.3.

6.6 Discussion and conclusions

In this chaper we presented a method for cardiac-respiratory MRI acquisition and reconstruction in free-breathing. This method is based on the use of retrospective gating and the fact that the image function f was sought in a RKHS. From all the RKHS tested, Sobolev RKHS was found to give better reconstructions in both simulated and volunteer experiments, the quality of reconstructed images being comparable with the quality of the images reconstructed using the previous (less formalized) approach based simple sinc-exp interpolation. Nevertheless, the principal advantage of the method described in this chapter is that allows a better understanding of the compromise between blurring and aliasing artifacts by the variation of the kernel decay rate p.

In addition to the choice of the RKHS used for reconstruction, tuning the kernel opening parameter is of great importance. In the case of a sinc RKHS, the kernel opening can easily be interpreted as corresponding to the maximal frequency allowed in the function search space. Tuning this parameter may be difficult in practice, as in the present application, due to the non-uniform sampling of the cardiac-respiratory space. A wrong choice can lead either to excessive blurring or to major aliasing artifacts and the choice of parameter p may differ from an RKHS to another. Choosing to use other RKHS (spline or Sobolev) was found to be more flexible. In particular, Sobolev RKHS lead to robust reconstructions, with less dependency on the kernel opening parameter. This can be explained by the solution being sought for in a larger space of functions, with good regularity properties and stronger norm. This strategy can be thought of as integrating prior knowledge about the image into the reconstruction process, which makes it particularly useful when the Nyquist criterion is not fulfilled (i.e. in an attempt to find a good compromise between resolution and residual aliasing artifacts).

The reconstruction algorithm is composed of two steps. The first step consists of the calculus of the matrices G_k and $(G_k)^{-1}$ (see (6.5)), which are independent of the acquired signal as G_k only depends upon sampling times. This first step is of the order of $O(N_y \times N_x \times I^2)$. Recall that (N_y, N_x) is the size of the image and I is the number of aquisition of each position of the k-space. In the second step the solution function f is calculated according to (6.6). An advantage of the method is that, once the first step has been performed, an arbitrary number of images and channels can be reconstructed with minimal additional computational effort using (6.6).

Our work shows that it is possible to obtain heart images from a subject at different cardiac or respiratory phases, with a comparatively short acquisition time in free-breathing. This may be particularly important in clinical situations where breath-holding is impractical or extremely difficult, as is the case of the patients with cardiac arrhythmia. It is possible, with this method, to choose not only the respiratory and cardiac phases to build images but also the value of the RR interval. Therefore, an appropriate window for RR cycles may be selected. Too short or too long cardiac cycles or cycles following a premature contraction may be rejected for reconstruction with only "normal" cycles remaining. Another interesting aspect of the method is that it is

possible to study the cardiac and respiratory interactions which are clinically relevant. These preliminary data should be confirmed by a clinical study.

Acknowledgements

We thank here the help, for image analysis, of Pr Pierre-Yves Marie MD PhD from the department of Nuclear Medicine, University Hospital of Nancy.

7. Wave propagation seen by magnetic resonance imaging

In this chapter, we consider the problem of the reconstruction of a source term in the wave equation from the restriction of the Fourier transform of the wave equation's solution to an open and nonempty set. We prove an indentifiability result and we give some illustrative numerical examples.

7.1 Introduction

Let $\Omega = (0,1)^2$ be the unit square in $\mathbb{R}^2$ and $\mathcal{O} \subset \mathbb{R}^2$ an open and nonempty set. We consider the following wave equation :

$$\ddot{w}(\boldsymbol{x},t) - \Delta w(\boldsymbol{x},t) = \lambda(t) f(\boldsymbol{x}), \qquad \boldsymbol{x} \in \Omega,\ t > 0 \tag{7.1}$$

$$w(\boldsymbol{x},t) = 0, \qquad \boldsymbol{x} \in \partial\Omega,\ t > 0 \tag{7.2}$$

$$w(\boldsymbol{x},0) = \dot{w}(\boldsymbol{x},0) = 0, \qquad \boldsymbol{x} \in \Omega, \tag{7.3}$$

where $\lambda : [0,\infty) \to \mathbb{R}$ is a given function and $f \in L^2(\Omega)$ is the unknown source. In this chapter, we study an inverse problem which consists to identify the source f from the observation y given by

$$y(t) = \widehat{w}(\cdot,t)|_{\mathcal{O}}, \tag{7.4}$$

where by $\widehat{w}$ we denote the Fourier transform of w. Note that we extend the solution of (7.1)-(7.3) by zero outside the domain Ω and in this way the Fourier transform of w is well defined. This problem corresponds to the identification of the wave source from a magnetic resonance imaging (MRI) measurement y (see, for instance, Haacke, Brown, Thompson and Venkatesan [33]).

In order to solve this inverse problem, one important question is the *identifiability* of f :

is the mapping $f \mapsto y$ one to one?

We give a positive answer to this question combining some classic Fourier analysis results with an adapted version of the general framework for solving inverse source problems, described in Alves, Silvestre, Takahashi and Tucsnak [2].

The main result of this chapter is the following theorem :

Theorem 7.1. *Let $\tau > 0$ and $\lambda \in H^1(0,\tau)$ be a function satisfying $\lambda(0) \neq 0$. The application $\mathbb{E}_\tau : L^2(\Omega) \to L^2(0,\tau;\ L^2(\mathcal{O}))$ which associates to the source f in (7.1)-(7.3), the observation y given by (7.4), is one to one.*

The proof of this theorem makes the object of the second section of this chapter.

The third section describes two strategies for recovering the initial state of an infinite dimensional system.

The forth and the last sections illustrate numerically the reconstruction of a source term in the wave equation and give some perspectives to apply this approach to MRI.

7.2 Proof of Theorem 7.1

This section is mainly dedicated to the proof of Theorem 7.1. Firstly we introduce some notation.

Denote $H = L^2(\Omega)$ and consider the operator $A_0 : \mathcal{D}(A_0) \to H$ defined by

$$\mathcal{D}(A_0) = H^2(\Omega) \cap H_0^1(\Omega), \qquad A_0\varphi = -\Delta\varphi \qquad (\varphi \in \mathcal{D}(A_0)).$$

It is well known that A_0 is a self-adjoint, positive operator with compact resolvents. Therefore, as we already done before in this thesis, we introduce the space $H_{\frac{1}{2}}$. Here we have $H_{\frac{1}{2}} = H_0^1(\Omega)$. Let $Y = L^2(\mathcal{O})$ and $C_0 \in \mathcal{L}(H,Y)$ defined by

$$C_0\varphi = \hat{\varphi}|_{\mathcal{O}} \qquad (\varphi \in H),$$

where

$$\hat{\varphi}(\boldsymbol{\xi}) = \int_{\mathbb{R}^2} \varphi(\boldsymbol{x}) e^{-i2\pi\boldsymbol{\xi}\cdot\boldsymbol{x}}\, \mathrm{d}\boldsymbol{x}, \qquad (\boldsymbol{\xi} \in \mathbb{R}^2)$$

is the Fourier transform of φ extended by zero outside Ω. As usually we write (7.1)-(7.3) as a first order system. In order to do this, we denote $X = H_{\frac{1}{2}} \times H$ and $A : \mathcal{D}(A) \to X$

$$\mathcal{D}(A) = H_1 \times H_{\frac{1}{2}}, \qquad A = \begin{bmatrix} 0 & I \\ -A_0 & 0 \end{bmatrix}.$$

Applying Lumer-Phillips theorem, A generates a strongly continuous semigroup $(\mathbb{T}_t)_t$ in X (see, for instance, Tucsnak and Weiss [80, pp.112-113]). Let $C \in \mathcal{L}(X,Y)$ be defined by $C = [C_0,\ 0]$ and $F = \left[\begin{smallmatrix} 0 \\ f \end{smallmatrix}\right]$. With these notations we can write (7.1)-(7.4) as

$$\dot{z}(t) = Az(t) + F, \qquad z(0) = 0 \tag{7.5}$$

$$y(t) = Cz(t), \tag{7.6}$$

where $z(t) = \left[\begin{smallmatrix} w(t) \\ \dot{w}(t) \end{smallmatrix}\right]$. In other words, Theorem 7.1 says that, if $\lambda \in H^1(0,\tau)$ with $\lambda(0) \neq 0$, then the application which associates y given by (7.6), to $F \in X$ from (7.5), is one to one.

Proof of Theorem 7.1. If $F \in X$, it is well-known that the solution of (7.5) satisfies $z \in C([0,\tau];\mathcal{D}(A)) \cap C^1([0,\tau],X)$. Morever, by Duhamel formula we obtain

$$z(t) = \int_0^t \mathbb{T}_{t-s}\lambda(s)F \, \mathrm{d}s = \int_0^t \lambda(t-s)\mathbb{T}_s F \, \mathrm{d}s, \qquad (t \in [0,\tau]). \tag{7.7}$$

Applying the operator C to both sides of (7.7), we obtain

$$y(t) = \int_0^t \lambda(t-s)C\mathbb{T}_s F \, \mathrm{d}s, \qquad (t \in [0,\tau]). \tag{7.8}$$

We denote $y_1(t) = C\mathbb{T}_t F$ and then (7.8) can be written as a Volterra first kind integral equation

$$y(t) = \int_0^t \lambda(t-s)y_1(s) \, \mathrm{d}s, \qquad (t \in [0,\tau]), \tag{7.9}$$

with the unknown y_1. We introduce the operator $S : L^2(0,\tau;Y) \to H^1_L([0,\tau],Y)$ which associates y to y_1 as in (7.9). It is a well-known fact that the operator S defined in this way is an isomorphism (see Kress [43, pp. 33-34]). Moreover, in [2] this operator is extended to another isomorphism from $H^1_R([0,\tau],Y)'$ onto $L^2(\Omega)$. Therefore, there exists a positive constant M_S such that

$$\|y\|_{H^1_L([0,\tau],Y)} = \|Sy_1\|_{H^1_L([0,\tau],Y)} \geqslant M_S \|y_1\|_{L^2(0,\tau;Y)}. \tag{7.10}$$

The identifiability of $f \in L^2(\Omega)$ from the observation y is nothing else that "$y = 0$ implies $f = 0$". Assume that $y = 0$. Then from (7.10) we easily obtain that $y_1 = 0$, i.e.

$$C\mathbb{T}_t F = 0, \qquad (t \in [0,\tau]). \tag{7.11}$$

Recall that $V(t) = \mathbb{T}_t F$ is the solution of

$$\dot{V}(t) = AV(t), \qquad V(0) = F.$$

Denoting $V(t) = \begin{bmatrix} v(t) \\ \dot{v}(t) \end{bmatrix}$, $v(t)$ satisfies the following wave equation

$$\ddot{v}(\boldsymbol{x},t) - \Delta v(\boldsymbol{x},t) = 0, \qquad \boldsymbol{x} \in \Omega, \ t \in [0,\tau] \tag{7.12}$$

$$v(\boldsymbol{x},t) = 0, \qquad \boldsymbol{x} \in \partial\Omega, \ t \in [0,\tau] \tag{7.13}$$

$$v(\boldsymbol{x},0) = 0, \quad \dot{v}(\boldsymbol{x},0) = f(\boldsymbol{x}), \qquad \boldsymbol{x} \in \Omega \tag{7.14}$$

and, moreover, from (7.11) we have

$$\hat{v}(\cdot,t)|_{\mathcal{O}} = 0, \qquad (t \in [0,\tau]).$$

To define the Fourier transform of $v(\cdot,t)$, we extended $v(\cdot,t)$ by zero outside the domain Ω. Therefore, the extended $v(\cdot,t)$ can be seen as a function with compact support. Applying Paley-Wiener theorem (see Stein and Weiss [74, Theorem 4.9]), $\hat{v}(\cdot,t)$ is an entire function. Therefore, $\hat{v}(\cdot,t)$ is an analytic function which is null on an open and nonempty set $\mathcal{O}$ and, so, $\hat{v}(\cdot,t) \equiv 0$. This implies that $v(\cdot,t) \equiv 0$ for every $t \in [0,\tau]$ and finally $f = 0$. □

7.3 Two strategies for recovering the initial state of an infinite dimensional system

This section describes two strategies for recovering the initial data of infinite dimensional systems and follows closely the ideas from Ramdani, Tucsnak and Weiss [65]. As in [65], we assume that the pair (A, C) is *estimatable* with bounded injection, i.e., there exists an operator $K \in \mathcal{L}(Y, X)$ such that $A + KC$ is the generator of an exponentially stable semigroup. Moreover, we assume that (A, C) is *backward estimatable* with bounded injection, i.e., there exists an operator $K_b \in \mathcal{L}(Y, X)$ such that the operator $-A + K_bC$ is the generator of an exponentially stable semigroup.

A classical method to approach the state $z(t)$ of (7.5)-(7.6), when t is large, is to use an *observer*, i.e., another system which, using y given by (7.6) as an input, converges to $z(t)$ when $t \to \infty$ for any initial state. Assuming that, for a given $\tau > 0$, the state $z(\tau)$ is "well" approximated by this observer, we can consider a *backward observer* which in time τ will approximate $z(0)$. This idea is described in Subsection 7.3.1. This method is generalized in [65] and we describe it in Subsection 7.3.2.

7.3.1 Forward and backward observers

Let $K \in \mathcal{L}(X, Y)$ be a bounded linear operator such that $A + KC$ is the generator of an exponentially stable semigroup. Consider the following system

$$\dot{w}(t) = (A + KC)w(t) - Ky(t), \qquad (t \geqslant 0) \tag{7.15}$$

$$w(0) = w_0, \tag{7.16}$$

where $w_0 \in X$ and y is given by (7.6). Under the hypothesis that (A, C) is estimatable, the system (7.15)-(7.16) is an observer associated to (7.5)-(7.6). Indeed, if we denote $\varepsilon(t) = w(t) - z(t)$ the estimation error, we have

$$\begin{aligned} \dot{\varepsilon}(t) &= \dot{w}(t) - \dot{z}(t) \\ &= (A + KC)w(t) - Ky(t) - Az(t) \\ &= (A + KC)w(t) - KCz(t) - Az(t) \\ &= (A + KC)\varepsilon(t). \end{aligned}$$

Recall that (A, C) estimatable means that $(A + KC)$ generates an exponentially stable semigroup. This shows that $\varepsilon(t)$ converges exponentially to zero when $t \to \infty$. A backward observer for (7.5)-(7.6) is given by the following system

$$\dot{w}_b(t) = (A - K_bC)w_b(t) + K_by(t) \tag{7.17}$$

$$w_b(\tau) = w_{b\tau}, \tag{7.18}$$

where $K_b \in \mathcal{L}(Y, X)$ is such that $(-A + K_bC)$ generates an exponentially stable semigroup on X. The existence of such an operator is guaranteed by the backward estima-

bility of the pair (A, C). Denoting $\varepsilon_b(t) = w_b(t) - z(t)$, we obtain

$$\begin{aligned}\dot{\varepsilon}_b(t) &= \dot{w}_b(t) - \dot{z}(t)\\ &= (A - K_bC)w_b(t) + K_by(t) - Az(t)\\ &= (A - K_bC)w_b(t) + K_bCz(t) - Az(t)\\ &= (A - K_bC)\varepsilon_b(t).\end{aligned}$$

Therefore, the estimation error is given by $\varepsilon_b(0) = e^{\tau(-A+K_bC)}\varepsilon_b(\tau)$ and goes to zero when τ goes to ∞.

To recover the initial state z_0 from the observation (7.5), using these two observers, we put $w_b(\tau) = w(\tau)$. The error between z_0 and $w_b(0)$ is given by

$$\varepsilon_b(0) = e^{\tau(-A+K_bC)}e^{\tau(A+KC)}\varepsilon(0). \tag{7.19}$$

From the forward and backward estimability of (A, C) we can easily see that the error given by estimate above goes exponentially fast to zero when τ goes to infinity.

Remark 7.2. Historically, one of the first papers where observers for finite dimensional systems are described is due to Luenberger [50] and dates from 1964. The construction of the operators $K, K_B \in \mathcal{L}(Y, X)$ is generally non trivial. More precisely, for finite dimensional systems, construction of the matrices K involve the placement of all the eigenvalues (the poles) of $A + KC$ to the left of imaginary axis. This can be realized by solving a Ricatti equation, which is computationally expensive. As is the case for the wave equation, when the operator A is skew-adjoint we can choose $K = -C^*$.

7.3.2 Iterative forward and backward observers

In this subsection we describe briefly the iterative method for recovering the initial state of infinite dimensional systems from [65]. This method consists to iterate the method from previous subsection with the purpose to obtain a better precision for the initial data approximation with a shorter observation time.

With the same assumptions as at the beginning of this section we consider the following forward and backward systems

$$\dot{w}^{(n)}(t) = (A + KC)w^{(n)}(t) - Ky(t), \qquad t \geqslant 0 \tag{7.20}$$

$$w^{(n)}(0) = \begin{cases} w_0, & \text{if } n = 1\\ w_b^{(n-1)}(0), & \text{if } n > 1\end{cases} \tag{7.21}$$

and

$$\dot{w}_b^{(n)}(t) = (A - K_bC)w_b^{(n)}(t) + K_by(t), \qquad t \leqslant \tau \tag{7.22}$$

$$w_b^n(\tau) = w^{(n)}(\tau). \tag{7.23}$$

If we solve $N > 0$ times (7.20)-(7.23) the error in the approximation of the z_0 by $w_b^N(0)$ is given by

$$\varepsilon_b^{(N)}(0) = (w_b^{(N)} - z)(0) = \left(e^{(-A+K_bC)\tau}e^{(A-KC)\tau}\right)^N \varepsilon^{(0)}(0).$$

Indeed, applying N times the error estimates proven in the previous subsection we obtain the estimate above. If (A, C) is forward and backward estimatable, and that K and K_b are such that $A + KC$ and $A - K_bC$ are exponentially stable, then there exists a time $\tau > 0$ such that

$$\|e^{(-A+K_bC)\tau}e^{(A-KC)\tau}\| < 1$$

and therefore

$$\|\varepsilon^{(N)}(0)\| \leqslant \|e^{(-A+K_bC)\tau}e^{(A-KC)\tau}\|^N \|\varepsilon^{(0)}(0)\|.$$

Remark 7.3. In practice, both methods are easy to implement numerically. The advantage of this approach compared with the non-iterative one is that we have the convergence of the approximation for a "short" observation time τ. The dual of this method for the construction of exact controls for second order infinite dimensional systems was described from a numerical point of view in Chapter 4.

7.4 Numerical simulations

In this section we give a numerical example of recovering the source term f in the wave equation (7.1)-(7.4) using observers.

Following the steps from the proof of Theorem 7.1, first of all we solve a Volterra integral equation of the first kind. For solving numerically this integral equation we used a simple quadrature method, or more precissely, a repeated Simpson rule. In this way the unknown source term is placed in the initial data of the wave equation (7.12)-(7.14).

The method described in this chapter needs a numerical solver for the following type of equations

$$\begin{aligned} \ddot{w}(x,t) - \Delta w(x,t) + F(w,x,t) = 0, &\qquad \text{in } \Omega \times [0,\tau] \\ w(x,t) = 0, &\qquad \text{on } \partial\Omega \times [0,\tau] \\ w(x,0) = w_0(x), \quad \dot{w}(x,0) = w_1(x), &\qquad \text{in } \Omega, \end{aligned}$$

with different values of F. For solving numerically this equation we use an approximation of the solution by functions with a finite number of eigenmodes.

Let $\phi_{mn}(x, y) = \sin(m\pi x)\sin(n\pi y)$ be the eigenvectors of the Dirichlet Laplacian in the unit square Ω and assume that the unknown source term f, and therefore, the initial data in (7.12)-(7.14), has a finite number of eigenmodes, i.e.

$$f(x,y) = \sum_{m,n=1}^{M,N} c_{mn}\phi_{mn}(x,y).$$

Also, the solution of (7.12)-(7.14) has the form

$$v(x,y,t)=\sum_{m,n=1}^{M,N} v_{mn}(t)\phi_{mn}(x,y). \tag{7.24}$$

Replacing (7.24) in (7.12)-(7.14), we obtain

$$\ddot{v}_{mn}(t)+(m^2+n^2)\pi^2 v_{mn}(t)=0, \qquad 1\leqslant m\leqslant M,\ 1\leqslant n\leqslant N, t\geqslant 0 \tag{7.25}$$

$$v_{mn}(0)=0, \quad \dot{v}_{mn}(0)=c_{mn}, \qquad 1\leqslant m\leqslant M,\ 1\leqslant n\leqslant N. \tag{7.26}$$

The observation becomes

$$y(\xi_1,\xi_2,t)=\sum_{m,n=1}^{M,N}\frac{mn\pi^2\left(1-(-1)^m e^{-i\xi_1}\right)\left(1-(-1)^n e^{-i\xi_2}\right)}{(m^2\pi^2-\xi_1^2)(n^2\pi^2-\xi_2^2)}w_{mn}(t), \qquad (\xi_1,\xi_2\in\mathcal{O}). \tag{7.27}$$

In fact, we consider in (7.27) only a finite number P of observation points $(\xi_{p,1},\xi_{p,2})$ uniformly distributed in the interior of the disc $B(0,r)$. Therefore, the system (7.25)-(7.27) can be written as a finite dimensional system. For this purpose, denote

$$W(t)=(w_{mn}(t))_{\substack{1\leqslant m\leqslant M\\ 1\leqslant n\leqslant N}}\in\mathbb{R}^{MN}, \qquad F=(c_{mn})_{\substack{1\leqslant m\leqslant M\\ 1\leqslant n\leqslant N}}\in\mathbb{R}^{MN}$$

and $\tilde{A}_0=(a_{jk})_{j,k}\in\mathcal{M}_{MN,MN}(\mathbb{R})$, given by

$$a_{jk}=\begin{cases}0, & j\neq k\\ m^2+n^2, & i=j=(m-1)N+n.\end{cases}$$

With this notation, (7.25)-(7.27) becomes

$$\begin{cases}\ddot{W}(t)+\tilde{A}_0W(t)=0, & (t\geqslant 0)\\ W(0)=0, \quad \dot{W}(0)=F\end{cases} \tag{7.28}$$

and $y(t)=C_0W(t)$, where $C_0=(c_{p,\ (m-1)N+n})_{\substack{1\leqslant p\leqslant P\\ 1\leqslant m\leqslant M,\ 1\leqslant n\leqslant N}}\in\mathcal{M}_{P,MN}(\mathbb{C})$

$$c_{p,(m-1)N+n}=\frac{mn\pi^2(1-(-1)^m e^{-i\xi_{p,1}})(1-(-1)^n e^{-i\xi_{p,2}})}{(m^2\pi^2-\xi_{p,1}^2)(n^2\pi^2-\xi_{p,2}^2)}.$$

Moreover, putting $Z(t)=\begin{bmatrix}W(t)\\ \dot{W}(t)\end{bmatrix}$, $\tilde{A}=\begin{bmatrix}0 & I\\ -\tilde{A}_0 & 0\end{bmatrix}$, $C=[C_0\ 0]$ and $Z_0=\begin{bmatrix}W_0\\ 0\end{bmatrix}$ we can write the above second order system as a first order system :

$$\dot{Z}(t)=AZ(t), \qquad Z(0)=Z_0$$
$$y(t)=CZ(t).$$

To solve this last problem we use the two approaches described in Section 7.3. For illustrating the efficiency of this method we consider the problem of reconstruction of

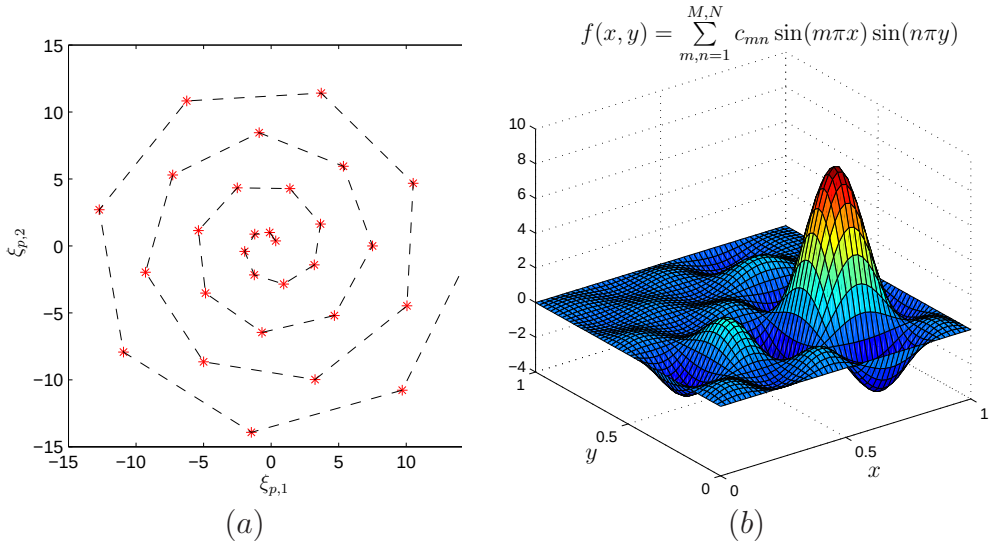

Figure 7.1: (a) The set of points $(\xi_{p,1}, \xi_{p,2})_{p=1,\cdots,P}$ from the definition of C_0. (b) The source $f(x, y)$.

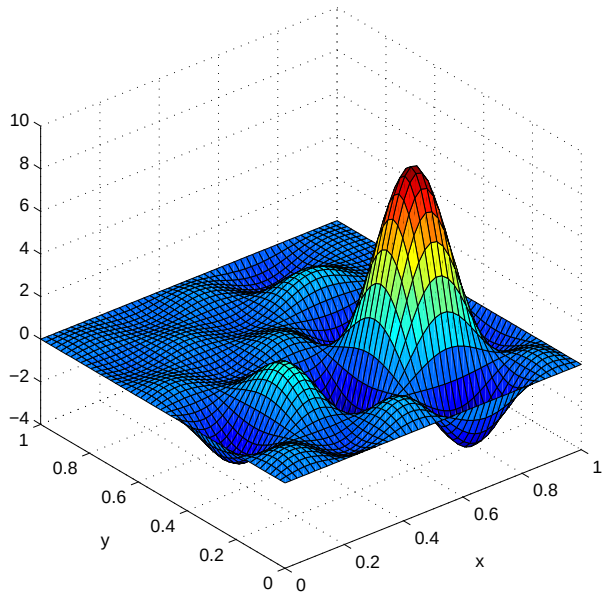

Figure 7.2: Reconstructed initial data after 9 iterations.

the source term $F = (c_{mn})_{1 \leqslant m,n \leqslant M}$ with $M = N = 5$ and the observation $y(t) \in \mathbb{C}^P$ with $P = 30$ points distributed on a spiral in the interior of the disc $B(0, r)$ with $r = 15$ (Figure 7.1(a). We set $\lambda(t) = e^{-t}$, $\tau = 0.25$ and

$$c_{mn} = \sin\left(\frac{2m\pi}{3}\right) \sin\left(\frac{n\pi}{3}\right),$$

which corresponds to the profile described in the Figure 7.1(b).

All the computations were realized in Matlab (MathWorks, Natick, MA). The source

term reconstructed after 9 iterations of the algorithm, corresponding to the method described in Subsection 7.3.2 is displayed in Figure 7.2.

The evolution of the relative error, in norm L^2, between the exact initial data and the reconstructed one, in rapport with the number of iterations is displayed in Figure 7.3. The value of the relative error after the 9-th iteration is 0.02%.

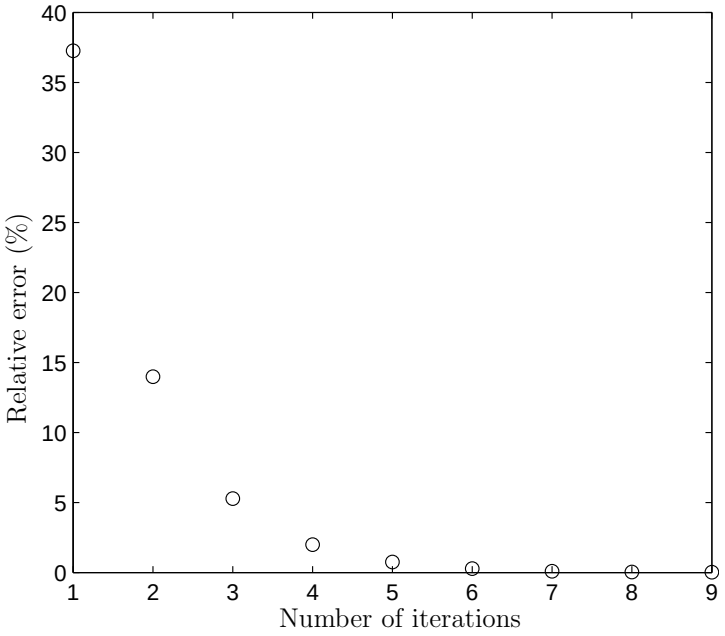

Figure 7.3: Relative error between the estimated and reconstructed source.

Remark 7.4. To construct the matrices K and K_b, such that the operators $A + KC$, $-A+K_bC$ are the generators of two exponentially stable semigroups, we used the Matlab command `pole` from the `Control System Toolbox`. The number of poles which can be placed with this command can't be very large, because the pole placement algorithms are numerically unstable.

Remark 7.5. A numerical study of the errors realized by replacing our original observation ($y(t) \in L^2(\mathcal{O})$, with $\mathcal{O} = B(0, r)$) by an observation in a finite dimensional space, will be very interesting.

In the remaining part of this section we give two examples of finite dimensional observation operators corresponding to (7.27). More precisely, from a MRI practical point of view, several acquisition sequences are possible, two of them being the following: first one consists in a random path inside the disc $B(0, r)$ (Figure 7.4(a)) and second one follows a rectangular grid path (Figure 7.4(b)).

For both acquisition sequences described above we obtained very similar results with relative errors after 10 iterations equal to 0.4% for the random sequence and 0.3% for the Cartesian sequence.

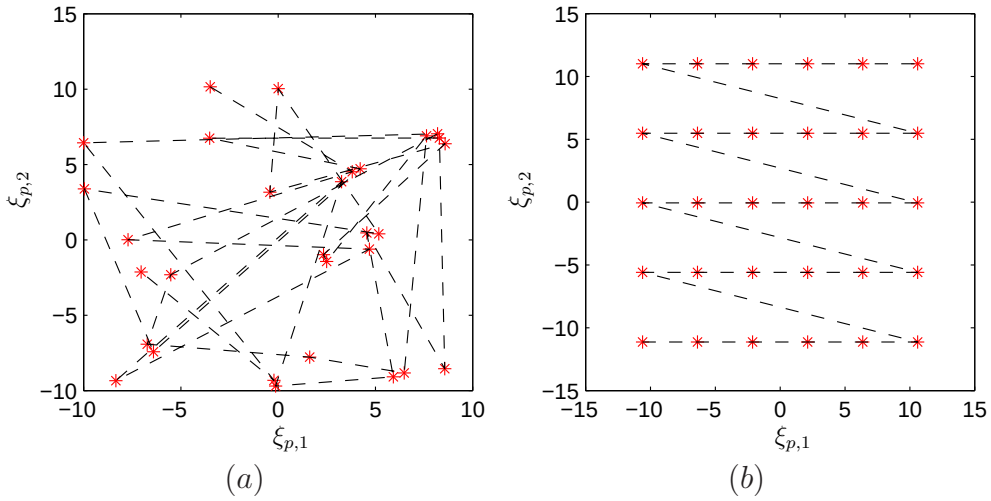

Figure 7.4: Two examples of acquisition sequences. (a) A random acquisition sequence. (b) A rectangular grid sequence.

7.5 A perspective to MRI

In this section we assume that the object (or a slice of the object) imaged by MRI has a motion which can be described by a partial differential equation of the form

$$\dot{z}(t) = Az(t) + \lambda(t)F$$

and that we are capables to record

$$y(t) = Cz(t),$$

corresponding to the Fourier transform of the image. How we already seen in this chapter, for this kind of systems, if (A, C) is exactly observable (or, even if we have an identifiability property), we can develop a method, based on observers, to reconstruct the unknown source term F from the acquired data y. The wave equation and the plate equations which were the subject of the first part of this thesis are good examples of partial differential equations of this type.

Unfortunately, the organs of human body, as for example the heart, have much more complicated motions, and the model of motion is aprioiri unknown. In [72], Sermesant et al proposed a model for cardiac motion and using a data assimilation technique, they calibrate this model to the MR images from a specific patient. One very intersting research direction, for applying the method described in this chapter to cardiac MRI, is to try to assimilates directly the MR raw data to the model proposed in [72] in the purpose to reconstruct an image of the heart (for example the initial data) and so a complete cardiac cycle.

At I.A.D.I. Laboratory, we tried to realize an experiment consisting to place in a MRI machine, a system which is governed by the wave equation. More precisely, the object that we imaged is a recipient containing some liquid (water for example). We

can generate surface waves using a vibrating system and by MRI we can measure the Fourier transform of the two dimensional function defined by the liquid height in each point. Figure 7.5 displays one of the first images realized in this experiment and Figure (b) display the source considered in Section 7.4 as an image.

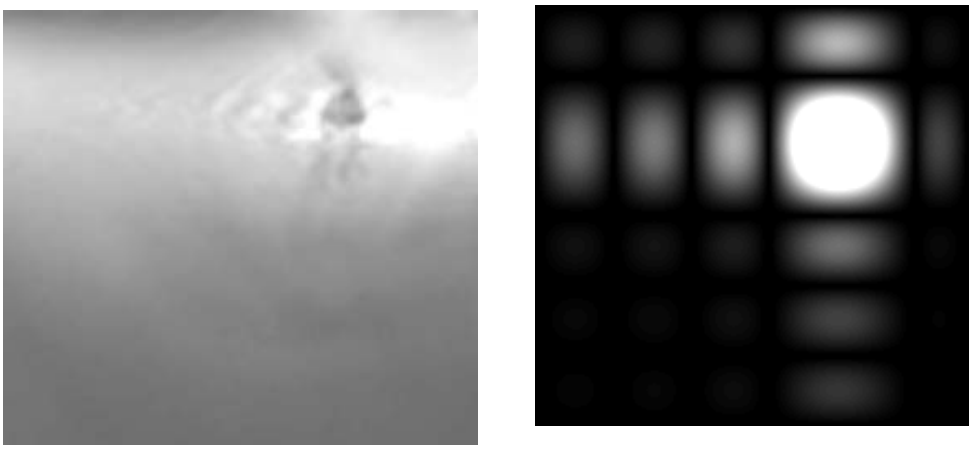

(a) (b)

Figure 7.5: (a) A first MR image of a surface wave in a water recipient. (b) The source term for the wave equation simulated in Section 7.4.

This experimental part is in progress, at I.A.D.I. Laboratory developing adequate sensors to record the signal of the vibrating system generating the wave, which corresponds to the function $\lambda(t)$, supposed known in the previous sections.

Conclusion and perspectives to MRI inverse problems

In this second part of the thesis, the main topic was the reconstruction of magnetic resonance images of moving objects from the magnetic resonance data acquired during the motion. The medical example that we have in mind is the cardiac magnetic resonance imaging with data acquired in free-breathing.

In the first chapter of this part, corresponding to Chapter 5 of the thesis, we described shortly the basic physical principles of the magnetic resonance imaging, explaining the process of image formation. We present the problematic of motion during the acquisition of MR data and we give the main ideas used by the standard clinical methods in cardiac MRI.

In Chapter 6 we develop a new method for the reconstruction of cardiac magnetic resonance images from data acquired in free-breathing. The idea of this method is to assume that the protons density in time is a function in a reproducing kernel Hilbert space. Using the properties of these spaces we formulate the reconstruction as a problem of moments in a Hilbert space. The results obtained for different reproducing kernel Hilbert spaces were compared using data from five healthy volunteers and from a simulated cardiorespiratory phantom.

The last chapter of this thesis combines the methods described in the first part of the thesis concerning the exact observability of differential system with an inverse problem from magnetic resonance imaging. More precisely, we solved the inverse problem consisting in the reconstruction of the initial data in the wave equation from an observation corresponding to a magnetic resonance signal.

This part of the thesis have two main perspectives.

First of these perspectives is to do a clinical study in order to measure the evolution of some parameters of cardiac function (par example the volume of left ventricle) along the respiration, using the reconstruction method described in Chapter 6. Concerning the same method, a mathematical study of the influence of the sampling density to the quality of the reconstruction will be very intersting.

The methodology presented in Chapter 7 can be applied to other models such plate equations and, why not, to the finite element model of the heart described in [72].

Bibliography

[1] A. Aldroubi and K. Gröchenig, *Nonuniform sampling and reconstruction in shift-invariant spaces*, SIAM Rev., 43 (2001), pp. 585–620 (electronic).

[2] C. Alves, A. L. Silvestre, T. Takahashi, and M. Tucsnak, *Solving inverse source problems using observability. Applications to the Euler-Bernoulli plate equation*, SIAM J. Control Optim., 48 (2009), pp. 1632–1659.

[3] W. Arendt, C. J. K. Batty, M. Hieber, and F. Neubrander, *Vector-valued Laplace transforms and Cauchy problems*, vol. 96 of Monographs in Mathematics, Birkhäuser Verlag, Basel, 2001.

[4] N. Aronszajn, *Theory of reproducing kernels*, Trans. Amer. Math. Soc., 68 (1950), pp. 337–404.

[5] D. Atkinson, D. L. Hill, P. N. Stoyle, P. E. Summers, and S. F. Keevil, *Automatic correction of motion artifacts in magnetic resonance images using an entropy focus criterion.*, IEEE Transactions on Medical Imaging, 16 (1997), pp. 903–910.

[6] S. A. Avdonin and S. A. Ivanov, *Families of exponentials*, Cambridge University Press, Cambridge, 1995. The method of moments in controllability problems for distributed parameter systems, Translated from the Russian and revised by the authors.

[7] G. Baker, *Error estimates for finite element methods for second order hyperbolic equations*, SIAM J. Numer. Anal., 13 (1976), pp. 564–576.

[8] J. M. Ball, *Initial-boundary value problems for an extensible beam*, J. Math. Anal. Appl., 42 (1973), pp. 61–90.

[9] C. Bardos, G. Lebeau, and J. Rauch, *Sharp sufficient conditions for the observation, control and stabilization of waves from the boundary*, SIAM J. Control. and Optim., 30 (1992), pp. 1024–1065.

[10] H. M. Berger, *A new approach to the analysis of large deflections of plates*, J. Appl. Mech., 22 (1955), pp. 465–472.

[11] D. A. Bluemke, J. L. Boxerman, E. Atalar, and E. R. McVeigh, *Segmented k-space cine breath-hold cardiovascular MR imaging: Part 1. principles and technique.*, AJR Am J Roentgenol, 169 (1997), pp. 395–400.

[12] D. E. Bohning, B. Carter, S. S. Liu, and G. M. Pohost, *Pc-based system for retrospective cardiac and respiratory gating of nmr data.*, Magn Reson Med, 16 (1990), pp. 303–316.

[13] S. Brenner and L. Scott, *The mathematical theory of finite element methods*, vol. 15 of Texts in Applied Mathematics, Springer-Verlag, New York, 1994.

[14] N. Burq and M. Zworski, *Geometric control in the presence of a black box*, J. Amer. Math. Soc., 17 (2004), pp. 443–471.

[15] G. Chen, *Control and stabilization for the wave equation in a bounded domain*, SIAM J. Control Optim., 17 (1979), pp. 66–81.

[16] N. Cîndea, S. Micu, and M. Tucsnak, *An approximation method for exact controls of vibrating systems*, submitted, (November, 2009).

[17] N. Cîndea, F. Odille, G. Bosser, J. Felblinger, and P.-A. Vuissoz, *Three dimensional reproducing kernel Hilbert spaces for heart modulated cadio-respiratory magnetic resonance imaging*, Proceedings 16th Scientific Meeting, International Society for Magnetic Resonance in Medicine, Toronto, (2008).

[18] N. Cîndea and M. Tucsnak, *Fast and strongly localized observation for a perturbed plate equation*, International Series of Numerical Mathematics, 158 (2009), pp. 73–83.

[19] N. Cîndea and M. Tucsnak, *Local exact controllability for Berger plate equation*, Mathematics of Control, Signals, and Systems (MCSS), 21 (2009), pp. 93–110.

[20] N. Cîndea, F. Odille, G. Bosser, J. Felblinger, and P.-A. Vuissoz, *Reconstruction from free-breathing cardiac MRI data using reproducing kernel Hilbert spaces.*, Magn Reson Med, 63 (2010), pp. 59–67.

[21] R. W. Dickey, *Free vibrations and dynamic buckling of the extensible beam*, J. Math. Anal. Appl., 29 (1970), pp. 443–454.

[22] ——, *Dynamic stability of equilibrium states of the extensible beam*, Proc. Amer. Math. Soc., 41 (1973), pp. 94–102.

[23] S. Dolecki and D. L. Russell, *A general theory of observation and control*, SIAM J. Control Optimization, 15 (1977), pp. 185–220.

[24] H. Du and M. Cui, *Representation of the exact solution and a stability analysis on the Fredholm integral equation of the first kind in reproducing kernel space*, Appl. Math. Comput., 182 (2006), pp. 1608–1614.

[25] S. Ervedoza, *Spectral conditions for admissibility and observability of wave systems: applications to finite element schemes*, Numer. Math., 113 (2009), pp. 377–415.

[26] S. Ervedoza and E. Zuazua, *Hilbert Uniqueness Method and Regularity: Applications to the order of convergence of discrete controls for the wave equation*, (2009). Private communication.

[27] ——, *Uniformly exponentially stable approximations for a class of damped systems*, J. Math. Pures Appl. (9), 91 (2009), pp. 20–48.

[28] J. Felblinger and C. Boesch, *Amplitude demodulation of the electrocardiogram signal (ECG) for respiration monitoring and compensation during MR examinations.*, Magn Reson Med, 38 (1997), pp. 129–136.

[29] J. O. Fredrickson, H. Wegmller, R. J. Herfkens, and N. J. Pelc, *Simultaneous temporal resolution of cardiac and respiratory motion in MR imaging.*, Radiology, 195 (1995), pp. 169–175.

[30] A. V. Fursikov and O. Y. Imanuvilov, *Controllability of evolution equations*, vol. 34 of Lecture Notes Series, Seoul National University Research Institute of Mathematics Global Analysis Research Center, Seoul, 1996.

[31] R. Glowinski, C. H. Li, and J.-L. Lions, *A numerical approach to the exact boundary controllability of the wave equation (i). Dirichlet controls: Description of the numerical methods*, Japan J. Appl. Math., 7 (1990), pp. 1–76.

[32] R. Glowinski and J.-L. Lions, *Exact and approximate controllability for distributed parameter systems*, Acta Numer., (1996), pp. 159–333.

[33] M. E. Haacke, R. W. Brown, M. R. Thompson, R. Venkatesan, M. E. Haacke, R. W. Brown, M. R. Thompson, and R. Venkatesan, *Magnetic Resonance Imaging: Physical Principles and Sequence Design*, Wiley-Liss, June 1999.

[34] A. Haraux, *Une remarque sur la stabilisation de certains systèmes du deuxième ordre en temps*, Portugal. Math., 46 (1989), pp. 245–258.

[35] O. Y. Imanuvilov and J.-P. Puel, *Global Carleman estimates for weak solutions of elliptic nonhomogeneous Dirichlet problems*, Int. Math. Res. Not., (2003), pp. 883–913.

[36] A. E. Ingham, *Some trigonometrical inequalities with applications to the theory of series*, Math. Z., 41 (1936), pp. 367–379.

[37] K. Ito, K. Ramdani, and M. Tucsnak, *A time reversal based algorithm for solving initial data inverse problems*, Discrete Contin. Dyn. Syst. Ser. S., (2010). to appear.

[38] S. Jaffard, *Contrôle interne exact des vibrations d'une plaque rectangulaire*, Portugal. Math., 47 (1990), pp. 423–429.

[39] H. Jung, J. C. Ye, and E. Y. Kim, *Improved k-t blast and k-t sense using focuss.*, Phys Med Biol, 52 (2007), pp. 3201–3226.

[40] J.-P. Kahane, *Pseudo-périodicité et séries de Fourier lacunaires*, Ann. Sci. École Norm. Sup. (3), 79 (1962), pp. 93–150.

[41] P. Kellman, C. Chefd'hotel, C. H. Lorenz, C. Mancini, A. E. Arai, and E. R. McVeigh, *Fully automatic, retrospective enhancement of real-time acquired cardiac cine MR images using image-based navigators and respiratory motion-corrected averaging.*, Magn Reson Med, 59 (2008), pp. 771–778.

[42] V. Komornik, *On the exact internal controllability of a Petrowsky system*, J. Math. Pures Appl. (9), 71 (1992), pp. 331–342.

[43] R. Kress, *Linear integral equations*, vol. 82 of Applied Mathematical Sciences, Springer-Verlag, Berlin, 1989.

[44] H. J. Landau, *Necessary density conditions for sampling and interpolation of certain entire functions*, Acta Math., 117 (1967), pp. 37–52.

[45] I. Lasiecka and R. Triggiani, *Exact controllability and uniform stabilization of Euler-Bernoulli equations with boundary control only in* $\Delta w|_\Sigma$, Boll. Un. Mat. Ital. B (7), 5 (1991), pp. 665–702.

[46] G. Lebeau, *Contrôle de l'équation de Schrödinger*, J. Math. Pures Appl. (9), 71 (1992), pp. 267–291.

[47] Z.-P. Liang, H. Jiang, C. P. Hess, and P. C. Lauterbur, *Dynamic imaging by model estimation.*, International Journal of Imaging Systems and Technology, 8 (1997), pp. 551–557.

[48] J.-L. Lions, *Contrôlabilité exacte, perturbations et stabilisation de systèmes distribués. Tome 1*, vol. 8 of Recherches en Mathématiques Appliquées, Masson, Paris, 1988.

[49] K. Liu, *Locally distributed control and damping for the conservative systems*, SIAM J. Control Optim., 35 (1997), pp. 1574–1590.

[50] D. Luenberger, *Observing the state of a linear system*, IEEE Transactions on Military Electronics, 8 (1964), pp. 74–.

[51] G. P. Menzala and E. Zuazua, *Timoshenko's beam equation as limit of a nonlinear one-dimensional von Kármán system*, Proc. Roy. Soc. Edinburgh Sect. A, 130 (2000), pp. 855–875.

[52] L. Miller, *Controllability cost of conservative systems: resolvent condition and transmutation*, Journal of Functional Analysis, 218 (2005), pp. 425–444.

[53] R. Narayan and R. Nityananda, *Maximum entropy image restoration in astronomy.*, Annual Review of Astronomy and Astrophysics, 24 (1986), pp. 127–170.

[54] A. H. Nayfeh and D. T. Mook, *Nonlinear oscillations*, Wiley-Interscience [John Wiley & Sons], New York, 1979. Pure and Applied Mathematics.

[55] K. Nehrke, P. Bornert, D. Manke, and J. C. Bock, *Free-breathing cardiac MR imaging: study of implications of respiratory motion–initial results*, Radiology, 220 (2001), pp. 810–5.

[56] F. Odille, N. Cîndea, D. Mandry, C. Pasquier, P.-A. Vuissoz, and J. Felblinger, *Generalized MRI reconstruction including elastic physiological motion and coil sensitivity encoding.*, Magn Reson Med, 59 (2008), pp. 1401–1411.

[57] F. Odille, C. Pasquier, R. Abaherli, P.-A. Vuissoz, G. P. Zientara, and J. Felblinger, *Noise cancellation signal processing method and computer system for improved real-time electrocardiogram artifact correction during MRI data acquisition.*, IEEE Trans Biomed Eng, 54 (2007), pp. 630–640.

[58] F. Odille, P.-A. Vuissoz, P.-Y. Marie, and J. Felblinger, *Generalized reconstruction by inversion of coupled systems (grics) applied to free-breathing MRI.*, Magn Reson Med, 60 (2008), pp. 146–157.

[59] A. Pazy, *Semigroups of linear operators and applications to partial differential equations*, vol. 44 of Applied Mathematical Sciences, Springer-Verlag, New York, 1983.

[60] G. Perla Menzala, A. F. Pazoto, and E. Zuazua, *Stabilization of Berger-Timoshenko's equation as limit of the uniform stabilization of the von Kármán system of beams and plates*, M2AN Math. Model. Numer. Anal., 36 (2002), pp. 657–691.

[61] C. Plathow, S. Ley, J. Zaporozhan, M. Schobinger, E. Gruenig, M. Puderbach, M. Eichinger, H. P. Meinzer, I. Zuna, and H. U. Kauczor, *Assessment of reproducibility and stability of different breath-hold maneuvres by dynamic MRI: comparison between healthy adults and patients with pulmonary hypertension*, Eur Radiol, 16 (2006), pp. 173–9.

[62] J. P. W. Pluim, J. B. A. Maintz, and M. A. Viergever, *Mutual-information-based registration of medical images: a survey*, 22 (2003), pp. 986–1004.

[63] A. Quarteroni and A. Valli, *Numerical approximation of partial differential equations*, vol. 23 of Springer Series in Computational Mathematics, Springer-Verlag, Berlin, 1997.

[64] K. Ramdani, T. Takahashi, G. Tenenbaum, and M. Tucsnak, *A spectral approach for the exact observability of infinite-dimensional systems with skew-adjoint generator*, J. Funct. Anal., 226 (2005), pp. 193–229.

[65] K. Ramdani, M. Tucsnak, and G. Weiss, *Recovering the initial state of an infinite-dimensional system using observers*, submitted, (2009).

[66] R. Rebarber and G. Weiss, *An extension of russell's principle on exact controllability*, in Proc. of the Fourth ECC, 1997. CD-ROM.

[67] J. B. T. M. Roerdink and M. Zwaan, *Cardiac magnetic resonance imaging by retrospective gating: mathematical modelling and reconstruction algorithms*, European J. Appl. Math., 4 (1993), pp. 241–270.

[68] D. Russell, *Exact boundary value controllability theorems for wave and heat processes in star-complemented regions*, in Differential games and control theory (Proc. NSF—CBMS Regional Res. Conf., Univ. Rhode Island, Kingston, R.I., 1973), Dekker, New York, 1974, pp. 291–319. Lecture Notes in Pure Appl. Math., Vol. 10.

[69] ——, *Controllability and stabilizability theory for linear partial differential equations: recent progress and open questions*, SIAM Rev., 20 (1978), pp. 639–739.

[70] C. L. Schultz, R. J. Alfidi, A. D. Nelson, S. Y. Kopiwoda, and M. E. Clampitt, *The effect of motion on two-dimensional fourier transformation magnetic resonance images*, Radiology, 152 (1984), pp. 117–21.

[71] A. D. Scott, J. Keegan, and D. N. Firmin, *Motion in cardiovascular MR imaging.*, Radiology, 250 (2009), pp. 331–351.

[72] M. Sermesant, P. Moireau, O. Camara, J. Sainte-Marie, R. Andriantsimiavona, R. Cimrman, D. Hill, D. Chapelle, and R. Razavi, *Cardiac function estimation from MRI using a heart model and data assimilation: Advances and difficulties*, Medical Image Analysis, 10 (2006), pp. 642 – 656. Special Issue on Functional Imaging and Modelling of the Heart (FIMH 2005).

[73] A. Sigfridsson, J.-P. E. Kvitting, H. Knutsson, and L. Wigström, *Five-dimensional MRI incorporating simultaneous resolution of cardiac and respiratory phases for volumetric imaging.*, J Magn Reson Imaging, 25 (2007), pp. 113–121.

[74] E. M. Stein and G. Weiss, *Introduction to Fourier analysis on Euclidean spaces*, Princeton University Press, Princeton, N.J., 1971. Princeton Mathematical Series, No. 32.

[75] G. Strang and G. J. Fix, *An analysis of the finite element method*, Prentice-Hall Inc., Englewood Cliffs, N. J., 1973. Prentice-Hall Series in Automatic Computation.

[76] G. Tenenbaum and M. Tucsnak, *Fast and strongly localized observation for the Schrödinger equation*, Trans. Amer. Math. Soc., 361 (2009), pp. 951–977.

[77] R. B. Thompson and E. R. McVeigh, *Cardiorespiratory-resolved magnetic resonance imaging: measuring respiratory modulation of cardiac function*, Magn Reson Med, 56 (2006), pp. 1301–10.

[78] M. Tucsnak and G. Weiss, *Simultaneous exact controllability and some applications*, SIAM J. Control Optim., 38 (2000), pp. 1408–1427 (electronic).

[79] ——, *How to get a conservative well-posed linear system out of thin air. Part II: Controllability and stability*, SIAM J. Control Optimization, 42 (2003), pp. 907–935.

[80] ——, *Observation and Control for Operator Semigroups*, Birkhäuser Advanced Texts / Basler Lehrbücher, Birkhäuser Basel, 2009.

[81] R. J. van den Hout, H. J. Lamb, J. G. van den Aardweg, R. Schot, P. Steendijk, E. E. van der Wall, J. J. Bax, and A. de Roos, *Real-time MR imaging of aortic flow: influence of breathing on left ventricular stroke volume in chronic obstructive pulmonary disease.*, Radiology, 229 (2003), pp. 513–519.

[82] G. Weiss and M. Tucsnak, *How to get a conservative well-posed linear system out of thin air. Part I: Well-posedness and energy balance*, ESAIM Control Optim. Calc. Var., 9 (2003), pp. 247–274.

[83] A. M. Weissler, W. S. Harris, and C. D. Schoenfeld, *Systolic time intervals in heart failure in man.*, Circulation, 37 (1968), pp. 149–159.

[84] G. A. Whalley, H. J. Walsh, G. D. Gamble, and R. N. Doughty, *Comparison of different methods for detection of diastolic filling abnormalities.*, J Am Soc Echocardiogr, 18 (2005), pp. 710–717.

[85] M. L. Wood and R. M. Henkelman, *MR image artifacts from periodic motion*, Med Phys, 12 (1985), pp. 143–51.

[86] R. M. Young, *An introduction to nonharmonic Fourier series.*, Pure and Applied Mathematics, 93. New York etc.: Academic Press, a Subsidiary of Harcourt Brace Jovanovich, Publishers. X, 246 p., 1980.

[87] E. Zuazua, *Contrôlabilité exacte d'un modèle de plaques vibrantes en un temps arbitrairement petit*, C. R. Acad. Sci. Paris Sér. I Math., 304 (1987), pp. 173–176.

[88] ——, *Propagation, observation and control of waves approximated by finite difference methods*, SIAM Rev., 47 (2005), pp. 197–243.

Problèmes inverses et contrôlabilité avec applications en élasticité et IRM

Mots-clés : Contrôlabilité, équations des plaques, problèmes inverses, imagerie par résonance magnétique.

Résumé

Le but de cette thèse est d'étudier, du point de vue théorique, la contrôlabilité exacte de certaines équations aux dérivées partielles qui modélisent les vibrations élastiques, et d'appliquer les résultats ainsi obtenus à la résolution des problèmes inverses provenant de l'imagerie par résonance magnétique (IRM).

Cette thèse comporte deux parties. La première partie, intitulée "Contrôlabilité et observabilité de quelques équations des plaques", discute la problématique de la contrôlabilité exacte, respectivement de l'observabilité exacte, de l'équation des plaques perturbées avec des termes linéaires ou non linéaires. Ainsi, dans le Chapitre 2 de cette thèse nous avons démontré l'observabilité interne exacte de l'équation des plaques perturbées par des termes linéaires et dans le Chapitre 3 la contrôlabilité exacte locale d'une équation des plaques non linéaire attribuée à Berger. Le Chapitre 4 introduit une méthode numérique pour l'approximation des contrôles exactes dans des systèmes d'ordre deux en temps.

La deuxième partie de la thèse est dédiée à l'imagerie par résonance magnétique. Plus précisément, on s'intéresse aux méthodes de reconstruction des images pour des objets en mouvement, l'exemple typique étant l'imagerie cardiaque en respiration libre. Dans le Chapitre 6, nous avons formulé la reconstruction d'images cardiaques acquises en respiration libre comme un problème des moments dans un espace de Hilbert à noyau reproductif. L'existence d'une solution pour un tel problème des moments est prouvée par des outils bien connus dans la théorie du contrôle. Nous avons validé cette méthode en utilisant des images simulées numériquement et les images de cinq volontaires sains.

La connexion entre les deux parties de la thèse est réalisée par le Chapitre 7 où l'on présente le problème inverse d'identification d'un terme source dans l'équation des ondes à partir d'une observation correspondante à un enregistrement IRM.

En conclusion, nous avons montré qu'on peut utiliser les outils de la théorie de contrôle pour des problèmes inverses provenant de l'IRM des objets en mouvement, à la condition de connaître l'équation du mouvement.